

Yasushi Asami
Yukio Sadahiro
Ikuho Yamada
Kimihiro Hino *Editors*

Studies in Housing and Urban Analysis in Japan

New Frontiers in Regional Science: Asian Perspectives

Volume 75

Editor-in-Chief

Yoshiro Higano, University of Tsukuba, Tsukuba, Ibaraki, Japan

This series is a constellation of works by scholars in the field of regional science and in related disciplines specifically focusing on dynamism in Asia.

Asia is the most dynamic part of the world. Japan, Korea, Taiwan, and Singapore experienced rapid and miracle economic growth in the 1970s. Malaysia, Indonesia, and Thailand followed in the 1980s. China, India, and Vietnam are now rising countries in Asia and are even leading the world economy. Due to their rapid economic development and growth, Asian countries continue to face a variety of urgent issues including regional and institutional unbalanced growth, environmental problems, poverty amidst prosperity, an ageing society, the collapse of the bubble economy, and deflation, among others.

Asian countries are diversified as they have their own cultural, historical, and geographical as well as political conditions. Due to this fact, scholars specializing in regional science as an inter- and multi-discipline have taken leading roles in providing mitigating policy proposals based on robust interdisciplinary analysis of multifaceted regional issues and subjects in Asia. This series not only will present unique research results from Asia that are unfamiliar in other parts of the world because of language barriers, but also will publish advanced research results from those regions that have focused on regional and urban issues in Asia from different perspectives.

The series aims to expand the frontiers of regional science through diffusion of intrinsically developed and advanced modern regional science methodologies in Asia and other areas of the world. Readers will be inspired to realize that regional and urban issues in the world are so vast that their established methodologies still have space for development and refinement, and to understand the importance of the interdisciplinary and multidisciplinary approach that is inherent in regional science for analyzing and resolving urgent regional and urban issues in Asia.

Topics under consideration in this series include the theory of social cost and benefit analysis and criteria of public investments, socio-economic vulnerability against disasters, food security and policy, agro-food systems in China, industrial clustering in Asia, comprehensive management of water environment and resources in a river basin, the international trade bloc and food security, migration and labor market in Asia, land policy and local property tax, Information and Communication Technology planning, consumer “shop-around” movements, and regeneration of downtowns, among others.

Researchers who are interested in publishing their books in this Series should obtain a proposal form from Yoshiro Higano (Editor in Chief, higano@jrsai.jp) and return the completed form to him.

Yasushi Asami • Yukio Sadahiro • Ikuho Yamada •
Kimihiro Hino

Editors

Studies in Housing and Urban Analysis in Japan



Springer

Editors

Yasushi Asami
Department of Urban Engineering
The University of Tokyo
Bunkyo-ku, Tokyo, Japan

Ikuho Yamada
Center for Spatial Information Science
The University of Tokyo
Kashiwa-shi, Chiba, Japan

Yukio Sadahiro
Interfaculty Initiative in Inform. Stud.
The University of Tokyo
Bunkyo-ku, Tokyo, Japan

Kimihiro Hino
Department of Urban Engineering
The University of Tokyo
Bunkyo-ku, Tokyo, Japan

ISSN 2199-5974

ISSN 2199-5982 (electronic)

New Frontiers in Regional Science: Asian Perspectives

ISBN 978-981-99-8026-0

ISBN 978-981-99-8027-7 (eBook)

<https://doi.org/10.1007/978-981-99-8027-7>

© The Editor(s) (if applicable) and The Author(s), under exclusive license to Springer Nature Singapore Pte Ltd. 2024

This work is subject to copyright. All rights are solely and exclusively licensed by the Publisher, whether the whole or part of the material is concerned, specifically the rights of translation, reprinting, reuse of illustrations, recitation, broadcasting, reproduction on microfilms or in any other physical way, and transmission or information storage and retrieval, electronic adaptation, computer software, or by similar or dissimilar methodology now known or hereafter developed.

The use of general descriptive names, registered names, trademarks, service marks, etc. in this publication does not imply, even in the absence of a specific statement, that such names are exempt from the relevant protective laws and regulations and therefore free for general use.

The publisher, the authors, and the editors are safe to assume that the advice and information in this book are believed to be true and accurate at the date of publication. Neither the publisher nor the authors or the editors give a warranty, expressed or implied, with respect to the material contained herein or for any errors or omissions that may have been made. The publisher remains neutral with regard to jurisdictional claims in published maps and institutional affiliations.

This Springer imprint is published by the registered company Springer Nature Singapore Pte Ltd. The registered company address is: 152 Beach Road, #21-01/04 Gateway East, Singapore 189721, Singapore

Paper in this product is recyclable.

Preface

This book contains a collection of papers published in Japanese by researchers closely associated with our laboratory. They are translated into English with the permission of the academic societies where the original papers were published and compiled into a single volume on the occasion of my retirement from the University of Tokyo. Hopefully, this book provides an overview of the research activities of our laboratory.

The laboratory is called the Laboratory of Housing and Urban Analysis and has long operated with urban housing theory and urban analysis as the mainstay of its research. The first professor of the laboratory was Dr. Masahiko Honjo, who studied the spatial configuration of residential areas. The second professor was Dr. Kaoru Shimofusa, who studied housing issues from the perspective of housing economics, including the appropriate setting of rents. Dr. Shimofusa was also interested in analytical research methods and offered a course entitled “Urban Analysis.” Dr. Kozo Okudaira, an associate professor under Dr. Shimofusa, was also involved in the production of architectural models and compiled a book on urban analysis methods entitled *Urban Engineering Reader: Analyzing the City* (Okudaira 1976), which is still a bible for researchers who aim at urban analysis. However, Dr. Okudaira passed away suddenly in 1979. The third professor of the laboratory was Professor Atsuyuki Okabe, who explored the methodology of spatial analysis, especially summarized in *Spatial Tessellations. Concepts and Applications of Voronoi Diagrams* (Okabe et al. 1992) and *Spatial Analysis along Networks: Statistical and Computational Methods* (Okabe and Sugihara 2012) and others to establish spatial analysis methods. Then, Yasushi Asami became the fourth professor.

It was in 1981, when I was a senior in the Department of Urban Engineering at the University of Tokyo, that I decided to join the Laboratory of Housing and Urban Analysis organized by Professor Shimofusa and Associate Professor Atsuyuki Okabe. At the time, I was strongly attracted by the approach to research that considered urban events analytically and captured the city on a quantitative basis. Dr. Shimofusa gave me advice on the direction of my research from a broad perspective, and Dr. Okabe specifically guided me on methods and logical thinking,

and I completed my graduation thesis, “Factor Analysis of Urbanization: Using Takasaki City Mesh Data” (Asami 1982). In my graduation thesis, I considered population growth to be a major indicator of urbanization, and used multiple regression analysis to explore what factors promote urbanization. I then went on to a master’s program in the Department of Urban Engineering, Graduate School of Engineering, the University of Tokyo, where I conducted my master’s research in the same laboratory. I received guidance under the same system, and in particular, Dr. Okabe taught me in detail the basic concepts of research, how to construct analytical methods, how to handle actual data, and how to summarize my research. My current approach to research is largely due to the teachings of Dr. Okabe. I summarized my master’s research and presented it as my master’s thesis, “Distribution and Location Analysis of Population and Facilities in Urban Areas” (Asami 1984). During that time, he encouraged me to study in the USA and I was able to decide to study in the Department of Regional Science at the University of Pennsylvania.

At the University of Pennsylvania, I studied under the supervision of Dr. Tony Smith and Dr. Masahisa Fujita, who led a regional science workshop where researchers from inside and outside the university presented and discussed their research every week. I also presented my research every semester, and the comments I received were very helpful in improving my research. In my doctoral research, I was interested in land use theory, which considers the spatial organization of cities through the real estate market, and I reexamined the concept of land rent as a key concept in the theory. In doing so, I applied game theory, which was relatively new at the time, in an attempt to establish an academic foundation for land use theory. My doctoral dissertation, “Game-Theoretic Approaches to Bid Rent” (Asami 1987), was reviewed by Dr. Tony Smith, Dr. Masahisa Fujita, and Dr. Xavier Vives. I owe a great deal to Dr. Tony Smith and Dr. Masahisa Fujita for my axiomatic methods and urban economics approach.

After receiving Ph.D. degree, I returned to my old “home,” the Laboratory of Housing and Urban Analysis, as an assistant professor in the Department of Urban Engineering, Faculty of Engineering, the University of Tokyo in 1987. At that time, Dr. Okabe and I ran the laboratory together and taught students. I asked myself how to establish my area of expertise and decided to utilize my strengths. My background in urban planning and urban economics led me to try to open up a new field by fusing these two fields.

When I returned to Japan in 1987, Japan was in the midst of a real estate price bubble that soared, and shortly thereafter the bubble burst, fundamentally damaging the urban structure. The power of the real estate market was clearly demonstrated. Under these circumstances, urban planning scholars argued that strong planning regulations were necessary to break the market’s malady. On the other hand, urban economists argued that too much regulation distorts the market and leads to inefficient urban structures. The two disciplines on which I was relying had reached completely opposite conclusions. Since I was relying on them, I had to resolve this contradiction. Therefore, I considered what the premises of both theories were and what differences led to their different conclusions. At the time,

urban planning studies was weak in its conception of planning that incorporates the market, and urban economics was weak in its model that fully incorporates external diseconomies among land uses. If we can compensate for these weaknesses, we can obtain a consistent form of real estate for both fields. This became the focus of my subsequent research activities.

Some of the papers in this book are studies in which I was directly involved, while others were conducted independently by the respective authors. However, I expect that some of the authors may have been influenced in some small way by the way they approached their research in the process of research guidance and discussion of their research.

This book consists of two parts: Part I, Housing analysis, which contains research related to housing and residential life, and Part II, Urban analysis, which contains research related to urban analysis and spatial analysis. Our laboratory is called the Laboratory of Housing and Urban Analysis, and we have put up two signs in the front of the book. Part I, Housing analysis, contains papers on housing markets, housing environments, the lives of the older adults, urban crime, and photovoltaic panels installed on houses. The second part, Urban analysis, contains papers on methodology development, analysis, urban activity analysis, and traffic analysis.

An important area of Housing Analysis is the analysis of the housing market. Housing is a special good that has heterogeneity (no two houses are alike), durability (it is used for a long period of time), and high price (it is expensive and therefore not something that can be purchased many times). For this reason, they form a field of study in economics, as in the field of housing economics. Suzuki-Asami paper analyzes the price and market residence time of existing detached houses. In the case of existing houses, if demand is high, the house can be sold normally, but when demand falls, sellers are faced with the choice of selling at a lower price or giving up on the sale. This creates a somewhat unique housing market. Baba-Shimizu-Asami paper also analyzes the probability of rebuilding older condominiums. In Japan, each owner of a condominium unit has a special ownership right called strata title. In order to rebuild a condominium, it is necessary to obtain the agreement of the unit owners by a special majority vote of 80% or more. Therefore, it is difficult to rebuild a condominium unless the circumstances are very favorable for rebuilding, which is directly related to the high demand in the housing market.

In Housing Analysis, the living environment around a house is also an important subject of analysis. The term “living environment” covers a wide range of factors, including safety, health, convenience, amenity, and sustainability. This field analyzes how these factors ultimately affect people’s housing behavior. For this purpose, it is necessary to comprehensively measure the living environment. Ai paper analyzes the relationship between housing environment scores and population growth.

As Japan’s population ages, it is important to accurately understand the lives of the older adults and consider necessary housing policies. Kim et al. paper analyzes the relationship between social participation of the older adults and the density of neighborhood facilities. Sekiguchi paper analyzes the problem of accessibility to stores for the older adults by examining not only distance but also road conditions

in detail. This kind of steady analysis of the behavior of the older adults produces hints for building a society that takes the older adults into consideration.

Crime is one of the most important safety-related issues in the living environment. One of the crimes involving housing is residential burglary. There are certain characteristics of houses and areas where residential burglary is most likely to occur. Conversely, if we can analyze trends, we can determine what countermeasures should be taken to reduce residential burglary, and this information can be used to improve safety. This book includes Hino-Kojima paper, which constructs a model to predict the risk of residential burglary, and Uesugi-Hino paper, which analyzes the relationship between the socioeconomic status of a neighborhood and residential burglary.

The use of renewable energy has been increasing in recent years due to heightened environmental awareness. For homes, a relatively easy renewable energy source to use is solar panels. The installation of solar panels has advanced considerably due to the feed-in tariff system, but at the same time, it has caused landscape problems. In Okazawa-Hino-Asami paper, the relationship between the installation of residential solar panels and the home and surrounding environment is analyzed.

Urban Analysis deals with the problem of analyzing spatial arrangements and spatial representations. A time map is a map that shows the time required between points intuitively in terms of the distances between each other by changing the location of the points themselves so that the time required is as proportional as possible to the distances between the points. In general, the method differs depending on what and how much importance is placed on actual position of points and precise representation of time since it is not possible to make the time required completely proportional to the distance between points. Therefore, it can be said that the methods of creating time maps are diverse and still in the process of development. Nishi-Asami paper develops a method for constructing time maps and shows examples of their application.

Predicting how a building will be constructed on a given site is important for analyzing the formation process of urban areas. The owner of a site will develop the site in a way that is optimal for himself based on the site conditions. In Taima et al. paper, a method is constructed to predict what kind of building will be built in a given site in a highly commercial area, and examples of the prediction results are presented.

One method often used to estimate housing prices is hedonic analysis. In hedonic analysis, a regression analysis is conducted with housing land prices and housing prices as the objective variables and variables representing the status of factors expected to affect prices as explanatory variables. Hiruta-Asami paper analyzes the severity of multicollinearity and shows how to obtain appropriate regression results.

In urban planning, the setback of a building (how far a building is set back from the street), the length of frontage of site to the adjacent road, and the depth of the site have been considered and analyzed as important indicators to express the urban environment. Usui-Asami paper presents a framework that allows for a

comprehensive analysis of these relationships and analyzes their relationship with building density.

The vitality of a city center depends on the location and activity of commercial establishments. Therefore, how shopping areas develop or decline is an important concern in urban planning. Inasaka paper develops a method to express which direction commercial facilities are spreading and presents the results of this analysis.

Urban transportation is an important factor in determining the convenience of an urban area. Urban transportation has been undergoing major changes in recent years due to the development of ICT technology, including the spread of sharing services and the development of demand-responsive transit. Hasegawa-Suzuki paper theoretically analyzes what kind of public transportation system is desirable.

Looking at the topics of the papers gathered in this way, I am deeply moved by a renewed appreciation of the breadth of research that our laboratory has conducted. I also feel the joy of having nurtured so many researchers. I hope that the younger members of our laboratory will continue to develop and deepen their research fields in the future.

When my former teacher, Dr. Atsuyuki Okabe, retired, we translated Japanese papers by researchers who had been under his care into English and compiled them into a book (Asami et al. 2009). This stimulated us to plan this book. I am grateful to Yukio Sadahiro, Ikuho Yamada, Kimihiro Hino, and Hiroyuki Usui, for their support in the planning of this project. I would like to express my deep gratitude to them.

We hope that this book will help readers learn more about the current status of housing and urban analysis research in Japan and assist in its future development.

Tokyo, Japan

Yasushi Asami

References

- Asami Y (1982) Factor analysis of urbanization: using mesh data of Takasaki City. Graduation Thesis, Department of Urban Engineering, Faculty of Engineering, The University of Tokyo
- Asami Y (1984) Distribution and location analysis of population and facilities in Tokyo. Master's thesis, Department of Urban Engineering, Faculty of Engineering, The University of Tokyo
- Asami Y (1987) Game-theoretic approaches to bid rent. Ph.D. dissertation, Department of Regional Science, University of Pennsylvania University Microfilms Inc., Ann Arbor, Michigan
- Asami Y, Sadahiro Y, Ishikawa T (eds) (2009) New frontiers in urban analysis. In Honor of Atsuyuki Okabe. CRC Press, Boca Raton
- Okabe A, Boots B, Sugihara K (1992) Spatial tessellations. Concepts and applications of Voronoi diagrams. J. Wiley and Sons

- Okabe A, Sugihara K (2012) Spatial analysis along networks: statistical and computational methods. John Wiley & Sons
- Okudaira K (1976) Toshi Kogaku Dokuhon: Toshi wo Kaisekisuru [Urban Engineering Reader: Analyzing the City]. Shokoku-sha Publishing Co.

Contents

Part I Housing Analysis

1 Demand –Supply Relationship in the Resale Housing Market in the Suburbs of Tokyo	3
Masatomo Suzuki and Yasushi Asami	
2 Old Condominiums and Their Tendency to Be Rebuilt: A Case Study of the Tokyo Metropolitan Area	21
Hiroki Baba, Chihiro Shimizu, and Yasushi Asami	
3 Significance of “Living Environment Score” in Quantifying Attractiveness of Regions During Residence Selection	41
Hisatoshi Ai	
4 Relationship Between Participation of Older Adults in Hobby Clubs and Sports Groups and Density of Neighborhood Facilities: A Case of Nagoya City Using JAGES Panel Data	65
Hongjik Kim, Kimihiro Hino, Hiroyuki Usui, Masamichi Hanazato, Daisuke Takagi, Naoki Kondo, and Katsunori Kondo	
5 Environmental Factors Causing Inconvenience of Store Accessibility for Older Adults in Tokyo: Objective Indicators of Road Environments for Estimating People’s Inconvenience	81
Tatsuya Sekiguchi	
6 Relationship Between Crime Rate of Residential Burglary and Local Context	101
Kimihiro Hino and Takaya Kojima	

7 A Spatial Analysis of the Effects of Neighborhood Socio-economic Status on Residential Burglaries in Tokyo: Focusing on the Spatial Heterogeneity and the Interactions with Built Environment	115
Masaya Uesugi and Kimihiro Hino	
8 Factors Affecting Installation of Residential Photovoltaics in Housing Estates in Kakegawa City, Shizuoka: Focusing on Housing and Surrounding Environment Characteristics	133
Yuki Okazawa, Kimihiro Hino, and Yasushi Asami	

Part II Urban Analysis

9 Statistical Multi-dimensional Scaling with a Geographical Penalty: Development of Bayesian Multi-dimensional Scaling and Its Application to Time–Space Mapping	153
Hayato Nishi and Yasushi Asami	
10 Factors that Influence Estimation of Building Location in City Blocks in Tokyo Commercial Zones	169
Masahiro Taima, Yasushi Asami, Kimihiro Hino, and Wataru Morioka	
11 A Diagnostic Approach to the Multicollinearity Problem for Better Model Selection in the Hedonic Pricing Method	185
Yuki Hiruta and Yasushi Asami	
12 Theoretical Relationships Between Building Setback, Plot Frontage, and Plot Depth in Terms of Road and Building Densities	215
Hiroyuki Usui and Yasushi Asami	
13 A Method of Visual Analytics and Data Visualization in Design Context: Case Study of Spatiotemporal Data Visualization of Urban Retail Agglomeration Growth	235
Akiyoshi Inasaka	
14 Theoretical Approach for Selection of Public Transport System Considering Urban Density and Travel Distance	271
Daisuke Hasegawa and Tsutomu Suzuki	

Part I

Housing Analysis

Chapter 1

Demand–Supply Relationship in the Resale Housing Market in the Suburbs of Tokyo



Masatomo Suzuki and Yasushi Asami

Abstract Vacant houses are currently being promoted for use in the resale housing market, and the purchase of resale houses has become an important option in society. This chapter investigates the demand–supply relationship in the resale housing market on the outskirts of the Tokyo metropolitan area. Focusing on the two established market-clearing factors: “price” and “time required to sell a property,” we investigated the manner in which potentially disadvantageous properties—in terms of building and locational characteristics—are sold in the market. In suburbs less than 30 km from central Tokyo, we show that such properties tend to be sold quickly or fetch high prices, suggesting a strong demand for resale houses for young households. In addition, in the outer suburbs (40 km or farther away from central Tokyo), potentially disadvantageous properties required longer time to sell or fetch low prices. Moreover, certain owners were found attempting to dispose their properties quickly at a low price, suggesting that they consider it costly to maintain their unnecessary properties.

Keywords Housing market analysis · Resale housing market · Price · Time on the market · Population decline

The contents of this chapter are based on the following paper originally published in a Japanese journal: Suzuki M, Asami Y (2017) The demand-supply relationship in the resale housing market: Evidence from the outskirts of the Tokyo metropolitan area. Journal of the City Planning Institute of Japan 52(3): 514–520 (in Japanese).

M. Suzuki (✉)

Yokohama City University, Yokohama, Kanagawa, Japan
e-mail: suzuki.mas.ke@yokohama-cu.ac.jp

Y. Asami

Department of Urban Engineering, The University of Tokyo, Tokyo, Japan
e-mail: asami@csis.u-tokyo.ac.jp

1.1 Introduction

The outskirts of the Tokyo metropolitan area is experiencing a decrease in the population (or number of households). Thus, the number of vacant houses is increasing. For spatial planning to enhance the long-term sustainability of the area, the relationship between neighborhood characteristics and population dynamics, including decreasing population (or number of households) (Ai 2014; Miyake et al. 2014), generation balance (Ai 2016; Fujii 2008; Fujii and Oe 2005, 2006), and increasing number of vacant houses (Sakamoto and Yokohari 2016; Ujihara et al. 2006, 2016a, 2016b; Yamanshita and Morimoto 2015), has been investigated.

Recently, vacant houses have been promoted for use in the resale housing market, and purchasing resale houses has become an important option in society (Hirayama 2011). Several city-planning studies have investigated owners' willingness to utilize vacant houses (e.g., Ito and Kaido 2013). However, real estate markets have rarely been investigated. Among the few who have investigated these markets, Todoroki (2011) and Umeda and Hirayama (2002) only investigated special cases such as foreclosure sales and properties whose prices had dropped significantly.

The resale housing market is crucial for clarifying the building and locational characteristics that new residents consider when purchasing resale houses, thus clarifying the boundaries of the urban area that are expected to be sustained in the long run. Consequently, the resale housing market becomes inactive before the population (or number of households) starts to decrease, and vacant houses begin to increase in number. Focusing on utilizing resale houses, the similarities and differences between the building/locational characteristics that determine the demand-supply relationship of resale housing markets and the neighborhood dynamics documented in the literature must be clarified.

The demand-supply relationship in real estate markets is characterized by two indicators: "price" and "time on the market" (TOM) (Han and Strange 2015). As in the hedonic analysis, price represents the value of the building or locational characteristics. However, the TOM has rarely been investigated in the city planning literature. It is a liquidity measure that measures the time from the initial listing in the market to the completion of sales. A short TOM indicates a "hot" market with more buyers than sellers. For buyers searching for desirable houses across several properties/regions, there is a trade-off between price and TOM. Their determination in the market is dependent on the micro-level segments of the building or locational characteristics (Piazzesi et al. 2020). Thus, both must be investigated to understand the housing resale market. Ong and Koh (2000) investigated the effect of building or locational characteristics on price and TOM, focusing on heterogeneities in the floor levels of high-rise apartments.

This chapter investigates the relationship between building or locational characteristics in the context of population shrinkage in Japan and price and TOM, which are the basic components of real estate markets. It clarifies the demand-supply relationship of the resale housing markets in the suburbs of the Tokyo metropolitan area. We focus on the area along the Tobu Tojo/Ogose lines in Saitama Prefecture because certain of these areas are now facing population shrinkage (or a

decreasing number of households) (Miyake et al. 2014). We categorized the building characteristics by age, floor area, etc. and categorized their location based on distance from central Tokyo, time from the nearest station, etc. From the estimated price/TOM equations, we obtained the following demand–supply relationship in the resale housing market. Overall, relative to supply, the demand for resale houses was low (high) in areas with typical characteristics of population shrinkage (growth). However, the demand–supply relationship for potentially disadvantageous properties changed with the distance from central Tokyo. In other words, demand strongly exists even for potentially disadvantageous properties in the suburbs relatively close to central Tokyo; on the outskirts farther away from central Tokyo, such properties exhibit long TOM, and certain owners may reduce prices to quickly dispose of their properties.

The remainder of this chapter is organized as follows. Section 1.2 describes the target area and data. Section 1.3 describes the empirical methods considered in this study. Section 1.4 presents and discusses the results. Finally, Sect. 1.5 concludes the paper with certain policy implications.

1.2 Target Area and Data

In the Tokyo metropolitan area, characteristics of areas vary significantly across train lines even within the same distance from central Tokyo. To compensate for the factors that affect price and TOM, we focused on the area along the Tobu Tojo/Ogose lines in Saitama Prefecture.¹ Certain of these areas, particularly those 40 km or further from central Tokyo, are now facing population shrinkage (and a decreasing number of households) (Miyake et al. 2014). The area covers the town of Moroyama, where vacant houses are rapidly increasing in number (Hasegawa 2005). Therefore, this area is suitable for our analysis in the context of population shrinkage.

We employed the list price data of resale houses from a real estate market database collected by At Home Co., Ltd. The data included the list price, date of listing, building characteristics, and (geocoded) locational characteristics for each property listed in the database between January 1, 2011 and August 31, 2014. We employed a time interval that includes sufficient samples to capture recent trends in the resale housing market, whose importance is growing.² As shown in Fig. 1.1,

¹ The cities include Wako, Niiza, Asaka, Shiki, Fujimi, Fujimino, Kawagoe, Tsurugashima, Hidaka, Sakado, Higashi-matsuyama, and Kumagaya. The towns include Ogose, Miyoshi, Moroyama, Kawashima, Yoshimi, Hatoyama, Tokigawa, Namerigawa, Ranzan, Ogawa, and Yorii.

² After the bubble burst, the resale housing market became important in Japan. Indeed, the proportion of resale houses to all the transacted houses (resale houses and newly built ones) is exhibiting an increasing trend (MLIT 2017). The transaction volume of newly built houses fluctuates over time, while that of resale houses are stable over time; this suggests that the macroeconomic effect on the resale housing market in the analysis periods is relatively small. Notably, we control the macroeconomic trend by season/year dummies.

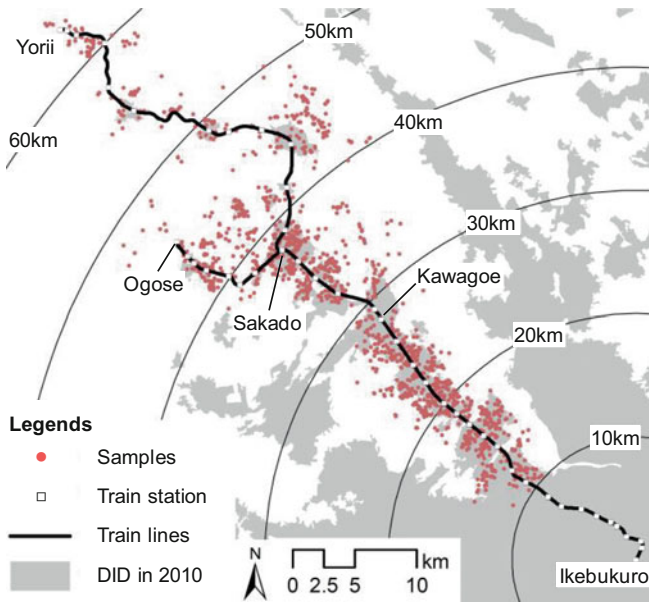


Fig. 1.1 Spatial distribution of resale houses on the market

we restricted the sample to houses whose nearest train station was on the Tobu Tojo/Ogose lines. To investigate suburban areas, the samples were restricted to those located 10 km or farther from central Tokyo (in this case, Ikebukuro station). In particular, within a distance of 30–50 km from central Tokyo, many houses in the market are far away from the nearest station. We measured the TOM by employing houses listed on or after April 1, 2011 with the listing ending on or before May 31, 2014. We assumed that (i) transactions were made at the list price one day after the final listing³ and (ii) if the listing interval became 3 months or greater, the property was sold once and again listed for sale (note that the properties are usually listed once a month if they are not yet sold). We omitted samples with TOM longer than 2 years (730 days).

Table 1.1 summarizes the variables used in the analysis. The explanatory variables include the markup ratio (M), which is the ratio of list price to expected sale price; variables of macroeconomic environments (E); variables of building characteristics (B); and variables of locational characteristics (R), where bold indicates the vectors.

The markup ratio (M) is the ratio of the list price to the expected sale price (see Sect. 1.3 for details), showing individual circumstances. Engelhardt (2003) and Genesove and Mayer (1997, 2001) provide an example. In the US, households

³ Most of the previous literature assumes that properties once listed on the real estate market database are finally transacted, at which time the listing ends (Shimizu et al. 2004).

Table 1.1 Summary statistics

Variables	Mean	S.D.	Min.	Max.
Price/TOM				
List price (1000 JPY)	17,366	11,261	1300	120,000
Sale price (1000 JPY)	16,718	10,848	1300	120,000
Time on the market (day)	94.8	126.2	1.0	727.0
Markup ratio (M)				
Markup ratio	1.098	0.374	0.187	4.331
Variables of macroeconomic environment (E)				
Fall	0.272	0.445	0	1
Year 2013	0.316	0.465	0	1
Year 2014	0.083	0.276	0	1
Variables of building characteristics (B)				
Lot size: less than 50 m ²	0.050	0.219	0	1
Lot size: 250 m ² or more	0.082	0.275	0	1
Lot size (m ²)	143.5	132.2	25.3	1939.8
Floor space (m ²)	94.7	34.6	23.8	405.1
Building age: less than 5 years	0.076	0.265	0	1
Building age: 30 years or more	0.279	0.449	0	1
Building age (year)	21.6	12.1	0.0	66.0
Variables of locational characteristics (R)				
Time to nearest station: less than 10 min	0.262	0.440	0	1
Bus to nearest station	0.167	0.373	0	1
Max. slope: 10 degrees or more	0.057	0.232	0	1
Proportion of elderlies: 25% or more	0.052	0.222	0	1
Detached owner-occupied housing district	0.376	0.484	0	1
Densely inhabited districts in 1960	0.021	0.145	0	1
Densely inhabited districts in 2010	0.662	0.473	0	1
Low-rise residential zones	0.279	0.449	0	1
Medium-to-high-rise residential zones	0.170	0.376	0	1
Distance from central Tokyo: 20–30 km	0.250	0.433	0	1
Distance from central Tokyo: 30–40 km	0.271	0.445	0	1
Distance from central Tokyo: 40–50 km	0.225	0.418	0	1
Distance from central Tokyo: 50–70 km	0.071	0.256	0	1

that have remaining mortgage debt are likely to experience a longer TOM to sell their houses at high prices. However, in the suburbs of the Tokyo metropolitan area, typical owners who wish to sell their resale houses are typically elderly and have already finished mortgage payments (Hirayama 2011); thus, such a situation in the US is not likely to apply to our analysis.

The macroeconomic environment variables (**E**) include a seasonality dummy (fall: July–September) and year dummies (2013 and 2014) for the listing date.

The variables of building characteristics (**B**) included land area, floor area, and building age. We also prepared the following special dummy variables to capture

the differences from typical houses. As the average land area is 143.5 m², dummy variables for “less than 50 m²” and for “250 m² or greater” are constructed. For building age, dummy variables are constructed for “less than five years” and for “30 years or greater” (i.e., built under the former earthquake-resistance standards). We omitted samples with a building age of 100 years or older as an exception.

For the variables of locational characteristics (**R**), we prepared the following special dummy variables that captured differences from typical houses. Previous literature has investigated neighborhood characteristics of population shrinkage using the following variables: distance from the nearest station, slope of the residential district, balance of the age of residents, variety of building types, periods of development, zoning, and distance from the metropolitan center (Fujii 2008; Miyake et al. 2014; Ujihara et al. 2016a, 2016b). Therefore, for the distance from the nearest station, we constructed dummy variables for “within a 10 min walk to the nearest station” and “more than a 30 min walk to the nearest station (i.e., need to take a bus).”

For the slope of the residential district, a dummy variable was constructed if the maximum slope was 10 degrees or greater. For the balance the age of residents, a dummy variable was constructed if the proportion of elderly residents (i.e., the ratio of households whose members are all 65 years old or older to all households) was 25% or greater. For varieties of building types, we constructed a dummy variable for “detached owner-occupied housing districts,” wherein the detached housing ratio was 80% or greater and the owner-occupied housing ratio was 80% or greater, following the method of Fujii (2008). For the development periods, dummy variables were constructed for densely inhabited districts (DIDs) in 1960 and 2010. For zonings that protect the nice residential environments, we constructed dummy variables for “category I exclusive low building residential zone” (hereafter, “low-rise residential zones”) and “category I exclusive high and medium building residential zone” (hereafter, “medium-to-high-rise residential zones”).

For the distance from the metropolitan center, we categorized the area by 10 km intervals from central Tokyo; here, the 50–70 km interval was used to maintain sufficient samples for analyses. The previous literature on population dynamics in the Tokyo metropolitan area (Fujii 2008; Fujii and Oe 2005, 2006; Miyake et al. 2014) employed 10 km intervals from central Tokyo to discuss the characteristics of the area. Thus, we employed the same distance intervals to discuss our results in Sect. 1.4 along with the previous literature. To prepare the variables, we used property geocodes to overlap with the spatial data.⁴

⁴ We calculated the time distance from the nearest station (we employed the digital national land information, MLIT) by measuring the Euclidean distance and dividing it by the walking speed (80 m/min). For maximum slopes (250 m mesh) and DID areas, we employed the digital national land information (MLIT). For the proportion of elderly persons, detached housing ratio, and owner-occupied housing ratio, we employed the district-level 2010 Population Census.

Table 1.2 Price and TOM in each distance interval from central Tokyo

	10–20 km	20–30 km	30–40 km	40–50 km	50–70 km
Sale price (1000 JPY)	24,154	17,749	16,182	12,413	9492
	(14,587)	(10,987)	(7962)	(7029)	(5352)
Time on the market (day)	88.9	82.1	104.1	94.5	105.5
	(118.5)	(116.9)	(137.1)	(130.4)	(117.8)
Number of observations	284	386	419	348	109

Notes: For the sales price and TOM, we show the average (standard deviations in parentheses)

We used 1546 houses after omitting samples with missing information. As shown in Table 1.1, the average TOM was 94.8 days, and the list price was, on average, 9.8% higher than the sale price. The average age of the buildings was 21.6 years. Table 1.2 summarizes the price and TOM for each distance interval from central Tokyo. At the metropolitan level, sales prices declined and TOM increased farther away from central Tokyo.

1.3 Empirical Methods

Following Ong and Koh (2000), we investigated the effect of the building/locational characteristics of housing units on their prices and TOM.⁵

Step 1: A hedonic analysis (OLS) was conducted using building characteristics (**B**) and locational characteristics (**R**) as explanatory variables. The dependent variable is the log of sale price, P_S . We then estimated the expected sale price.

$$\ln \hat{P}_S = \hat{\alpha}_0 + \mathbf{B}'\hat{\alpha}_B + \mathbf{R}'\hat{\alpha}_R \quad (1.1)$$

The “dash” for the vectors shows the transposed matrix, α_0 is the constant, α_i ($i \in \{B, R\}$) is the corresponding vector of coefficients, and the “hat” represents the estimated value.

Step 2: From Eq. (1.1), we define the markup ratio (M) as the ratio of the list price P_L to the expected sale price:

$$M \equiv \frac{P_L}{\hat{P}_S} \quad (1.2)$$

⁵ Housing markets are determined with price and TOM, and the following two types of assumptions exist: (i) the TOM is independently determined as a function of M , \mathbf{E} , \mathbf{B} , and \mathbf{R} ; or (ii) the TOM is determined simultaneously with price as a function of \mathbf{E} . In this study, we employed the former assumption to investigate the effect of building characteristics (**B**) and locational characteristics (**R**) on both price and TOM, as in the analysis by Ong and Koh (2000).

Step 3: TOM is explained as a function of the markup ratio (M), macroeconomic environment variables (\mathbf{E}), building characteristic variables (\mathbf{B}), and locational characteristic variables (\mathbf{R}).

$$\text{TOM} = \Phi(M, \mathbf{E}, \mathbf{B}, \mathbf{R}) \quad (1.3)$$

While prices are determined from the “universal” components such as building and locational characteristics, the TOM becomes short if the list price is lower than its original value (i.e., its expected sale price) and if the market is in the active period (Eq. (1.3)). Specifically, we conducted a survival analysis that analyzed the time since the event (i.e., final sales) occurred, assuming a Weibull distribution.⁶ Let $f(t)$ be the probability density function of the TOM in period t , and its cumulative distribution (i.e., the probability that the TOM is shorter than t) becomes

$$F(t) = \int_0^t f(s)ds = \Pr(\text{TOM} \leq t) \quad (1.4)$$

However, the probability that the properties are still in the market in period t (i.e., the probability that the TOM is t or longer) is

$$S(t) = 1 - F(t) = \Pr(\text{TOM} \geq t) \quad (1.5)$$

From Eq. (1.5), the probability (or hazard) that properties that are still in the market in period t will be sold in the next period (or instance) becomes

$$h(t) = \frac{f(t)}{S(t)} \equiv \lambda p t^{p-1} \quad (1.6)$$

which is assumed to follow a Weibull distribution. The hazard function $h(t)$ is an increasing (decreasing) function of time t if parameter $p > 1$ ($p < 1$); that is, properties are more likely to be sold (properties are more likely to remain listed) with increase in the TOM. Therefore, the estimation of Eq. (1.3) becomes the estimation of parameters p and λ in Eq. (1.6). Note that the coefficients of explanatory variables for the TOM and hazard of sales, λ , are reversed:

$$\lambda = \exp(\gamma_0 + \gamma_M M + \mathbf{E}' \boldsymbol{\gamma}_E + \mathbf{B}' \boldsymbol{\gamma}_B + \mathbf{R}' \boldsymbol{\gamma}_R) \quad (1.7)$$

where γ_0 is the constant, γ_M is the coefficients of the markup ratio, and $\boldsymbol{\gamma}_i$ ($i \in \{E, B, R\}$) are the corresponding coefficient vectors.

⁶ Compared to the direct estimate of the TOM by OLS, we confirm that the survival analysis better fits the model with larger log-likelihood. In addition, we employed the Weibull distribution in the survival analysis after comparing the log-likelihoods in exponential and log-normal distributions.

1.4 Empirical Results

Table 1.3 presents the estimation results of the sale price for the entire sample and the subsamples at each distance interval from central Tokyo.⁷ If the coefficients of explanatory variables are positive (negative) and statistically significant, the variables exert an effect on pushing up (down) the price. The basic determinants included lot size, floor area, building age, and distance from central Tokyo.

Table 1.4 shows the estimation results of TOM (specifically, the hazard of sale, λ , in Eq. (1.7)) for the entire sample and for the subsamples of each distance interval from central Tokyo.⁸ In each estimation, the parameter p satisfies $p < 1$, showing the reasonable trend that properties are more likely to remain listed with increase in the TOM.⁹ If the coefficients of the explanatory variables are positive (negative) and statistically significant, the variables have an effect on pushing down (up) the TOM. The basic determinants include the seasons and years of the initial listing and the markup ratio. For building or locational characteristics, variables such as lot size, building age, bus access to the nearest station, detached owner-occupied housing districts, and distance from central Tokyo had a statistically significant effect on the TOM.¹⁰ In general, the TOM is determined within the search and matching framework. Thus, the TOM typically contains considerable larger random components, and the accuracy of its estimation is relatively low compared with the price (Yavas and Yang 1995). Even in the study by Ong and Koh (2000), which employs methods similar to our analysis, only certain building or locational characteristics affected the TOM compared to price. Thus, Table 1.4 presents reasonable estimation results. In particular, in the 50–70 km interval from central Tokyo, a clearer effect on TOM than on price was observed; this implies that the market is adjusted both by prices and TOM. Therefore, we confirmed the importance of both price and TOM in capturing the demand–supply relationship in the resale housing market.

At the metropolitan level, sales prices declined and TOM increased in areas farther away from central Tokyo (see Table 1.2). Considering this metropolitan-level trend, from Tables 1.3 and 1.4, we summarize the effect of each property characteristic on the demand–supply relationship within each distance interval

⁷ Since the VIF is below 5, a multi-collinearity problem does not exist.

⁸ In contrast to the estimation of price, in the survival analysis on TOM, we do not include the controls such as lot size, floor area, and building age, as these variables do not exhibit statistical significance.

⁹ This confirms that the Weibull distribution is more appropriate than exponential distribution ($p = 1$).

¹⁰ We compared the log-likelihood to choose the survival analysis with Weibull distribution to estimate TOM. In addition, to estimate TOM with the entire sample, we constructed or selected the appropriate explanatory variables after comparing the log-likelihoods between each estimated model. For the entire sample, the likelihood ratio test (the null hypothesis is without any explanatory variables) yielded $\chi^2 = 154.08$ with statistical significance (at 1% level); thus, we confirmed the validity of the entire estimates.

Table 1.3 Determinants of sale price

	Entire sample			10–20 km			20–30 km		
	Coef.	t-value		Coef.	t-value		Coef.	t-value	
Distance from central Tokyo:									
Explanatory variables									
Lot size: less than 50 m ²	-0.326	-8.01	***	-0.036	-0.44		-0.248	-5.24	***
Lot size: 250 m ² or more	0.023	0.54		-0.556	-2.61	**	-0.827	-6.58	***
Building age: less than 5 years	0.041	1.08		-0.027	-0.35		-0.032	-0.54	
Building age: 30 years or more	0.046	1.39		0.184	1.94	*	0.107	1.81	*
Time to nearest station: less than 10 min	0.069	3.36	***	0.200	4.34	***	0.050	1.33	
Bus to nearest station	-0.073	-2.82	***	-0.102	-1.32		-0.228	-3.66	***
Max. Slope: 10 degrees or more	-0.119	-3.03	***	-0.008	-0.03				
Proportion of elderlies: 25% or more	0.054	1.42		0.095	1.02		-0.052	-0.43	
Detached owner-occupied housing district	-0.112	-5.20	***	-0.095	-1.21		-0.153	-4.65	***
Densely inhabited districts in 1960	0.169	2.91	***	0.043	0.50		0.064	0.60	
Densely inhabited districts in 2010	0.150	6.05	***	0.363	3.81	***	0.181	3.40	***
Low-rise residential zones	0.094	4.60	***	0.065	1.06		-0.035	-1.02	
Medium-to-high-rise residential zones	0.095	3.79	***	0.080	1.74	*	-0.039	-0.86	
Lot size (m ²)	0.001	12.06	***	0.006	7.67	***	0.006	11.93	***
Floor space (m ²)	0.007	22.23	***	0.007	7.40	***	0.004	6.78	***
Building age (year)	-0.021	-15.88	***	-0.022	-6.96	***	-0.024	-10.78	***
Distance from central Tokyo: 20–30 km	-0.195	-7.26	***						
Distance from central Tokyo: 30–40 km	-0.359	-13.53	***						
Distance from central Tokyo: 40–50 km	-0.631	-20.31	***						
Distance from central Tokyo: 50–70 km	-0.758	-16.98	***						
Constant	9,430	195.75	***	8.774	61.25	***	9.139	113.48	***
Adjusted-R ²	0.74			0.69			0.83		
Number of observations	1546			284			386		

Distance from central Tokyo:	30–40 km		40–50 km		50–70 km	
	Coef.	t-value	Coef.	t-value	Coef.	t-value
Explanatory variables						
Lot size: less than 50 m ²	-0.300	-1.61	-0.382	-1.84	*	
Lot size: 250 m ² or more	-0.058	-0.75	0.230	3.93	***	0.195 1.54
Building age: less than 5 years	0.028	0.38	0.096	1.12	0.220	1.04
Building age: 30 years or more	0.005	0.09	0.042	0.70	-0.192	-1.84 *
Time to nearest station: less than 10 min	0.066	1.87	* -0.075	-1.65	0.194	2.27 **
Bus to nearest station	-0.121	-2.12	** -0.044	-1.18	-0.086	-0.92
Max. Slope: 10 degrees or more			-0.193	-4.20	***	-0.075 -1.16
Proportion of elderlys: 25% or more	-0.034	-0.41	0.024	0.38	0.123	1.26
Detached owner-occupied housing district	-0.077	-2.00	** -0.118	-2.76	***	-0.138 -1.45
Densely inhabited districts in 1960	-0.036	-0.11	0.247	2.17	**	
Densely inhabited districts in 2010	0.199	4.67	*** 0.141	3.23	***	-0.050 -0.30
Low-rise residential zones	0.043	1.14	0.155	3.64	***	0.433 4.23 ***
Medium-to-high-rise residential zones	0.115	2.31	** 0.185	3.07	***	0.139 0.85
Lot size (m ²)	0.002	8.31	*** 0.001	4.98	***	0.001 4.75 ***
Floor space (m ²)	0.004	7.29	*** 0.006	11.04	***	0.004 2.63 **
Building age (year)	-0.020	-7.91	*** -0.023	-8.76	***	-0.019 -2.70 ***
Constant	9.168	109.23	*** 8.982	103.10	***	8.875 34.99 ***
Adjusted-R ²	0.60		0.73		0.74	
Number of observations	419		348		109	

Notes: The dependent variable is the log of the sale price (1000 JPY). Significance level: ***1%, **5%, *10%

Table 1.4 Determinants of TOM

Distance from central Tokyo:		Entire sample		10–20 km		20–30 km	
	Coeff.	<i>z</i> -value		Coeff.	<i>z</i> -value	Coeff.	<i>z</i> -value
Explanatory variables							
Lot size: less than 50 m ²	0.235	1.90	*	0.039	0.16	0.356	2.13
Lot size: 250 m ² or more	0.180	1.84	*	0.493	1.06	0.428	1.07
Building age: less than 5 years	0.208	2.09	**	0.447	2.21	0.139	0.72
Building age: 30 years or more	-0.047	-0.79		-0.008	-0.06	-0.141	-1.16
Time to nearest station: less than 10 min	-0.074	-1.15		-0.009	-0.06	-0.195	-1.31
Bus to nearest station	-0.148	-1.81	*	-0.131	-0.53	-0.375	-1.57
Max. Slope: 10 degrees or more	-0.058	-0.47		0.504	0.70		
Proportion of elderlys: 25% or more	0.042	0.35		-0.268	-0.96	0.863	1.86
Detached owner-occupied housing district	-0.116	-1.69	*	0.115	0.46	-0.215	-1.68
Densely inhabited districts in 1960	0.115	0.63		-0.035	-0.13	1.074	2.66
Densely inhabited districts in 2010	-0.093	-1.17		0.033	0.11	-0.269	-1.33
Low-rise residential zones	-0.066	-1.04		0.012	0.06	-0.138	-1.07
Medium-to-high-rise residential zones	0.026	0.34		0.117	0.79	-0.005	-0.03
Distance from central Tokyo: 20–30 km	0.141	1.68	*				
Distance from central Tokyo: 30–40 km	-0.017	-0.20					
Distance from central Tokyo: 40–50 km	0.099	1.03					
Distance from central Tokyo: 50–70 km	-0.007	-0.05					
Fall	-0.106	-1.80	*	0.031	0.21	0.053	0.43
Year 2013	0.267	4.67	***	0.298	2.11	0.388	3.35
Year 2014	0.925	9.32	***	0.887	3.87	1.141	6.03
Markup ratio	-0.384	-5.33	***	-0.166	-1.13	-0.366	-2.28
Constant	-2.224	-15.60	***	-2.841	-7.00	***	-5.92
Parameter <i>p</i>	0.63 ***			0.65 ***		0.60 ***	
Log-likelihood	-3207.66			-576.77		-814.93	
Number of observations	1546			284		386	

	30–40 km		40–50 km		50–70 km	
	Coeff.	z-value	Coeff.	z-value	Coeff.	z-value
Explanatory variables						
Lot size: less than 50 m ²	0.564	0.93	0.155	0.21		
Lot size: 250 m ² or more	-0.067	-0.36	0.116	0.78	0.940	3.10 ***
Building age: less than 5 years	0.196	0.93	0.041	0.15	0.640	0.98
Building age: 30 years or more	-0.086	-0.78	-0.007	-0.05	0.568	2.13 **
Time to nearest station: less than 10 min	-0.028	-0.25	-0.210	-1.29	-0.436	-1.43
Bus to nearest station	-0.197	-1.05	-0.231	-1.76 *	0.221	0.68
Max. Slope: 10 degrees or more			0.029	0.18	-0.214	-0.89
Proportion of elderlys: 25% or more	-0.052	-0.20	0.269	1.19	0.240	0.63
Detached owner-occupied housing district	0.015	0.12	-0.122	-0.77	-1.475	-4.06 ***
Densely inhabited districts in 1960	0.577	0.57	-0.018	-0.05		
Densely inhabited districts in 2010	-0.129	-0.91	0.058	0.37	-2.205	-2.82 ***
Low-rise residential zones	-0.105	-0.88	0.087	0.59	0.029	0.08
Medium-to-high-rise residential zones	-0.012	-0.07	-0.036	-0.17	1.791	2.20 **
Fall	-0.197	-1.72 *	-0.233	-1.85 *	0.090	0.38
Year 2013	0.184	1.62	0.061	0.47	0.401	1.78 *
Year 2014	0.903	4.60 ***	0.758	3.30 ***	1.003	1.83 *
Markup ratio	-0.496	-3.55 ***	-0.524	-2.95 ***	-1.303	-3.61 ***
Constant	-2.163	-8.94 ***	-1.822	-6.70 ***	-1.311	-2.31 **
Parameter <i>p</i>	0.65 ***		0.61 ***		0.85 **	
Log-likelihood	-832.78		-728.83		-196.46	
Number of observations	419		348		109	

Notes: The dependent variable is hazard λ (probability of sale). Significance level: ***1%, **5%, *10%. The significance level for parameter *p* is based on the Wald test, where the null hypothesis is $\ln(p) = 0$; that is, $p = 1$

Property characteristics	10–20km	20–30km	30–40km	40–50km	50–70km
Lot size: less than 50m ²		*		-	
Lot size: 250m ² or more	-	-		+	+
Building age: less than 5 years	+				
Building age: 30 years or more	+	+			*
Time to nearest station: less than 10 min	+		+		+
Bus to nearest station	-	-	-	-	
Max. slope: 10 degrees or more				-	
Proportion of elderlies: 25% or more		+			
Detached owner-occupied housing district		-	-	-	-
Densely Inhabited Districts in 1960		+		+	
Densely Inhabited Districts in 2010	+	+	+	+	-
Low-rise residential zones				+	+
Medium-to-high-rise residential zones	+		+	+	+
Market demand (relative to supply)	--	-		+	++
	Low				High

Fig. 1.2 Demand–supply relationship for building/locational characteristics in each distance interval from central Tokyo

in Fig. 1.2. Demand relative to supply is high (low) if the price has a positive (negative) premium and/or the TOM reduces (increases). Thus, we showed the degree of demand as “++” (“—”) if both the price and TOM indicated high (low) demands with statistical significance; and “+” (“—”) if either price or TOM showed high (low) demands with statistical significance, while considering the other cases as a reference. In the case wherein the price and TOM indicated demands in opposite directions, the price and TOM reduced; we indicated the state as “*.” The significance level was set at 10%, and the diagonal lines indicate the cases without such samples.

From Tables 1.3 and 1.4 and Fig. 1.2, we first discuss the overall trends and then proceed to the discussion for suburbs close to central Tokyo and for outskirts farther from central Tokyo.

1.4.1 Overall Trends

Overall, relative to the supply, the demand for resale houses is low (high) in areas with typical characteristics of population shrinkage (growth).¹¹ First, strong demand exists in districts with convenient access to the nearest station and/or zones that protect the residential environment. For houses located within 10 min of walking distance to the nearest station, demand was relatively high in almost all distance intervals (10–20, 30–40, and 50–70 km), suggesting that convenient locations

¹¹ For small properties whose lot size is less than 50 m², demand is low within a 40–50 km interval, and price is reduced with a short TOM in an interval 20–30 km away from central Tokyo. For new properties that are less than 5 years old, strong demand exists within 10–20 km from central Tokyo.

sustain demand even on the outskirts farther away from central Tokyo. In the entire Tokyo metropolitan area, Ai (2014, 2016) shows that the population increases in areas located within 500 m of the nearest station; thus, our results suggest that purchasing a resale house may be suitable as an option to live in these convenient locations. In addition, properties in “medium-to-high-rise residential zones” tend to exhibit high demand in each distance interval (10–20 and 30–70 km).

However, the demand tends to be low in each distance interval for properties without convenient access to the nearest station and/or in detached owner-occupied housing districts. For houses that require taking a bus to the nearest station, the demand decreases at almost all distance intervals (20–50 km). Specifically, prices decline within the 20–40 km interval, and TOM increases within the 40–50 km interval.¹² In addition, in detached owner-occupied housing districts, the demand is low in all distance intervals (20–70 km), particularly in those characterized by a long TOM in the 50–70 km interval. This corresponds to a small population influx in areas that lack a variety of building types (Fujii 2008; Miyake et al. 2014).

The tendency of resale houses influencing the renewal of districts varies according to their distance from Tokyo. For properties located in the 1960 DID, demand is relatively high within 20–30 and 40–50 km intervals. For properties located in the DID of 2010, demand was relatively high in 10–50 km intervals, whereas it decreased with increased TOM in the 50–70 km interval. This may be attributed to the fact that the population declines in the newly developed residential districts within 50 km of central Tokyo. Moreover, the population shrinks in the traditional districts on the outskirts, 50 km or farther from central Tokyo (Miyake et al. 2014).

1.4.2 Suburbs Close to Central Tokyo

Demand is strong in the suburbs, relatively close to (within 30 km) central Tokyo. For houses that are 30 years old or older, demand is relatively high within 10–30 km intervals; for properties in aging districts (where the proportion of elderly residents is 25% or more), demand is relatively high, and properties are sold quickly. A potential reason for this strong demand is that, within commutable distance to central Tokyo, young households with children can purchase spacious houses at reasonable prices. This may explain why new residents who have settled in existing residential districts tend to be large households (Yoshida et al. 2007). Another potential reason for purchasing resale houses is to live close to parents within commutable distance from central Tokyo (Nakashima et al. 2011); these areas are likely to be occupied by elderly parents.

¹² There is no such effect beyond 50 km from central Tokyo, possibly because daily life does not rely on public transports.

1.4.3 *Outskirts Farther Away from Central Tokyo*

However, in the outskirts farther away (40 km or greater) from central Tokyo, the demand for potentially disadvantageous properties is low as the population (and number of households) declines. Specifically, houses in detached owner-occupied housing districts and/or those in the 2010 DIDs tended to exhibit an increased TOM in the 50–70 km distance interval. Furthermore, for properties located in inclined districts with a maximum slope of 10 degrees or greater, negative price premiums existed in the 40–50 km interval.

In certain cases, for old properties, the price declined while the TOM became short. Indeed, properties that were 30 years old or older exhibited a shorter TOM with a lower price. Recently, certain owners of vacant houses have found it costly to maintain their property (e.g., due to the holding tax). As reported by Hirayama (2011), the value of homeownership becomes negative unless the owner finds a buyer. Thus, our results suggest that certain owners are motivated to dispose of their property quickly by reducing their prices.

On the outskirts farther away from central Tokyo, where the demand is shrinking, the demanded properties exhibit characteristics that are suitable for the location. In other words, for large houses with lot sizes of 250 m² or greater, demand is low within 10–30 km of central Tokyo, whereas there is a strong demand within 40–70 km of central Tokyo. In particular, in suburbs 40 km or farther from central Tokyo, the reason may be that spacious resale houses are more reasonable to purchase than newly built houses. Furthermore, properties in “low-rise residential zones” attract demands within 40–70 km from central Tokyo, suggesting the zones with nice residential environments result in a population influx. However, these characteristics are typically observed in the low-demand “detached owner-occupied housing districts”; thus, the absolute demand may not be that high.

1.5 Conclusion

This chapter investigated the relationship between building and locational characteristics in the context of population shrinkage in Japan and price and TOM, which are the basic components of real estate markets. It clarified the demand–supply relationship of the resale housing markets in the suburbs of the Tokyo metropolitan area. Overall, relative to the supply, the demand for resale houses was low (high) in areas with typical characteristics of population shrinkage (growth). However, the demand–supply relationship for potentially disadvantageous properties varied according to distance from central Tokyo. Thus, there is a strong demand in the suburbs relatively close to (within 30 km) central Tokyo, even for old houses in areas with a large proportion of elderly residents. However, in the outskirts farther away (more than 40 km) from central Tokyo, houses in the detached owner-occupied

housing area are losing demand, exhibiting an increased TOM, and certain owners may reduce their prices to quickly dispose of their properties.

The results suggest the potential of the suburbs relatively close to central Tokyo, where the resale housing market plays a role in circulating built-up residential areas where old houses and elderly residents are concentrated. In addition to the utilization of vacant properties, resale houses are a new option beyond purchasing costly newly built houses or renting tiny flats. However, the results suggest that in the outskirts farther away from central Tokyo, market demands for resale houses in the detached owner-occupied housing area are limited; thus, these property owners must continue maintenance, utilize them within their neighborhood communities, or utilize them as land after demolishing the building. The results also suggest that certain owners feel that it is costly to maintain vacant houses. An effective strategy may be getting the neighbors to agree to use the land and/or maintain houses before the properties are inherited and owners become unknown to the public.

This chapter conducted a basic analysis to capture the unexplored demand-supply relationship in the resale housing market in the suburbs of Tokyo. It is necessary to understand the market dynamics, including vacant houses that do not enter the resale housing market. Moreover, the reasons behind purchasing resale houses and the characteristics of such households in the suburbs relatively close to central Tokyo must be clarified using survey data of the population influx.

References

- Ai H (2014) How living environment indices effect on population change patterns of local districts. *J City Plan Inst Jpn* 49(3):567–572
- Ai H (2016) Indexing of living environment attracts young and productive age generations. *J City Plan Inst Jpn* 51(3):860–866
- Engelhardt GV (2003) Nominal loss aversion, housing equity constraints, and household mobility: evidence from the United States. *J Urban Econ* 53(1):171–195
- Fujii T (2008) A micro-level analysis on generational changes and district characteristics in the Tokyo metropolitan area. *J Archit Plan* 633:2399–2407
- Fujii T, Oe M (2005) An analysis of the population structure in the Tokyo metropolitan area in terms of generation balance. *J Archit Plan* 593:123–130
- Fujii T, Oe M (2006) A study on generational changes in the suburbs of the Tokyo metropolitan area: a comparative analysis from 1980 to 2020 among cohorts by GBI. *J Archit Plan* 605:101–108
- Genesove D, Mayer C (2001) Loss aversion and seller behavior: evidence from the housing market. *Q J Econ* 116(4):1233–1260
- Genesove D, Mayer CJ (1997) Equity and time to sale in the real estate market. *Am Econ Rev* 87(3):255–269
- Han L, Strange WC (2015) The microstructure of housing markets: search, bargaining, and brokerage. In: Duranton G, Henderson JV, Strange WC (eds) *Handbook of regional and urban economics*, vol 5B. Elsevier, Amsterdam, pp 813–886
- Hasegawa H (2005) Study on changes of small lots and houses in suburban detached houses estates built in mass-housing period: part 2, case study in Moroyama town, Saitama, Tokyo metropolitan area. *Proceedings of the Architectural Institute of Japan (F-1)*, pp 1545–1546
- Hirayama Y (2011) *Urban conditions: housing, life, and sustainability*. NTT Publishing, Tokyo

- Ito S, Kaido K (2013) The transformation of the spatial uses of vacant houses and vacant lots and the demographic structures of the residences in suburban housing estates. *J City Plan Inst Jpn* 48(3):999–1004
- Ministry of Land, Infrastructure, Transport and Tourism (2017) Housing economics data: change in the share of used houses in the housing transactions. http://www.mlit.go.jp/statistics/details/t-jutaku-2_tk_000002.html. Accessed 3 Aug 2017
- Miyake R, Koizumi H, Okata J (2014) Research on the distribution of the households-decreasing districts and district characteristics in the Tokyo metropolitan area. *J City Plan Inst Jpn* 49(3):1029–1034
- Nakashima T, Ito N, Lee YG, Tsukuda H, Otsuki T (2011) Analysis of real-estate transaction in “new town” in local city over 30 years for depopulation and aging society. Proceedings of the Architectural Institute of Japan (F-1), pp 69–72
- Ong SE, Koh YC (2000) Time on-market and price trade-offs in high-rise housing sub-markets. *Urban Stud* 37(11):2057–2071
- Piazzesi M, Schneider M, Stroebel J (2020) Segmented housing search. *Am Econ Rev* 110(3):720–759
- Sakamoto K, Yokohari M (2016) Dynamic characteristics of emerging vacant houses and abandoned lands in residential neighborhoods. *J City Plan Inst Jpn* 51(3):854–859
- Shimizu C, Nishimura KG, Asami Y (2004) Search and vacancy costs in the Tokyo housing market: attempt to measure social costs of imperfect information. *Rev Urban Reg Dev Stud* 16(3):210–230
- Todoroki O (2011) A basic study on the trends of the mortgaged real estate market at the city planning area. *J City Plan Inst Jpn* 46(3):565–570
- Ujihara T, Abe H, Murata N, Washio N (2016b) Reality of “spongy urban area” in local city: based on situation of development and loss, vacant house. *J Jpn Soc Civ Eng D3* 72(1):62–72
- Ujihara T, Abe H, Nonaka S (2016a) Reality of spongy urban area based on state analysis of residential districts. *J City Plan Inst Jpn* 51(3):466–473
- Ujihara T, Taniguchi M, Matsunaka R (2006) The reality of urban retreat: reverse sprawl and its relation with residential zone types. *J City Plan Inst Jpn* 41(3):977–982
- Umeda N, Hirayama Y (2002) Crisis in the home ownership system? The spatial distribution of the financially troubled property in Kobe. *Proc Archit Inst Jpn (Kinki)* 42:841–844
- Yamanshita S, Morimoto A (2015) Study on occurrence pattern of the vacant houses in the local hub city. *J City Plan Inst Jpn* 50(3):932–937
- Yavas A, Yang S (1995) The strategic role of listing price in marketing real estate: theory and evidence. *Real Estate Econ* 23(3):347–368
- Yoshida T, Koyama Y, Hasegawa H (2007) Characteristics of householders newly moving in suburban neighborhood districts of detached houses. *J City Plan Inst Jpn* 42(3):703–708

Chapter 2

Old Condominiums and Their Tendency to Be Rebuilt: A Case Study of the Tokyo Metropolitan Area



Hiroki Baba, Chihiro Shimizu, and Yasushi Asami

Abstract Condominiums are important housing stock in Japan, but they often need to be rebuilt. This research investigates the factors and spatial distribution of condominium rebuilding. To this end, data on rebuilt condominiums was integrated with data on old condominiums defined as the ones with old earthquake resistance standards. Using a probit model, the tendency of certain factors to contribute to rebuilding was assessed. Findings reveal that building age, land area, distance to the city center, number of housing units, and floor area possible for expansion are statistically significant, which is consistent with the findings of previous studies on the qualitative analysis of condominium rebuilding in Japan. When the marginal effects of the factors were calculated, a four-year increase in the average building age, for instance, increases the probability of rebuilding by 1.49 percentage point. We also confirmed that condominiums with high rebuild probability are concentrated in the western part of central Tokyo and are also likely to exist in suburban areas.

Keywords Condominium · Rebuilding · Real estate · Probit model · Spatial distribution · Floor area ratio

The contents of this paper are based on the following paper originally published in a Japanese journal: Baba, H., Shimizu, C., Asami, Y. (2020) Factors and spatial distribution of rebuilding of old condominium: Case study of Tokyo metropolitan area. Journal of City Planning Institute of Japan 55(3): 1143–1150 (in Japanese).

H. Baba (✉) · C. Shimizu
Graduate School of Social Data Science, Hitotsubashi University, Tokyo, Japan
e-mail: h.baba@r.hit-u.ac.jp

Y. Asami
Department of Urban Engineering, The University of Tokyo, Tokyo, Japan

2.1 Introduction

2.1.1 Background and Research Aim

Condominiums are important housing stock in Japan, with an estimated 6.5 million units as of the end of 2018 (MLIT n.d.-a). Demand for this type of housing increases as urban agglomeration intensifies (Rosen and Walks 2013). Once a building is supplied, it deteriorates and should be ultimately rebuilt, but demolition and rebuilding are more difficult than that for detached housing (Saito and Hasegawa 2001). Condominiums have multiple owners, which raises various issues such as rebuilding consensus and handling of mortgage (Hasegawa 1999). Therefore, it is not simple to renew condominiums, and they might be left as they are, even if they deteriorate or become mismanaged in the future (Asami and Saito 2019). To deal with this problem, Baba (2020) constructed a database of condominiums from private company data and visualized the geographical distribution of aging condominiums, but it is not clear to what extent rebuilding is realistic.

Condominiums are generally durable goods, and it is difficult to make elastic quantity adjustments for future population increase and decrease (Glaeser and Gyourko 2005). Nevertheless, it is natural to rebuild condominiums to some degree when real estate property values rise significantly in areas of excess demand. Nevertheless, in Japan, as rebuilding requires the agreement of 80 percent of unit owners and eviction of tenants, the number of condominiums that have been completed or are undergoing rebuilding as of April 2019 is merely 267 (MLIT n.d.-b). Therefore, although previous studies have chosen case studies of rebuilt condominiums (Hasegawa 1999), establishing general trends is a challenging task.

This study focuses on old condominiums, defined as the ones with old earthquake resistance standards,¹ and examines the trends in rebuilding factors and the spatial distribution of rebuilding probability. Specifically, We examine the difference between existing condominiums with old earthquake resistance standards and those that have been rebuilt, and analyze the difference in trends using a probit model. In particular, the rebuilding issue is associated with the economic load of the unit owners (Tanaka and Kumata 1999). Therefore, We considered variables such as the size of land area, floor area, and expandable floor area by rebuilding. In addition, after estimating the probability of rebuilding, We demonstrated the spatial distribution of grid cells that are (or are not) expected to be rebuilt.

The target area in this study is the Tokyo metropolitan area (Tokyo, Saitama, Chiba, and Kanagawa Prefectures), where old condominiums have been supplied since early stages (Fig. 2.1). Given that approximately 60.6% of the rebuilt condominiums across Japan exist here, this area is suitable for analyzing the

¹ Condominiums with old earthquake resistance standards refer to the ones whose building permit was approved by May 1981. This is because a new earthquake resistance standard had been implemented in June 1981. In this study, considering the period of construction, condominiums completed before 1982 were used as the data for analysis.

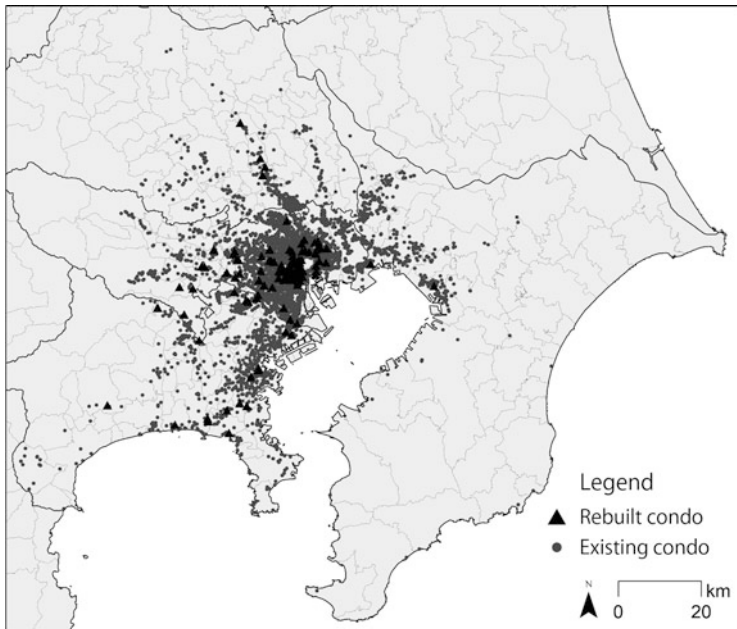


Fig. 2.1 Geographical location of rebuilt and existing condominiums with old earthquake resistance standards in the Tokyo metropolitan region

trend of rebuilding through market mechanisms. Condominiums here that have old earthquake resistance standards are being actively considered for rebuilding due to aging and seismic performance issues.

2.1.2 Current Situation of Rebuilding Condominiums

With the advent of condominiums, the housing system enables us to build dense urban areas (Rosen and Walks 2015). Particularly in areas where housing demand is high, such as Hong Kong and Singapore, most people live in either condominium or apartment housing. Despite their necessity and amenity, condominiums face many challenges. In Hong Kong, during the redevelopment of residential high-rise neighborhoods, private developers struggled with absent housing owners (Yau and Ling Chan 2008). In Singapore, the owners could not reach a consensus on the sale of sites in areas with high development potential, and the government amended the law to allow sale with 80% consensus (Sim et al. 2002). In the case of the Gold Coast, where more than 50% of the condominiums are more than 30 years old, the cityscape of the area is degraded due to aging condominiums and the difficulty of updating the area (Warnken et al. 2003). Even in Toronto, Canada, condominium neighborhoods sometimes face an anticommons problem (Webb and

Webber 2017). Lastly in Japan, while an oversupply of new condominiums is being built, the accumulation of old condominiums has become a problem (Baba 2020; Ronald and Hirayama 2006). Aging is one of the keywords considering future condominium issues, and it is appropriate to target Japanese cities for analysis as many condominiums are already old.

In Japan, previous research has focused on the aging of condominiums and the difficulties of rebuilding, including the development of a legal framework, land constraints, and consensus building in management associations (e.g., Asami et al. 2012). The pioneering work on the issue of condominium rebuilding is conducted by Takamizawa and Go (1989), where the authors anticipate that the issue of condominium rebuilding will arise in the future, and proposed that the possibility of floor space increase, location, and the floor area per unit are important factors. Hasegawa (1999) analyzed cases where reconstruction was completed at an early stage, and he identified rebuilding factors such as floor area ratio, location, the amount of self-pay burden for owners, and the number of owners. Thus, some of the rebuilding factors include the physical characteristics and location of the condominium.

Consensus building of the management association is another important factor for rebuilding. Previous studies have been conducted in this regard, including one that discusses optimal consensus building requirements from the perspective of the rebuilding benefits (Asami 2009), one that enumerates the consensus building process and describes its characteristics (Saito and Hasegawa 2001), and one that ranks the consensus building capacity of management associations (Saito et al. 1999). Although these discussions offer important findings for promoting condominium rebuilding, they do not fully consider factors that indicate the potential for physical reconstruction, such as the possibility of floor area increase, location, and floor area per unit, as advocated by Takamizawa and Go (1989) and Hasegawa (1999). This may be attributed to the fact that there are only a few examples of condominium rebuilding in Japan.

Recent increases in condominium rebuilding enable researchers to conduct quantitative analysis of their physical characteristics. For instance, Hanazato (2017) used discriminant analysis to show the difference in trend between two groups: rebuilds and massive renovations. Although the author revealed the limited nature of successful rebuilds, they cannot be representative of older condominiums as a whole, as the control group (massive renovation group) consisted of 47 cases. Therefore, although quantitative analysis of the potential for condominium rebuilding provides useful insights into what types of old condominiums are suitable for future rebuilding, previous studies have not collected sufficient number of the samples.

Considering the previous studies above, this study has the following originalities. First, this study covers most of the condominiums with old earthquake resistance standards, enabling a more general discussion of condominium rebuilding. Second, this study explicitly introduces physical characteristics such as the possibility of floor area increase and location into a model, which have been difficult to deal with in previous studies. Third, using the regression results, this study identifies areas where condominium rebuilding is likely to occur in the future and areas where condominiums are likely to remain unmaintained.

2.2 Data and Method

2.2.1 Data

We used the data on condominiums completed before 1982 by the Real Estate Economic Institute, Co., Ltd.² regarding the characteristics of condominiums. This is because a new earthquake resistance standard had been implemented in June 1981. Property data had been collected between 1967 and 1982, containing a variety of information associated with building and location characteristics. Pieces of information for this analysis were extracted and used as variables: property name, location, site area, total floor area, number of floors, total number of units, year of completion, and average private floor area per unit. The average private floor area per unit was categorized into single occupancy (-40 m^2), two-person household ($40\text{--}55\text{ m}^2$), and family (55-m^2), referring to the guideline floor area levels described in the Basic Plan for Housing and Living Standards (MLIT n.d.-c). This is because data representing a range of floor area exist for each property and cannot be expressed as an interval scale. Note that as the condominium data in this study is a compilation of information on sales, there may be multiple rows of data for the same property depending on the time of release. Therefore, all data were sorted by property name to avoid duplicate use of data.

We used 462,635 housing unit samples on condominiums with old earthquake resistance standards. Before analysis, it is necessary to consider whether these samples are representative of all the condominiums. According to the statistics issued by MLIT (n.d.-a), the national stock of condominiums with old earthquake resistance standards is approximately 1.03 million units, and Baba (2020) illustrated that approximately 56.8% of these units are located in Tokyo and three prefectures. However, the government statistics refers to the number of condominiums based on confirmation of the building code, including properties that were never built, so it might lead to an overcount of the number of condominium units. Although the data used in this study are approximately 20% less than the value presented by the government statistics, it is considered to be within a sufficient range to measure statistical properties.³

The reconstruction data were extracted from the cases published by the Urban Renewal Association of Japan for Tokyo, Chiba, Saitama, and Kanagawa prefectures.⁴ Of the 157 reconstruction cases in Tokyo and three prefectures, 114 were selected as the sample for analysis. We considered the case of overlap with data for condominiums with old earthquake resistance standards and reconstructed condominiums, and the 14 duplicate property names were then removed.

² <https://www.fudousankeizai.co.jp/publicationCateList?cateId=8&id=52>.

³ As listwise deletion is performed for missing variables, the sample size is smaller than above. However, given the large sample size, this should not be a problem when analyzing statistical trends.

⁴ <http://m-saisei.info/index.html>.

In addition to the condominium data, data related to the surrounding environment and land use regulations were also added. Specifically, distance to the city center,⁵ distance to the nearest station, and land use zoning were measured from the National Land Numerical Information.⁶ The land use zoning was broadly classified into exclusively residential, residential, commercial, and industrial areas. It is true that introducing land price into a model is effective for increasing the explanatory power, but the land price would explain most location factors as an important proxy for the economic value of condominiums. Therefore, land price value and location may face the problem of multicollinearity. As this study focuses on the predictive spatial distribution of condominium rebuilding, the location factors supersede the land price. This study thus proceeded with the analysis assuming that the land price is controlled by location variables such as distance to the nearest station, distance to the city center, and land use zoning dummies.

We generated data of floor area available for expansion considering both regulations designated by land use zoning and by the width of the road frontage. The land use zoning was judged by overlaying zoning polygons from the National Land Numerical Information. When considering the regulation by the width of the road frontage, the entire road width was estimated from the road centerline line data provided by the Conservation GIS-consortium Japan.⁷ Road widths were classified as -3.0 m, 3.0–5.5 m, 5.5–13.0 m, 13.0–19.5 m, and 19.5-m, the maximum floor area ratio was calculated using road widths of 3.00 m, 4.25 m, 9.25 m, 16.25 m, and 20.00 m, respectively, for convenience. Although the range of road width thresholds appears to be wide, most cases where the standard floor area ratio is restricted are narrow roads with road widths of 4 m or less in Japan. As the road frontage could not be identified from the building point data, the width of the road frontage was calculated as an approximation. Specifically, assuming a square site area of am^2 , for the road edge overlapped with a circle whose radius is the distance $\sqrt{2a}/2m$ from the building center point to the farthest building edge, We adopted the widest road as the width of the road frontage. Finally, We compared the maximum floor area ratios by both land use zoning and the regulation by the width of the road frontage, and the smaller one was defined as the floor area ratio available for expansion.

To remove outliers from the dataset, preprocessing was then performed in the following steps. First, We omitted properties whose latitude and longitude were not identified to the street level using the geocoder provided by the University of

⁵ If the city center is defined by a single point such as Tokyo Station, municipalities in the western part of Tokyo may be overmeasured. Therefore, the definition of the city center is based on the following assumptions: the distance to the city center is measured as 0 m if the location is in the six central wards of Tokyo (Chiyoda, Chuo-ku, Minato-ku, Shinjuku, Bunkyo-ku, and Shibuya-ku); otherwise, the minimum distance to five stations with a large number of passengers on the Yamanote Line (Shinjuku, Ikebukuro, Tokyo, Shinagawa, and Shibuya stations) is measured.

⁶ <https://nlftp.mlit.go.jp/ksj/>.

⁷ <http://cgisj.jp>. Note that this data was generated based on the Numerical Map 2500 provided by the Geospatial Information Authority of Japan (GSI) and is not a basic survey result.

Table 2.1 Descriptive statistics

Variable	Unit	Mean	S.D.	Min.	Median	Max.
Land area	1000 m ²	2.178	5.956	0.100	0.881	149.983
Total floor area	1000 m ²	4.710	7.762	0.128	2.716	170.502
Number of stories	Story	7.148	2.745	2	7	25
Number of housing units	Unit	66.182	100.733	4	40	2233
Building age as of 2020	Year	43.551	4.258	38	42	93
Dummy on single layout	–	0.180	0.384	0	0	1
Dummy on two-person layout	–	0.327	0.469	0	0	1
Dummy on family layout	–	0.493	0.500	0	0	1
Distance to the nearest station	1000 m	0.447	0.409	0.013	0.331	7.971
Distance to the city center	1000 m	10.081	11.347	0.000	6.252	79.275
Dummy on exclusively residential land use	–	0.250	0.433	0	0	1
Dummy on residential land use	–	0.228	0.419	0	0	1
Dummy on commercial land use	–	0.392	0.488	0	0	1
Dummy on industrial land use	–	0.131	0.337	0	0	1
Floor area ratio	%	277.336	142.804	60	200	800
Observation		5821				

Tokyo,⁸ properties whose year of completion was after 1983, and properties whose site area or total floor space was less than 100m². In addition, We performed listwise deletion, by which properties with at least one of the variables missing were omitted. As a result, 5821 samples were obtained. The descriptive statistics of the data is shown in Table 2.1.

2.2.2 Method

First, the floor area available for expansion, add_floor_i, is calculated in a simplified manner as follows.

$$\text{addfloor}_i = (\text{FAR}_i^{\max} - \text{FAR}_i^{\text{use}}) \text{ lotsize}_i \quad (2.1)$$

where FAR_i^{max} represents the maximum floor area ratio considering the land use and the building code regulations, FAR_i^{use} represents the current floor area ratio, and lot_size_i represents the land area. Equation (2.1) indicates the extent of floor area that can be increased by rebuilding, which can be an indicator related to the financial burden for owners at the time of rebuilding. During the analysis, to identify spatial

⁸ <https://geocode.csis.u-tokyo.ac.jp/geocode-cgi/geocode.cgi?action=start>.

trends in floor area available for expansion, We visualized the floor area divided by the total number of units per municipality.

A probit model was then used to analyze the characteristics of rebuilt condominiums. The model is often used where the variables are on a nominal or ordinal scale and has been applied to various analysis targets, such as occupant satisfaction evaluation (Choi and Asami 2004) and analysis of trends in rebuilding when the building code regulations are tightened (Hanazato 2017). The model in this study used the status of a condominium with old earthquake resistance standard i as a binary explained variable, that is, whether the condominium i is rebuilt or not. The rebuilding choice of the stakeholders (e.g., condominium management association) of the condominium i is denoted as y_i , and $y_i = 1$ is defined as rebuilding, and $y_i = 0$ is otherwise. In the model, the dependent variable for the potential preference y_i^* behind the choice can be expressed linearly with J variables:

$$y_i^* = \alpha + \beta \mathbf{x}'_i + u_i \quad (2.2)$$

where α is the parameter, β is the $1 \times J$ parameter vector, \mathbf{x}_i is the i -th $1 \times J$ variable vector, and u_i is the error term. Now assume that the choice to rebuild is taken when the potential preference is greater than 0 and not to rebuild when it is less than 0. Given the probability when $y_i = 1$:

$$\Pr(y_i = 1) = \Pr(y_i^* > 0) = \Pr(-(\alpha + \beta \mathbf{x}'_i) < u_i) \quad (2.3)$$

Assuming that u_i is standard normal distribution, $\Pr(\bullet)$ can be expressed in terms of the cumulative distribution function, so let $F(\bullet)$ be the cumulative density function⁹:

$$\Pr(y_i^* > 0) = 1 - F(-(\alpha + \beta \mathbf{x}'_i)) = F(\alpha + \beta \mathbf{x}'_i) \quad (2.4)$$

In the case of no rebuilding ($y_i = 0$), it can be expressed as:

$$\Pr(y_i^* \leq 0) = 1 - F(\alpha + \beta \mathbf{x}'_i) \quad (2.5)$$

For more details on this model, please see Wooldridge (2016).¹⁰

The explanatory variables include the ones related to possibility of floor area increase, building characteristics, and location, according to previous studies. Therefore, We added land area, number of housing units, number of stories, floor

⁹ The cumulative density function of the standard normal distribution can be identified as $F(\alpha + \beta \mathbf{x}'_i) = \int_{-\infty}^{\alpha + \beta \mathbf{x}'_i} \frac{1}{\sqrt{2\pi}} \exp\left(-\frac{y^2}{2}\right) dy$.

¹⁰ Parameter estimation is performed by the maximum likelihood method. The likelihood function $L(\alpha, \beta) = \prod_{m=1}^{N_1} F(\alpha + \beta \mathbf{x}'_i) \prod_{n=1}^{N_2} (1 - F(\alpha + \beta \mathbf{x}'_i))$ where N_1 is the sum of condominium owners that choose to rebuild and N_2 that do not, and the sum of both is the number of observations. The parameters, α, β , are estimated by maximizing the likelihood function.

layout dummies, total floor area, and floor area available for expansion. Moreover, distances to the nearest station and to the city center are important variables describing the location characteristics of condominiums, and land use zoning is also considered an important indicator of the location, so these variables were also added. Moreover, the building age was also added as it correlates with the physical aging of the condominium, which is directly related to the likelihood of rebuilding.

2.3 Results

2.3.1 Geographic Distribution of Floor Area Available for Expansion

Figure 2.2 shows the total sum of the floor area available for expansion by municipality, and Fig. 2.3 shows the average values of the floor area available for expansion divided by the number of housing units. The former allows us to consider the potentiality of future development, whereas the latter represents the extent of rebuilding incentive for condominium owners. By observing both figures, the following findings were obtained.

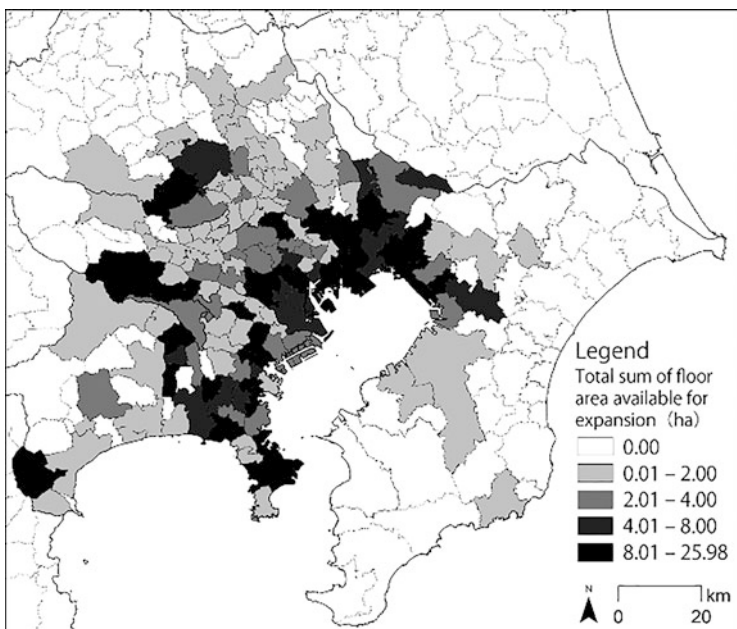


Fig. 2.2 Geographical distribution of the total sum of floor area available for expansion by municipality

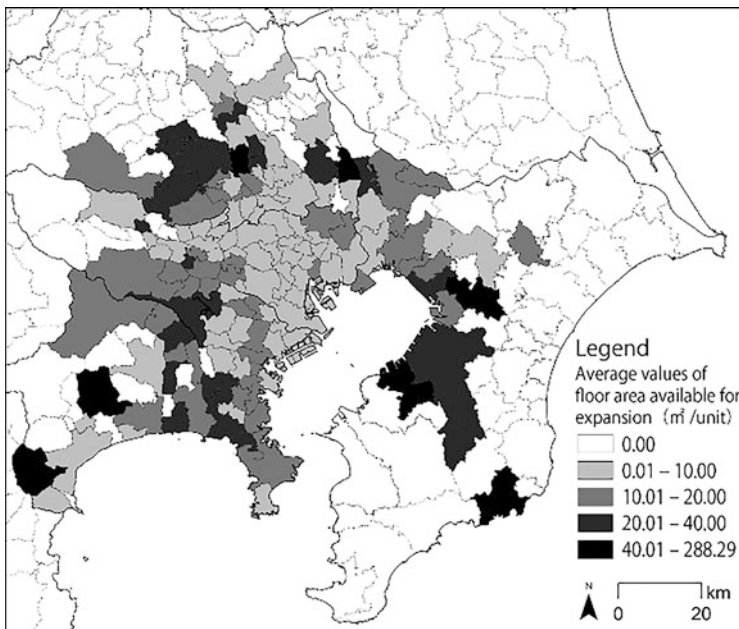


Fig. 2.3 Geographical distribution of average values of floor area available for expansion by municipality

First, the total floor area available for expansion is high in both eastern parts (e.g., Sumida and Edogawa wards) and western parts (e.g., Shibuya ward) of central Tokyo, and it is low in the southern part of Saitama prefecture. However, the average floor area available for expansion tended to be higher in the suburban areas of the Tokyo metropolitan area such as Sodegaura, Yoshikawa, and Hadano Cities, and lower in the central Tokyo area. This suggests that although there is room for development based on the total floor area available for expansion in central Tokyo, it is difficult for the owners of condominiums to benefit from floor space expansion. In suburban areas, the total sum of the floor area available for expansion is estimated to be low, but the floor area available for expansion per housing unit is large because there is a surplus land area for condominiums. Nevertheless, there is not a one-size-fits-all decision as to whether rebuilding is better than new development in the surrounding area, considering the costs of demolition and redevelopment.

2.3.2 Difference in Averaged Characteristics Values of Condominiums with Old Earthquake Resistance Standards and Rebuilt Ones

Rebuilt condominiums were compared to existing condominiums with old earthquake resistance standards using averaged characteristics as an indicator (Table 2.2). The results showed that the rebuilt condominiums had a relatively larger land area, lower number of stories, larger total number of housing units, and older building age. Furthermore, the distance to the nearest station was significantly closer for the rebuilt condominiums, whereas the distance to the city center was not significant. In addition, the floor area available for expansion per unit was found to be significantly larger for the rebuilt condominiums. Thus, although the number of rebuilt condominiums is relatively small, the results support the observations of previous studies. In particular, land area and floor area available for expansion per unit were approximately 2.4 times and 7.3 times larger, respectively, which is likely to be an important factor for condominium rebuilding. Nonetheless, we cannot deny the correlation and confounding among variables. For example, the assumption is that apartments located closer to the city center tend to be closer to the nearest train station. Therefore, We conducted a regression analysis using a probit model that considers the correlation of the explanatory variables in the next subsection.

2.3.3 Statistical Difference Between Condominiums with Old Earthquake Resistance Standards and the Rebuilt Ones

The characteristics of the rebuilt condominiums were analyzed using a probit model (Table 2.3). The results revealed the following points.

First, land area was positively correlated with the probability of rebuilding, while the number of stories was negatively correlated with the probability of rebuilding. These results imply that rebuilding occurs in condominiums with large sites and originally low-rise buildings. The condominiums planned and completed by the Japan Housing Corporation (now the Urban Renaissance Agency) are representative of such cases of rebuilding. Second, a significant negative correlation was found between the probability of rebuilding and the number of housing units. Assuming that there is one owner per unit, this could mean that rebuilding occurs in areas where the number of owners is small, which supports the results of previous studies (Asami et al. 2012). Furthermore, there was a weak positive correlation between the probability of rebuilding and the floor layout dummy. This was only for two-person households. Although the trend was not strong, the two-person household layout may be more likely to be rebuilt to accommodate for the demand to rent single-person households and buy family households. It is also conceivable that housing styles have changed over time. Although housing units of about 50 m² were sold for families in the 1970s, demand for small family-oriented units is thought

Table 2.2 Difference between the average values of condominiums with old earthquake resistance standards and those that were rebuilt

Variable	Unit	Mean		Standard error		Difference with statistical significance
		Rebuilding Yes	No	Rebuilding Yes	No	
Land area	1000 m ²	5.14	2.12	9.54	5.85	-3.29 Diff > 0 ***
Number of stories	Story	5.92	7.17	2.38	2.75	5.44 Diff < 0 ***
Number of housing units	Unit	86.65	65.79	103.55	100.65	-2.08 Diff > 0 *
Building age as of 2020	Year	54.69	43.34	11.66	3.67	-10.15 Diff > 0 ***
Dummy on single layout	-	0.23	0.18	0.42	0.38	-1.23
Dummy on two-person layout	-	0.37	0.33	0.05	0.01	-0.88
Dummy on family layout	-	0.40	0.50	0.05	0.01	1.92 Diff < 0 *
Distance to the nearest station	1000 m	0.40	0.45	0.03	0.01	1.53 Diff < 0 †
Distance to the city center	1000 m	8.94	10.10	1.17	0.15	0.98
Dummy on exclusively residential land use	-	0.30	0.25	0.04	0.01	-1.21
Dummy on residential land use	-	0.26	0.23	0.04	0.01	-0.70
Dummy on commercial land use	-	0.38	0.39	0.05	0.01	0.34
Dummy on industrial land use	-	0.06	0.13	0.02	0.00	2.83 Diff < 0 **
Floor area available for expansion	m ² /unit	54.69	7.52	8.78	0.34	-5.37 Diff > 0 ***

Notes: Statistical significance ***0.1%, **5%, †1%; observation: rebuilt condo = 109, existing condo = 5712; diff = mean(rebuilt)-mean(existing)

Table 2.3 Statistical trend of rebuilt condominiums

Variable	Estimation result			
	Coeff.	Robust S.E.	Standardized Coeff.	<i>z</i> -value
Ln(land area)	0.520	0.132	0.549	3.94 ***
Ln(number of stories)	-0.458	0.198	-0.181	-2.32 *
Ln(number of housing units)	-0.345	0.139	-0.291	-2.48 *
Ln(building age as of 2020)	6.446	0.528	0.579	12.20 ***
Dummy on two-person layout	0.312	0.170	0.146	1.84 †
Dummy on family layout	-0.018	0.178	-0.009	-0.10
Ln(distance to the nearest station)	-0.037	0.073	-0.032	-0.51
Ln(distance to the city center)	-0.061	0.014	-0.236	-4.35 ***
Dummy on exclusively residential land use	-0.352	0.233	-0.152	-1.51
Dummy on residential land use	0.233	0.220	0.098	1.06
Dummy on commercial land use	0.578	0.217	0.282	2.66 **
Ln(floor area available for expansion)	0.211	0.044	0.290	4.85 ***
Observation	5821			
Wald χ^2	248.54***			
Pseudo R^2 (McFadden)	0.470			

Notes: Statistical significance ***0.1%, **1%, *5%, †10%; Coeff. = Coefficient, S.E. = Standard Error

to have declined. Finally, the probability of rebuilding was significantly positively correlated with the floor area available for expansion per unit. This result is in line with previous studies (Hasegawa 1999; Takamizawa and Go 1989) and is confirmed here quantitatively.

Unlike the discussion in the previous subsection, the probability of rebuilding was not correlated with distance to the nearest station, whereas distance to the city center was significantly negatively correlated. This result indicates that rebuilding occurs when proximity to the city center takes precedence over neighborhood convenience. Furthermore, the probability of rebuilding was positively correlated with the commercial land use dummy. This implies that reaching a consensus with neighbors in commercial areas is less difficult than in residential areas. In other words, this trend could be caused by the cost of seeking a building consensus with neighbors as oppositional movements occur when a massive condominium is built in residential areas.

Comparing each factor with standardized coefficient values, the absolute values of the coefficients are larger in the order of building age, land area, number of housing units, floor area available for expansion, commercial land use dummy, distance to the city center, and number of stories. This shows that the aging of the condominiums is not only linked to rebuilding, but the possibility of floor area increase has a relatively large effect on condominium rebuilding.

In general, the above results quantitatively confirm the effects of physical rebuilding factors, including the floor area available for expansion, location, and building size, as argued by Takamizawa and Go (1989) and Hasegawa (1999). The only exception is that the influence of floor layout is not necessarily strong, and rebuilding is explained primarily by building age, size, room for floor area expansion, and location to the city center.

Having interpreted general trends, We then analyzed changes in the probability of rebuilding when the average characteristics of condominiums were varied. Specifically, We looked at what change is assumed when the standardized explanatory variables are increased in the 1σ range, and the average marginal probability effect (AMPE) was used to quantify the change.¹¹

Observing AMPEs (Table 2.4), the increase in the probability of rebuilding was positively correlated with building age, land area, commercial land use dummy, and floor area available for expansion, while it was significantly negatively correlated with the number of stories, number of housing units, and distance to the city center. This is similar to the trend of the coefficients in the model of estimation results. We also examined the specific change in the probability of rebuilding, that is, the extent of the AMPE. To illustrate the interpretation in terms of building age, if We compare a condominium that is approximately 44 years old with one that is 48 years old, the probability of rebuilding is 1.49 percentage points higher for the 48-year-old condominium. The most influential variables are the building's age, land area, floor area available for expansion, number of housing units, and distance to the city center. The first three aforementioned factors increase the probability of rebuilding by 1.49, 1.42, and 0.75 percentage points, respectively, and the latter two decrease the probability of rebuilding by 0.75 and 0.61 percentage points, respectively. However, note that this is a marginal probability effect for the average of the observed values, and the marginal effect for each observation should be calculated one by one.

2.3.4 Geographical Distribution of the Predictive Probability of Rebuilding

Taking advantage of the probit model that was used in the previous subsection, We calculated the predictive probability of rebuilding and estimated the total floor area in areas with a high or low probability of condominium rebuilding. The geographical unit is an approximately 1 km^2 grid cell, which can indicate location trends in more detail than municipal units.

¹¹ Average marginal probability effects can be expressed by $\text{AMPE}_j = \frac{1}{n} \sum_{i=1}^N \frac{\partial \Pr(y_i|\mathbf{x})}{\partial x_{ij}} = \frac{1}{n} \sum_{i=1}^N F'(\boldsymbol{\beta}'\mathbf{x}'_i) \beta_j$ when we want to see the effect of the j th explanatory variable x_{ij} on the i -th observed value. Here, N is the number of observations and $F'(\bullet)$ is the derivative of the cumulative density function.

Table 2.4 AMPE of each characteristic

Variable	Average marginal probability effect		Mean	S.D.	Unit
	AMPE	S.E. (Delta method)			
Ln (land area)	0.0142	0.004	***	2178	5956 m ²
Ln (number of stories)	-0.0047	0.002	*	7.15	2.75 Story
Ln (number of housing units)	-0.0075	0.003	*	66.18	100.73 Unit
Ln (building age as of 2020)	0.0149	0.001	***	43.55	4.26 Year
Dummy on two-person layout	0.0038	0.002	†	0.33	0.47 –
Dummy on family layout	-0.0002	0.002		0.49	0.50 –
Ln (distance to the nearest station)	-0.0008	0.002		446.51	409.35 m
Ln (distance to the city center)	-0.0061	0.001	***	10,081	11,347 m
Dummy on exclusively residential land use	-0.0039	0.003		0.25	0.43 –
Dummy on residential land use	0.0025	0.002		0.23	0.42 –
Dummy on commercial land use	0.0073	0.003	*	0.39	0.49 –
Ln (floor area available for expansion)	0.0075	0.002	***	8.41	29.21 m ²
Observation					
Wald χ^2					
Pseudo R^2 (McFadden)					

Notes: Statistical significance ***0.1%, **1%, *5%, †10%; S.E. = Standard Error, S.D. = Standard Deviation; AMPE = Average Marginal Probability Effect; All the variables are standardized for measuring AMPE.; Means and S.Ds are modified from logarithmic values

Figure 2.4 represents the number of rebuilt condominiums when the entire sample is divided into 10 equal parts, with the range of predictive probability of rebuilding on the horizontal axis. The average predictive probability for condominiums with old earthquake resistance standards is about 1.88%, and the predictive probability for the bottom 80% is less than 1%. It is likely that condominium rebuilding occurs when the predictive probability of rebuilding is low due to factors other than physical characteristics, such as the ability of the management association to form a consensus and the presence of troublesome tenants. Furthermore, cases of reconstruction due to exogenous shocks, such as the designation of urban redevelopment promotion zones and seismic disguises, are also difficult to predict with this model. Nevertheless, given that approximately 83% of all reconstruction cases are included in the top 10% sample, the accuracy of the model is still guaranteed at a certain level.

We observed the geographical distribution of the total floor area in the top 10% of the predictive probability of rebuilding (Fig. 2.5). On the one hand, the condominiums

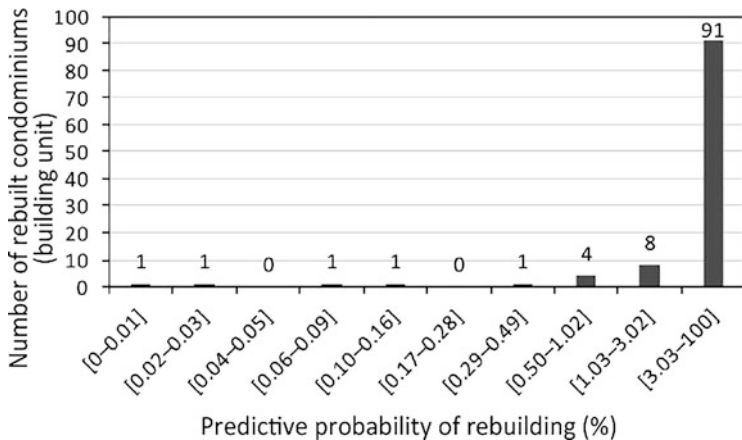


Fig. 2.4 Relationship between the number of rebuilt condominiums and the predictive probability of rebuilding (All samples are divided into 10 equal parts)

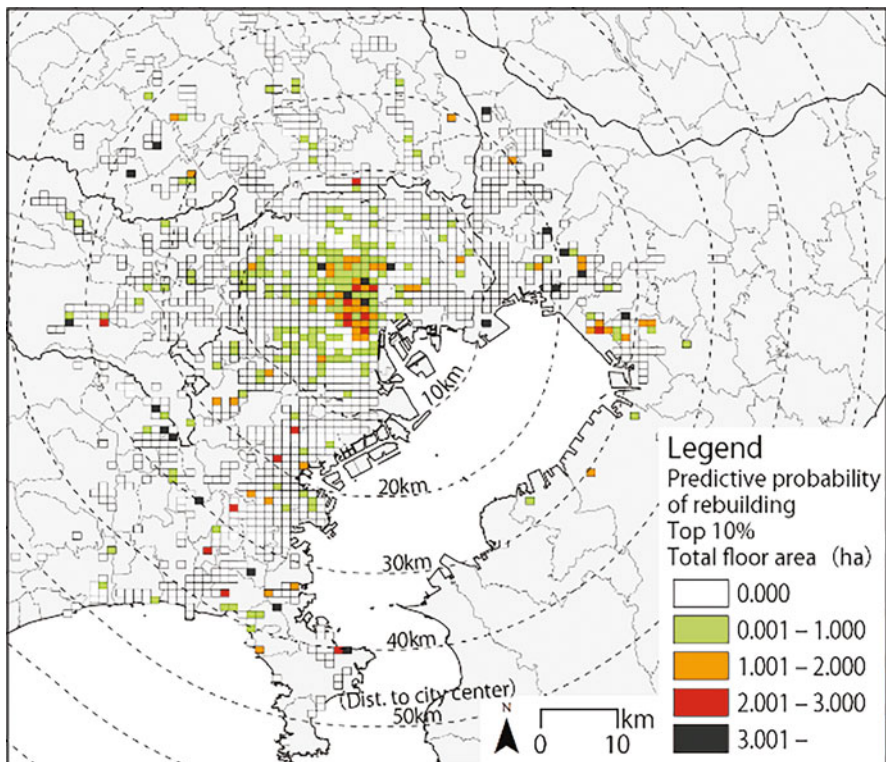


Fig. 2.5 Geographical distribution of total floor area in the top 10% of predictive probability of rebuilding

ums with a high probability of rebuilding are concentrated in Minato, Shibuya, and Shinjuku wards, indicating that the possibility of rebuilding is high in the central and western parts of the central Tokyo. On the other hand, even in the suburban areas 20–30 km away from the city center, there are grid cells of condominiums with a large total floor area. It is conceivable that such condominiums are planned and sold during a period of high economic growth; these condominiums have a relatively high floor area ratio and a low number of floors, reflecting a high probability of rebuilding. However, the model does not include information on the demand side conditions; thus, the condominiums located in suburban areas might not be rebuilt in anticipation of a future decline in demand.

In terms of the total floor area in the bottom 10% of the predictive probability of rebuilding (Fig. 2.6), the values are particularly high in the eastern and southern parts of central Tokyo. In some areas of Koto and Sumida wards, condominiums have already exploited most of the floor area ratio, and the number of housing units is likely to be high, resulting in a pushdown for the probability of rebuilding in this model. In the suburban area, grid cells with a total floor area of 1 ha or less

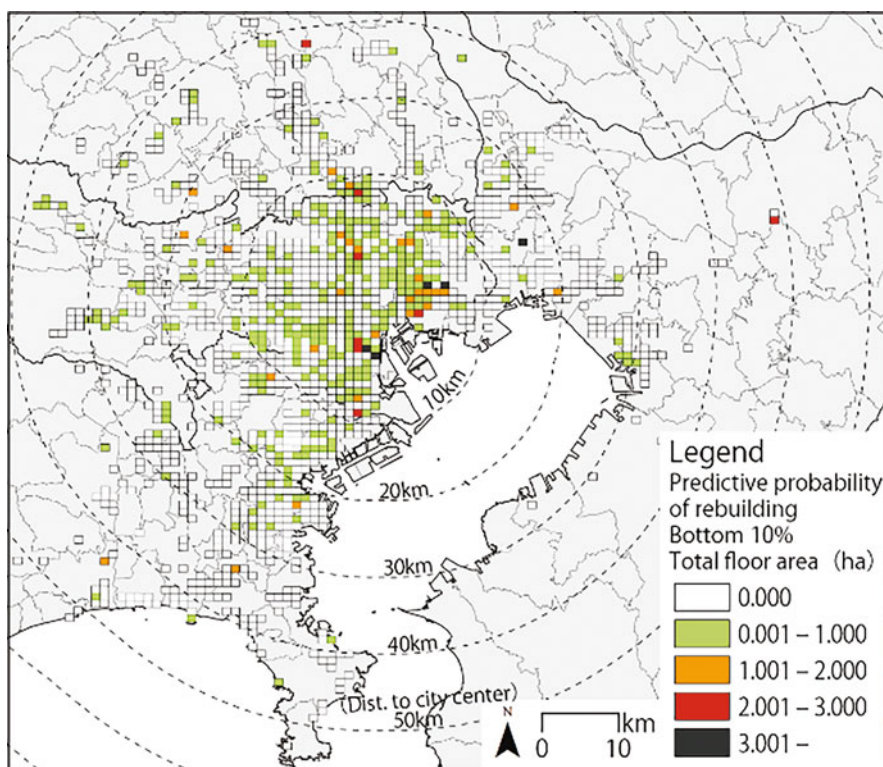


Fig. 2.6 Geographical distribution of total floor area in the bottom 10% of predictive probability of rebuilding

are widely distributed. Therefore, areas where condominiums will be rebuilt and the ones will accumulate are expected to occur simultaneously in central Tokyo. Moreover, as many grid cells with a low probability of rebuilding are also distributed in the suburban areas, the accumulation of old condominiums is expected to progress widely and gradually.

2.4 Conclusion

This study compared rebuilt condominiums to existing condominiums with old earthquake resistance standards. This revealed the trends, predicted the geographical distribution, and the probability of condominium rebuilds in the future. The following are the main findings.

We found that the trend of condominiums rebuilt with old earthquake resistance standards follows the results of previous studies. This shows that the potential of rebuilding is associated with building and location characteristics, such as the floor area available for expansion, location, and floor area per unit. This is as per the arguments of Takamizawa and Go (1989), Hasegawa (1999), and Hanazato (2017). The correlation of floor layout to the probability of rebuilding in this study was weak, and condominium rebuilding was largely influenced by building age, land and building size, room for expansion, and its distance to the city center. In addition, We showed the marginal effects of condominium characteristics on rebuilding. Specifically, We found that building age, land area, and floor area available for expansion increased the probability of rebuilding by 1.49, 1.42, and 0.75 percentage points, respectively, whereas the number of housing units and distance to the city center decreased the probability of rebuilding by 0.75 and 0.61 percentage points, respectively.

Furthermore, We visualized the areas with a high or low probability of rebuilding using a 1 km grid cell and showed that the central Tokyo and suburban areas tend to differ. Condominiums with a high probability of rebuilding were concentrated in the central and western parts of central Tokyo, whereas in the eastern and southern parts of central Tokyo, the concentration of condominiums with a low probability of being rebuilt was small. In the suburban areas, however, areas with a high probability of rebuilding are scattered throughout the city, whereas areas with a low probability of rebuilding are not concentrated but are widely distributed. There is concern that hotspots of old condominiums may emerge in the eastern and southern parts of central Tokyo in the future.

Although this study discussed the probability of rebuilding condominiums, We only used building and location characteristics as explanatory variables. Therefore, factors such as the ability of management associations, the existence of troublesome tenants, district-specific planning regulations, and exogenous shocks are not considered in the forecast. In addition, the price of housing is inherently determined by the supply–demand relationship, and the decision to rebuild is thought to change in relation to the equilibrium. Therefore, We need to build a structural model

assuming more realistic settings. The construction of such a model would deepen our discussion on the likelihood of condominium rebuilding.

Acknowledgments This work was supported by JSPS KAKENHI Grant Numbers 20H00082, 20K14898.

References

- Asami Y (2009) Optimization of majority rule for consensus building: resolution for rehabilitation of condominiums. *Urban Hous Sci* 64:137–143. https://doi.org/10.11531/uhs1993.2009.64_137. (in Japanese)
- Asami Y, Fukui H, Yamaguchi M (2012) Condominium rebuilding: how to prepare for aging of building. *Nippon-Hyoron-sya*. (in Japanese)
- Asami Y, Saito H (Eds.) (2019) Considering the end of life in condominium. Progress. (in Japanese)
- Baba H (2020) Potentialities and issues of privately-owned data on Condominium Studies. *Jpn J Real Estate Sci* 33(4):79–83. https://doi.org/10.5736/jares.33.4_79. (in Japanese)
- Choi J, Asami Y (2004) A study of the relation between sense of values and residential evaluation. *J Archit Plan* 69(576):133–139. https://doi.org/10.3130/aija.69.133_2. (in Japanese)
- Glaeser E, Gyourko J (2005) Urban decline and durable housing. *J Pol Econ* 113(2):345–375. <https://doi.org/10.1086/427465>
- Hanazato T (2017) Feasibility evaluation for condominium reconstruction by means of the application of discriminant analysis on real estate data. *Jpn J Real Estate Sci* 31(3):119–128. https://doi.org/10.5736/jares.31.3_119. (in Japanese)
- Hasegawa H (1999) Countermeasures for problems in condominium reconstruction projects. *J Archit Plan* 64(523):235–242. https://doi.org/10.3130/aija.64.235_4. (in Japanese)
- MLIT (n.d.-a) Number of condominium units. <https://www.mlit.go.jp/jutakukentiku/house/content/001488548.pdf> (in Japanese)
- MLIT (n.d.-b) Current situation of condominium rebuilding. <https://www.mlit.go.jp/jutakukentiku/house/content/001488550.pdf> (in Japanese)
- MLIT (n.d.-c) Basic plan for housing (national plan). <https://www.mlit.go.jp/common/001392030.pdf> (in Japanese)
- Ronald R, Hirayama Y (2006) Housing commodities, context and meaning: transformations in Japan's urban condominium sector. *Urb Stud* 43(13):2467–2483. <https://doi.org/10.1080/00420980600970680>
- Rosen G, Walks A (2013) Rising cities: condominium development and the private transformation of the metropolis. *Geoforum* 49:160–172. <https://doi.org/10.1016/j.geoforum.2013.06.010>
- Rosen G, Walks A (2015) Castles in Toronto's sky: condo-ism as urban transformation. *J Urban Aff* 37(3):289–310. <https://doi.org/10.1111/juaf.12140>
- Saito H, Hasegawa H (2001) A study on process of consensus-building in initial stage of condominiums reconstruction project and its problems: case of large-scale condominiums in the suburb. *J Archit Plan* 66(543):239–245. https://doi.org/10.3130/aija.66.239_1. (in Japanese)
- Saito H, Hasegawa H, Souda O, Yagisawa S (1999) Capability for consensus-building of condominium reconstruction project by homeowners' association. *J City Plan Inst Jpn* 34:307–312. <https://doi.org/10.11361/journalcpij.34.307>. (in Japanese)
- Sim L, Lum S, Malone-Lee LC (2002) Property rights, collective sales and government intervention: averting a tragedy of the anticommons. *Habitat Int* 26(4):457–470. [https://doi.org/10.1016/S0197-3975\(02\)00021-8](https://doi.org/10.1016/S0197-3975(02)00021-8)
- Takamizawa K, Go Y (1989) Survey of the actual condition of decrepit condominium apartment and analysis for their reconstruction. *J Archit Plan Environ Eng* 404:89–97. https://doi.org/10.3130/ajax.404.0_89. (in Japanese)

- Tanaka M, Kumata Y (1999) Problems of decrepit condominiums furthering aggravation of urban environment is rebuilding possible by means of reverse mortgage system? *Stud Reg Sci* 29(2):41–61. https://doi.org/10.2457/srs.29.2_41
- Warnken J, Russell R, Faulkner B (2003) Condominium developments in maturing destinations: potentials and problems of long-term sustainability. *Tour Manag* 24(2):155–168. [https://doi.org/10.1016/S0261-5177\(02\)00063-8](https://doi.org/10.1016/S0261-5177(02)00063-8)
- Webb B, Webber S (2017) The implications of condominium neighbourhoods for long-term urban revitalisation. *Cities* 61:48–57. <https://doi.org/10.1016/j.cities.2016.11.006>
- Wooldridge J (2016) Introductory econometrics: a modern approach. Southwestern Publishing House, Nashville
- Yau Y, Ling Chan H (2008) To rehabilitate or redevelop? A study of the decision criteria for urban regeneration projects. *J Place Manag Dev* 1(3):272–291. <https://doi.org/10.1108/17538330810911262>

Chapter 3

Significance of “Living Environment Score” in Quantifying Attractiveness of Regions During Residence Selection



Hisatoshi Ai

Abstract Japan’s conventional city planning is based on the assumption that population growth and urbanization will continue in the future. However, it is extremely likely that the population growth assumption will no longer hold in the future, so the city planning system is at a critical juncture. Notably, the development of compact cities maintains the quality of life in cities and administrative service efficiency even in the era of population decline. In order to make a city more compact through effective planning, municipalities should formulate policies encouraging relocation, such as developing urban areas with attractive living environments and the introduction of subsidies for relocation-associated expenses. Hence, a quantitative and objective index to assess the living environment of each area from the perspective of whether it corresponds to residents’ preferences is needed.

The living environment score (LES) focuses on various living environment indices and takes into account the magnitude of the influence of these indices on residence selection in order to assess the overall attractiveness of an area as a residence. We analyzed population increases from 2000 to 2010 in the Tokyo

The contents of this paper are based on the following papers originally published in a Japanese journal: Ai, H. (2014) How living environment indices effect on population change patterns of local districts: An analysis on urban area in the Greater Tokyo Area. *Journal of City Planning Institute of Japan*, 49 (3), pp. 567–572 (in Japanese). Ai, H. (2016) Indexing of living environment attracts young and productive age generations: An analysis based on local districts within the Greater Tokyo Metropolitan Area, *Journal of City Planning Institute of Japan*, 51 (3), pp. 860–866 (in Japanese). Ai, H. (2020) Calculating living environment index forecasting population increase in a grid based spatial units: Comparison of the result between a census grid basis and a basic unit block basis, *Journal of City Planning Institute of Japan*, 55 (1), pp. 41–48 (in Japanese). Ai, H. (2021) A relationship between residential reallocation based on living environment score and disaster risk reduction: Focusing on land slide risk, flood risk, and heavily build-up areas, *Journal of City Planning Institute of Japan*, 56 (3), pp. 587–594 (in Japanese).

H. Ai (✉)

Department of Contemporary Liberal Arts, Showa Women’s University, Tokyo, Japan
e-mail: hisaai@swu.ac.jp

metropolitan area and attempted to calculate the LES at both the census grid and local district levels. The results showed that there was a significant expected population increase tendency in regions with a high LES. However, the accuracy rate was around 60%, and further improvements are needed in order to use this as a basis for decision-making.

Indices related to disaster safety have not been considered in the LES. Thus, when we verified the relationship between population-increase tendencies or the LES with disaster risk, it was suggested that population increases might continue in regions with flood risk or risks associated with dense urban areas. Disaster risk is something that people seek to minimize, and this should be considered as a property that is different from other living environment indices that should be pursued to an appropriate level. For the future work, it is imperative to improve the LES calculation method so that disaster risk can be reduced while improving accuracy.

Keywords City planning · Living environment · Comprehensive evaluation · Attractiveness of regions

3.1 Era of Declining Population and Compact Cities

For the first time since World War II, Japan's population registered a natural decline in 2007, and it is estimated that this trend will continue in the future (Statistics Bureau, Ministry of Internal Affairs and Communications, 2014). Most prefectures have already shown a population decline trend, and from 2015 to 2020, only 8 of 47 prefectures reported no population decline (Ministry of Internal Affairs and Communications 2021). Although the population decline trend is evident at both national and prefectural levels, it is not uniform within each area. For example, Ogawa (2011) reported that areas with population growth and decline coexist in a mosaic pattern.

Population changes can be broadly attributed to natural causes, such as births and deaths, as well as social changes driven by relocations associated with employment, personnel transfer, and advancement to higher education. Koike (2006) analyzed populations by municipality and cohort in the Hokkaido Prefecture and indicated that social changes have a major impact on population changes. Specifically, this can be attributed to not only the direct impact of immigration and emigration but also the indirect influence on birth rates due to immigration and emigration of generations that have children. Although the place of residence is restricted at the prefectural level, it can be said that there is a greater degree of freedom in residence selection at the more detailed municipality or local district level. Specifically, relocating individuals are considered to select an area that matches their own residence preferences among such options with a certain spatial extent. Additionally, the 1986 and 1991 migration surveys reported that 40% of individuals relocated citing housing conditions (Arai and Ohki 1999), and that these individuals' assessment of the living environment had an impact on residence selection. Accordingly, it is

considered that population changes are largely impacted by social changes and that it is highly likely that the living environment of areas with increasing social changes is seen to match the preferences of more residents.

Next, Japan’s conventional city planning is a growth management system design that is based on the assumption that population growth and urbanization will continue in the future. However, as mentioned earlier, it is extremely likely that the population growth assumption will no longer hold in the future, so the city planning system is at a critical juncture. Notably, the development of compact cities maintains the quality of life in cities and administrative service efficiency even in the era of population decline. It is envisioned that compact cities in Japan, also characterized as “compact and network,” consolidate urban areas along railway lines and strengthen commerce, administration, and medical welfare around railway stations, which are transportation nodes between railway and bus networks. The localization normalization plan is introduced to make cities more compact in addition to land use zoning system which is the earlier method of land use control. If there are multiple railway stations in the same municipality or an urban area, then that station may be hierarchical depending on its importance as a transportation hub in the localization normalization plan. Objective decision-making is important, such as deciding which railway station surroundings should be set as higher-order hubs and how far the scope of urbanization extends from the railway station within the hub surroundings. The former plays an important role when formulating the localization normalization plan, and the latter while setting specific residential promotion areas. Therefore, indices are imperative for assessing regions that have already been developed and urbanized.

In order to make a city more compact through effective planning, it is imperative to follow population movement so that it corresponds with the direction of the compact city plan. In Japan’s present-day social system, plan-based forced migration and mass relocation are not realistic options, and municipalities, which are the main implementers of city planning, should formulate policies encouraging relocation, such as developing urban areas with attractive living environments and the introduction of subsidies for relocation-associated expenses. Discussing cost-effectiveness is essential for projects and policies that involve expenditures such as urban development and subsidies for relocation, and a quantitative and objective assessment index is needed. Essentially, as mentioned earlier, it is imperative to assess the living environment of each area from the perspective of whether it corresponds to residents’ preferences.

3.2 Concept and Features of Living Environment Score

3.2.1 *Conceptualization and Calculation of Living Environment Score*

The living environment score is calculated as a comprehensive assessment index that combines multiple living environment indices. This can be attributed to the fact that during the selection process, individuals do not choose a residence based on a single factor and could have multiple preferences. Furthermore, the spatial unit is assumed to be a local district or a census grid, or so-called a mesh, rather than a municipality. The details of each will be described later, although the calculation method explained here is identical regardless of the spatial unit used.

The procedure for comprehensive assessment can be broadly divided into two stages. The first is to derive the standard that leads to population increase for each living environment index. For example, metropolitan areas in Japan have developed railway networks that connect the city center and its suburbs, and urban development has advanced mainly along these railway lines; therefore, areas surrounding railway stations are often popular among people searching for homes. When areas within 1 km from the railway station have exhibited, marked population increases and areas farther away have not shown much population increase, then the 1 km-radius from the railway station is considered a demarcation point leading to population increases. These standards can be derived using statistical methods by creating a cross-tabulation table with population increase tendencies for each living environment index and performing a chi-square test. The living environment indices used in the assessment will be described later.

For the second stage, when combining multiple living environment indices and calculating the living environment score, the magnitude of impact, or so-called weight, of each index on residence selection is considered. This corresponds to the consideration of multiple living environment indices that are reported to impact the resident selection, such as distance to the railway station, presence, or absence of nearby parks, and whether the land is on a slope. Although equal importance is not given to each, some are deemed important and others are used only as a reference.

The concept of discriminant analysis is used for this stage. Discriminant analysis with population increase tendency as the independent variable and standardized version of each living environment index as the explanatory variable yields a discriminant coefficient. As the explanatory variables were standardized, the magnitude of the absolute value of this discriminant coefficient is considered to reflect the magnitude of the impact of each living environment index on population increase tendencies.

When calculating the final living environment score, each of the living environment indices in individual local districts or census grids is first judged based on whether it satisfies the standard calculated in the first stage. For indices that meet the standard, the absolute value of the discriminant coefficient obtained in the second stage is added up as the raw living environment score. Specifically, the raw score

enhances when living environment indices increasingly satisfy the standard leading to population growth or when living environment indices that satisfy the standard have a greater impact on residence selection. Finally, the living environment score is obtained by converting this raw score into a deviation value for the entire target region. Since it is a deviation value, a local district or census grid with average living environment regarding leading to population increase is given a score of 50, and those with higher scores could be interpreted as having a living environment that is advantageous in terms of residence selection.

If the living environment score appropriately reflects residents’ preferences in residence selection, it is believed that residential promotion can be achieved by prioritizing areas with high scores. The derivation process of the living environment score can also identify which living environment index in each local district or census grid has failed to satisfy the standard at which population increase is expected. Furthermore, the magnitude of impact of each living environment index on population increase has been calculated. Therefore, discussions can be held as to which index should be improved in each local district or census grid to effectively increase the living environment score.

3.2.2 Living Environment Indices Used for Calculating Living Environment Score

When selecting living environment indices to be used in the analysis, it is important to examine what type of living environment indices impact population increase while considering residential promotion that aims for compact cities. Table 3.1 summarizes the living environment assessment items that Maene et al. (2012) surveyed among residents. Likely important items include those marked *, which had low satisfaction levels in the surveyed area, and §, considered to be important for future residential areas. We considered that our items should correspond with

Table 3.1 Living environment assessment items surveyed among residents. *Based on Maene et al. (2012)

Public transportation *§	Retail stores of daily goods*	Access to downtown*
Medical care services§	Ambulance and firefighting§	Natural disaster prevention
Migration of young generation§	Vitality of the community	Activities of local communities
Relationship with neighborhood	Sports and health care facilities	Social welfare services
Administrative services	Education and child-rearing environment	Richness of nature
Crime prevention activities	Comprehensive comfort	

* Low satisfaction levels in the surveyed area

§ considered to be important for future residential areas

these items and also could be compared in relatively small spatial units and that they should be indices that express the socioeconomic circumstances of cities. Accordingly, we analyzed 13 living environment indices in this study. It should also be noted that the data were collected and published in spatial units at the local district level or following the census grid system as a time-series data.

Maene et al. (2012) reported low satisfaction levels for three items—public transportation, shopping, and ease of going outside the area. Essentially, the level of demand by residents for these elements was high, and they are considered to have a strong impact on living environment assessments. When calculating the living environment score, we reflect these by the *distance to the railway station* and the *number of stores*.

Maene et al. also reported that items that were considered important for future residential areas were access to medical care, emergency services, and firefighting services; disaster prevention; and housing for young people. This signifies that even residents who are not necessarily dissatisfied with the current situation focus on these elements and that they ultimately impact living environment assessments. Access to *hospitals* and *firefighting services*, *slopes* as terrain, and the *aging rate* as resident attributes are used to consider these elements when calculating the living environment score.

Asami (2001) emphasized the importance of considering sustainability in addition to convenience, safety, comfort, and health when assessing living environment indices. The above-mentioned living environment indices were mainly related to convenience, safety, and health. Regarding safety, not only disaster prevention but also crime prevention is important; thus, *access to police* is also considered in the living environment score. The *presence or absence of parks* is believed to contribute to comfort and health. Regarding sustainability, given that residents remain in a region for a certain number of years, the following factors are considered to correspond to sustainability: *aging rate*, which reflects the age-group of residents; *average number of household members* and *detached house rate*, which reflect housing styles; *population density* and *vacant lot ratio*, which reflect the land use situation and the status of urban development; and the *number of businesses*, which is related to employment opportunities.

Table 3.2 summarizes the above-mentioned living environment indices together with data sources.

3.3 Setting of Target Regions and Definition of Population Increase in This Study

3.3.1 Setting of Target Regions

The target regions in this study are “city planning areas” of the Tokyo, Saitama, Chiba, and Kanagawa Prefectures. These four prefectures form the wide and

Table 3.2 Living environment indices used for calculating living environment scores and their data sources *Edited and reproduced based on Ai (2014)

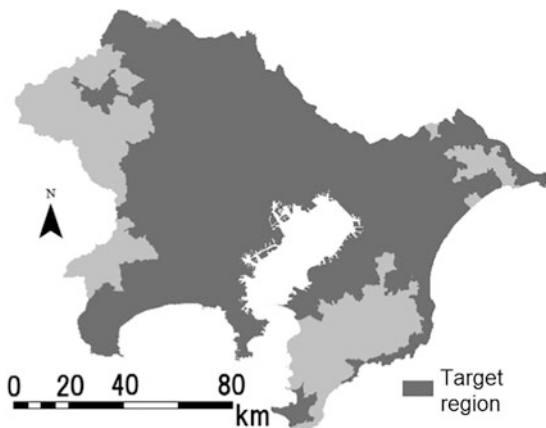
Index	Abbreviations	Unit	Data source
Distance to railway station	Station	Meters	DNLI, railway time-series data
Distance to hospital	Hospital	Meters	DNLI, public facility data (2006); hospitals, medical centers
Distance to police	Police	Meters	DNLI, public facility data (2006); police stations, police boxes
Distance to firefighting services	Firefighting	Meters	DNLI, public facility data (2006); fire departments, fire houses
Presence or absence of parks	Park		DNLI, urban park data (2011)
Number of stores	Stores		Establishment and Enterprise Census (2006); stores, restaurants
Number of businesses	Businesses		Establishment and Enterprise Census (2006); establishments, offices
Slopes	Slopes	Degrees	DNLI, elevation and slope data/fifth level census grid (2011)
Population density	Density	Person/km ²	National Census (2000)
Aging rate	Aging	%	National Census (2000)
Average number of household members	Household	Person	National Census (2000)
Vacant lot rate	Vacant	%	DNLI, detailed land use data/fifth level census grid (2011)
Detached house rate	Detached	%	National Census (2000)

* DNLI: digital national land information

integrated Tokyo metropolitan area, where there is a daily flow of people commuting to work and schools across the borders of these prefectures. Considering its size, the entire region does not necessarily simultaneously fall into the set of options available during residence selection, but the urban areas are continuous. Subdividing these regions into mutually independent areas is difficult regarding population flow, so the four prefectures were treated as an integrated region. Additionally, we limited our study to “city planning areas” because there are restrictions to the scope of the provision of land use data, which is one of the living environment indices used in this analysis (Fig. 3.1).

When attempting analyses with a spatial unit that is more detailed than municipalities, local districts or census grids can be considered as candidates. A local district is an administrative place name that is more detailed than a municipality in Japan. Although it does not have legal status, it is used as an address for postal items and is a spatial unit that has been widely recognized by residents. The census grid is divided at regular intervals, such as 500 m or 1 km, and in the case of Japan, the division method system (standard region census grid) is defined based on latitude

Fig. 3.1 Four prefectures and the target region of this study * Cited from Ai (2014) and translated into English



and longitude. In addition to the population census, various statistical data use the same census grid system, facilitating the superimposition of data.

One of the advantages of using the local district as the spatial unit for analysis is that natural topography, such as rivers and transportation networks, is often used as boundary lines, and movement within the same local district is relatively easier than moving in and out of the local district, and although there are exceptions, the living environment within a local district is generally homogenous. Meanwhile, local districts are often re-organized in areas undergoing development, such as land re-adjustment, and estimation processing, such as proportional division, may be required when comparing time-series data. Areas with large population fluctuations, which are of particular interest in this study, often fall under this category, and it can be indicated as a point worth noting when conducting analyses.

In the case of the census grid, one of the advantages is that it has a uniform spatial unit shape and size. Additionally, the use of standard region grids enables the seamless superimposition and analysis of population statistics, economic statistics, topographic data, and so on. The position and shape of the spatial units do not change between each time point, so time-series comparisons are also easy. Since the space is divided mechanically, it should be noted that areas that straddle rivers, major roads, administrative boundaries, etc. are often included in the same census grid and that the homogeneity of the living environment is not necessarily guaranteed within the same census grid. Residents are not aware of the division of census grids on a daily basis, so there are not many cases where the residents are aware of the census grid number of their own residences.

In this chapter, we consider the results for both when the spatial unit is set to census grids of 500 m intervals and when it is set to local districts.

3.3.2 Definition of Population Increase and Method of Proportional Division by Population

Population changes were calculated using population data from 2000, 2005, and 2010 population census sub-regional tabulations. The local district areas were based on the 2005 data, and the population as of 2000 of the local districts that were merged from 2000 to 2005 (“A” in Fig. 3.2) were totaled and then compared with the post-merger population in 2005 in chronological order. In contrast, the population in 2000 of local districts that were divided from 2000 to 2005 (“B” in Fig. 3.2) were estimated by proportional division by population of the 2005 data and then compared in chronological order. In the example of B in Fig. 3.2, since it is divided into two, the population of B in 2000 was halved, and this was compared with the populations of B1 and B2 after the division. The reason why proportional distribution by area was not implemented for the division was because, when dividing a local district with a concentrated population in one part, it is the densely populated zone that is divided, so it is assumed that the population of each local district after division will be roughly the same. The population as of 2010 in the local districts that were merged from 2005 to 2010 (“C” in Fig. 3.2) were estimated using the proportional division method by population and then compared in chronological order with the 2005 data. The population as of 2010 in the local districts that were divided from 2005 to 2010 (“D” in Fig. 3.2) were totaled and then compared with the 2005 data. However, cases where complex restructuring of local districts, such as the combination of divisions and mergers, were excluded from the analysis since there are limits to the estimation of population using proportional division. As mentioned above, there are no changes in the census grid in the spatial unit. Therefore, this type of proportional division by population is not implemented for this case.

In this study, “population change” was defined as follows: when comparing time-series population data of the same local district, an “increase” was defined as “when a population increased at one of two time points, and when, even for the other time point, the population of the census grid/local district exceeded the expected population based on the population change tendency of the entire target region” or “when the population of the census grid/local district was at least 2%

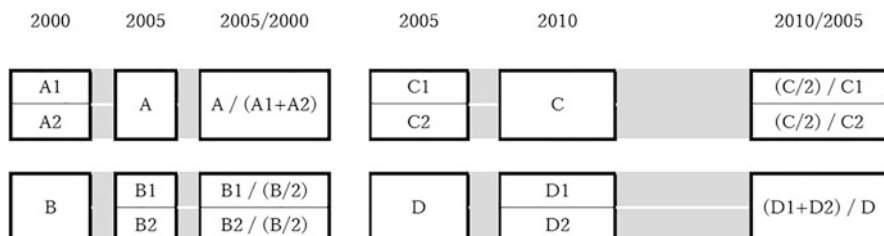


Fig. 3.2 Population estimation method when local district area changes

higher than the estimated population based on the population change tendency of the entire target region at both time points.” An “increase” was set not as a simple comparison of population data between two time points, but as a comparison with the overall population increase rate as described above, in order to take into account the population change due to the population flow within as well as in and out of the entire target region (i.e., the four prefectures defined earlier), while extracting the changes that exceed those tendencies and make them the subject of discussion in this study. Additionally, comparisons of population data cannot be made if the population was zero at any single time point from 2000 to 2010 or if the population data was confidential due to few population; accordingly, these cases were excluded from the analysis.

The youth population (under the age of 18) decreased by 8.3% from 2000 to 2005, and by 0.5% from 2005 to 2010. On the other hand, the productive age population (18 to under 60) decreased by 7.1% from 2000 to 2005, and by 1.2% from 2005 to 2010. Therefore, it should be noted that, although the population decreased in terms of absolute numbers, there are cases in this study that would be classified as “increases.”

3.4 Calculation of Living Environment Score

3.4.1 *Cross-Tabulation of Population Growth Tendencies and Living Environment Levels*

When calculating the living environment score, the population data for each local district or census grid are compared chronologically and classified according to whether the population increased or decreased. Although this can be done with any generation, here, we calculate the living environment score for both the youth and productive age population based on the findings of Ai (2016). It is expected that calculating the living environment score for each age-group based on the age-group-specific population change tendencies will enable the observation of whether residence preferences differ according to age-group or lifestyle. First, the productive age population corresponds to the generation that works and pays taxes, and it is an important generation for maintaining the vitality of a city and securing tax revenue. Meanwhile, the youth population rarely changes their place of residence alone and generally reflect the dynamics of the child-rearing generation. The youth population and productive age population are essentially mutually exclusive in terms of generational divisions, but when considering the household unit, the dynamics of the productive age population should be interpreted as partially including the dynamics of the youth population.

When calculating the living environment score, we sought to determine the necessary level for the living environment index at which population increase can be expected by conducting a chi-square test and residual analysis, verifying

whether each living environment index has a significant relationship with population increase. Table 3.3, which demonstrates the results, is a series of cross-tabulation tables for each index, and the spatial units of the census grid and local district are shown simultaneously so that they can be compared. In the “increase” column for each spatial unit, the number of census grids and local districts that correspond to each spatial unit is shown in the left column and adjusted residuals are in the center column. The adjusted residuals for “non-increase,” which is the case that does not correspond to an increase, have an absolute value that is equal to the “increase” values, differing only in sign; hence, they are omitted here and the number of census grids and local districts that are “non-increase” are shown in the right column.

In Table 3.3, the squares where the absolute value of the adjusted residual exceeds 1.96 and can be said to be significant at the 5% level are colored. For the classes where A.R. is over 1.96, the actual number of census grids/local districts was significantly higher than the assumed number of census grids/local districts if the living environment index and population increase were unrelated; and conversely, for the classes where A.R. is 1.96 or lower, the actual number was significantly lower. For example, for the distance to the nearest railway station in Table 3.3, it could be read that the population increase was significantly higher for the youth generation in grids within 1500 m and for the productive age generation in grids within 1000 m. When the local district was set as the spatial unit, it could be read that the population increase was significantly higher for both generations in local districts within 500 m from the railway station. A summary of whether each level of the living environment index resulted in a significantly higher population increase is listed in the standard column of Table 3.4. In Table 3.4, the left side shows the case where the census grid is the spatial unit, and the right side shows the case where the local district is the spatial unit. The interpretation here is that, if the living environment index is included in this standard, then population increase is expected in the census grid/local district from the perspective of that index.

Several indices, such as the distance to the nearest railway station or hospital, as well as the number of stores, can be seen in Table 3.4, where there are differences in the value range that significantly impacts population increase at the fourth-order census grid unit and local district unit. Differences in the area and shape between the two spatial units can be raised as one factor for this. Although there are some differences depending on the latitude, the fourth-order grid has a side length of approximately 500 m and an area of approximately 0.25 sq.-km. In contrast, local districts have considerable differences in area and shape. In general, local districts in city centers tend to have a smaller area, whereas local districts in suburbs tend to have a larger area. The number of stores and businesses are not density indices. Therefore, even if these numbers are distributed at the same density, in case the area of the tabulated spatial unit is larger, it would result in a larger number of stores and businesses that are used as indices. Additionally, distance indices such as the distance to the nearest railway station are calculated from the outer circumference of the grid or local district, excluding cases where the facility exists within the area and has a distance of zero. On this basis, if the area of the tabulated unit is larger, then the distance from the center of that spatial unit is more likely to be underestimated. For

Table 3.3 Chi-square test and residual analysis results for each living environment index *Edited and reprinted from Ai (2020) Table 1

		Census grids				Local districts			
		Youth population		Productive age population		Youth population		Productive age population	
		Increase	A.R.	Non-increase	A.R.	Increase	A.R.	Non-increase	A.R.
		$\chi^2 = 786.7$	$p = 0.00$	$\chi^2 = 1084.5$	$p = 0.00$	$\chi^2 = 191.5$	$p = 0.00$	$\chi^2 = 521.6$	$p = 0.00$
(A) Station (meters)	0	404	7.62	1008	487	18.20	930	413	4.30
	0-500	1633	13.45	4467	1556	20.29	4593	1981	6.51
	500-1000	1387	10.37	4000	965	20.9	4481	1161	0.652
	1000-1500	855	2.84	2971	601	-2.31	3280	568	-1.13
	1500-2000	479	-3.85	2216	364	-5.19	2382	255	-2.39
	2000-3000	504	-8.43	2835	351	-10.80	3058	168	-5.77
	3000-	396	-22.55	4279	345	-19.49	4447	94	-10.8
		$\chi^2 = 1055.1$	$p = 0.00$	$\chi^2 = 790.0$	$p = 0.00$	$\chi^2 = 237.7$	$p = 0.00$	$\chi^2 = 257.5$	$p = 0.00$
(B) Hospital (meters)	0	423	8.35	1022	380	9.71	1081	410	3.36
	0-500	1818	16.25	4744	1572	17.37	5052	2041	7.69
	500-1000	1535	10.83	4454	1147	5.26	4887	1325	3.20
	1000-1500	893	3.13	3079	675	-0.02	3352	488	-4.37
	1500-2000	399	-5.46	2041	318	-5.53	2164	174	-5.95
	2000-3000	315	-13.83	2596	299	-10.43	2683	137	-7.15
	3000-5000	191	-17.89	2449	312	-13.04	2486	47	-8.75
(C) Police (meters)	5000-	84	-14.57	1391	66	-13.43	1466	18	-3.29
	0	713	8.16	1958	737	15.62	1945	745	4.41
	0-500	2685	16.97	7661	2155	13.44	8276	2830	7.24
	500-1000	1451	0.15	5563	1065	-4.72	6051	834	-5.88
	1000-2000	725	-18.28	5240	626	-15.46	5485	219	-8.85
	2000-	84	-14.23	1354	86	-11.76	1414	12	-4.37
	$\chi^2 = 692.9$	$p = 0.00$	$\chi^2 = 667.4$	$p = 0.00$	$\chi^2 = 249.4$	$p = 0.00$	$\chi^2 = 514.2$	$p = 0.00$	$p = 0.00$

		$\chi^2 = 913.1$	$p = 0.00$	$\chi^2 = 683.6$	$p = 0.00$	$\chi^2 = 832.3$	$p = 0.00$	$\chi^2 = 2726.7$	$p = 0.00$
(D) Firefighting (meters)	0	260	5.97	653	237	7.50	679	252	3.40
0–500	1585	15.78	4081	1352	16.15	4295	1817	9.16	4197
500–1000	1755	12.60	4991	1373	8.64	5434	1579	2.85	4195
1000–2000	1539	-3.95	6507	1198	-6.18	6992	863	-8.30	3244
2000+	519	-26.60	594	509	-20.89	5771	129	-11.7	1016
(E) Stores	0	$\chi^2 = 747.7$	$p = 0.00$	$\chi^2 = 891.7$	$p = 0.00$	$\chi^2 = 73.2$	$p = 0.00$	$\chi^2 = 249.7$	$p = 0.00$
0	731	-22.05	5877	638	-19.19	6244	205	-4.69	831
1–10	2700	-0.56	10,483	2018	-6.87	11,290	1568	-5.29	5040
11–20	980	14.07	2290	717	8.37	2556	907	0.735	2517
21–30	411	6.36	1109	343	6.22	1177	527	1.19	1417
31–40	218	5.17	560	186	5.40	592	345	2.67	833
41–	618	10.73	1457	767	25.53	1312	1088	5.77	2572
		$\chi^2 = 1019.2$	$p = 0.00$	$\chi^2 = 1613.3$	$p = 0.00$	$\chi^2 = 296.9$	$p = 0.00$	$\chi^2 = 698.9$	$p = 0.00$
(F) Businesses	0	102	-13.02	1335	130	-9.13	1424	327	-5.69
1–10	1211	-23.82	8349	1067	-19.34	8729	2033	-10.8	7009
11–20	779	-1.33	3150	566	-4.51	3394	838	2.18	2201
21–30	612	5.92	1810	433	1.45	1997	415	3.22	986
31–40	477	7.15	1269	338	2.97	1410	265	5.00	523
41–	2477	24.56	5863	2135	25.71	6217	762	13.9	1191
		$\chi^2 = 890.0$	$p = 0.00$	$\chi^2 = 774.3$	$p = 0.00$	$\chi^2 = 57.6$	$p = 0.00$	$\chi^2 = 72.3$	$p = 0.00$

(continued)

Table 3.3 (continued)

		Census grids				Local districts				Productive age population		
		Youth population		Productive age population		Youth population		Local districts		A.R.	Non-increase	Increase
		Increase	A.R.	Non-increase	Increase	A.R.	Non-increase	Increase	A.R.	Non-increase	A.R.	Non-increase
(G) Parks	YES	3089	29.83	7196	2568	27.83	7749	2711	7.59	6865	3214	8.50
	NO	2569	-29.83	14,580	2101	-27.83	15,422	1929	-7.59	6345	2318	-8.50
(H) Density (People/km ²)	-2000	1804	-29.12	11,674	1586	-23.80	12,294	639	-12.2	2921	748	-15.3
	2000-4000	763	3.76	2539	554	-0.02	2752	491	8.11	907	487	3.23
4000-10,000	4000	1903	22.52	4268	1371	12.98	4800	1764	10.4	3928	1882	4.45
	10,000-15,000	758	8.69	2060	663	10.13	2155	994	0.805	2756	1260	4.22
	15,000-20,000	314	5.76	834	349	12.62	799	457	-1.66	1416	692	6.14
	20,000-	116	1.03	401	146	7.05	371	295	-6.91	1282	463	-1.29
(I)	1-1.5	16	1.39	41	26	1.98	83	33	3.03	48	39	0.542
	Household (persons)											79
1.5-2	391	11.43	760	439	19.33	735	621	10.5	1073	789	15.0	913
	2-2.5	1492	22.06	3076	1347	24.72	3268	1593	9.17	3597	2030	15.3
2.5-3	2133	13.13	6245	1392	-0.85	7063	1600	0.226	4531	1631	-8.83	4515
	3-3.5	1119	-12.59	6109	937	-10.51	6369	587	-9.22	2452	719	-9.48
3.5-4	321	-20.73	3590	334	-15.17	3627	136	-11.8	1052	221	-9.54	976
	4-	186	-14.2	1955	194	-10.64	2036	70	-6.75	4572	93	-7.17
(J) Aging (%)	-10	259	3.07	804	415	18.42	711	916	-3.83	2964	1540	12.9
	10-15	783	5.26	2462	796	12.42	2466	1565	6.00	3834	1693	1.02
15-20	1551	11.24	4459	1190	6.97	4838	1356	3.87	3473	1497	0.299	3344
	20-25	1586	6.59	5181	1180	1.52	5613	523	-4.36	1821	550	-8.31
25-30	803	-8.27	4122	566	-11.13	4392	179	-4.91	756	171	-8.81	782
	30-	676	-16.58	4748	522	-17.10	5151	101	-2.08	362	81	-7.08

		$\chi^2 = 287.6$	$p = 0.00$	$\chi^2 = 298.2$	$p = 0.00$	$\chi^2 = 27.9$	$p = 0.00$	$\chi^2 = 87.9$	$p = 0.00$	$\chi^2 = 226.1$	$p = 0.00$	$\chi^2 = 226.1$	$p = 0.00$
(K) Slopes (degrees)	0	162	1.59	542	149	2.97	565	26	1.33	54	43	4.47	37
0-1	3225	9.88	10.807	2712	10.74	11,463	2296	1.04	6419	2940	7.69	5846	
1-3	1587	1.57	5881	1291	0.80	6275	1536	4.66	3890	1729	1.71	3735	
3-5	438	-5.77	2242	341	-6.37	2397	510	-3.25	1693	584	-4.82	1634	
5-10	204	-8.97	1486	127	-10.86	1605	223	-2.06	740	190	-7.78	782	
10-	45	-11.59	818	49	-9.40	866	49	-7.66	414	46	-9.94	422	
$\chi^2 = 102.0$		$p = 0.00$	$\chi^2 = 157.4$		$p = 0.00$	$\chi^2 = 15.7$		$p = 0.01$	$\chi^2 = 44.6$		$p = 0.01$	$\chi^2 = 44.6$	$p = 0.00$
(L) Vacant (%)	0	4518	-9.23	18,491	3685	-9.95	19,650	3531	1.06	9950	4298	4.77	9264
0-5	462	4.37	1419	348	1.83	1,555	683	-3.00	2193	741	-6.62	2158	
5-10	245	2.82	770	215	3.66	811	221	1.61	555	246	0.412	534	
10-20	239	5.17	626	216	6.27	664	133	1.18	336	161	1.18	324	
20-30	119	3.05	332	124	5.81	339	27	-0.511	86	40	0.488	82	
30-	75	5.28	138	81	7.38	152	45	1.95	90	46	0.719	91	
$\chi^2 = 1158.7$		$p = 0.00$	$\chi^2 = 1939.4$		$p = 0.00$	$\chi^2 = 249.4$		$p = 0.00$	$\chi^2 = 1266.5$		$p = 0.00$	$\chi^2 = 1266.5$	$p = 0.00$
(M) Detached (%)	-20	714	13.73	1526	852	27.06	1455	929	10.3	1808	1332	20.9	1476
20-40	1025	13.34	2495	1096	24.26	2442	1053	3.57	2671	1621	18.8	2117	
40-60	1086	12.89	2730	825	8.31	3029	902	0.722	2504	1083	1.36	2331	
60-80	1184	11.38	3202	750	0.38	3671	869	2.15	2289	753	-9.35	2412	
80-	1649	-33.71	11,823	1146	-37.05	12,574	887	-14.1	3938	743	-27.4	4120	

Table 3.4 Living environment indices used for calculating living environment score, and value range and weighting indices in which population increased significantly *Edited and reprinted from Ai (2020) Table 2

Indices	Census grids			Local districts		
	Youth	Productive	Youth	Productive	Standard	Coefficient
Station	<1500 m	0.162	<1000 m	0.154	<500 m	0.156
Hospital	<1500 m	0.254	<1000 m	0.076	<1000 m	0.254
Police	<500 m	0.148	<500 m	0.058	<500 m	0.235
Firefighting	<1000 m	0.210	<1000 m	0.030	<1000 m	0.301
Parks	Present	0.077	Present	-0.007	Present	-0.214
Stores	11+	-0.042	11+	-0.008	31+	0.263
Businesses	11+	-0.019	11+	-0.080	11+	-0.474
Slopes	0–1 degree	0.091	<1 degree	0.096	1–3 degrees	0.213
Density	2000 persons/km ² +	0.362	4000 persons/km ² +	-0.135	2000–10,000 persons/km ²	0.226
Aging	<25%	-0.166	<20%	0.395	10%–20%	-0.051
Household	1.5–3 persons	0.138	2.5人未満	0.044	1–2.5 persons	0.166
Vacant	0% +	-0.091	5% +	-0.132	Not	Applicable
Detached	<80%	0.527	<60%	0.881	<40% OR 60%–80%	-0.040
					<40%	0.302

both cases, the aim is not to establish absolute standards for residential promotion but rather to quantify the assessment of a relative living environment within an urban area, so even if the differences in the tabulated spatial unit impact the results, it is unlikely to be a major problem.

Next, we look at some of the items in Table 3.4 that have different results by age-group. For distances to the nearest railway station or hospital, there is a general tendency that local districts and census grids that are closer to these facilities are more likely to lead to population increase, but the result shows that population increases are expected at slightly longer distances for the youth population. These results can be interpreted as follows: the child-rearing generation, which lives with the youth population, tolerates regions slightly farther away from railway stations or hospitals as residences than the productive age populations of married couples without children or single people.

Finally, when looking at the association with the aging rate, both generations did not seem to prefer living in regions with a high aging rate, but a population increase was expected in regions with a marginally higher aging rate for the youth population. This indicates that the child-rearing generation preferred areas where relatively diverse generations, including elderly people, live, whereas married couples and single people preferred regions with a large productive age population similar to themselves. In terms of the detached house rate, neither age-group preferred regions with a high level of 80% or more, but the youth generation preferred the detached house rate to a level close to 80%. This can be interpreted as follows: the child-rearing generation preferred detached houses, whereas married couples and single people preferred apartment houses.

3.5 Relationship Between Living Environment Score and Actual Population Increase

Are there actual population increase tendencies in regions with a high living environment score derived by the above-mentioned method? Table 3.5 demonstrates the results of applying the chi-square test and residual analysis in order to create a cross-tabulation table of living environment score levels and actual population increases. As mentioned above, the results for the census grid unit and local district unit are shown together.

A significant relationship between the living environment score level and actual population increase was seen for both spatial units and for both age-groups. Specifically, there were significant population increases in census grids and local districts with a living environment score of at least 50 for the youth generation and significant population increases in census grids and local districts with a living environment score of at least 55 for the productive age generation. Furthermore, fewer population increases were registered in census grids and local districts with a living environment score of less than 50 for both age-groups. These results

Table 3.5 Living environment scores and actual population increases *Re-organized and reprinted from Ai (2016) Table 10 and Ai (2020) Table 3

		Youth population		Productive age population		
		Increase	Non-increase	Increase	Non-increase	
Census grids	LES	$\chi^2 = 1373.4$	$p = 0.00$	$\chi^2 = 1682.8$	$p = 0.00$	
	-50	1523	-35.95	11,698	1624	-38.56
	50-55	647	5.00	2010	314	1.91
	55-60	1044	10.55	2825	309	4.35
	60-	2444	28.53	5243	2422	38.64
Local districts	LES	$\chi^2 = 448.8$	$p = 0.00$	$\chi^2 = 1261.3$	$p = 0.00$	
	-50	1716	-20.53	7866	1656	-30.63
	50-55	747	4.32	1974	797	0.17
	55-60	845	8.99	1882	863	9.19
	60-	1209	14.04	2444	1768	30.20
						2016

demonstrate that a population increase can be expected when the living environment score is high, which is the fundamental property that should be satisfied by the living environment score.

The number of census grids and local districts with a living environment score of 50 or more, exhibiting a population increase, as well as those with a living environment score of less than 50, exhibiting a population non-increase, as a percentage of the total number of census grids and local districts, is set as the accuracy rate. Specifically, this is the percentage of areas where high living environment scores and population increases are consistent with each other, in line with the aim of this study. The accuracy rate was 57.7% for the youth population and 65.1% for the productive age population when the spatial unit was the census grid, and 57.1% for the youth population and 60.4% for the productive age population when the spatial unit was the local district. Although the census grid unit was marginally higher, the overall accuracy rate was generally around 60%. This result suggests that referring to the living environment score in order to determine areas where it is expected that people would continue to live in the future is better than when there is no reference data. However, the results cannot be said to have reached an accuracy rate that can be held accountable during plan formulation and decision-making. Therefore, improving this accuracy rate is a task for future study.

3.6 Relationship Between Residential Promotion by Living Environment Score and Disaster Risk

In Japan, considering that natural disasters occur frequently, disaster risk mitigation in urban areas is an important issue. Typhoons and heavy rains, in particular, have become a major concern in recent years, frequently causing river and inland water flooding and landslides. Disaster risks cannot be sufficiently considered with the

living environment scores analyzed so far, but could disaster risks also be reduced if residence selection was conducted based on the living environment, such as convenience and comfort, or if residential promotion for the consolidation of urban areas based on this residence selection was conducted. This is an important issue from the perspective of living environment safety and sustainability.

A basic principle of city planning operation guidelines is that residential promotion should not include areas with major concerns with regard to disaster prevention and safety, such as landslide disasters and tsunami disaster special warning areas. However, landslide and tsunami disaster warning areas, which have lower levels of concern, are subject to comprehensive assessment not only in terms of risks but also to warning and evacuation systems, and there is nevertheless room for their inclusion in residential promotion areas under certain conditions. In practice, as reported by Nishii et al. (2019), 70–80% of all municipalities exclude areas with disaster risk from the residential promotion area setting conditions. Warabi et al. (2019) conducted interviews with municipalities and surveys of city planning zone setting records, where they indicated that disaster risk was not clearly understood on a spatial scale when urbanization promotion areas were initially set, due to location restrictions, despite disaster risks. In this backdrop, it is fully assumed that urbanization has already expanded to areas with disaster risk. Consequently, it is possible that residential promotion areas have been set even in regions with potential disaster risk. However, when considering the purpose of city planning operation guidelines, residential promotion should be planned in areas with lower disaster risk in the medium to long term.

When comparing Kiuchi et al. (2003), who investigated the availability of the living environment during residence selection, and Kita (2017), who investigated the prioritized items in a living environment, the former had about 10–20% of respondents citing natural disaster safety and earthquake/fire safety as factors, whereas the latter showed that regions with limited concerns of disasters were the third highest priority, surpassing items like transportation convenience. It cannot be assumed that the subjects of the two surveys were homogenous, but it is possible that disaster risk has assumed priority in the approximately 10-year period straddling the Great East Japan Earthquake that occurred in 2011. However, Sakamoto (2020) conducted surveys of tsunami inundation assumptions and residence reasons, where it was discussed that there was a trade-off between consideration of disaster prevention and convenience to the city center. Based on the above results, whether disaster risk can also be reduced is an important question during residential promotion based on the living environment score.

Open data of hazard maps are used to assess disaster-based damage risk. Specifically, we used the Digital National Land Information “Landslide warning areas,” “Flood inundation areas,” and “Dense urban areas that are extremely dangerous during earthquakes” in order to compare with the living environment score that was calculated at the fourth-order census grid spatial unit, which is approximately 500 m square.

We created a cross-tabulation table between the presence or absence of disaster risk based on the three disaster classifications (henceforth, “landslide risk,” “flood

risk,” and “dense urban area”) and the change of population by age-group and conducted a chi-square test on these values. The results showed that, with the exception of the population change for the youth generation in regions with flood risk, significant relationships were found at the 5% significance level (Table 3.6). Residual analysis also showed significant population increases in areas with no landslide risk or areas corresponding to dense urban areas for both the youth generation and productive age generation. Basically, this could be interpreted as follows: given present-day population movement tendencies, landslide risk will decrease, but dense urban area risk due to building collapses and fires during earthquakes will not abate. Regarding flood risk, it cannot be said that the risk would increase or decrease for the youth generation, whereas population movements tended to increase in higher risk areas for the productive age population. If summarizing without considering disaster risk, then the results could be interpreted as follows: steep slopes are being avoided, whereas populations are returning to urban centers on flat land with dense populations. However, as mentioned above, this is not necessarily a change in direction that will lead to a reduction in disaster damage risk.

Similar results are also obtained when limiting the analysis scope to areas with a living environment score of 50 or higher and conducting the same chi-square test and residual analysis mentioned above (Table 3.7). Considering present-day population movement tendencies, residential promotion based on the living environment score does not produce a change in the direction of reducing disaster damage risk.

Summarizing the analysis in this section based on the above results, there currently was a tendency for significant population increases in census grids with flood risk and dense urban areas, with similar tendencies noted even when limited to census grids with a living environment score of at least 50, which are believed to have an attractive environment in terms of residential promotion. Essentially, even if residential promotion is conducted with the aim of developing compact cities, it is unlikely to contribute to disaster risk in particular.

When setting residential promotion areas in location normalization plans, although regions with disaster risk are generally excluded, in practice, existing urban areas are centered around such risky locations, and it may be unavoidable to conduct residential promotion even in areas with disaster risk, such as by planning soft measures like disaster prevention activities. Assuming that the population will decline in the medium to long term, it is considered that flood risk could be effectively reduced by prioritizing disaster prevention activities in areas around railway stations and hospitals, which have a large magnitude when calculating the living environment score (i.e., has a major impact on population changes). This means that we set a high priority to improve the disaster resilience of areas where it is highly probable that residential promotion will progress. Railway stations are locations with a larger non-permanent than permanent resident population, and hospitals are bases for life-saving and rescue activities. Thus, improving the disaster resilience of these surroundings is expected to effectively reduce the scale of damage beyond just a simple comparison of estimated affected populations based on population distributions.

Table 3.6 Relationship between population change and disaster risk by age-group.*Edited and reproduced from Ai (2021) Table 4

		Youth population		Productive age population	
		Increase	Non-increase	Increase	Non-increase
Landslide	$\chi^2 = 59.2$		$p = 0.00$	$\chi^2 = 130.6$	$p = 0.00$
	YES	2087	-7.71	1701	-11.44
Flood	NO	9002	7.71	8013	11.44
		$\chi^2 = 3.6$	$p = 0.16$	$\chi^2 = 22.1$	$p = 0.00$
Dense urban areas	Above floor	3859	1.63	5452	4.67
	Under floor	461	-1.22	719	415
	None	6769	-1.08	9938	5829
		$\chi^2 = 53.0$	$p = 0.00$	$\chi^2 = 52.8$	$p = 0.00$
	YES	191	7.33	122	172
	NO	10,898	-7.33	15,987	9542

Table 3.7 Relationship between population change and disaster risk in regions with high living environment score. *Edited and reproduced from Ai (2021)

		Youth population		Productive age population	
		Increase	Non-increase	Increase	Non-increase
		$\chi^2 = 49.8$	$p = 0.00$	$\chi^2 = 40.0$	$p = 0.00$
Landslide	YES	1024	-7.08	754	-6.35
	NO	5192	7.08	6304	6.35
Flood		$\chi^2 = 2.7$	$p = 0.26$	$\chi^2 = 16.1$	$p = 0.00$
	Above floor	2185	-0.04	2814	1950
	Under floor	245	-1.60	359	198
	None	3786	0.70	4825	2968
Dense urban areas		$\chi^2 = 37.5$	$p = 0.00$	$\chi^2 = 11.8$	$p = 0.00$
	YES	190	6.18	122	166
	NO	6026	-6.18	7876	4950

3.7 Conclusion

The living environment score focuses on various living environment indices and takes into account the magnitude of the influence of these indices on residence selection in order to assess the overall attractiveness of an area as a residence. In this section, we analyzed population increases from 2000 to 2010 in the Tokyo metropolitan area and attempted to calculate the living environment score at both the census grid and local district levels. The results showed that there was a significant expected population increase tendency in regions with a high living environment score. However, the accuracy rate was around 60%, and further improvements are needed in order to use this as a basis for decision-making.

Indices related to disaster safety have not been considered in the living environment score. Thus, when we verified the relationship between population-increase tendencies or the living environment score with disaster risk, it was suggested that population increases might continue in regions with flood risk or risks associated with dense urban areas. Disaster risk is something that people seek to minimize, and this should be considered as a property that is different from other living environment indices that should be pursued to an appropriate level. However, as mentioned above, it is imperative to improve the living environment score calculation method so that disaster risk can be reduced while improving accuracy.

References

- Arai Y, Ohki S (1999) Recent tendency of personnel transfers in Japan: new tabulation of the data of the third migration survey. *Komaba Stud Hum Geogr* 13:111–136. (in Japanese)
- Asami Y (ed) (2001) Residential environment: methods and theory for the evaluation. University of Tokyo Press, pp 17–22. (in Japanese)
- Kita Y (2017) Analysis on residential location choice and its evaluation indexes based on modal theory. *J Archit Plan (Trans AIJ)* 82(732):485–495. (in Japanese)
- Kiuchi N, Arita T, Tanaka N, Kawasaki N (2003) On home area definition and residential environment information acquisition of the government housing loan corporation contractors. *Urban Hous Sci* 43:162–167. (in Japanese)
- Koike S (2006) Mechanism of population decline as seen from regions. *Commun Oper Res Soc Jpn: Manag Sci* 51(1):30–36. (in Japanese)
- Maene M, Shimizu Y, Nakayama T (2012) Research on the change of living environment and land use in the northern Osaka suburb I: the analysis of residents’ living environment. *Proc AIJ Kinki Chap Archit Res Meet* 2012:445–448. (in Japanese)
- Ministry of Internal Affairs and Communications (2021) *2020 population census: basic statistics on population, summary of results*, p. 2 (in Japanese)
- Nishii S, Manabe R, Murayama A (2019) Policies and backgrounds for setting residential promotion areas in location normalization plans: through comparison of cities with contrasting area ratio of residential promotion area to urbanization promotion area. *J City Plann Inst Jpn* 54(3):532–538. (in Japanese)
- Ogawa H (2011) Characteristics of population dynamics of three major metropolitan area in population decline era: case study of the 2010 population census. *Proc AIJ Tohoku Chap Archit Res Meet* 74:223–228. (in Japanese)

- Sakamoto J (2020) An empirical analysis on the relationship between awareness of tsunami hazard risk and housing choice, travel mode. *J City Plann Inst Jpn* 55(3):836–842. (in Japanese)
- Warabi Y, Matsukawa T, Nakade B, Higuchi S (2019) Study on relation between urbanization promotion area and disaster risk area: focusing on comparison between original area and expanding area. *J City Plann Inst Jpn* 54(3):931–937. (in Japanese)

Chapter 4

Relationship Between Participation of Older Adults in Hobby Clubs and Sports Groups and Density of Neighborhood Facilities: A Case of Nagoya City Using JAGES Panel Data



Hongjik Kim, Kimihiro Hino, Hiroyuki Usui, Masamichi Hanazato,
Daisuke Takagi, Naoki Kondo, and Katsunori Kondo

Abstract Previous studies have suggested that the closer older adults live to urban facilities, the more likely they are to participate in recreational group activities. However, close proximity can also have a negative effect on participation. This study aimed to investigate the relationship between changes in the density of neighborhood facilities and changes in the participation of older Japanese adults. The data used in this study consisted of two waves of the Japan Gerontological Evaluation Study (JAGES) survey. The survey participants were not eligible for long-term public nursing care. The facilities were categorized as (1) leisure facilities; (2) cafés, pubs, and restaurants; (3) medical and welfare facilities; and (4) food stores. A multilevel ordered logistic model was used for the analysis. The results of this study indicate that several types of neighborhood facilities are associated with increased participation by older adults. However, light-hearted going out, especially during daily use of food stores, may have some limitations in promoting participation.

Keywords Social participation · Neighborhood facility · Promotion policy · Panel data · The Japan Gerontological Evaluation Study (JAGES)

H. Kim (✉) · K. Hino · H. Usui

Department of Urban Engineering, The University of Tokyo, Tokyo, Japan
e-mail: hj-kim@e.u-tokyo.ac.jp

M. Hanazato · K. Kondo

Center for Preventive Medical Sciences, Chiba University, Chiba, Japan

D. Takagi

Graduate School of Medicine, The University of Tokyo, Tokyo, Japan

N. Kondo

Department of Social Epidemiology, Kyoto University, Kyoto, Japan

4.1 Introduction

The importance of older adults' participation in group activities is increasing in countries with aging populations. Various administrative bodies, including the World Health Organization (World Health Organization 2007), are developing policies to promote the participation of older adults in group activities. Various types of group activities for older adults include hobbies, sports, community events, volunteering, and employment (Cabinet Office 2017). In particular, the effectiveness of hobbies and sports group activities in preventing care needs has been demonstrated (Kanamori et al. 2014), attracting attention from various fields, such as public health and administration. Furthermore, in Japan, although there is a high willingness among older adults to participate in hobbies and sports, the actual participation rate is low (Cabinet Office 2017).

Homes, community centers, and third places are locations where older people conduct and engage in group activities (Van den Berg et al. 2015). Third places are informal spaces where people interact socially (Oldenburg and Brissett 1982); these include public and commercial facilities, such as shopping malls (Jeffres et al. 2009). These facilities are expected to promote social interaction (Mouratidis 2018). Therefore, the establishment of these facilities near older adults' homes could aid in promoting activity participation.

Encounters outside third places also create opportunities for activity participation. According to a survey by the Ministry of Land, Infrastructure, Transport, and Tourism (Ministry of Land, Infrastructure, Transport, and Tourism 2015), older adults often go out for daily shopping, dining, socializing, and recreation. Additionally, the proportion of older adults attending medical appointments increases with age. Therefore, in addition to socialization and recreation, it is important to focus on shopping, dining, and medical appointments, which are among the main reasons for older adults going out.

Older adults tend to spend more time in their neighborhoods. The health of older adults is associated with social capital in the neighborhood, particularly social interactions. Furthermore, the distance that older adults can walk tends to decrease with age (Ministry of Land, Infrastructure, Transport, and Tourism 2015), and their walking ability is related to the frequency with which they go outdoors (Fujita et al. 2006). Owing to a decline in physical abilities, especially walking ability, the range of outings and social interactions among older adults is relatively small. Therefore, in an aging society, amenable neighborhoods are particularly important for older adults to promote walking and participating in group activities.

When considering a neighborhood environment conducive to activity participation for older adults from an urban structure perspective, the density of urban facilities (i.e., neighborhood facilities) in the vicinity is crucial. Facility density is not only related to the proximity of facilities in the neighborhood but also to the variety of choices available.

Previous studies have shown that neighborhood environment is related to the participation of older adults (Vaughan et al. 2016). In the case of neighborhood facilities, accessibility to facilities (such as grocery stores, recreational facilities, shopping malls, restaurants, cafés, and medical facilities) has been found to be positively related to older adults' activity participation (Levasseur et al. 2011; Richard et al. 2009, 2013). Thus, the more accessible the urban facilities are, the more easily older people can participate in group activities. However, if the distance to the facility is too short (e.g., if there are amenities on the ground floor of residential buildings), going to the destination may result in fewer opportunities for chance encounters or obtaining information about group activities. However, this was not considered in previous studies.

Most previous studies have used a cross-sectional design rather than a longitudinal design (Hand and Howrey 2019; Levasseur et al. 2011; Richard et al. 2009, 2013). Although cross-sectional surveys have shown that the density of neighborhood facilities is positively related to activity participation, it is not clear whether building additional facilities at the neighborhood scale results in greater participation by older adults. Therefore, a longitudinal survey is necessary to investigate how changes in the density of neighborhood facilities are related to changes in older adults' activity participation. If the increase in facility density is related to an increase in the frequency of activity participation, this provides empirical evidence that the establishment of urban facilities near older adults' homes is a policy option for facilitating participation in recreational group activities.

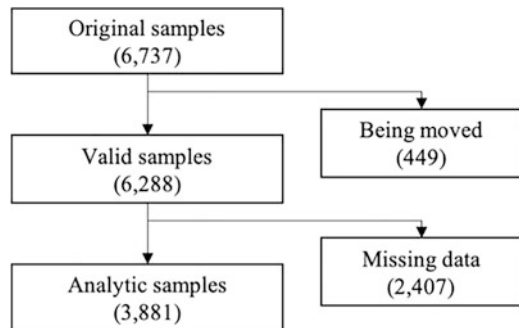
This study investigates the relationship between the density of neighborhood facilities and older adults' participation in hobby clubs and sports groups using panel data. The rest of the manuscript is organized as follows. Section 4.2 describes the target area and data. Section 4.3 describes the analytical methods used in the study. Section 4.4 presents and discusses the results. Finally, Sect. 4.5 presents the conclusions in the study, with additional policy implications.

4.2 Materials and Methods

4.2.1 Dataset

Panel data collected by the Japan Gerontological Evaluation Study (JAGES) in 2010 and 2016 were employed for the longitudinal analysis. The JAGES conducted a nationwide survey targeting older adults in 31 municipalities every 3 years from the 2010 survey, and the group surveyed approximately 180,000 people from 41 municipalities in 2016. The extraction was performed by municipality, and randomly sampled older adults were surveyed using questionnaires (see Kondo 2016 for more details). Given that the responses surveyed in different years were linked to each person, older adults' activity participation can be observed and traced using panel data. Among the 20 municipalities surveyed by the JAGES in both 2010

Fig. 4.1 Flowchart summarizing the selection of analytic samples



and 2016, Nagoya is one of three major metropolitan areas with a high population density (70 people/ha). This study aimed to investigate whether it is difficult to increase older adults' activity participation in areas where facility density is too high. This indicates that the distance to the nearest facility is too short (Koshizuka 1985). Thus, an area with a high level of facility density is required for the study area. Therefore, Nagoya was selected as the study area.

As shown in Fig. 4.1, several responses were excluded because the participants moved to another elementary school district within the study area (449 responses); this eliminates the effect of residence relocation. The relocation of older adult residences represents a process of selective migration. Several responses (2407) were also excluded because of missing data in the questionnaire items regarding the frequency of activity participation. Missing data for individual attributes other than participation in activities were included in the analysis as missing values. Therefore, the analytical sample consisted of 3881 responses. The average number of responses per elementary school was 14.8, and its standard deviation was 6.9. Nagoya comprises 262 elementary school districts. In the case of 200 neighborhoods, the level of 10 samples in each neighborhood was sufficient for model estimation without bias (Clarke and Wheaton 2007). According to this standard, the number of samples was sufficient to estimate a model.

The targets of the JAGES were people aged 65 years and older who did not require long-term nursing care services. The percentage of males within the analytic samples is 50.7%, and the average age and its standard deviation is 71.1 ± 4.66 (years). The characteristics of individuals, such as education, income, household type, walking ability, relationships with neighbors, and frequency of meeting friends, as well as their gender and age, were used as the control variables. These are assumed to be time-invariant variables, and the model uses the covariates measured in 2010.

4.2.2 Neighborhood Environment

The area where older adults spend their time in daily life has two levels of area (Nishino and Omori 2014): (1) the elementary school district (a scale of areas in which older adults can easily walk) and (2) the junior high school district (an area composed of two or three elementary school districts). The elementary school district in which individuals lived was used as a neighborhood unit to investigate the relationship between activity participation and neighborhood environment. Figure 4.2 illustrates the 262 elementary school districts in Nagoya.

The neighborhood environment was assessed by facility density, population density, and percentage of people aged 65 years and older estimated for each elementary school district (Table 4.1). Population density and the percentage of people aged 65 years and older were calculated based on the 2010 census survey. The high population density and high percentage of older adults indicate that there could be many peers with whom to conduct group activities, as well as the great availability of urban services owing to the large population.

Facility data from a telephone directory with associated location information (Zenrin Co., Ltd., Telepoint Pack!) for 2010 and 2016 were linked to the questionnaire responses. This was used to assess the density of facilities in the neighborhood and its changes. Facilities were grouped into (1) recreational facilities (libraries, movie theaters, adult education classes, karaoke boxes, sports facilities, fitness clubs, Mahjong clubs, community centers, etc.), (2) eating places (cafés, pubs, restaurants), (3) medical and welfare facilities (hospitals, welfare facilities for older

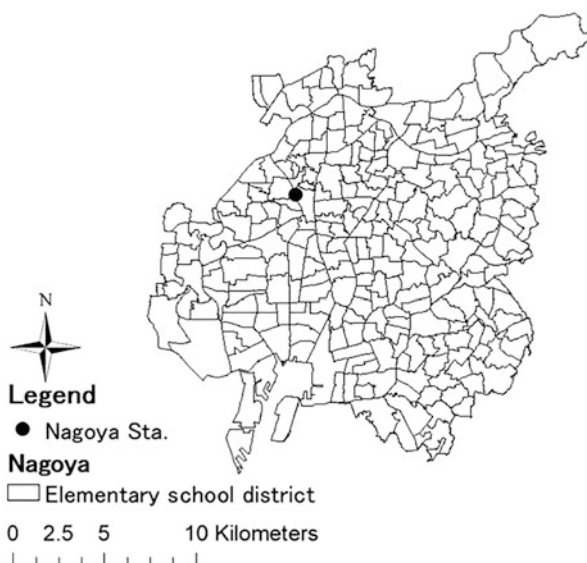


Fig. 4.2 Nagoya and its 262 elementary school districts

Table 4.1 Neighborhood-level variables

	Mean \pm SD
Population density (people/ha)	89.1 \pm 33.6
Percentage of people who aged 65 years and older	0.21 \pm 0.04
Facility density (facilities/ha)	
Recreational facilities	0.12 \pm 0.13
Eating places	0.50 \pm 0.72
Medical and welfare facilities	0.18 \pm 0.16
Food stores	0.13 \pm 0.11
Changes in facility density (facilities/ha)	
Recreational facilities	-0.02 \pm 0.03
Eating places	-0.11 \pm 0.12
Medical and welfare facilities	0.00 \pm 0.04
Food stores	-0.02 \pm 0.04

Note. The neighborhood is organized into 262 elementary school districts where individuals live.
SD: standard deviation

adults), or (4) food stores (grocery stores, convenience stores, and supermarkets). These facilities are places older adults can go to and interact with each other. The number of public recreational facilities was smaller than that of other categories, such as food stores. Recreational facilities include both public and private facilities. Public recreational facilities accounted for less than 10% of the total number of recreational facilities.

4.2.3 Frequency and Changes in Activity Participation

The two dependent variables were the frequency of participation in hobby clubs and sports groups. These variables were assessed using items from the survey regarding the frequency of respondent participation in hobbies or sports groups. The frequency of activity participation was answered on a six-point scale (four times a week or more, two to three times a week, once a week, once to three times a month, several times a year, and not participating).

To secure a certain number of participants, the frequency of activity participation was reclassified into three categories: (1) once a week or more, (2) several times a month or year, and (3) not participating. More precisely, participating in group activities four times a week and more, two to three times a week, and once a week are grouped into “once a week and more,” on the other hand, one to three times a month and several times a year are grouped into “several times a month or year.” Not participating remains as a category “not participating.” These reclassified categories corresponded to high and low frequencies of activity participation and no participation, respectively. This enables the model to assess

changes among participation levels in terms of frequency rather than changes within a high frequency of activity participation.

Based on the reclassified categories, changes in the frequency of activity participation of individual i living in area j between 2010 and 2016 were defined as follows:

$$\Delta y_{ij} = \begin{cases} 3, & \text{if } y_{ij}^{2016} - y_{ij}^{2010} > 0 \\ 2, & \text{if } y_{ij}^{2016} - y_{ij}^{2010} = 0 \\ 1, & \text{if } y_{ij}^{2016} - y_{ij}^{2010} < 0 \end{cases} \quad (4.1)$$

where y_{ij}^{2010} and y_{ij}^{2016} indicate the frequency of participation in activities of individual i living in area j in 2010 and 2016, respectively. Consequently, the changes in the frequency of activity participation are defined as “increase” if $\Delta y_{ij} = 3$, “no change” if $\Delta y_{ij} = 2$, and “decrease” if $\Delta y_{ij} = 1$.

4.3 Analytic Method

Multilevel ordinal logistic regression was used because of the non-uniformity of the samples and their hierarchical structure as well as ordinal dependent variables. The regression model was expressed as follows:

$$\log \frac{p(\Delta y_{ij} \geq c | X_s, Z_t, u_j)}{p(\Delta y_{ij} < c | X_s, Z_t, u_j)} = \alpha_c + \sum_s \beta_s X_s + \sum_t \gamma_t Z_t + u_j \quad (4.2)$$

where categories for the changes in the frequency of participation are denoted by $c(\in\{1, 2, 3\})$ and α_c indicates the intercept for category c . The random effect (which controls for the effects of other unobserved neighborhood-level variables of area j) is denoted by u_j . The numbers of individual- and neighborhood-level variables are denoted as s and t , respectively. Coefficient β_s indicates s -th individual-level variable X_s , and γ_t denotes t -th neighborhood-level variable Z_t .

The individual-level variables (a set of X_s) comprised both y_{ij}^{2010} and control variables (such as gender, age, education, income, household type, walking ability, relationships with neighbors, and frequency of meeting friends). Owing to the fact that there could possibly be differences in the increases and/or decreases (among the levels of the frequency of activity participation), y_{ij}^{2010} is included in the model. Meanwhile, neighborhood-level variables (a set of Z_t) are composed of demographic neighborhood-level variables (population density and percentage of people aged 65 years and older) and facility density. In addition, the neighborhood-level variables regarding facility density are composed of density of existing (observed in 2010) neighborhood facility of type k in area j (which is denoted by F_{jk}), change in density between 2010 and 2016 (which is denoted by ΔF_{jk}), and interaction term of the two ($F_{jk} \Delta F_{jk}$). Given that the interaction term is included,

each neighborhood-level variable is mean centered to avoid multicollinearity issues. All facility-related variables were simultaneously included at the same time.

The interaction term enables the model to express the nonlinear relationship between the frequency of activity participation and facility density. The interaction term is positive when both F_{jk} and ΔF_{jk} (mean-centered variables) have positive or negative values. When the interaction term is positively related to the change in the frequency of activity participation, a greater likelihood of participation is shown in neighborhoods where the number of facilities increases in areas with a high density of existing facilities, or their number decreases in areas with low density; this indicates a U-shaped relationship. However, the interaction term has a negative value when either F_{jk} or ΔF_{jk} has a positive value and the other has a negative value. When the interaction term shows a negative coefficient, there is a greater likelihood of participation in the neighborhood where the number of facilities decreases in the area with a high density of existing facilities, or their number increases in the area with a low density, indicating an inverted U-shaped relationship. In this case, there may be a certain facility density with the highest likelihood of increasing the frequency of participation in activities.

The model tests the relationship between the neighborhood environment and changes in the frequency of activity participation. From the model, $p(\Delta y_{ij} = 3)$ indicates that the probability of an increase in the frequency of activity participation can be expressed as a function of F_{jk} and ΔF_{jk} . Given that the model expresses Δy_{ij} using F_{jk} and ΔF_{jk} , the function is denoted as $\Delta y_{ij}(F_{jk}, \Delta F_{jk})$. The amount of change in $p(\Delta y_{ij} = 3)$ when the facility density increases slightly is the marginal effect of the density of neighborhood facilities, and is defined as follows:

$$\text{Marginal effect} = \frac{\partial p(\Delta y_{ij}(F_{jk}, \Delta F_{jk}) = 3)}{\partial F_{jk}} \quad (4.3)$$

The marginal effect enables the model to determine the density at which the likelihood of an increase in the frequency of activity participation has the highest/lowest value.

To facilitate the participation of older adults in recreational group activities, a sufficient level of facility density F_{jk}^* can be defined as the density at which the likelihood of an increase in the frequency of activity participation has the highest value. A sufficient level F_{jk}^* is found by the extremum \hat{F}_{jk} where the marginal effect is equal to 0.

$$\frac{\partial p(\Delta y_{ij}(F_{jk}, \Delta F_{jk}) = 3)}{\partial F_{jk}} = 0, \text{ where } F_{jk} = \hat{F}_{jk} \left(0 \leq \hat{F}_{jk} \leq \max F_{jk} \right) \quad (4.4)$$

Since it is hard to solve \hat{F}_{jk} analytically, it is numerically solved.

The analysis was conducted in three steps. First, multilevel ordinal logistic regression models were used to test the relationship between older adults' partici-

pation in hobbies and sports groups and the density of neighborhood facilities using panel data. It also tested whether a nonlinear relationship existed between the two. Finally, it estimates the density of facilities where the likelihood of an increase in the frequency of activity participation has the highest value based on the model, and visualizes the neighborhoods where a sufficient number of facilities are located.

4.4 Results and Discussion

4.4.1 *Change in the Frequency of Activity Participation Between 2010 and 2016*

Table 4.2 shows the frequency of participation in hobbies and sports groups in 2010 and 2016. Comparing the frequency of participation between the two time points, more people were found to not participate in hobbies clubs, even though the number of people participating at least once a week increased slightly (once a week or more: 1073 to 1094; several times a month or year: 935 to 843; not participating: 1873 to 1944). On the other hand, in the case of sports groups, the number of participants increased (once a week or more: 1002 to 1129 people; several times a month or year: 399 to 482 people; not participating: 2480 to 2270).

Table 4.3 shows the changes in the frequency of activity participation at each participation frequency level in 2010. Regarding the frequency of participation in hobby clubs, older adults showed an increase (620 responses; 16.0%), no change (2563 responses; 66.0%), and a decrease (698 responses; 18.0%). In terms of the frequency of participation in sports groups, older people showed an increase (552 responses; 14.2%), no change (2968 responses; 76.4%), and a decrease (361 responses; 9.3%). This indicates that older adults who do not need long-term nursing care services are able to continue participating in group activities, and some find and start new activities (Agahi et al. 2006).

Table 4.2 Frequency of participation in recreational group activities

	2010	2016
Hobby clubs		
Once/week and more	1073 (27.6)	1094 (28.2)
Several/month or year	935 (24.1)	843 (21.7)
Not participating	1873 (48.3)	1944 (50.1)
Sports groups		
Once/week and more	1002 (25.8)	1129 (29.1)
Several/month or year	399 (10.3)	482 (12.4)
Not participating	2480 (63.9)	2270 (58.5)

Table 4.3 Changes in the frequency of participation in recreational group activities from 2010 to 2016 ($N = 3881$)

	Increase	No change	Decrease
Hobby clubs			
Once/week and more	–	660 (17.0)	413 (10.6)
Several/month or year	237 (6.1)	413 (10.6)	285 (7.3)
Not participating	383 (9.9)	1490 (38.4)	–
Total	620 (16.0)	2563 (66.0)	698 (18.0)
Sports groups			
Once/week and more	–	756 (19.5)	246 (6.3)
Several/month or year	108 (2.8)	176 (4.5)	115 (3.0)
Not participating	444 (11.4)	2036 (52.5)	–
Total	552 (14.2)	2968 (76.4)	361 (9.3)

4.4.2 Relationships Between Participation and Facility Density

Table 4.4 presents the odds ratios (e^{γ_i}) estimated using this model. The odds ratio for population density (people/ha) indicates the likelihood of a change in the frequency of activity participation when 100 units increase, and the odds ratio for the percentage of older adults indicates the likelihood of change when the percentage increases by 1%. Regarding facility densities (people/ha), the odds ratios are the likelihood of a change in participation frequency when a facility is additionally built in an area comprising 10 ha.

Residents living in neighborhoods with larger populations are more likely to have relationships with those living in the same neighborhood (Boessen et al. 2018). However, population density and percentage of older adults were found to show insignificant relationships with changes in the frequency of participation in hobby clubs and sports groups. In densely populated urban areas (such as Nagoya), differences in population density and percentage of older adults between neighborhoods are not related to the ease of older adults' participation in recreational group activities. In other words, older residents living in urban areas do not suffer from a lack of colleagues or peers to conduct group activities. This suggests that the number of candidates for a group activity does not critically impact the likelihood of an increase in participation frequency once the number reaches a certain level.

The density of existing recreational facilities and their changes were found to show a negative relationship with an increase in participation in hobby clubs or sports groups (for hobby clubs, odds ratios: 0.80, 0.69, respectively; for sports groups, odds ratios: 0.76, 0.68, respectively). Even though public recreational facilities such as community centers function as places for facilitating social interactions among older adults (Hino and Ishii 2014; Makino and Imai 1999), most recreational facilities include private facilities (such as karaoke boxes, fitness clubs, and adult education classes). Although private recreational facilities provide

Table 4.4 Estimates [and 90% Confidence Intervals] for the odds ratio (e^{β_i}) of the changes in the frequency of participation in hobby clubs and sports groups ($N = 3881$)

	(1) Hobby clubs	(2) Sports groups
Population density ^a	0.94 (0.76–1.17)	0.83 (0.64–1.07)
Percentage of people who aged 65 and older ^b	1.00 (0.99–1.01)	0.99 (0.97–1.01)
Facility density		
Recreational facilities	0.80 (0.69–0.93)*	0.76 (0.63–0.91)*
Eating places	1.05 (1.01–1.08)*	1.10 (1.05–1.14)*
Medical and welfare facilities	1.11 (1.02–1.20)*	0.94 (0.86–1.04)
Food stores	0.89 (0.76–1.03)	0.90 (0.76–1.08)
Changes in facility density		
Recreational facilities	0.69 (0.52–0.92)*	0.68 (0.48–0.96)*
Eating places	1.07 (0.98–1.16)	1.01 (0.91–1.12)
Medical and welfare facilities	1.00 (0.79–1.25)	0.70 (0.54–0.92)*
Food stores	0.95 (0.71–1.27)	1.34 (0.95–1.91)
Facility density × changes in facility density		
Recreational facilities	1.03 (0.94–1.13)	1.01 (0.91–1.13)
Eating places	1.00 (1.00–1.00)	1.01 (1.00–1.01)
Medical and welfare facilities	1.08 (1.00–1.17)*	1.10 (1.00–1.20)*
Food stores	0.91 (0.77–1.08)	0.78 (0.64–0.96)*
AIC	5972.836	4784.692

Note. ^aOdds ratio when 100 units (people/ha) increased. ^bOdds ratio when the percentage increased by 1%. Odds ratio other than a and b occurred when 0.1 units (facility/ha) increased

* $p < 0.1$

activities that meet a variety of needs, this suggests that it is difficult to build social interaction in these facilities and that it could possibly be an obstacle.

On the other hand, areas with a high density of eating places were found to be positively associated with an increase in the frequency of participation in hobby clubs and sports groups (hobby clubs, odds ratio: 1.05; sports groups, odds ratio: 1.10). In the case of densely developed urban areas, there are few places where older people can relax and have conversations; however, eating places (such as cafés, pubs, and restaurants) provide opportunities for social interaction that promote their participation in sports groups, as well as hobby clubs.

However, an increase in the density of eating places was found to have an insignificant relationship with an increase in participation frequency. Although eating places provide places for social interaction, they do not form new social connections; therefore, an increased number of eating places in the neighborhood may not lead to further participation in group activities. Therefore, if the local government aims to encourage activity participation through eating places, it is necessary to create opportunities for collaboration with eating place operators.

In terms of medical and welfare facilities, the relationships between facility density and increase in participation frequency were found to differ between hobby clubs and sports groups. In the case of hobbies clubs, older adults living in areas

with a high density of medical and welfare facilities were more likely to participate (odds ratio: 1.11). In areas with a high density of existing medical and welfare facilities, older adults showed a positive relationship with increased participation in hobby clubs when the density increased further (odds ratio: 1.08). Interventions involving collaboration with local health sectors provide opportunities for older adults to participate in hobbies (Haseda et al. 2019; Hosokawa et al. 2019).

On the other hand, in the case of sports groups, increases in the density of medical and welfare facilities are found to show a negative relationship with the increases in the participation frequency (odds ratio: 0.70). However, in areas with a high density of existing medical and welfare facilities, older adults showed a positive relationship with an increase in participation in sports groups when the density increased further (odds ratio: 1.10). These are possible reasons why the density of medical and welfare facilities is related to participation in sports groups, even though the analytic samples included older adults who did not need long-term nursing care services.

In neighborhoods where the number of older adults with limited functional ability is relatively small, people living in the neighborhood, including healthy older adults, may have a negative perception of participation in recreational group activities. Therefore, it is difficult for participation frequency to increase because of fear of their peers' negative judgment. In other words, there could be factors that cause older adults to hesitate to participate. However, as the number of medical and welfare facilities increases, both the presence of older people with limited functional ability and participation in the prevention of functional disability become more common, and older adults may start to have health awareness, which positively influences participation in activities. By contrast, in neighborhoods with a low density of medical and welfare facilities, people are less likely to have a negative image of activity participation. Therefore, they show a higher likelihood of increased participation frequency than neighborhoods where factors that make older adults hesitate to participate in group activities exist. Consequently, there is a U-shaped relationship between the density of medical and welfare facilities and increases in the frequency of participation in sports groups (i.e., a higher likelihood of increases in participation frequency in neighborhoods with both a low and high level of facility density and a relatively lower likelihood in neighborhoods with a middle level of facility density).

In the case of food stores, older adults living in neighborhoods where the number of facilities increased in areas with a high density of existing facilities or decreased in areas with low density were found to be more likely to participate in sports groups (odds ratio: 0.78). This finding suggests that food store density may be sufficient to facilitate older adults' participation in sports. A high food store density means that the average distance to the destination is short when leaving home in daily life. In this case, there are few opportunities for social interaction and conversation. As an extreme example, people living in residential-commercial buildings, which are residential buildings with commercial uses on the ground floor, can easily visit these buildings for grocery shopping; however, going out rarely creates opportunities for chance encounters or obtaining information about sports group activities, owing to the short distance to the ground floor. The same is true at the neighborhood

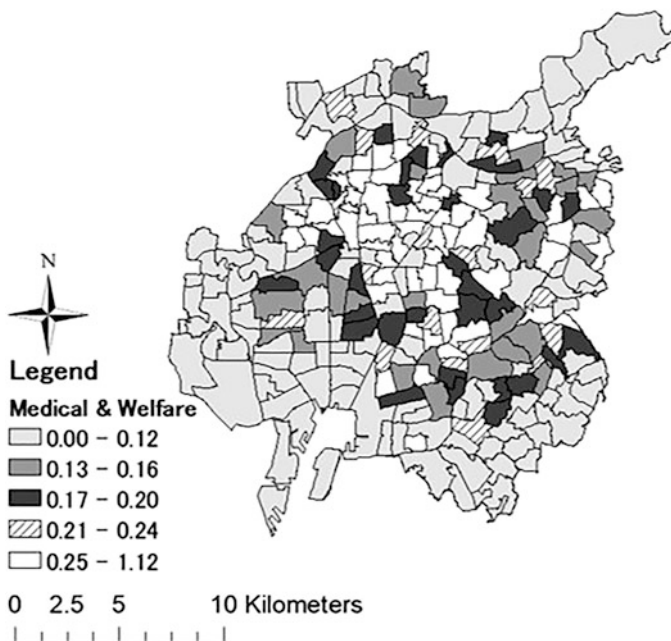


Fig. 4.3 Elementary school districts with the density of medical and welfare facilities where the likelihood of the increase in the frequency of participation in hobby clubs and sports groups is close to the local minimum (black colored areas)

scale. However, if the average distance is too long, willingness to go out decreases; therefore, the likelihood of an increase in participation frequency also decreases.

An extremum in the probability of an increase in participation frequency was found only in the cases of medical and welfare facilities and food stores. Figures 4.3 and 4.4 show neighborhoods (elementary school districts are colored black) with facility density where the likelihood of an increase in activity participation is close to the extremum (i.e., the marginal effect on the increase in participation frequency is close to 0). The density of medical and welfare facilities, where the likelihood of an increase in the frequency of participation in hobby clubs and sports groups has the lowest value, is estimated to be approximately 0.18 facilities/ha. In the case of food stores, the density, where the likelihood of an increase in the frequency of participation in hobby clubs and sports groups has the highest value, is estimated to be approximately 0.22 facilities/ha. In terms of geographical distribution, neighborhoods with facility density (both medical and welfare facilities and food stores) close to the extremum are located more than 2 km from Nagoya Station, which is close to the commercial center of Nagoya.

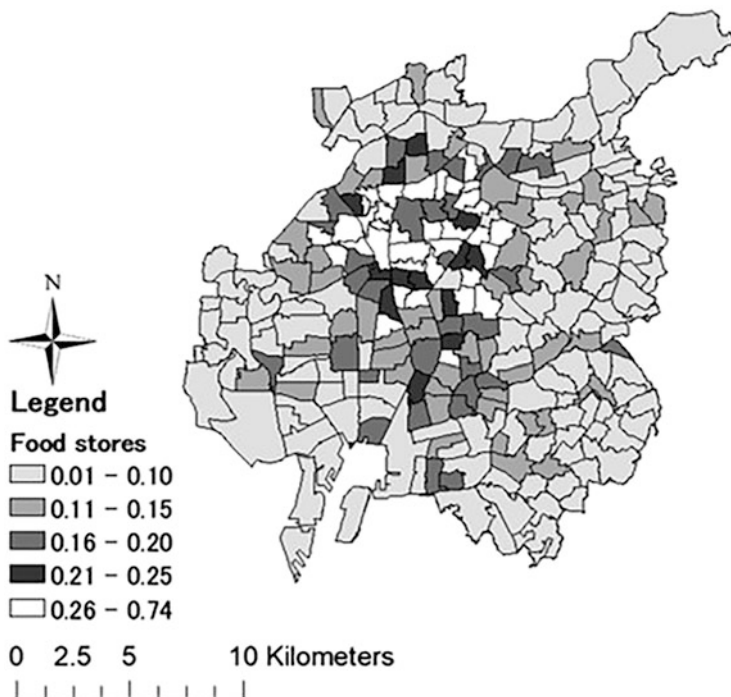


Fig. 4.4 Elementary school districts with a sufficient level of density of food stores in terms of older adults' participation in sports groups. Black colored areas indicate the neighborhoods with facility density where the likelihood of the increase in the frequency of participation in sports groups is close to the local maximum

4.5 Conclusion

This study investigated the relationship between the density of neighborhood facilities and changes in the frequency of older adults' participation in hobby clubs and sports groups. The results of the analysis using panel data to consider self-selection bias indicate that the density of urban facilities is related to participation of older adults in recreational group activities, not just the frequency of their activity participation. In other words, building additional facilities in urban areas at the neighborhood scale can be a solution to promote older adults' participation in recreational group activities, even though its impact on facilitating activity participation could possibly decrease.

In the case of food stores, an inverted U-shaped relationship was found between facility density and increased frequency of participation in sports groups (i.e., a closer distance to food stores is not always better in terms of facilitating older adults' participation in sports groups). In an aging society, it is necessary to consider the opportunities that help form new social connections, as well as proximity to

food stores, when policymakers consider the neighborhood environment in which residents can easily shop groceries. For example, in addition to online shopping and home delivery services, it is necessary to focus on the social exchanges involved in shopping among older adults who are unable to shop.

However, there are some limitations because the facility density (the density of unweighted point features) is used to assess each type of facility. When building urban facilities, the scale, attractiveness, and number of facilities are important. In addition, given that it is difficult to obtain detailed information about the geographical location of older adults' homes, elementary school districts where they reside are used as neighborhood units. Therefore, it is unclear exactly how far away urban facilities can still have an effect on older adults' participation. The scale, service quality, and attractiveness of each facility could also be related to the distance that each facility can affect; however, these aspects were not considered in this study. Further studies that consider these issues are warranted.

References

- Agahi N, Ahacic K, Parker MG (2006) Continuity of leisure participation from middle age to older age. *J Gerontol B Psychol Sci Soc Sci* 61(6):S340–S346
- Boessen A, Hipp JR, Butts CT, Nagle NN, Smith EJ (2018) The built environment, spatial scale, and social networks: do land uses matter for personal network structure? *Environ Plan B Urban Anal City Sci* 45(3):400–416
- Cabinet Office (2017) Annual report on the ageing Society; 2017. https://www8.cao.go.jp/kourei/english/annualreport/2017/2017pdf_e.html
- Clarke P, Wheaton B (2007) Addressing data sparseness in contextual population research: using cluster analysis to create synthetic neighborhoods. *Sociol Methods Res* 35(3):311–351
- Fujita K, Fujiwara Y, Chaves PH, Motohashi Y, Shinkai S (2006) Frequency of going outdoors as a good predictors for incident disability of physical function as well as disability recovery in community-dwelling older adults in rural Japan. *J Epidemiol* 16(6):261–270
- Hand CL, Howrey BT (2019) Associations among neighborhood characteristics, mobility limitation, and social participation in late life. *J Gerontol B Psychol Sci Soc Sci* 74(3):546–555
- Haseda M, Takagi D, Kondo K, Kondo N (2019) Effectiveness of community organizing interventions on social activities among older residents in Japan: a JAGES quasi-experimental study. *Soc Sci Med* 240:112527
- Hino K, Ishii N (2014) Utilization of third places among elderly people and their significance. *J Archit Plan* 79(705):2471–2477
- Hosokawa R, Kondo K, Ito M, Miyaguni Y, Mizutani S, Goto F, Abe Y, Tsuge Y, Handa Y, Ojima T (2019) The effectiveness of Japan's community centers in facilitating social participation and maintaining the functional capacity of older people. *Res Aging* 41(4):315–335
- Jeffres LW, Bracken CC, Jian G, Casey MF (2009) The impact of third places on community quality of life. *Appl Res Qual Life* 4:333–345
- Kanamori S, Kai Y, Aida J, Kondo K, Kawachi I, Hirai H, Shirai K, Ishikawa Y, Suzuki K, JAGES Group (2014) Social participation and the prevention of functional disability in older Japanese: the JAGES cohort study. *PLoS One* 9(6):e99638
- Kondo K (2016) Progress in aging epidemiology in Japan: the JAGES project. *J Epidemiol* 26(7):331–336
- Koshizuka T (1985) On the relation between the density of urban facilities and the distance to the nearest facility from a point in a given area. *J City Plan Inst Jpn* 20:85–90

- Levasseur M, Gauvin L, Richard L, Kestens Y, Daniel M, Payette H, NuAge Study Group (2011) Associations between perceived proximity to neighborhood resources, disability, and social participation among community-dwelling older adults: results from the VoisiNuAge study. *Arch Phys Med Rehabil* 92(12):1979–1986
- Makino Y, Imai N (1999) The place where the elderly relaxing and pleasuring viewed from the residential style of the elderly. *J Archit Plan* 64(522):131–138
- Ministry of Land, Infrastructure, Transport, and Tourism (2015) National survey on urban transportation characteristics. https://www.mlit.go.jp/toshi/tosiko/toshi_tosiko_fr_000024.html
- Mouratidis K (2018) Built environment and social well-being: how does urban form affect social life and personal relationships? *Cities* 74:7–20
- Nishino T, Omori K (2014) A case study of senior care services area settings based on junior high school districts: a comparative study of official service area settings and actual living spheres of the elderly in a regional core city. *J Archit Plan* 79(699):1109–1118
- Oldenburg R, Brissett D (1982) The third place. *Qual Soc* 5(4):265–284
- Richard L, Gauvin L, Gosselin C, Laforest S (2009) Staying connected: neighbourhood correlates of social participation among older adults living in an urban environment in Montreal, Quebec. *Health Promot Int* 24(1):46–57
- Richard L, Gauvin L, Kestens Y, Shatenstein B, Payette H, Daniel M, Moore S, Levasseur M, Mercille G (2013) Neighborhood resources and social participation among older adults: results from the VoisiNuage study. *J Aging Health* 25(2):296–318
- Van den Berg P, Kemperman A, De Kleijn B, Borgers A (2015) Locations that support social activity participation of the aging population. *Int J Environ Res Public Health* 12(9):10432–10449
- Vaughan M, LaValley MP, AlHeresh R, Keysor JJ (2016) Which features of the environment impact community participation of older adults? A systematic review and meta-analysis. *J Aging Health* 28(6):957–978
- World Health Organization (2007) Global age-friendly cities: a guide. Retrieved from <https://apps.who.int/iris/handle/10665/43755>

Chapter 5

Environmental Factors Causing Inconvenience of Store Accessibility for Older Adults in Tokyo: Objective Indicators of Road Environments for Estimating People's Inconvenience



Tatsuya Sekiguchi

Abstract The problem of disadvantaged shoppers has become more serious in Japan. People feel difficulties for grocery shopping. Inconvenience of store accessibility is a factor of the difficulties. To address this problem, it is necessary to specify the elements in the concepts. However, few studies have focused on factors other than distance.

Focusing the older adults, this study aims to (1) clarify the characteristics of dissatisfaction with various road environments, (2) clarify what kinds of road environment dissatisfaction affect inconvenience, and (3) to develop decision tree models that estimate people's dissatisfaction with the objective condition.

A series of analyses were conducted based on data from an online questionnaire survey. First, the results indicated that the degree of tolerance and the amounts of each road elements were related to dissatisfaction. Elderlies tend to avoid several elements. Second, several road element can lead to inconveniences in accessing stores. Additionally, we created decision tree models by combining these data with indicators of objective road conditions. These models provided the threshold values of the objective conditions that significantly changed the subjective evaluation. These results allow us to compare the conditions of regions more efficiently or to identify regions requiring a more detailed survey.

The contents of this paper are based on the following paper originally published in a Japanese journal: Sekiguchi, T. (2023) Factors of inconvenience of store accessibility for older adults in Tokyo: Objective indicators and thresholds for estimating dissatisfaction of road environments that cause the inconvenience. MERA Journal 46(3): 1–10 (in Japanese).

T. Sekiguchi (✉)

Graduate School of Life and Environmental Sciences, Kyoto Prefectural University, Kyoto, Japan
e-mail: ta-sekiguchi@kpu.ac.jp

Keywords Disadvantaged shoppers · Road environments · Questionnaire survey · Subjective evaluation · Objective indicator · Inconvenience of store accessibility

5.1 Introduction

5.1.1 *Background and Purpose of Study*

The “disadvantaged shopper” problem, where an increasing number of people in a region experience difficulty in daily grocery shopping, has recently become a social issue in Japan. In the administrative context, the term “disadvantaged shopper” has varied ambiguous meanings, such as “elderly people who feel inconvenienced in purchasing groceries” or “people who feel dissatisfied with the shopping environment” (Ministry of Internal Affairs and Communications 2017; Hachioji City 2013). Therefore, the disadvantaged shopper problem is often investigated and evaluated by using subjective indices such as “inconvenience of the shopping” or “the dissatisfaction of the store” (Hirai and Minami 2013; Yakushiji et al. 2013; Sekiguchi and Hino 2021). In addition, studies have pointed out that negative subjective evaluations of the food shopping environment lead to less frequent shopping and inadequate food intake, causing health problems (Sekiguchi and Hino 2021; Hino 2002; Nakamura and Asami 2019).

In Japan, a practical approach for improving this problem is “ensuring accessibility to grocery stores” or “decreasing the inconvenience.” However, treating “accessibility” and “inconvenience” as fuzzy concepts prevents the development of concrete countermeasures. It is, therefore, necessary to specify the elements in these concepts. Previously, “distance to stores” has been regarded as the main factor of inconvenience of accessibility globally (Nakamura and Asami 2019; Larsen and Gilliland 2008; Russell and Heidkamp 2011). However, several studies have indicated out the influence of factors other than distance (Sekiguchi and Hino 2021; Takeshima 2007), which must be analyzed when considering these concepts.

This study aimed to answer the following research questions (RQs) based on the results of an online questionnaire survey and the spatial data of road elements in the Tokyo metropolitan area.

- (RQ1) Clarify conditions that cause dissatisfaction with each road element
- (RQ2) Clarify road elements that cause inconvenience of accessibility to the store
- (RQ3) Develop statistical models to describe the objective conditions that cause dissatisfaction with the important road elements using specific objective indicators

We focused on multiple road elements that could become obstacles to traveling to stores, including distance. Additionally, negative evaluations of each element are considered as “dissatisfaction.” Our analysis is based on the subjective evaluation structure that dissatisfaction with multiple or single elements of the road environment causes “inconvenience” of accessibility.

Clarifying these RQs will enrich our understanding of store accessibility inconvenience, which is conventionally treated as an abstract concept. Moreover, it helps to create appropriate and concrete countermeasures to overcome disadvantaged shoppers' difficulties. This study will provide a new perspective in the field of research dealing with the issue of disadvantaged shoppers.

5.1.2 *Literature Review*

Previously, “distance to stores” was regarded as a main factor contributing to the inconvenience of accessibility globally (Nakamura and Asami 2019; Larsen and Gilliland 2008; Russell and Heidkamp 2011). However, in addition to distance, elderly people with declined mobility skills due to aging find other road elements as problems (Takeshima 2007; Shibata et al. 2017; Matsumura et al. 2021).

Several studies have attempted to clarify the specific conditions that cause negative evaluation. Kato et al. (1995) studied the width and slope of sidewalks, whereas Nitta et al. (2004) studied the evaluations of elderly people on slopes and clarified the objective condition of these road elements in which they feel burdened. However, in travel situations such as shopping, people set the travel routes between the starting point and destination. Therefore, the amount and distribution of each element along the route are important; however, existing studies did not consider these points.

This study quantitatively analyzed the relationship between “inconvenience” in visiting stores and “dissatisfaction” with various road elements. In addition, we extract threshold values of each road elements that may lead to dissatisfaction. Clarifying the objective conditions that affect people's negative evaluation of the shopping route will help to set a target value for how much improvement of the road environments is needed and develop an efficient maintenance plan that considers the balance of the entire route, such as focusing on improving the specific sidewalks used by numerous people.

5.2 Materials and Methods

5.2.1 *The Survey Area and Overview*

The study area was the Tokyo metropolitan area, excluding island areas. This capital area of Japan has the highest population and well-developed public transportation system. People do not depend on cars, and high-density stores are located within walking distance, resulting in a high percentage of people who go shopping on foot. Due to such urban characteristics, road environment factors other than distance are considered problems during shopping travel.

Table 5.1 Demographic attributes of the respondents

Attributes	All respondents	Elderly people
Area of residence		
Tokyo 23 wards	773	381
Suburban Tokyo	227	119
Gender		
Male	544	312
Female	456	188
Age		
Under 65	500	0
65–74	431	431
75–79 (over 75)	69	69
Walking ability		
No difficulty in walking on my own	966	476
Some difficulty in walking on my own, but do not need a supporting device	21	15
Some difficulty in walking on my own, and need a supporting device	13	9
Significant difficulty in walking on my own	0	0
Degree of bulk buying		
Buy just for 1 day	207	102
Buy in bulk for 2 or 3 days	596	317
Buy in bulk for 4 or 5 days	114	53
Buy in bulk for 1 week or more	83	28
Leisure time walking habit (more than 10 min)		
Almost everyday	253	163
4 or 5 days a week	126	77
2 or 3 days a week	159	83
Once a week	115	46
Less than once a week	159	66
No such habit	188	65

An online questionnaire survey was conducted in December 2020 (survey via internet was commissioned by My Voice Communications, Inc.). Thousand responses were received from the respondents living in Tokyo Metropolitan area. The 500 responses were from elderly peoples aged 65–79 years and the rest from non-elderly peoples. All respondents were responsible for their households' shopping and usually went shopping on foot. All of them were selected based on screening questions. Table 5.1 lists the respondents' basic attributes.

5.2.2 Analysis Flow

In this study, we mainly focused on the elderly group and performed the following analysis.

In the Sect. 5.3, we analyzed how the tolerance level and the amount of each road element affect the dissatisfaction ratio. In Sect. 5.4.1, we extract dissatisfaction factors in the road environment elements that cause inconvenience in accessibility. In the first half of Sect. 5.4.2, we measured the distribution amount of each road element on each respondent's route to make objective indices for the next analysis. Finally, by analyzing the relationship between the respondent's subjective evaluations and objective indices, we extracted a threshold value using decision tree analysis for the objective situation where the tendency of evaluated satisfaction changed (latter half of Sect. 5.4.2). The method is suitable for extracting the threshold values where the respondents' evaluation trends and the decision tree can visually describe the multi-layered effects explanatory variables. Based on the results, we conclude this study by discussing the application and contribution of the developed models to the disadvantaged shoppers' problem (Sects. 5.4.3 and 5.5).

5.3 Analysis 1: Dissatisfaction of Elderly People with Various Road Elements

5.3.1 Dissatisfaction Ratio for Each Road Elements

First, we focused on dissatisfaction with road environment factors. In this section, we deal with the case of the store which respondents most frequently use. Table 5.2 shows the dissatisfaction ratio (the ratio of respondents who evaluated “dissatisfied” and “rather dissatisfied”, excluding those who answered “No such element exists”) for each item among the elderly respondents.

The dissatisfaction ratio with “Many bicycles run on the sidewalk” is the highest at over 30%, followed by “narrow sidewalks” at over 25%. Therefore, it is important to solve these dissatisfactions to create comfortable walking environment. Other dissatisfaction ratios for the following 15 items were around 15%, though “No rest space,” “Steps between road and sidewalk,” and “Distance to the store” were below 10%. In particular, the ratio of “Distance to stores” was the lowest. This indicates that elderly people decide the route to stores by prioritizing avoiding long distance. It is presumed that this causes unacceptable road elements in route selection or a large number of dissatisfaction factors on the route, which will leave dissatisfaction with other road elements other than distance.

Table 5.2 Dissatisfaction ratio for each item among the elderly respondents

Item	Ratio (%)	Item	Ratio (%)
Many bicycles run on the sidewalk	31.5	Stairway	14.2
Narrow sidewalk	26.4	Pedestrian bridge	13.8
Hard to walk in summer	18.6	Slope difficult to use	13.4
No sidewalk	17.6	Steep slope	13.3
Crosswalk with short green light	17.0	Many cars run on the road (no sidewalk)	12.9
Hard to walk in bad weather	16.2	Crosswalk with many cars	12.8
Obstacles on the sidewalk	15.7	Many cars run on the road (with sidewalk)	12.2
No nighttime lights	15.5	No rest space	9.1
Many pedestrians on the sidewalk	14.3	Step between road and sidewalk	8.4
Bumpy surface of the sidewalk	14.2	Distance to the store	7.8

5.3.2 *Influence of “Tolerance Level” and the “Amount” of the Road Elements on the Respondent’s Dissatisfaction*

Next, we investigate the influence of “tolerance level” and the “amount” of the road elements on the respondent’s dissatisfaction. Table 5.3 summarizes the tolerance level for each factor other than distance and the dissatisfaction ratio by the amount on the route among the elderly respondents.

First, the influence of the tolerance level is significant. When the amount of each element is the same, the dissatisfaction ratio of those who want to avoid such an element (“Unacceptable group”) tends to greatly exceed the ratio of the group that accepts the element. In particular, when the amount level of each element is high, the dissatisfaction ratio of the unacceptable group exceeded 50% for 15 out of the 19 items. To solve the dissatisfaction with each road environments, it is important to understand the characteristics of people who do not tolerate each element and estimate the elements likely to be avoided in each region based on residents attributes.

On the other hand, the degree of amount of each element affected the dissatisfaction ratio. Even in the unacceptable group, the dissatisfaction ratio decreases to 20–30% when the amount of each element is “Medium.” This indicates that dissatisfaction can be significantly improved by reducing the amount of each element.

However, for several road elements, the dissatisfaction ratio does not decrease significantly even if the amount level of element is reduced to a “Medium” level in the unacceptable group (e.g., narrow sidewalks, steps between sidewalks and roadways, bicycles on sidewalks, crosswalks with short green lights, and no lighting at night). The dissatisfaction with these items cannot be improved unless the amount of their presence becomes “small.” In addition, for factors such as narrow sidewalks,

Table 5.3 Dissatisfaction ratio by tolerance/amount for each road element among the elderly respondents

Road elements	Tolerance	Distribution amount		
		Much	Medium	Little
Narrow sidewalk	Acceptable	23.5	22.2	10.4
	Unacceptable	73.2	33.3	16.1
No sidewalk	Acceptable	12.2	0.0	5.1
	Unacceptable	45.1	25.8	9.3
Bumpy surface of the sidewalk	Acceptable	0.0	15.4	4.3
	Unacceptable	71.4	16.1	10.7
Steps between road and sidewalk	Acceptable	7.1	2.8	3.8
	Unacceptable	33.3	31.3	7.1
Obstacles on the sidewalk	Acceptable	0.0	22.2	4.5
	Unacceptable	76.0	22.9	9.8
Many pedestrians on the sidewalk	Acceptable	17.9	0.0	0.0
	Unacceptable	55.6	24.4	5.0
Many bicycles run on the sidewalk	Acceptable	43.8	10.5	7.1
	Unacceptable	73.8	41.9	9.0
Many cars run on road(with sidewalk)	Acceptable	5.5	0.0	1.8
	Unacceptable	52.3	16.7	6.3
Many cars Runn on road(no sidewalk)	Acceptable	14.3	0.0	0.0
	Unacceptable	52.2	24.1	8.0
Crosswalk with many cars	Acceptable	5.6	4.8	2.7
	Unacceptable	50.0	22.9	9.6
Crosswalk with short green light	Acceptable	16.7	4.5	5.1
	Unacceptable	48.0	35.9	10.3
Pedestrian bridge	Acceptable	0.0	0.0	9.1
	Unacceptable	66.7	20.0	15.7
Steep slope	Acceptable	14.3	16.7	0.0
	Unacceptable	57.1	20.0	15.7
Stairway	Acceptable	0.0	0.0	0.0
	Unacceptable	57.1	20.0	15.7
Slope difficult to use	Acceptable	0.0	0.0	0.0
	Unacceptable	100.0	29.4	11.5
No nighttime lights	Acceptable	0.0	0.0	0.0
	Unacceptable	50.0	50.0	8.6
No rest space	Acceptable	1.2	0.0	2.8
	Unacceptable	36.8	40.0	20.0
Hard to walk in summer	Acceptable	21.4	2.9	2.7
	Unacceptable	67.2	16.7	9.8
No rest space	Acceptable	0.0	0.0	0.0
	Unacceptable	65.7	23.3	5.7

Note: The answer of “very unacceptable” and “unacceptable” were integrated into the “Unacceptable” group, while “rather acceptable” and “acceptable” were integrated into the “Acceptable” group. The answer of “very much” and “somewhat much” groups were integrated into the “Much,” group, the “neutral” group as “Medium,” and the “somewhat little” and “very little” were integrated into the “Little” groups

pedestrian bridges, stairs, and lack of other facilities, the dissatisfaction ratio of the unacceptable group was slightly higher than 10%, even when their level was small. Therefore, these road elements should be eliminated from the route to the store to decrease dissatisfaction dramatically.

5.4 Analysis 2: What Kind of Elements' Dissatisfaction Constitutes the Inconvenience of Accessibility? Objective Conditions that Define Dissatisfaction with Road Elements

5.4.1 *Dissatisfaction with Road Elements Related to the Inconvenience of Accessibility*

In this section, we attempt to identify the road element dissatisfaction related to the inconvenience of store accessibility.

To ensure a sufficient sample for analysis, we targeted up to three frequently used stores by elderly respondents: 500 respondents answered the first store, 438 answered the second store, and 275 answered the third. The access inconvenience ratio (the percentage of respondents who answered “inconvenient” and “somewhat inconvenient”) was 7.0%, 10.5%, and 11.6% for the first, second, and third stores, respectively.

A characteristic of this dataset is that a respondent can have multiple store information. Therefore, an appropriate regression model should be selected based on the data structure. Therefore, we calculated the value of the intraclass correlation coefficients for evaluating the inconvenience of accessibility when all stores used by each individual were considered. The value of intraclass correlation coefficients was 0.545, indicating that it is desirable to assume a structure in which the store evaluation is nested in the individual.

Therefore, ordinal logistic regression was conducted using the data from a total of these 1213 individual evaluations of each store, considering the characteristics of evaluations among respondents as a random effect. The dependent variable was the evaluation of the inconvenience of accessibility (ordered variable on a 5-point scale from 1: inconvenient to 5: not inconvenient), and the explanatory variable was the dissatisfaction level for each road environment element and distance (scored on a 5-point scale from 1: not dissatisfied to 5: dissatisfied, with a cross term of their existing condition on the route: exist (1) and not exist (0)).

The regression results are presented in Table 5.4. It notes that the correlation coefficient of dissatisfaction with “steep slope” and “stairs” exceeded 0.9. In order to avoid multi-collinearity, “stairs” were excluded from the candidate explanatory variables considering of correlation with other variables.

The AIC of the final model is 1915.01, which is smaller than the AIC of 2089.00 when random effects are not considered; model fitting by the likelihood ratio test

Table 5.4 Road elements whose dissatisfaction is statistically related to the inconvenience of store accessibility

Variables	Coefficient	S. E.	Z value	p
Narrow sidewalk	-0.234	0.080	-2.905	0.004*
Steep slope	-0.194	0.082	-2.372	0.018**
Distance to the store	-2.200	0.145	-15.172	<0.001*

Note: Significance level *: 1%, **: 5%

Random effect: Deviance 6.266, Standard deviation 2.503

is also significant at the 1% level. The regression coefficients of narrow sidewalks, steep slopes, and distance to the store were significant. The distance had the greatest effect. In addition, the slope and the width of the sidewalk are factors that are often considered in other studies as factors of difficulty for the elderly (Takeshima 2007; Kato et al. 1995; Mizoguchi and Yamakawa 2001; Satoh et al. 2006).

5.4.2 Developing Decision Tree Models Describing Objective Conditions that the Dissatisfaction of the Road Elements Appear

5.4.2.1 Preparation of Quantitative Indicators of Road Elements' Distribution on the Route of Each Respondent

The distance or amount of these road elements extracted in Sect. 5.4.1 is represented by objective indices for the following analysis. To reduce costs, we used a method that does not require a field survey to prepare the objective data.

We randomly selected 203 respondents from the 500 elderly respondents to develop objective data. In addition, only the stores most frequently used by each respondent were selected for ease of interpretation of the model in the next analysis. Figure 5.1 shows an image and outline of data preparation for each respondents. The steps for this preparation are described below in order.

Estimating the Routes Used by Each Respondents

First, we estimated the routes used by respondents. The stores most frequently used, and the bus stops nearest to their residence were identified based on the respondent's answers to the questionnaire. Subsequently, using QGIS (ver. 3.18, one of the GIS (geographical information system) software), each respondent's shortest route and its distance from the bus stop to the store were calculated. For the road network data, we used the road centerline data of the Digital Map (Basic Geospatial Information) published by the Geospatial Information Authority of Japan.

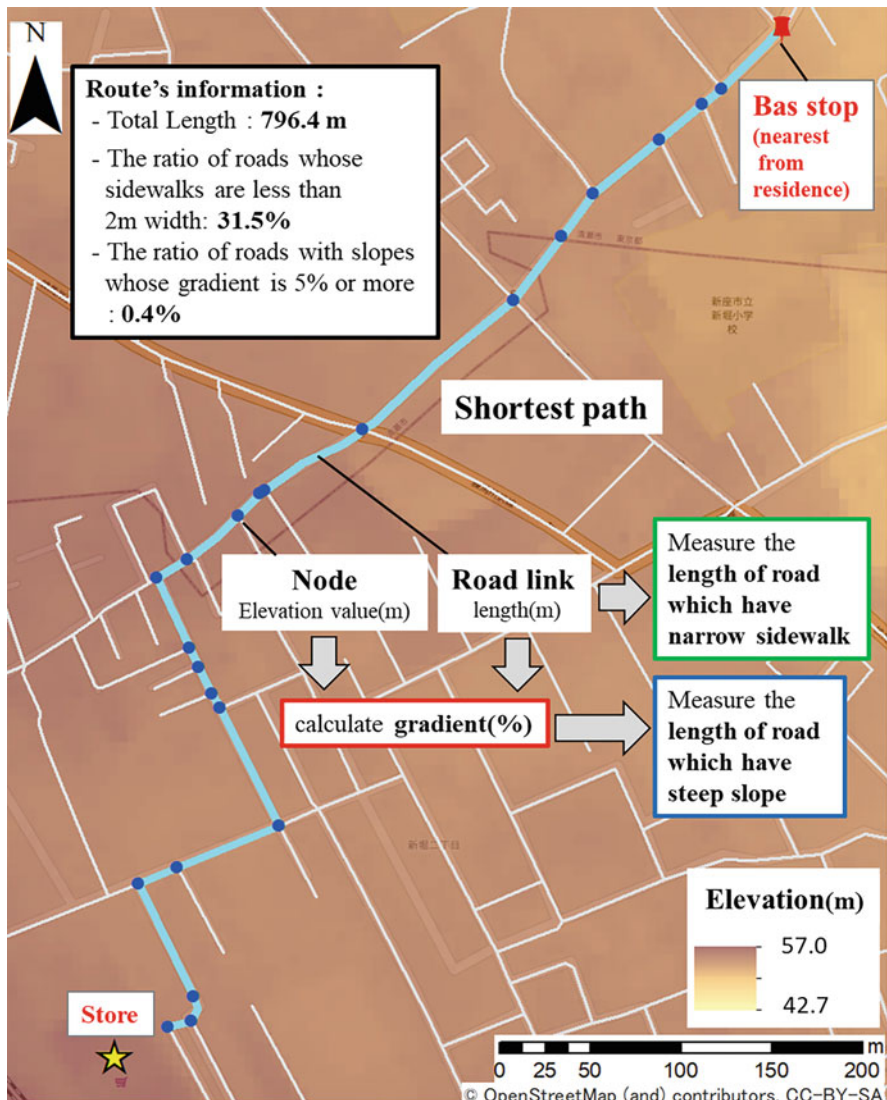


Fig. 5.1 Illustrative example of the data preparation of each respondents

Estimating the Distance to the Store

Using the aforementioned road network data, the lengths of the individual road links were obtained using a GIS tool. The total length of the links comprising the shortest route was used as the total route distance to the store.

Estimating Amount of Steep Slopes

As shown in Fig. 5.1, nodes were created at the endpoints of each link using GIS. Then, the elevation values from a 5 m resolution digital elevation model (The Geospatial Information Authority of Japan) were added to each node using the spatial merging function of GIS. The gradient of each slope was calculated as the percentage of the difference in elevation between the two ends of a road link to the length of the link.

In developing the index of “steep slope,” we used the gradient criterion of “5% or more” as steep slope, referring to the results of existing study (Nitta et al. 2004). The ratio of the total length of road links with slopes whose gradient are 5% or more to the total route length (%) (hereafter, “the ratio of roads with slopes whose gradient is 5% or more”) was used as an index to evaluate the amount of steep slopes in our analysis.

Estimating Amount of the Roads Which Have Narrow Sidewalks

Commonly available road data do not contain detailed information on the width of the sidewalks on each road. Therefore, we used Google Maps to measure the width of each road link that constituted the shortest path for each individual. The distance measure function was used to measure the width of the walkable parts of each sidewalk. In cases where the width was not constant due to the presence of fences, street trees, and other structures, we divided the walkable part into several sections, and the width of the section with the largest percentage of the road link length was used as the representative value. We used the width of “less than 2 m” as a criterion of “narrow sidewalk” (Doi and Amano 1986). The “ratio of the road links whose sidewalks are less than 2 m width to the total route length (%)" (hereafter, “ratio of roads whose sidewalks are less than 2 m in width”) was used as an indicator to evaluate the amount of “narrow” roads.

5.4.2.2 Extraction of Evaluation Bifurcation Points of Dissatisfaction for Each Road Elements by Decision Tree Models

In this section, by combining the indicators prepared, personal attributes and subjective evaluation of the dissatisfaction of each road elements obtained from the questionnaire, decision tree models were developed to identify objective criteria in which the people’s evaluation of their satisfaction level for each road elements changes significantly.

Each decision tree model was developed for each road element to describe the respondents’ dissatisfaction evaluation structure. The CART (classification and regression tree) method was used to select the model variables. The dependent variable was the dissatisfaction level with each road element, and the explanatory variables were the indices of objective road environments (distance, the ratio of roads with a slope of 5% or more, and the ratio of roads whose sidewalks were less than 2 m in width) of each element on each person’s route, the level of acceptance of each road element, and variables of personal attributes (Table 5.5).

Table 5.5 List of variables for developing decision tree models

	Variable name	Explanation of the variable
Dependent variable	Dissatisfaction with each road element	Prepared for each distance to the store, steep slope, and narrow sidewalk. – Three levels(※1): (1)dissatisfied, (2)neutral, and (3) not dissatisfied
Explanatory variables	Objective road environments (distance to the store, steep slope, and narrow sidewalk)	(1) Total length of route, (2)the ratio of roads with slopes whose gradient are 5% or more, and (3) ratio of roads whose sidewalks are less than 2 m in width
	Level of tolerance	Prepared for each distance to the store, steep slope and narrow sidewalk. – Three levels(※2): Unacceptable, neutral, and acceptable – this index was not used for the model of distance dissatisfaction)
	Male_D	Male: 1, Female: 0
	Age over 75_D	Age over 75: 1, otherwise: 0
	Walking difficulty_D	“No difficulty in walking on my own”: 0, otherwise: 1
	Walking regularly_D	If a respondent does leisure time walking (more than 10 min) at least once a week:1, otherwise: 0
	Large baggage_D	If a respondent usually buy groceries in bulk for 1 week or more:1, otherwise: 0

Note: (※1) The answer of “dissatisfied” and “rather dissatisfied” was aggregated into “dissatisfied” category, and the answer of “rather not dissatisfied” and “not dissatisfied” was aggregated into “not dissatisfied” category

(※2) The answer of “very unacceptable” and “unacceptable” was aggregated into “unacceptable” category, and the answer of “rather acceptable” and “acceptable” was aggregated into “acceptable” category

In the analysis, respondents who answered that “I have no such element in their route” were excluded from the 203 candidates. We also calculated the ratio of correct predictions, that is, the percentage of actual responses that matched the predicted response (i.e., predicted responses were estimated as the majority dissatisfaction level in each final node reached by following the branching conditions of the tree model along the respondents’ attributes or answers). The results are presented below in order.

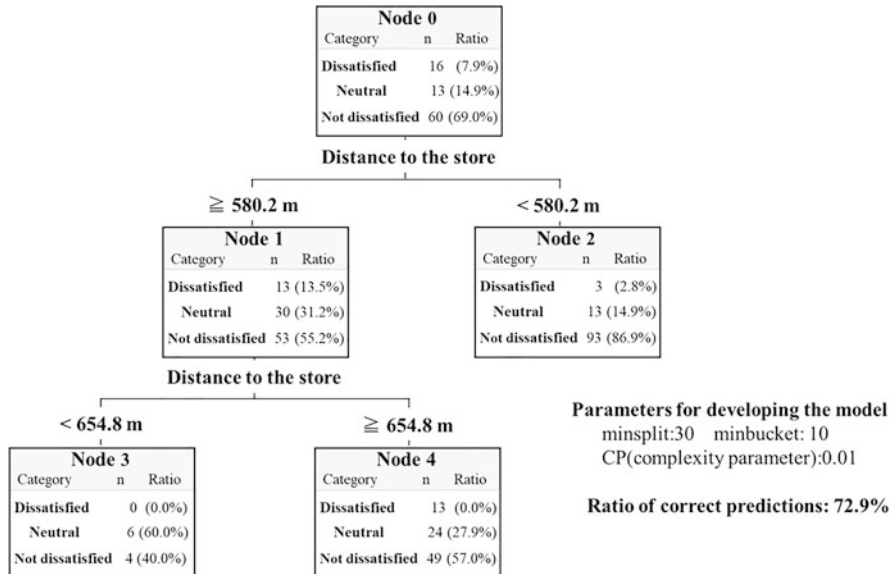


Fig. 5.2 The decision tree model for dissatisfaction of the distance to the store

Decision Tree for Dissatisfaction with the Distance to the Store

Figure 5.2 shows the results. Only the variables about distance value were used as the branching condition, and no personal attributes were included in the model. This finding suggests that the threshold for subjective evaluations does not depend on individual attributes in distance dissatisfaction.

When the respondent's distance was greater than 580.2 m, the overall dissatisfaction level increased. In detail, all dissatisfied respondents at Node 1 have a distance to the store of 654.8 m or more. We assume that the number of "not dissatisfied" respondents decreased when their distance exceeded approximately 580 m, and the number of "dissatisfied" respondents increased after a distance of 650 m.

Decision Tree for Dissatisfaction of the Steep Slope

Figure 5.3 shows the results. First, the nodes were branched according to their tolerance. Almost all respondents answered "not dissatisfied" when they could tolerate the use of steep slopes (Node 2). However, all respondents dissatisfied with the slope did not tolerate its use; thus, it can be said that whether they can tolerate of the steep slope was important in judging their dissatisfaction. Furthermore, the results diverged according to the objective conditions of the slopes on the route. When the "the ratio of roads with a slope of 5% gradient or more" exceeds 2.45%, the dissatisfaction level tends to increase (Node3 vs. Node4). Node 4 was further split according to whether the respondent's age was over 75.

From the above results, the tolerance of steep slopes influences dissatisfaction with steep slopes. Additionally, among those who cannot tolerate steep slopes, the

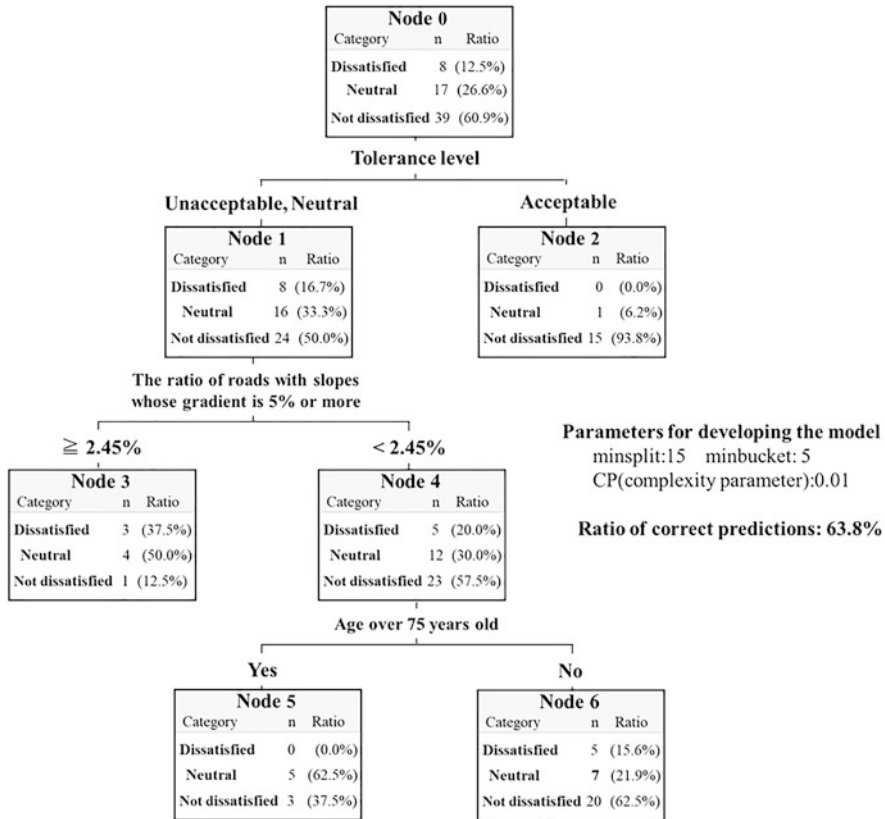


Fig. 5.3 Decision tree model for dissatisfaction with the steep slope

dissatisfaction rate was higher when the road had steep slopes (5% gradient or more) of more than 2.45%.

Decision Tree for Dissatisfaction with the Narrow Sidewalk

Figure 5.4 shows the results. First, the nodes were branched according to their tolerances. If the tolerance is anything other than not acceptable, the respondents were classified as Node 2. The dissatisfaction level is generally low at this node, suggesting that dissatisfaction is unlikely to occur when people are relatively tolerant of roads with narrow sidewalks. However, Node 1 is further divided by the objective condition of the “ratio of roads whose sidewalks are less than 2 m in width.” Compared to Node 4, Node 3, with road-to-narrow sidewalk ratios above 22.8%, showed a higher level of dissatisfaction. Additionally, 19 of the 21 respondents who has dissatisfaction in Node 1 were reclassified as belonging to Node 3.

These results indicate that even among those who do not tolerate narrow sidewalks, the ratio of those dissatisfied with the road element tends to be relatively

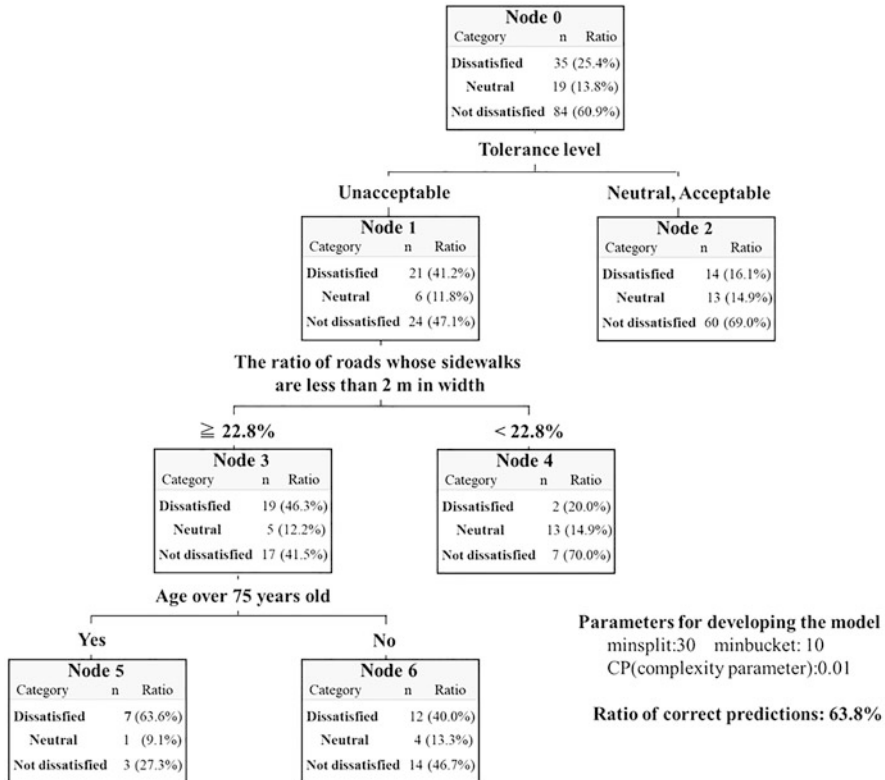


Fig. 5.4 Decision tree model for dissatisfaction with the narrow sidewalk

higher when approximately a quarter of the roads on the route are occupied by narrow sidewalks.

In addition, Node 3, with many roads having narrow sidewalks in the route, was further divided into deeper nodes according to the respondents' age. Comparing Nodes 5 and 6, the ratio of dissatisfied people was higher at Node 5, which was a group of elderly people over 75; in addition, the overall dissatisfaction level was also higher. This suggests that the elderly people over 75 are more likely to be dissatisfied with the roads having many narrow sidewalks.

The above results indicate that tolerance for narrow sidewalks and steep slopes influence dissatisfaction with the road elements. In addition, people tend to feel dissatisfied when narrow sidewalks occupy more than 22.8% of roads. The result also suggests that elderly people over 75 were more likely to feel dissatisfied with narrow sidewalks and steep slopes.

5.4.3 Applications of the Developed Models

In the previous section, we extracted the objective conditions likely to cause dissatisfaction with road elements. The results in Sect. 5.4.2 show that dissatisfaction with these elements affects the inconvenience of accessibility. Therefore, in order to solve disadvantaged shoppers' problems, it is important to improve road conditions of such road elements. Based on the results of our study, the amount of such problematic road elements should be kept below a certain ratio throughout the entire route to prevent dissatisfaction; hence, removing them altogether is unnecessary. This is a useful information for efficient road maintenance planning that prioritizes roads likely to become travel routes of many people.

Furthermore, the results allow easier comparisons of the progress of problems among several regions by estimating the subjective evaluation of people from the objective condition, without time-consuming and expensive questionnaire surveys. Such a simplified estimation can help to narrow problematic regions requiring more detailed field or questionnaire surveys. For estimation, we hypothetically assume an individual with attributes or subjective evaluations representing an area's residents. We set personal attributes with reference to existing local statistics and estimated route used by the person. Once a tentative route is established, we measure its distance or the percentage of roads with steep slopes or narrow sidewalks. We then apply the assumed individual attributes and the objective conditions of road elements to the decision tree models. Based on these settings, we follow the branches of the decision tree. Finally, when reach the final node, we use the majority rating of the classified node as the result of the estimation of the subjective evaluation estimation of the representative resident.

To set a representative individual's characteristics, local statistics can provide statistical information such as age and gender, which can be easily obtained from the national census. In addition, several individual attributes are required to adjust the tolerance level if it is likely to change owing to differences in attributes (see Sekiguchi 2022 to know the individual attributes are used for estimating the tolerance of each road element). For example, walking habits, which is relevant to estimating the tolerance level of steep slopes, can also be set by referring to statistics such as "walking and light exercise" by region, obtained from the Basic Survey of Social Life. In the elderly respondents, the distribution of the degree of tolerance for "narrow sidewalks" and "steep slopes" was as follows: unacceptable: 38.2% and 57.0%; undecided: 18.6% and 17.4%; acceptable: 43.2% and 25.6%, respectively. Based on these percentages, we weighed the aforementioned attributes by multiplying them with a magnification factor to set the tolerance degree of the assumed representative resident. In addition, for estimating the level of tolerance, the following values can be used as a reference: Women are 1.60 times more likely to be "unacceptable" for narrow sidewalks, 2.21 times more likely to be "unacceptable" for steep slope than men, and those whose leisure walking frequency is less than once a week are 1.66 times more likely to be "unacceptable" for steep

slopes than those whose frequency is once a week or more (see Sekiguchi 2023 for the details of the derivation).

One of the major strengths of our method for estimating subjective evaluations is the low cost of data collection and the analysis environment. In particular, it can be conducted with a much lower budget than a regional questionnaire survey and can be analyzed for free using applications such as QGIS and R. Objective data, such as elevation data and road width information, can be also obtained at no extra cost. Although obtaining road data (road centerline data) incurs some costs, the cost is low compared with that of distributing and collecting questionnaires in each area. Therefore, our method can be used in many situations requiring efficient surveys with limited budgets, such as by local governments.

5.5 Conclusion

5.5.1 *Summary of the Study*

This study conducted a series of analyses to clarify people's consciousness structure regarding the inconvenience of store accessibility and dissatisfaction with road elements. These are important concepts because solving the problems associated with these inconvenience and dissatisfaction will help improve the problem of disadvantaged shoppers.

We analyzed road elements contributing to dissatisfaction among the elderly. Dissatisfaction with distance was unexpectedly lower than that of other factors, suggesting that elderly people chose the routes that minimized distance dissatisfaction. However, other environmental factors could not be avoided, leading to dissatisfaction with these road elements.

Furthermore, the results also show that the dissatisfaction ratio for each element was closely related to people's tolerance levels and the amount of each element on the route to the store. Several road elements had high dissatisfaction ratio because of their large amount on the route, even if the use of these element is "acceptable." Conversely, other road elements had high dissatisfaction ratio because they denied to use despite their low occurrence along the route. These results will be useful in deciding which roads or road elements should be prioritized to improve the region.

We also extracted road elements that could cause inconvenience to accessibility. From the ordinal logistic regression analysis, dissatisfaction with narrow sidewalks, steep slopes, and distance to stores are closely related to "inconvenience." Based on the results, we successfully developed decision tree models that describe the objective conditions that can significantly change people's satisfaction levels, considering personal attributes and tolerance levels for each road element. Although the case study was limited to the Tokyo metropolitan area, the significance of this study is that the extracted elements and threshold values can be applied to other road environments. The models developed in this study can help estimate

people's subjective evaluations of objective road conditions with high simplicity. Furthermore, the objective data used in the models are generally available at a low cost or can be easily estimated from available data, enabling a more effective estimation of subjective estimation under limited time, human and financial costs.

5.5.2 Future Research Directions

In the future, the applicability of the method to other regions and improvements in prediction accuracy should be considered. If other elements can be indexed in addition to the road elements, and data maintenance can be made more efficient, it will be possible to predict dissatisfaction with various elements. For example, replacing manual acquisition of road widths with image analysis from bird's-eye view images or street views or using machine learning method will allow evaluation of other types of road elements in other regions easily.

In addition, using the proposed concept of "tolerance" to evaluate people's shopping inconvenience and dissatisfaction precisely will improve the prospects for discussing the problems of vulnerable shoppers in the future. These results can help conduct more detailed surveys among regions and take measures to eliminate dissatisfaction, thereby creating a comfortable shopping environment free from inconvenience and dissatisfaction.

Acknowledgments This study was funded and supported by the JSPS KAKENHI (grant number JP20K14901).

This manuscript is an English translation based on the original article "Factors of inconvenience of store accessibility for older adults in Tokyo: Objective indicators and thresholds for estimating dissatisfaction of road environments that cause the inconvenience" in MERA Journal (Vol. 25, No. 2, pp. 1–10). We thank to the Man-Environment Research Association for agreeing to translate the article.

References

- Doi M, Amano K (1986) A survey of pedestrian behaviour to determine sidewalk width under desirable service level. *Infrastruct Plan Rev* 4:237–243
- Hachioji City (2013) Report on the survey of shopping environments in Hachioji City. https://www.city.hachioji.tokyo.jp/kurashi/sangyo/sonota/001/p006343_d/fil/hyousi.pdf. Accessed 11 July 2023
- Hino K (2002) Connection between inconvenience for shopping and eating habits of old people: analysis of shopping habit of old people in Itabashi area. *J Archit Plan (Trans AJ)* 67:235–239
- Hirai H, Minami M (2013) Distribution change in grocery store and people with the disadvantage of shopping in Morioka City. *J City Plan Inst Jpn* 48(3):969–974
- Kato F, Wake I, Kawamoto Y (1995) Constructing an easy walking sidewalk for elderly. *Infrastruct Plan Rev* 17:991–994
- Larsen K, Gilliland J (2008) Mapping the evolution of 'food deserts' in a Canadian city: supermarket accessibility in London, Ontario 1961–2005. *Int J Health Geogr* 7:16

- Matsumura Y, Manabe R, Murayama A (2021) Urban environment that encourages going-out activities of elderly people in the suburban planned residential area—a case study in Koganehara area, Matsudo City. *J City Plan Inst Japan* 56(1):24–31
- Ministry of Internal Affairs and Communications (2017) Report on the survey on measures for disadvantaged shoppers. https://www.soumu.go.jp/main_content/000496982.pdf. Accessed 11 July 2023
- Mizoguchi H, Yamakawa H (2001) A study of pedestrian transportation concerning with slopes in hilly residential areas. *J City Plan Inst Jpn* 36:841–846
- Nakamura E, Asami Y (2019) The food desert caused by the economic difficult of access—in Azabu and Takanawa district of Minato-ku, Tokyo. *J Archit Plan (Trans AJ)* 84(756):437–445
- Nitta Y, Koyama K, Inoi H, Nakamura A (2004) The burden of elderly and disable walker on a slope. *Infrast Plann Rev* 29:102–105
- Russell SE, Heidkamp CP (2011) Food desertification': the loss of a major supermarket in New Haven, Connecticut. *Appl Geogr* 31:1197–1209
- Satoh E, Yoshikawa T, Yamada A (2006) Investigation of converted walking distance considering resistance of topographical features and changes in physical strength by age: model for location planning of regional facilities considering topographical condition and aging society part 1. *J Archit Plan (Trans AJ)* 71(610):133–139
- Sekiguchi T (2022) Older adults' inconvenience of store accessibility and dissatisfaction caused by the various road environments(Part1): focusing the tolerance and amounts of each road elements. *AIJ J Technol Design* 28(70):1465–1470
- Sekiguchi T (2023) Factors of inconvenience of store accessibility for older adults in Tokyo: objective indicators and thresholds for estimating dissatisfaction of road environments that cause the inconvenience. *MERA J* 25(2):1–10
- Sekiguchi T, Hino K (2021) How individual's various evaluations for the grocery shopping environments affects their shopping behaviors and dietary intake? an empirical study based on a questionnaire survey in a high-aged residential area in an outskirt of Central Tokyo. *J City Plan Inst Jpn* 55(3):1013–1020
- Shibata F, Niwa Y, Oie H, Ito K (2017) The perceived burdens felt by elderly pedestrians in street environments-differences between trips with and without rollators. *J Archit Plan (Trans AJ)* 82(732):451–457
- Takeshima Y (2007) Research on the walk environment maintenance for the aged -the order of the barrier and how to cope those barriers in the daily going out. *J Archit Plan (Trans AJ)* 611:1–6
- Yakushiji T, Takahashi K, Tanaka K (2013) Difficulties in accessing food from local Residents' viewpoint: factors of inconvenience and laboriousness involved in shopping for food. *J Rural Econ* 85(2):45–60

Chapter 6

Relationship Between Crime Rate of Residential Burglary and Local Context



Kimihiro Hino and Takaya Kojima

Abstract This study aimed to assess the risk of residential burglary by examining factors representing the physical and socio-demographic context of the neighborhoods. Structural equation modeling was employed to establish their relationship. The main findings of this study provide evidence-based insights on crime reduction. Particularly, higher density, a larger family size, and daytime population reduced the risk, potentially enhancing natural surveillance. Conversely, neighborhoods with a high rate of rented houses exhibited a higher risk, while those with a high building coverage ratio demonstrated an increased risk, and those with a high floor area ratio demonstrated low risk. In conclusion, considering community safety as an integral aspect of quality of life, a holistic approach is suggested.

Keywords Crime prevention · Residential burglary · Structural equation modeling · Safer places

6.1 Introduction

6.1.1 *Background and Purpose*

In response to citizens' increasing awareness of crime and the trend toward information disclosure, maps displaying various crimes in each neighborhood have

This content is based on the following article originally published in a Japanese journal: Hino, K., and Kojima, T. (2007). Relationship between crime rate of dwelling burglary and local context: On neighbourhoods in 29 wards and cities in Tokyo. *Journal of Architecture and Planning (Transactions of AJ)*, 616, 107–112 (in Japanese).

K. Hino (✉)

Department of Urban Engineering, The University of Tokyo, Tokyo, Japan
e-mail: hino@ua.t.u-tokyo.ac.jp

T. Kojima

Faculty of Human Sciences, Waseda University, Tokyo, Japan

been published in recent years. These maps aim to inform residents and encourage them to take appropriate measures. However, crime occurrence maps do not offer guidance on promoting community development to prevent crime. The measures proposed mainly focus on individual buildings, sites, and general patrol activities (Schneider and Kitchen 2002).

In July 2003, the Council of Ministries and Agencies compiled research and studies conducted in six model areas across Japan, along with specific measures taken by the relevant Ministries and Agencies, in a report titled “Promotion of Crime-Prevention Community Development.” Despite this report providing desirable measures for each type of urban area, a more universal and objective theory must be developed for the widespread implementation of community development to prevent crime.

In this study, a causal model was constructed to assess the risk of residential burglary based on social indicators such as households and population, as well as spatial indicators such as housing type and land use (“neighborhood characteristic indicators”). The premise of this study was the crime opportunity theory, which posits that the environment plays a role in inducing crime. By establishing the causal relationship between crime and the environment through the developed model, this study enables the implementation of community-specific safety measures.

6.1.2 Literature Review

Previous studies have investigated the relationship between community characteristics and crime occurrence using various methodologies. For instance, one study utilized factor analysis to explore the relationship between the number of crimes in each city and socioeconomic indicators (Shimada and Harada 1999a), while another study investigated the relationship between the number of crimes in each neighborhood and spatial indicators (Shimada and Harada 1999b). Recent studies have also investigated the number and rate of residential burglaries in neighborhoods, based on various indicators such as land use area (Hino 2006) and social and spatial indicators based on the crime prevention through environmental design (CPTED) theory (Seo et al. 2006).

Building upon previous studies, this study explains crime occurrence using both social and spatial indicators, selected following a comprehensive crime prevention guideline, described in the next section. Additionally, this study employed structural equation modeling to demonstrate causal relationships among the indicators, contributing to the development of more crime-resistant communities.

6.1.3 “Safer Places”

To select hypothetical neighborhood characteristics indicators, we referred to “Safer Places - The Planning System and Crime Prevention” (ODPM and Home Office 2003), a guideline for crime prevention in the United Kingdom. Safer Places was published in 2003 by the Office of the Deputy Prime Minister and the Home Office. Additionally, it is referenced as a guide in Planning Policy Statement 1 (PPS1) (2005), which outlines the government’s national policies on various aspects of land use planning in England. Crime prevention is an integral part of the broader objective of “Delivering Sustainable Development,” the title of PPS1. Section 17 of the Crime and Disorder Act requires all planning authorities to exercise their functions with due regard to their likely effect on crime and disorder, and to do all they reasonably can to prevent them. Safer Places was developed in response to requests from professionals such as planners, designers, and architects, which aim to provide practical guidance in line with these requirements.

Safer Places outlines seven attributes derived from a comprehensive review of crime prevention theory, urban design theory, and past practices (Table 6.1). This approach combines traditional theories with insights from multiple researchers, aiming to promote effective crime prevention measures while considering the values that must be emphasized in different practical contexts. Furthermore, it addresses the criticism that traditional theories alone have not consistently yielded positive results in real-world situations.

When comparing the seven attributes of Safer Places with the four from CPTED, which serve as the foundation for various standards in Japan, the following characteristics become evident:

- Broad concept: “Access and movement” consider access for residents, users, and potential offenders, while “Surveillance” focuses on increasing the presence of people and assigning them in appropriate ways.

Table 6.1 Overview of the seven attributes in “Safer Places”

Access and movement: places with well-defined routes, spaces, and entrances that provide for convenient movement without compromising security
Structure: places that are structured so that different uses do not cause conflict
Surveillance: places where all publicly accessible spaces are overlooked
Ownership: places that promote a sense of ownership, respect, territorial responsibility, and community
Physical protection: places that include necessary, well-designed security features
Activity: places where the level of human activity is appropriate to the location and creates a reduced risk of crime and a sense of safety at all times
Management and maintenance: places that are designed with management and maintenance in mind, to discourage crime in the present and the future

Source: ODPM and Home Office (2003)

- Detailed concepts: “Activity” and “Management and maintenance” provide more nuanced perspectives on the human impact on the environment compared to CPTED.
- Existence of higher-level concepts: The higher-level concept of “Structure” addresses housing form, use, and layout planning.

These characteristics arise from Safer Places’ emphasis on diversity and resident participation because its goal is not solely crime prevention but also the development of sustainable communities (Hino and Amemiya 2005; Hino and Koide 2006; Hino and Amemiya 2006). Because Safer Places targets the district level, its seven attributes apply to the Japanese neighborhoods examined in this study.

6.2 Methodology

6.2.1 Target Area

The research focused on 3048 neighborhoods located within the 23 wards of Tokyo and six adjacent cities (Musashino, Mitaka, Chofu, former Tanashi, former Hoya, and Komae). These neighborhoods were selected based on the availability of necessary data and having a minimum of 300 households. Neighborhoods were chosen as the geographical units for this study owing to their ease of understanding and familiarity to residents. Moreover, they can be readily associated with community development to prevent crime, serving as actionable measures for both residents and local governments.

6.2.2 Residential Burglary Rate—Dependent Variable

During the fiscal years 2002–2004, there was a tendency for increased residential burglaries in neighborhoods with a larger number of households that could be potential targets. Figure 6.1 categorizes the neighborhoods into five equally sized groups based on the number of residential burglaries. The neighborhoods highlighted in red are concentrated around Suginami, Nakano, Nerima, and Edogawa. Furthermore, the correlation coefficient between the number of residential burglaries per neighborhood and the number of households was 0.644. To account for the effect of size, this study employed the number of residential burglaries per 1000 households as the dependent variable, which was explained by the neighborhood characteristics index. To address the distributional bias, “crime rate” presented in the equation below was utilized in this study. For logarithmization, the minimum number of residential burglaries in each neighborhood was set at 0.5.

$$\text{Crime rate} = \ln \left(\frac{\text{number of residential burglaries}}{\text{number of households}^* 1000} \right)$$

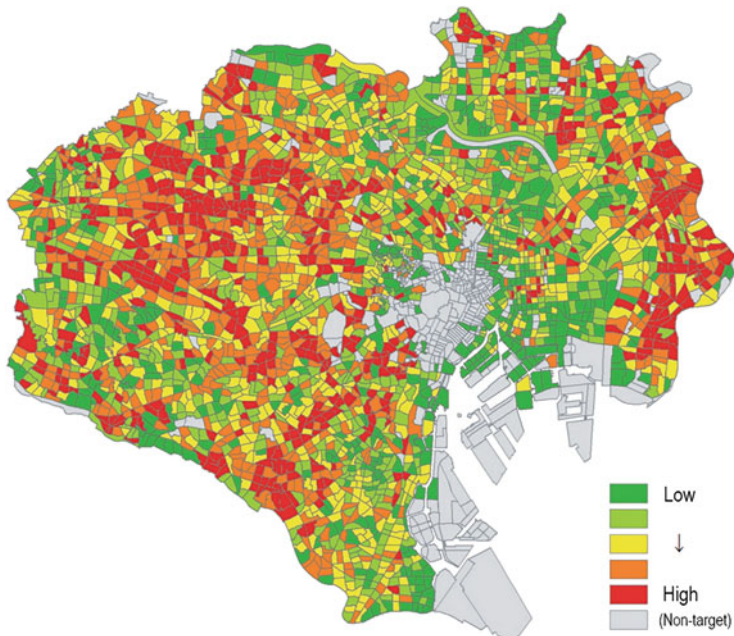


Fig. 6.1 Distribution of neighborhoods divided into five equally sized groups based on crime rate (residential burglary: FY 2002–2004)

The crime rate ranged from a minimum value of -1.60 to a maximum value of 3.95 , with a mean value of 2.29 and a standard deviation of 0.72 .

6.2.3 Neighborhood Characteristics—Explanatory Variables

Each neighborhood characteristic indicator was developed hypothetically based on the seven attributes of Safer Places (Table 6.2). The housing characteristics indicators were divided into two categories: ownership type (category a) and building type (category b) (apartment buildings were categorized by building floor). Separate models for each category were created to analyze their respective effects.

First, as indicators of neighborhood location, the distance to the nearest station, time distance to central Tokyo (train time from the Yamanote Line to the nearest station in minutes), and road area ratio (which is higher along arterial roads) were utilized. These indicators are related to the “Access and movement” attribute of Safer Places. To capture the attributes of “Activity” and “Surveillance,” indicators including the number of persons per household, population density, and daytime population ratio were employed. These indicators influence the amount of natural

Table 6.2 Neighborhood characteristic indicators set with reference to attributes of Safer Places

Categories	Variables	Data sources ^a	Related attributes ^b	Remarks ^c
Population	Number of persons per household Population density Daytime population ratio	A, B	Access, surveillance	= ln (daytime pop/night pop)
Location	Nearest station distance Time distance to central Tokyo	C	(Access)	
Land use	Road area ratio Commercial–residential area ratio	C	(Access), structure	= Road area/nbhd area = ln (com area/res area)
Spatial density	Building coverage ratio Floor area ratio	C	Structure	= $\sum bldg\ area/nbhd\ area$ = $\sum (bldg\ area * \text{no of floors})/nbhd\ area$
Housing characteristics (a)	Owner-occupied household rate Public housing household rate Rented household rate	A	Ownership, management	
Housing characteristics (b)	Detached housing rate Low-rise household rate Midrise household rate High-rise household rate	A	Protection	≤ 2 stories $3\text{--}5$ stories ≥ 6 stories

^a(A): 2000 Population Census (Tabulation for Small Areas), (B): 2000 Population Census (Report by Ward, City, Town, and Village in Tokyo), (C) Tokyo city planning geographic information system (Wards: FY 2001, Cities: FY 2002)

^bAccess: Access and movement, Protection: Physical protection, Management: Management and maintenance

^cpop Population, nbhd Neighborhood, bldg Building. For logarithmization, the minimum values of commercial land area divided by neighborhood area and residential land area divided by neighborhood area were set to 0.005

Table 6.3 Summary statistics for neighborhood characteristics indicators

	Min	Max	Mean	S.D.	Corr.
Population					
Number of persons per household	1.16	3.41	2.18	0.30	-0.15
Population density	836	50,986	16,066	6197	-0.11
Daytime population ratio	-1.15	3.77	-0.03	0.66	-0.16
Location					
Nearest station distance	3.39	7.88	6.28	0.66	-0.04
Time distance to central Tokyo	0.00	33.00	10.76	7.07	0.09
Land use					
Road area ratio	0.00	0.52	0.19	0.06	-0.11
Commercial–residential area ratio	-4.93	3.65	-1.55	1.10	-0.21
Spatial density					
Building coverage ratio	0.01	0.57	0.33	0.09	0.09
Floor area ratio	0.08	7.53	1.05	0.53	-0.23
Housing characteristics (a: ownership type)					
Owner-occupied household rate	0.00	0.91	0.42	0.13	0.08
Public housing household rate	0.00	1.00	0.07	0.16	-0.40
Rented household rate	0.00	1.00	0.45	0.14	0.40
Housing characteristics (b: building type)					
Detached housing rate	0.00	0.83	0.32	0.16	0.27
Low-rise household rate	0.00	0.68	0.17	0.11	0.41
Mid-rise household rate	0.00	1.00	0.25	0.13	0.03
High-rise household rate	0.00	1.00	0.21	0.22	-0.40

Max Maximum, Min Minimum, S.D. Standard deviation, Corr. Correlation with crime rate

surveillance within households and neighborhoods. The attribute of “Ownership” is influenced by housing characteristics (category a), including the percentage of owner-occupied households. The level of ownership also impacts the maintenance status. For “Physical protection,” housing characteristics (category b) were used because they affect the number of accessible openings and the presence of security facilities. The “Structure” indicator encompasses the commercial–residential area ratio and spatial density. Additionally, it is a significant attribute among the seven attributes, which is connected to several other neighborhood characteristic indicators.

Table 6.3 presents the summary statistics for each variable in the target neighborhoods. To address distributional bias, log transformations were applied to the nearest station distance, daytime population ratio, and commercial–residential area ratio.

6.2.4 Statistical Analysis

First, multiple regression analyses were conducted to examine the relationship between the neighborhood characteristics indicators listed in the previous section (explanatory variables) and the crime rate (dependent variable). Model (a) utilized housing characteristics (a) as the explanatory variable, while model (b) employed housing characteristics (b). To address collinearity among the explanatory variables, a stepwise method ($p < 0.05$) was employed, and “time distance to central Tokyo” was excluded in model (b).

Next, structural equation modeling was employed to determine both the indirect effects on the dependent variable and causal relationships among the explanatory variables. While multiple regression analysis assumes that each explanatory variable is in a parallel relationship and the standardized coefficient of the multiple regression equation reflects the magnitude of the effect of each explanatory variable, structural equation modeling is more appropriate in cases where the explanatory variables do not exhibit a parallel relationship, regarding the neighborhood characteristics indicators in this study.

In this study, each neighborhood characteristic indicator was classified based on the relationship among the seven attributes of Safer Places. Indicators related to neighborhood location were placed at the first level, while indicators associated with the higher-level concept of “Structure” in Safer Places were positioned at the second level. Indicators related to “Ownership” and “Management and maintenance” were situated at the third level, and indicators of “Activity” and “Surveillance” were located at the fourth level. The assumption of the causal model can be summarized as follows: Variables at each level exert an effect on higher-level variables as well as crime rates. Three variables at the first level exhibit correlation. Additionally, there is a correlation between the error variables for each variable at every level.

6.3 Results

6.3.1 Multiple Regression Analysis

The coefficients and significance probabilities of the selected variables for each model are presented in Tables 6.4 and 6.5. The adjusted R-squared values, which indicate goodness of fit, were 0.316 for model (a) and 0.266 for model (b). The correlation coefficients between the estimated and actual number of residential burglaries for each model were 0.792 and 0.766, respectively. These coefficients were higher than the one obtained in the previous section between the number of residential burglaries and the number of households (0.644). Therefore, considering neighborhood characteristics enhanced the explanatory power of the number of residential burglaries.

Table 6.4 Coefficients of the multiple regression equations (Model (a))

	B	S.E.	β	t	p
Constant	1.21	0.29		4.18	0.00
Population					
Number of persons per household	-0.33	0.06	-0.14	-5.25	0.00
Population density	0.00	0.00	-0.27	-9.98	0.00
Daytime population ratio	-0.13	0.03	-0.11	-3.65	0.00
Location					
Nearest station distance	-0.07	0.02	-0.06	-3.30	0.00
Time distance to central Tokyo	0.00	0.00	0.04	2.20	0.03
Land use					
Road area ratio	0.95	0.22	0.08	4.40	0.00
Commercial–residential area ratio	-0.10	0.02	-0.15	-6.01	0.00
Spatial density					
Building coverage ratio	1.72	0.22	0.20	7.89	0.00
Floor area ratio	-0.24	0.04	-0.17	-5.94	0.00
Housing characteristics (a: ownership type)					
Owner-occupied household rate	1.90	0.27	0.34	6.94	0.00
Public housing household rate	0.81	0.26	0.18	3.10	0.00
Rented household rate	2.61	0.26	0.51	10.07	0.00

B Unstandardized coefficient, S.E. Standard error, β Standardized coefficient, t t-value, p p-value

Table 6.5 Coefficients of the multiple regression equations (Model (b))

	B	S.E.	β	t	p
Constant	1.93	0.29		6.67	0.00
Population					
Number of persons per household	-0.47	0.07	-0.19	-7.20	0.00
Population density	0.00	0.00	-0.33	-10.98	0.00
Daytime population ratio	-0.16	0.04	-0.14	-4.34	0.00
Location					
Nearest station distance	-0.10	0.02	-0.10	-4.90	0.00
Land use					
Road area ratio	1.13	0.23	0.10	4.95	0.00
Commercial–residential area ratio	-0.04	0.02	-0.07	-2.46	0.01
Spatial density					
Building coverage ratio	1.84	0.26	0.22	7.13	0.00
Floor area ratio	-0.12	0.05	-0.09	-2.61	0.01
Housing characteristics (b: building type)					
Detached housing rate	2.15	0.28	0.46	7.56	0.00
Low-rise household rate	2.63	0.27	0.40	9.62	0.00
Mid-rise household rate	1.82	0.26	0.34	7.14	0.00
High-rise household rate	1.39	0.26	0.42	5.36	0.00

B Unstandardized coefficient, S.E. Standard error, β Standardized coefficient, t t-value, p p-value

In model (a), which demonstrated higher explanatory power, standardized residuals were calculated based on estimated and measured crime rates. Out of the total, 393 neighborhoods (12.9%) had standardized residuals of -1 or less, suggesting the presence of environmental elements that may contribute to future increases in residential burglaries. Conversely, factors not addressed in this study, such as the prevalence of crime prevention equipment and frequency of crime prevention activities by residents, could potentially suppress burglaries in these neighborhoods. In terms of wards and cities, such neighborhoods were most prevalent in Chiyoda, Chuo, Taito, and Koto wards. Conversely, the 392 neighborhoods (12.9% of the total) with standardized residuals greater than one may attract burglars owing to factors not accounted for in this study, such as a higher average income that criminals expect to be associated with greater gains. In terms of wards and cities, such neighborhoods were more common in Minato, Sumida, and Edogawa wards. Other neighborhoods that exhibited a relatively good fit, despite having high crime rates, may possess the potential to deter burglars through long-term environmental improvements.

6.3.2 Structural Equation Modeling

Of the two models analyzed through multiple regression analysis in the previous section, model (a), which exhibited greater explanatory power, was further examined for causal relationships among the neighborhood characteristics indicators using structural equation modeling. The model, obtained by systematically eliminating paths with coefficients less than 0.1 while considering the interrelationships among variables, is depicted in Fig. 6.2, offering insights into the relationship between each variable and the crime rate. The direct and indirect effects of each variable on the

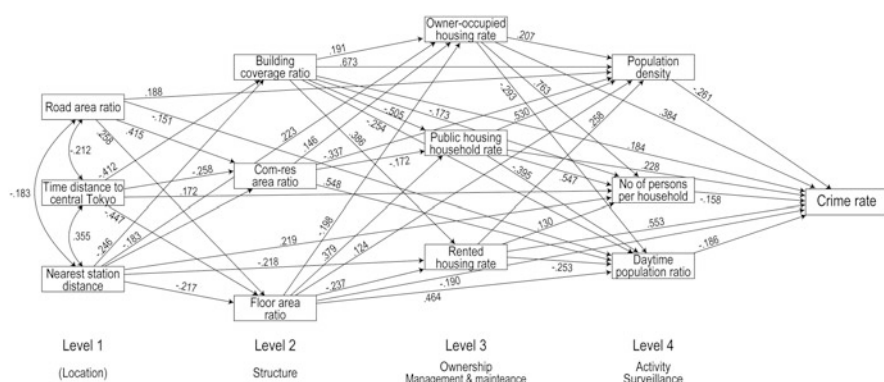


Fig. 6.2 Structural equation model of the residential burglary rate.

The estimated coefficients are standardized. The error terms and error correlations are not presented. Chi-square = 368.5, df = 22, $p = 0.00$

Table 6.6 Direct and indirect effects on residential burglary rate

Neighborhood characteristics indicator	Total effect	Direct effect	Indirect effect
1st level			
Nearest station distance	-0.064	—	-0.064
Time distance to central Tokyo	0.052	—	0.052
Road area ratio	-0.133	—	-0.133
2nd level			
Commercial–residential area ratio	0.012	—	0.012
Building coverage ratio	0.293	0.184	0.109
Floor area ratio	-0.453	-0.190	-0.263
3rd level			
Owner-occupied household rate	0.264	0.384	-0.120
Public housing household rate	0.077	0.228	-0.151
Rented household rate	0.513	0.553	-0.041
4th level			
Number of persons per household	-0.158	-0.158	—
Population density	-0.261	-0.261	—
Daytime population ratio	-0.186	-0.186	—

All the effects are standardized

crime rate are presented in Table 6.6. The goodness of fit indices, with a CFI of 0.987 and an RMSEA of 0.072, indicated a favorable fit for the model.

6.4 Discussion

6.4.1 Effects of Each Variable on Crime Rate

In this section, we discuss the effect of each neighborhood characteristic indicator on the crime rate, starting from the lowest level. To guide our discussion, we will refer to the seven attributes of “Safer Places.”

<Level 4>

Among the neighborhood characteristic indicators, population density exhibited the most significant negative direct effect on crime rates. Neighborhoods with high population density have enhanced natural surveillance and a lower risk of victimization. The number of persons per household demonstrated a negative direct effect on crime rates. Neighborhoods with a high number of persons per household have more households with occupants present during the day, reducing the risk of victimization compared to neighborhoods with a larger number of small households, such as single-person households and working couple households, which tend to be unoccupied. The daytime population ratio also showed a negative direct effect on crime rates. Neighborhoods with a higher daytime population ratio have a reduced risk of victimization owing to increased natural surveillance by visitors and

commuters, even during the daytime when homes are more likely to be unoccupied and residential burglaries are more probable to occur.

<Level 3>

Owner-occupied households, publicly owned households, and privately rented households each exerted a positive direct effect on crime rates. Based on the seven attributes of Safer Places, privately rented households, primarily consisting of low-rise rental apartments, are more susceptible to victimization owing to the lack of crime prevention measures (physical protection), a low sense of ownership, and insufficient maintenance (Building Research Institute 2006). The rate of public housing households indirectly affected the crime rate through population density and the number of persons per household, partially offsetting the direct effect. While slum-occupied public housing often serves as a crime hotspot in other countries, the risk of residential burglary in public housing is lower in Japan. This is because of the formation of communities owing to many homogeneous residents and the proper management and maintenance of housing by public entities. Additionally, the owner-occupied household rate indirectly affected the crime rate through the number of persons per household, with the total effect (including the direct effect) being approximately half that of the rented household. As aforementioned, these differences can be attributed to variations in physical protection, awareness of ownership, and maintenance.

<Level 2>

Neighborhood building coverage ratio exhibited a positive direct effect on crime rates. Neighborhoods with high building density, characterized by poor visibility and the potential for intrusion via adjacent buildings, are more susceptible to burglaries. The commercial–residential ratio did not have a direct effect on crime rates. Despite some concern that mixed use may increase the anonymity of residential neighborhoods and make them more prone to various types of crime, this study's analysis of residential burglaries did not yield such a result. There was a positive direct effect on the daytime population ratio, indirectly lowering the crime rate. However, the combined effect of all indirect effects almost offset this effect. Neighborhood floor area ratio had a negative direct and indirect effect on crime rates. The negative direct effect can be attributed to the presence of high-rise apartments in neighborhoods with high floor area ratios. These neighborhoods tend to have advanced crime prevention measures (physical protection) and fewer accessible openings (Hino 2005). The negative indirect effect was primarily attributed to higher daytime population ratios in neighborhoods with higher floor area ratios. The total effect, combining both direct and indirect effects, was the largest negative among the neighborhood characteristics variables.

<Level 1>

The road area ratio, time distance to central Tokyo, and nearest station distance did not have a direct effect on the crime rate, indicating that transportation accessibility was not a factor in target selection for residential burglars. However, when considering the total effect of both direct and indirect influences on the crime rate, the road area ratio showed a marginally negative effect.

6.4.2 Main Findings and Implications

Drawing from the crime opportunity theory, this study constructed a model to assess the risk of residential burglary by considering neighborhood characteristics that encompass both social and spatial factors. Furthermore, structural equation modeling was employed to reveal the causal relationships among the neighborhood characteristics indicators. The key findings of this analysis are summarized as follows:

- Neighborhoods characterized by high population density, many persons per household, and a high daytime population benefited from increased natural surveillance and face a lower risk of victimization. In conjunction with measures to revitalize shopping streets, housing policies that promote urban living and enhance the diversity of resident characteristics must be advocated for.
- Compared to neighborhoods with a high proportion of owner-occupied households, those with a high proportion of rented households faced a higher risk of victimization owing to disparities in physical protection, ownership awareness, and maintenance. Conversely, public housing exhibited a lower risk of victimization.
- A positive correlation was observed between the neighborhood building coverage ratio and the neighborhood floor area ratio. However, the former exhibited a positive effect on crime rates, while the latter had a negative effect. Neighborhoods with high building density had a higher risk of victimization, whereas those with a high proportion of high-rise apartments experienced a lower risk.
- The mixture of residential and commercial uses did not increase the risk of residential burglary. To guide community development to prevent crime, urban activities must be enhanced to attract more visitors, thereby increasing surveillance opportunities.
- Despite the presence of highly accessible transportation by railways and automobiles being associated with an increase in the number of crimes, it did not have a direct effect on the crime rate.

These findings are significant for residents and municipalities aiming to foster crime prevention and community development. As emphasized in “Safer Places,” a comprehensive perspective that incorporates crime prevention as an integral component of the living environment is essential. Despite the recent decline in the number of residential burglaries, the current level of security is still inadequate for citizens to feel completely safe. As part of our commitment to building a safer and more secure society, our future endeavor involves developing a model that incorporates neighborhood characteristics not examined in this study. This will be accomplished through conducting comprehensive on-site surveys to identify and analyze crucial factors for effective crime prevention.

Acknowledgments This study was supported by a research grant from the Research Foundation for Safe Society in 2005. The authors would like to express their gratitude.

References

- Building Research Institute (2006) Results of questionnaire survey on crime prevention in apartment buildings, Building Research Institute, Tsukuba, Japan
- Hino K (2005) Evaluation of crime prevention measures for houses: an analysis of the situation in Japan and UK and a residents' attitude survey. Summaries of technical papers of Annual Meeting, Architectural Institute of Japan. pp 1495–1496
- Hino K (2006) Relationship between number of crimes and land use. Reports City Plan Inst Japan 5(1):29–32
- Hino K, Amemiya M (2005) “Safer Places,” a guideline for crime prevention community planning in the U.K. Shintoshi 59(12):82–87
- Hino K, Amemiya M (2006) “Structure” and utilization of safer places. Shintoshi 60(5):95–103
- Hino K, Koide O (2006) Report on the survey on crime prevention community development in the U.K. Shintoshi 60(4):119–126
- ODPM, Home Office (2003) Safer places—the planning system and crime prevention, ICE Publishing, London
- Schneider RH, Kitchen T (2002) Planning for crime prevention. Routledge, New York
- Seo B, Suzuki T, Hino K (2006) A study on the geographical distribution and environmental of larceny in the Tokyo ward area. J Soc Saf Sci 8:79–82
- Shimada T, Harada Y (1999a) Relationship between crime and socioeconomic factors in large cities. Reports Natl Res Inst Police Sci, 39(2)
- Shimada T, Harada Y (1999b) Relationship between urban spatial configuration and crime occurrence. Reports Natl Res Inst Police Sci, 40(1)

Chapter 7

A Spatial Analysis of the Effects of Neighborhood Socio-economic Status on Residential Burglaries in Tokyo: Focusing on the Spatial Heterogeneity and the Interactions with Built Environment



Masaya Uesugi and Kimihiro Hino

Abstract This study explores the relationship between neighborhood socio-economic status (SES) and the crime rate of residential burglaries in the wards of Tokyo, focusing on the spatial heterogeneity of this relationship and the moderating role of SES on the relationship between crime rate and the built environment. The results are as follows: (1) While global model shows that the proportion of high-income neighbors is negatively and significantly associated with the neighborhood residential burglary rate, the local model, calibrated by geographically weighed regression estimation, indicates that there are local variations in this relationship. (2) Significant interactions between neighborhood income composition and physical indicators such as road area ratio and distance to the nearest rail station suggest that the links between the residential burglary rate and the built environment are conditioned by neighborhood SES.

Keywords Neighborhood · Residential burglary · Income distribution · Geographically weighed regression · Interaction effect · Tokyo

The contents of this paper are based on the following paper originally published in a Japanese journal: Uesugi, M. and Hino, K. (2015) A spatial analysis of the effects of neighborhood socio-economic status on residential burglaries in Tokyo. *Journal of City Planning Institute of Japan* 50(3): 608–615 (in Japanese).

M. Uesugi (✉)

Fukuoka Institute of Technology, Fukuoka, Japan
e-mail: uesugi@fit.ac.jp

K. Hino

Department of Urban Engineering, The University of Tokyo, Tokyo, Japan
e-mail: hino@ua.t.u-tokyo.ac.jp

7.1 Introduction

Spatial patterns of crime occurrences within cities are not necessarily determined only by built environment, such as road connectivity, land use, and building density. In terms of mid- and long-term crime prevention, it is equally important to pay attention to the relationships between crime occurrences and social environment, such as residential composition and industrial structure. Further, recognizing that crime prevention constitutes a constituent of the residential environment, a holistic approach encompassing both spatial and social dimensions becomes imperative (Hino and Kojima 2007).

Neighborhood socio-economic characteristics that reflect the social status and economic bracket of neighborhood residents have long been indicated in research outside of Japan as major explanatory factors of crime occurrence. Logically, a link between neighborhood socio-economic levels and crime is supported from the following perspectives, regardless of whether this relationship is positively or negatively correlated. One perspective stems from the social disorganization theory (Shaw and McKay 1942), which posits that socio-economic difficulties lead to a decrease in social control. This theory is applied in Western countries to explain why neighborhoods with a concentration of disadvantaged residents, including the poor and/or racial minorities, tend to have higher crime rates. Other viewpoints from the routine activity theory (Cohen and Felson 1979) and rational choice theory (Cornish and Clarke 1986) support an inverse relationship between neighborhood socio-economic levels and crime. These theories suggest that affluent neighborhoods are perceived as alluring targets, making crime occurrence within them more likely. Considering these conflicting theories, it is essential to examine which theory supports what kind of case and circumstances.

In Japan, Takagi et al. (2010) found that social capital in a neighborhood has inhibiting effects on residential burglary. With regard to one such element of social capital, Murayama et al. (2013) have demonstrated that social trust is affected by neighborhood social status, as defined by the occupational and educational backgrounds of residents. Of course, it is anticipated that local contexts in Japan differ from those in Western countries, whose circumstances have been emphasized in the development of the above-stated crime theories. Nevertheless, paying close attention to these theories is significant, especially when considering the expansion in economic disparity as well as trends in residential segregation in Tokyo since the 1990s (Uesugi and Asami 2011; Fujita and Hill 2012).

With the above background, this study examines the effects of neighborhood socio-economic status (SES) on crime occurrences in the wards of Tokyo. Residential burglaries in Tokyo have been analyzed in multiple previous studies (Kutsuzawa et al. 2007; Amemiya 2013). The present study contributes to the literature by investigating two characteristics hitherto not considered in Japanese neighborhood-level crime research. The first characteristic involves spatial variability (spatial heterogeneity) in the relationship between neighborhood SES and crime occurrences. Malczewski and Poetz (2005) demonstrated that there is a relationship

between crime risk and average house prices, which are an indication of the neighborhood SES, and neighborhoods in which the relationship becomes positive or negative are geographically mixed in a Canadian city. The same point has been indicated for the United States (Cahill and Mulligan 2007; Arnio and Baumer 2012; Zhang and Song 2014). However, residential segregation is not as distinct in Japanese cities as it is in the cities of Western countries. Therefore, to verify this characteristic for Japanese cities, a variety of residential neighborhood types, such as those found in Tokyo, needs to be studied and various built environment need to be controlled for as well.

The second characteristic examined in the present study is interaction effect, such that the relationship between built environment and crime occurrence changes according to neighborhood SES. Predictors previously used to explain crime rates have considered the built environment as independent from the social environment. However, in arguing for crime prevention through environmental design (CPTED), Taylor (2002) stressed that the relationship between environmental design and crime may rely upon neighborhood context. Even studies outside of Japan have conducted little verification work regarding this relationship. An exception is Ward et al. (2014) who found that in neighborhoods with a high concentration of the disadvantaged, the higher the road connectivity, the lower the crime rate, with the converse occurring in districts without such high road connectivity.

Previous studies on Tokyo have predominantly focused on the latter half of the 2000s decade and earlier. However, a significant reduction in the number of confirmed crimes has been observed subsequently, coinciding with geographical leveling (Amemiya and Shimada 2013). Given the contexts within large cities in Japan, understanding the spatial heterogeneity of the association between neighborhood SES and the crime rate of residential burglaries, as well as the moderating role of SES on the relationship between crime rate and the built environment, would contribute to enhancing the explanatory power concerning crime rates.

7.2 Methods

7.2.1 Data

We use data on crime numbers and neighborhood characteristics for *cho* districts for Tokyo. *Cho* districts are address/block divisions in urban areas of Japan. The numbers of crime were obtained from the geographical information database of Amemiya and Iwakura (2012), which provides the number of penal code offenses for *cho* districts by time series. These data are sourced from the confirmed penal code offenses records of the Tokyo Metropolitan Police Department (MPD), which classify these offenses by crime type and method. This study uses “residential burglaries,” which comprise the following three MPD classifications: breaking and entering (1) in the absence of residents, (2) in the presence of sleeping residents,

and (3) in the presence of residents who are home and awake, but are unaware of a crime occurring elsewhere in their residence. Regarding the statistical years, the three-year period spanning 2009, 2010, and 2011 was used.

For neighborhood characteristics, we use data on land use and building structures as well as population. Population characteristics were obtained from Population Census 2010 (Ministry of Internal Affairs and Communications) and Tokyo Metropolitan Government. Household income distribution, a neighborhood SES measure, was estimated using the method proposed by Uesugi and Asami (2011), with data from both the Comprehensive Survey of Housing Life (Ministry of Land, Infrastructure, Transport and Tourism) and Population Census. “High income” is defined as the upper 20% of household income, and “low income” is defined as the lower 20% of the household income within Tokyo. For land use and building characteristics, GIS data of the Basic City Planning Survey (Tokyo Metropolitan Government) and Zenrin Residential Maps (Zenrin Co., Ltd.) were used. Additionally, rail station location was obtained from the Digital National Land Information (Ministry of Land, Infrastructure, Transport and Tourism).

7.2.2 *Variables*

Dependent variable: Using the totals for residential burglaries during the three-year period, crime rate was considered to be the number of cases per 10,000 households; to manage zero cases, logarithmic transformation was performed after adding one (Amemiya 2013).

Independent variables: Referencing prior research (Hino and Kojima 2007; Amemiya 2013), the variables were shown in Table 7.1. First, social environment variables include population, housing, and neighborhood SES. For population variables, population density, daytime population ratio, average household size (the number of persons per household), and elderly people rate were used. Considering that the presence of visitors, work and school commuters, and work-at-home persons increase natural surveillance, crime prevention effects are anticipated. Homeownership rate, detached house rate, low-rise apartment rate (the proportion living in apartments 1 or 2 floor), and residential stability (the proportion living in the same residence 5 years previously) were set for housing variables. Homeownership rate and residential stability show the flow rate of residents. Higher flow rates are expected to indicate the weakening of informal social control, as demonstrated by lower awareness and concern of residents for neighborhood problems and unconventional behavior. Further, as it is easier to break into residence types that are detached dwellings and low-rise apartment buildings, these are expected to be easily linked to an increase in crime. Regarding neighborhood SES variables, economic strata are defined by the rates of high-income households and low-income households per resident, respectively.

Built environmental variables are those that represent accessibility, land use, and spatial density. Accessibility is represented by distance to nearest station (distance

Table 7.1 Descriptive statistics

Variables	Mean	SD
Residential burglary		
Count (2009–2011)	3.91	4.19
<i>Social environment</i>		
Population		
Population density (/km ²)	23,613	25,513
Daytime population ratio	2.86	10.57
Average household size	2.00	0.32
Elderly people rate (%)	19.96	5.62
Housing		
Homeownership rate (%)	45.03	14.51
Detached house rate (%)	28.05	16.56
Low-rise apartment rate (%)	13.58	10.34
Residential stability (%)	71.42	9.82
Neighborhood SES		
High-income household rate (%)	18.91	7.30
Low-income household rate (%)	18.83	7.26
<i>Build environment</i>		
Accessibility		
Distance to nearest station (m)	558.41	367.74
Distance to city center (m)	9347.8	4190.2
Land use		
Commercial-residential area ratio	1.65	7.98
Road area ratio	0.02	0.04
Spatial density		
District building coverage ratio	33.67	8.98
District floor area ratio	131.66	78.91

N = 2999

from residence to the nearest rail station) and city center (distance from residence to Tokyo station). Land use includes commercial-residential area ratio and road area ratio (the ratio of the road space to land area). Spatial density, such as district building coverage ratio (the ratio of the building footprint area to the land area) and district floor area ratio (the ratio of total of all the floor space to land area), shows how close buildings are built to each other, indicating poor visibility. All of these are considered elements that can attract or trigger crime. However, some research has indicated that accessibility and mixed land use may not necessarily be related to increased crime risk (Amemiya 2013).

Table 7.1 shows the basic statistics of the variables described above. It is noted that when creating the model, we used log transformations for some variables in consideration of their distribution characteristics.

7.2.3 Analysis Method

The neighborhoods studied comprised 2999 *cho* districts with 50 or more households (Population Census 2010) in the wards of Tokyo. The statistical analysis was divided into three major portions.

First, the dependent variable and independent variables mentioned in Sect. 7.2.2 were used to perform multiple regression analysis with an ordinary least squares (OLS) regression model. At this time, independent variables with strong correlations were first excluded to prevent multicollinearity. Then, to extract valid variables as predictive factors for crime occurrence, variables were selected using cross-validation. Here, we examine effects of neighborhood SES on the crime rate by variable significance (the significance level was set at 5%, unless otherwise noted) and model goodness-of-fit.

Next, regarding the relationships between neighborhood SES and crime, we employ geographically weighted regression (GWR) to investigate the spatial variations (spatial heterogeneity). Although the OLS model provides the uniform regression coefficients, *t* value, and coefficient of determination (R^2), these values were derived for each neighborhood location (in this study, this corresponds to *cho* district), by applying the GWR model of Fotheringham et al. (2002), as shown in Eq. (7.1).

$$y_i = \beta_{0i} + \sum_k \beta_{ki} x_{ik} + \varepsilon_i \quad (7.1)$$

where y_i is a dependent variable at location i , x_{ik} is an independent variable at number k at location i , and ε_i is an error term at location i . β_{ki} is the regression coefficient β_k of location i , and its estimated value $\hat{\beta}$ is determined using Eq. (7.2), as follows:

$$\hat{\beta}(i) = \left(\mathbf{X}^T \mathbf{W}(i) \mathbf{X} \right)^{-1} \mathbf{X}^T \mathbf{W}(i) \mathbf{Y} \quad (7.2)$$

where $\mathbf{W}(i)$ is the $n \times n$ spatial weights matrix whose off-diagonal elements are zero and whose diagonal elements denote w_{ij} for i (n is the number of observed values within regression point i). It should be noted that weight w_{ij} of j vis-à-vis regression location i is shown by Eq. (7.3), which uses a Gaussian distance decay function.

$$w_{ij} = \exp \left(-\frac{d_{ij}^2}{b^2} \right) \quad (7.3)$$

where d_{ij} is the direct distance from i to j , and b is the kernel bandwidth, which shows the extent of distance decay. The GWR result is dependent on this bandwidth.

Here, employing the cross-validation (CV) technique, Eq. (7.4) is used to find the optimal bandwidth of b for minimizing the CV score shown in the formula.

$$\text{CV} = \sum_i [y_i - \hat{y}_{\neq i}(b)]^2 \quad (7.4)$$

where $\hat{y}_{\neq i}(b)$ shows the predicted value of y (excluding location i) when using bandwidth b . The result estimated via GWR and OLS model can be examined using indices such as the adjusted degree of freedom R^2 , Akaike's Information Criteria (AIC), and Moran's I of the residual. At the same time, we can also use spatial pattern mapping to examine the t value of independent variables and coefficient of the neighborhood SES variable for each neighborhood.

Finally, we investigate the moderating effect of SES on the relationship between crime rate and the built environment. For the built environment variables not selected as significant variables in the OLS analysis, the interaction terms of the variables with the neighborhood SES variables were introduced. Here, to avoid multicollinearity with interaction terms, mean centering was employed (Cohen et al. 2003). For statistically significant interaction terms, we conducted simple slope analysis to confirm that neighborhood SES significantly changes the effects of the built environment on crime. It is noted that statistical environment R (ver. 3.0.3) was used for all the statistical analyses in this study.

7.3 Relationship Between Crime Rate and Neighborhood SES

In this section, the relationship between crime rate and neighborhood SES is examined using OLS model. First, independent variables with high mutual correlation were excluded. Specifically, population density, which correlated with daytime population ratio ($r = 0.58, p < 0.001$) and district floor area ratio, which correlated with district building coverage ratio ($r = 0.57, p < 0.001$), were excluded. Moreover, there were strong correlations between the rates of low-income and high-income household ($r = 0.81, p < 0.001$), which were used to represent neighborhood SES, therefore their simultaneous inclusion was avoided.

The estimated results are shown in Table 7.2. Model 0 does not include the neighborhood SES variable. Here, daytime population ratio and average household size were adopted as variables with positive significance with regard to crime rates. Conversely, detached house rate, low-rise apartment rate, and distance to city center were adopted as variables with negative significance.

Model 1 includes high-income household rate as the neighborhood SES variable. Here, daytime population ratio was excluded, and elderly people rate and commercial-residential area ratio were substituted as variables with negative significance. Then, even with consideration of these variables, high-income household

Table 7.2 OLS results for residential burglary

	Model 0			Model 1		
	Coefficient	t value		Coefficient	t value	
Constant	-1.576	-3.74	***	0.333	0.68	
Daytime population ratio (logged)	-0.270	-9.21	***			
Average household size	-0.634	-7.37	***	-0.594	-6.71	***
Elderly people rate				-0.030	-6.55	***
Detached house rate	0.019	12.67	***	0.018	11.06	***
Low-rise apartment rate	0.025	9.98	***	0.021	7.89	***
Distance to city center (logged)	0.462	8.56	***	0.358	6.39	***
Commercial-residential area ratio (logged)				-0.197	-8.37	***
High-income household rate				-0.030	-8.37	***
Adjusted R^2	0.334			0.345		
AIC	9451			9390		

***: $p < 0.1\%$, **: $p < 1\%$, *: $p < 5\%$

rate was adopted as a variable with negative significance. Here, the adjusted R^2 became 0.345, and the AIC improved from 9451 to 9390.

We can see below that variables with negative effects in relation to crime rates are consistent with prior research; for example, daytime population ratio, average household size, and elderly people rate. As can be imagined, these ratios are of people who are natural “neighborhood watchers,” like visitors and residents, and surveillance effects function effectively in these cases.

Conversely, variables that have positive effects with regard to crime rates are detached house rate and low-rise apartment rate. The latter result is especially consistent with prior research (Hino and Kojima 2007; Amemiya 2013). This strongly suggests that the presence of low-rise apartment households is a major predictor that increases crime risk, as such buildings are easier to burglarize.

Even when these variables are controlled for, the fact that the high-income household rate variable was negatively significant shows that higher neighborhood SES reduces crime risk. In other words, considering correlation, the lower the neighborhood SES, the higher the crime risk. Hence, the present study supports the social disorganization theory. In the context of Japan, as highlighted by Kutsuzawa et al. (2007), “persons vulnerable to crime” may exist owing to economic constraints. Moreover, as surmised by Amemiya (2013), it may be possible that neighborhoods with high asset values, which easily became targets of crime in the early 2000s decade, thereafter used their economic leeway to promote anti-crime measures, which may have led to improvements in crime rates.

7.4 Spatial Heterogeneity in the Relationship Between Crime Rate and Neighborhood SES

This section employs GWR to investigate the spatial heterogeneity in the neighborhood SES and crime relationship shown in the previous section. First, Table 7.3 describes the results estimated using GWR. Regarding the goodness-of-fit of the model, comparison with the OLS showed improvements in the adjusted R^2 from 0.417 to 0.345 and in AIC from 9390 to 9120. Moran's I , which shows the spatial autocorrelation of residuals, also reduced from 0.127 to 0.052. To test whether the coefficients are uniform for all neighborhoods, the $F(3)$ test was used (Leung et al. 2000). This test showed statistical significance at the 5% level for the spatial distribution of all independent variables.

Before we explore the effects of the neighborhood SES variable, we first highlight the characteristic points of the results obtained with the present model. Looking at the estimated coefficients in Table 7.3, we see a range in the plus and minus signs for such coefficients as average household size, distance to city center, and commercial-residential area ratio. Thus, we can glimpse spatial heterogeneity in relationships with crime rates, including for high-income household rate. Figure 7.1 shows the spatial distribution of local R^2 values. We can see major fluctuations by neighborhood: for example, in some neighborhoods (e.g., the southern part of Edogawa Ward), the value exceeds 0.5, and in some agglomeration neighborhoods (e.g., Shinjuku, Bunkyo, and Toshima Wards), it exceeds 0.4. On the contrary, the values of surrounding wards are less than 0.2. For such neighborhoods, predictors not considered in the present model are expected to play an important role. Additionally, for low-rise apartment rate variable, most neighborhoods had a t value with positive significance (Fig. 7.2). There are major differences in coefficient size across the east-west axis; this coefficient becomes larger in so-called *Shitamachi* neighborhoods (i.e., older districts in lower lands).

Table 7.3 GWR result for residential burglary

	Coefficient				
	Min	25%	Median	75%	Max
Constant	-4.253	-2.909	-0.506	2.917	20.140
Average household size	-1.713	-0.964	-0.801	-0.623	0.482
Elderly people rate	-0.069	-0.036	-0.030	-0.020	0.020
Detached house rate	0.005	0.017	0.019	0.023	0.031
Low-rise apartment rate	0.004	0.015	0.020	0.031	0.046
Distance to city center (logged)	-1.503	0.041	0.449	0.743	0.991
Commercial-residential area ratio (logged)	-0.297	-0.225	-0.174	-0.127	0.071
High-income household rate	-0.047	-0.026	-0.021	-0.015	0.018
Adjusted R^2	0.417				
AIC	9120				
Moran's I (residuals)	0.052				

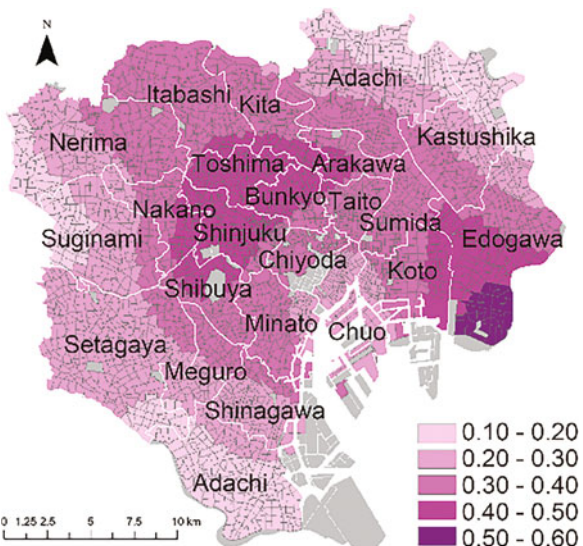


Fig. 7.1 Spatial variation of local R^2

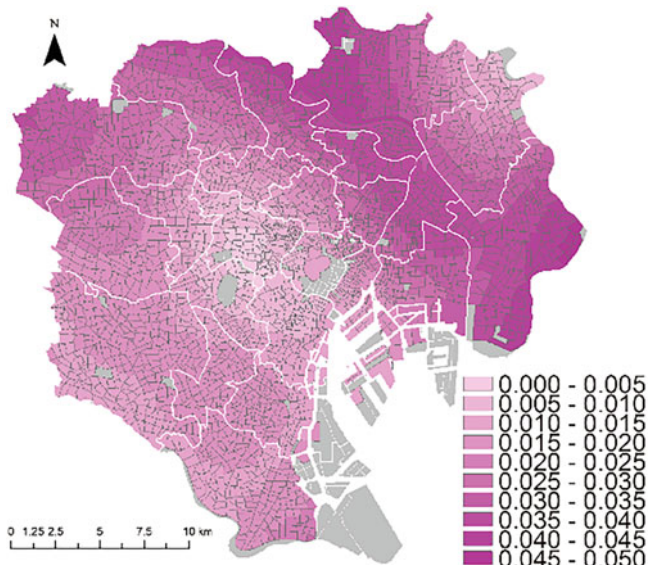


Fig. 7.2 Local coefficients of low-rise apartment rate

Figure 7.3 shows the distribution of the local coefficients of high-income household rate, the particular focus of the present study. In the OLS estimates, this coefficient was negatively significant. However, as shown in Fig. 7.4, neighborhoods with 5% significance ($t > 1.96$) account for only around half of the total (51.3%,

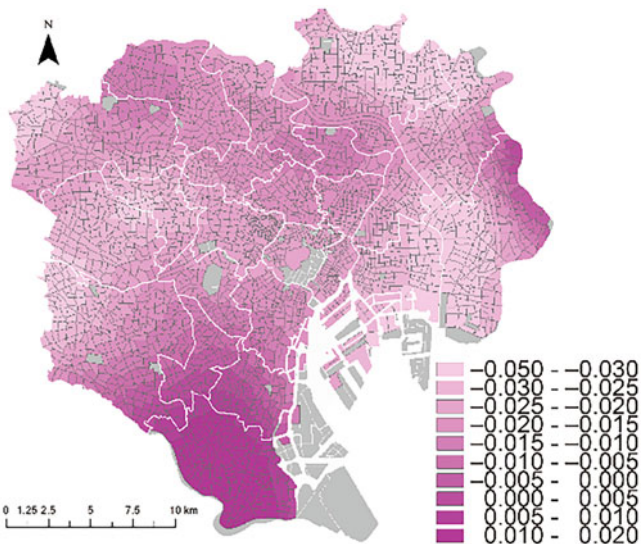


Fig. 7.3 Local coefficients of high-income household rate

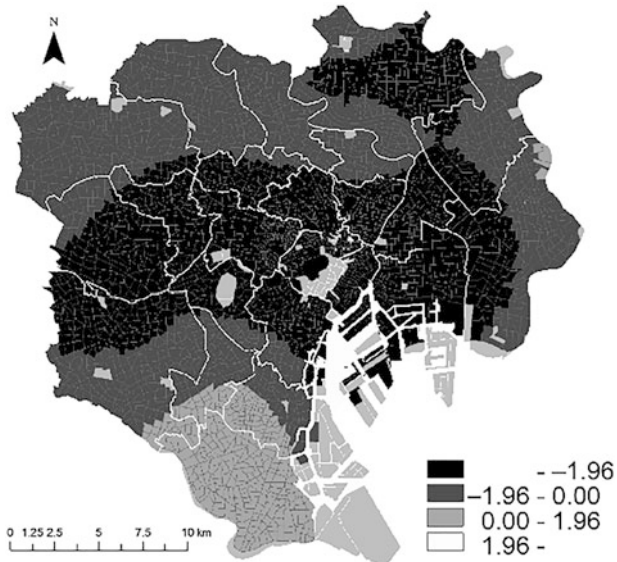


Fig. 7.4 *t* values for high-income household rate

$n = 1537$). Conversely, in some neighborhoods (10.2%, $n = 305$), the coefficient is positive; these neighborhoods are aggregated in the areas surrounding the Ota Ward. This means that, in contrast with other neighborhoods, the higher the high-income household rate is, the higher the crime rate becomes in these neighborhoods.

These geographical differences could be attributed to several potential reasons. For example, although social control could increase with an increase in high-income residents, in affluent neighborhoods where such social control factors were already functioning, there may also be an increase in the allure of concentration of high-income population for persons who are planning to commit crime. Regarding neighborhoods for which the coefficient was negative (e.g., Koto, Edogawa, Adachi, Suginami, and Nakano Wards), there is a tendency of higher income levels corresponding with lower risks of crime. These neighborhoods are among those for which the percentage of high-income strata is relatively low, except for a portion of these neighborhoods, such as the bayside area of Koto Ward, where urban redevelopment has progressed in recent years. The finding that in neighborhoods of low SES, there is a negative correlation between residential burglaries and neighborhood SES is consistent with the findings obtained for foreign cities (Malczewski and Poetz 2005; Zhang and Song 2014).

Conversely, the positive relationship between crime and neighborhood SES, as seen in Ota Ward, shows that in these regions where the percentage of high-income household is high, there is a tendency for increased crime risk. Ota Ward has a mix of relatively high and low economic strata neighborhoods in the south and north. Because neighborhoods where members of the high-income strata are concentrated are more easily targeted for crime, the nearby relatively low-income neighborhoods reduce the incentive to commit crime. However, since statistically significant results were not obtained for these coefficients, more detailed analysis is required.

Through these findings, this study has described geographical differences in crime occurrence factors within Tokyo. However, as confirmed in the beginning, the model goodness-of-fit was not necessarily high for all studied neighborhoods. Markowitz et al. (2001) claimed that trends of crime rates increasing in economically poor neighborhoods are weakened as a result of neighborhood cohesion. This likely suggests the importance of considering not only the demographic attributes of residents, but also dynamic processes (Brisson and Roll 2012). GWR is a superior means of exploring even more effective predictors (Gao and Asami 2002), and in possible future developments, these kinds of neighborhood characteristic variables can also be included within GWR perspectives.

7.5 Neighborhood SES Effects on the Relationships Between Crime Rates and Built Environment

This section analyzes the interaction terms of the neighborhood SES variable concerning the built environmental variables not used in the OLS estimates in Sect. 7.3. Here, we assume that the effects of built environment are dependent on neighborhood SES. The specific built environment variables are distance to nearest station, road area ratio, and district building coverage ratio. Of these, distance to nearest station and road area ratio can be considered variables that are statistically

Table 7.4 OLS results with interaction term (road area ratio)

	Model 1-0		Model 1-1		
	Coefficient	t value	Coefficient	t value	
Constant	0.346	0.71	0.344	0.71	
Average household size	-0.594	-6.71	*** -0.598	-6.76	***
Elderly people rate	-0.030	-6.56	*** -0.029	-6.34	***
Detached house rate	0.018	11.08	*** 0.018	11.10	***
Low-rise apartment rate	0.021	7.91	*** 0.021	7.97	***
Distance to city center (logged)	0.355	6.33	*** 0.356	6.35	***
Commercial-residential area ratio (logged)	-0.196	-8.33	*** -0.197	-8.40	***
High-income household rate	-0.031	-8.40	*** -0.031	-8.47	***
Road area ratio	0.389	0.67	-0.589	-0.88	
High-income household rate × road area ratio			0.163	2.98	**
Adjusted R^2	0.345		0.346		
AIC	9405		9398		

***: $p < 0.1\%$, **: $p < 1\%$, *: $p < 5\%$

insignificant when taken independently, but become significant when we added their interaction terms with neighborhood SES.

Tables 7.4 and 7.5 show each of their estimated results. Model 1-0 of Table 7.4 does not include an interactive term with neighborhood SES for road area ratio. When the other variables adopted in Model 1 of Sect. 7.3 are controlled for, road area ratio is not a statistically significant variable, and there is almost no improvement in model goodness-of-fit compared with Model 1 of Table 7.2. On the contrary, in Model 1-1, which includes the interaction term, the interaction term becomes a positive significant value at the 1% level. Further, goodness-of-fit is also improved in this model with measures of adjusted R^2 and AIC. Models 2-0 and 2-1 of Table 7.5 show the results for distance to nearest station, and similar results are obtained in that the interaction term becomes a negative significant variable at the 1% level.

Next, to interpret these results, we evaluated the conditional effect (simple slope) of some built environment variables on crime rate at various levels of high-income household rate. Here, “simple slope” is the regression coefficient, with regression of crime rates within built environmental variables under a specific level of neighborhood SES. We can perceive from Figs. 7.5 and 7.6 that the effects of built environment change according to neighborhood SES levels. For example, the effects of road area ratio on crime rate are negative when the high-income household rate in the area is smaller (Fig. 7.5). Conversely, with a higher high-income household rate, this effect becomes positive. Buffer portions show a 95% confidence interval for these effects. When the neighborhood high-income household rate is 10% or less, we observe a significant negative relationship between crime rate and road area ratio, while, conversely, when it exceeds 30%, a positive relationship emerges. Similarly,

Table 7.5 OLS results with interaction term (distance to nearest station)

	Model 2-0		Model 2-1	
	Coefficient	t value	Coefficient	t value
Constant	0.351	0.70	0.399	0.79
Average household size	-0.590	-6.28	*** -0.586	-6.24 ***
Elderly people rate	-0.030	-6.54	*** -0.031	-6.74 ***
Detached house rate	0.018	10.99	*** 0.018	10.78 ***
Low-rise apartment rate	0.021	7.89	*** 0.022	8.16 ***
Distance to city center (logged)	0.359	6.36	*** 0.360	6.39 ***
Commercial-residential area ratio (logged)	-0.197	-8.31	*** -0.204	-8.57 ***
High-income household rate	-0.030	-8.37	*** -0.031	-8.46 ***
Distance to nearest station (logged)	-0.006	-0.14	-0.017	-0.43
High-income household rate \times distance to nearest station (logged)			-0.014	-3.08 **
Adjusted R^2	0.344		0.346	
AIC	9406		9398	

***: $p < 0.1\%$, **: $p < 1\%$, *: $p < 5\%$

Fig. 7.5 Conditional effect of road area ratio at various levels of high-income household rate. The gray polygon is the 95% interval around the predictions

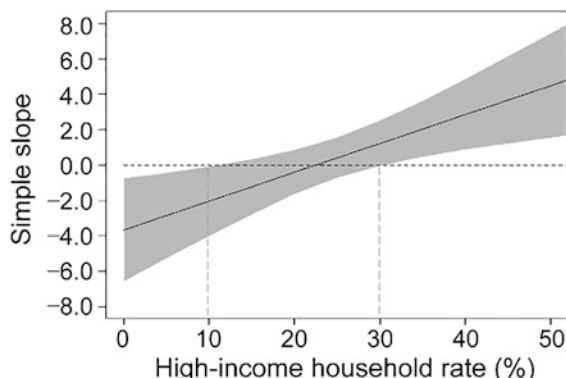
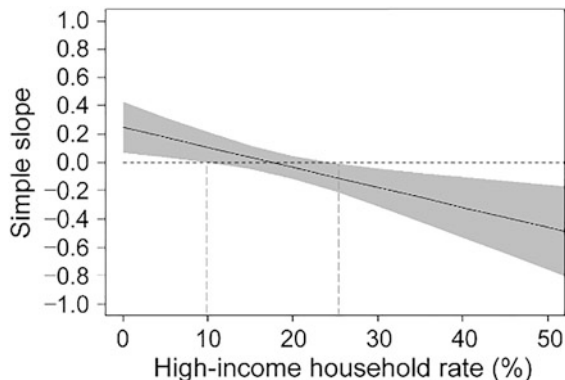


Fig. 7.6 shows that when the neighborhood high-income household rate is 10% or less, there is a significant positive relationship between crime rate and distance to the nearest rail station, but when it exceeds 26%, this becomes a negative relationship.

These findings indicate that in neighborhoods of high SES, larger road area ratios and smaller distances to the nearest rail station correspond with higher crime rates. Additionally, more convenient access to an arterial roadway and/or a nearby rail station is associated with a higher tendency for crime occurrence. Conversely, in neighborhoods where SES level is low, lower accessibility to roads and rail stations results in higher crime risk.

There are several possible reasons why the effects of accessibility vary according to neighborhood SES levels. Generally, social controls play a role in restraining

Fig. 7.6 Conditional effect of distance to nearest station at various levels of high-income household rate. The gray polygon is the 95% interval around the predictions



crime in high-income neighborhoods. However, good accessibility also means that unspecified numbers of people can enter and leave the neighborhood, which grants an anonymity that may be an inducement to crime. This may be hypothesized as an increase in crime rate due to the aforementioned anonymity nullifying the original crime restraint effects. In contrast, it is supposed that social controls cannot function in a low-income neighborhood. In such neighborhoods, the natural surveillance effects of residents and passers-by may play a significant role. However, surveillance effects lose their strength in neighborhoods of poor accessibility, where fewer people pass by and visibility is poor. Therefore, more than neighborhoods with good accessibility, these conditions may more readily invite an increase in crime.

7.6 Conclusion

This study focused on neighborhood SES and examined the relationship between neighborhood SES and residential burglary rates. With this approach, we highlighted spatial heterogeneity of the relationship and the interaction effects of neighborhood SES, which have previously not been considered in a Japanese context. The results revealed that neighborhood SES had significant negative effects on crime rates, even when built environment factors were considered. However, the results also revealed that in some neighborhoods, neighborhood SES may have positive effects. Further, in neighborhoods with high neighborhood SES, crime rates were found to be higher in districts with good accessibility in terms of road area ratios and distance to nearest rail station. It was also observed that the converse occurs in neighborhoods with lower district SES. In the past, the fact that there were contextual dependencies for built environment was largely disregarded. These findings suggest that neighborhood SES is useful clue for crime prevention measures in Japan as well, even though the spatial variation of neighborhood SES is smaller in Japan than in Western counties.

However, some aspects of neighborhood SES effects remain to be clarified. As indicated in Sect. 7.4, it will be necessary to pay close attention to how social capital can strengthen or weaken relationships between crime rates and neighborhood SES. Additionally, although the purpose of this study was to explain the current crime tendencies following the progress made in anti-crime measures in the first decade of the 2000s, from the perspectives of mid- and long-term measures to create cities with improved crime prevention, it becomes essential to delve deeper into the associations between trends in residential segregation and changes in the roles of neighborhood SES.

References

- Amemiya M (2013) Relationship between time series variations of residential burglary rates and the social and physical environments of local districts in Tokyo's 23 wards: an analysis using latent growth curve modeling. *J City Plan Inst Jpn* 48(3):351–356 (in Japanese)
- Amemiya M, Iwakura N (2012) Construction of a time series micro-scale geographical database of crimes and its potential application for temporal-spatial analysis of crime distribution in Tokyo. Papers and proceedings of the Geographic Information Systems Association 21, CD-ROM (in Japanese)
- Amemiya M, Shimada T (2013) Identifying changing patterns in the geographical distribution of residential burglaries in Tokyo: an analysis of crimes that have occurred in the past eleven years. *J City Plan Inst Jpn* 48(1):60–66 (in Japanese)
- Arnio A, Baumer E (2012) Demography, foreclosure, and crime: assessing spatial heterogeneity in contemporary models of neighborhood crime rates. *Demogr Res* 26:449–488
- Brisson D, Roll S (2012) The effect of neighborhood on crime and safety: a review of the evidence. *J Evid Based Soc Work* 9:333–350
- Cahill M, Mulligan G (2007) Using geographically weighted regression to explore local crime patterns. *Soc Sci Comput Rev* 25(2):174–193
- Cohen LE, Felson M (1979) Social change and crime rate trends: a routine activity approach. *Am Sociol Rev* 44(4):588–608
- Cohen J, Cohen P, West S, Aiken L (2003) Applied multiple regression/correlation analysis for the behavioral sciences. Erlbaum Associates, Hillsdale
- Cornish D, Clarke R (1986) Reasoning criminal: rational choice perspectives on offending. Springer-Verlag, New York
- Fotheringham AS, Brunsdon C, Charlton M (2002) Geographically weighted regression: the analysis of spatially varying relationships. Wiley, Chichester
- Fujita K, Hill RC (2012) Residential income inequality in Tokyo and why it does not translate into class-based segregation. In: Maloutas T, Fujita K (eds) Residential segregation in comparative perspective: making sense of contextual diversity. Ashgate, Farnham, pp 54–86
- Gao X, Asami Y (2002) Search for spatial influence on price determination for detached houses the quarterly journal of housing and land. *Economics* 44:10–21 (in Japanese)
- Hino K, Kojima T (2007) Relationship between crime rate of dwelling burglary and local context: on neighbourhoods in 29 wards and cities in Tokyo. *J Archit Plan* 616:107–112 (in Japanese)
- Kutsuzawa R, Mizutani N, Yamaga H, Ohtake F (2007) Regional crime rate, land price and housing rent. *Q J Hous Land Econ* 66:12–21 (in Japanese)
- Leung Y, Mei CL, Zhang WX (2000) Statistical tests for spatial nonstationarity based on the geographically weighted regression model. *Environ Plan A* 32(1):9–32
- Malczewski J, Poetz A (2005) Residential burglaries and neighborhood socioeconomic context in London, Ontario: global and local regression analysis. *Prof Geogr* 57(4):516–529

- Markowitz F, Bellair P, Liska A, Liu J (2001) Extending social disorganization theory: modeling the relationships between cohesion, disorder, and fear. *Criminology* 39:293–320
- Murayama H, Arami R, Wakui T, Sugawara I, Yoshie S (2013) Cross-level interaction between individual and neighbourhood socioeconomic status in relation to social trust in a Japanese community. *Urban Stud* 51(13):2770–2786
- Shaw CR, McKay HD (1942) Juvenile delinquency and urban areas. University of Chicago Press, Chicago
- Takagi D, Tsuji R, Ikeda K (2010) Crime control by local communities: focusing on social capital and cooperative behaviors in neighborhoods. *Japan J Social Psychol* 26(1):36–45 (in Japanese)
- Taylor R (2002) Crime prevention through environmental design (CPTED): yes, no, maybe, unknowable, and all of the above. In: Bechtel RB, Churchman A (eds) *Handbook on environmental psychology*. Wiley, New York, pp 413–426
- Uesugi M, Asami Y (2011) Neighborhood segregation by household income since the late 1990s: case study of Ota ward, Tokyo. *Geogr Rev Japan Ser A* 84(4):345–357 (in Japanese)
- Ward JT, Nobles MR, Youstin TJ, Cook CL (2014) Placing the neighborhood accessibility—burglary link in social-structural context. *Crime Delinquency* 60(5):739–763
- Zhang H, Song W (2014) Addressing issues of spatial spillover effects and non-stationarity in analysis of residential burglary crime. *GeoJournal* 79(1):89–102

Chapter 8

Factors Affecting Installation of Residential Photovoltaics in Housing Estates in Kakegawa City, Shizuoka: Focusing on Housing and Surrounding Environment Characteristics



Yuki Okazawa, Kimihiro Hino, and Yasushi Asami

Abstract This study identifies the factors affecting the installation of residential solar photovoltaics (PVs) in housing estates in Kakegawa City, Shizuoka Prefecture. Logistic regression analysis of 1327 houses in housing estates revealed that those that were lower, fully rebuilt, newly built, or larger as well as newly built were more likely to have PV installed. Furthermore, analysis of 1971 houses revealed that—compared to houses in adjacent blocks—those that were without building agreements, lower, fully rebuilt, newly built, or smaller as well as newly built were more likely to have PV installed. Accordingly, full rebuilds, new builds, building heights (measured in meters), and property areas (measured in square meters) were suggested as factors affecting PV installation.

Keywords Residential solar PV · Residential PV power generation · Housing estate · Building agreement · Logistic regression analysis

The contents of this paper are based on the following paper originally published in a Japanese journal: Okazawa, Y., Hino, K. and Asami, Y. (2022) Factors affecting residential solar photovoltaics installation in housing estates in Kakegawa City, Shizuoka Prefecture. *Journal of City Planning Institute of Japan* 57(3): 1049–1055 (in Japanese).

Y. Okazawa (✉) · K. Hino · Y. Asami

Department of Urban Engineering, The University of Tokyo, Tokyo, Japan
e-mail: okazawa-yuki986@g.ecc.u-tokyo.ac.jp; hino@ua.t.u-tokyo.ac.jp;
asami@csis.u-tokyo.ac.jp

8.1 Introduction

Residential photovoltaic (PV) power generation has been progressively introduced in Japan since the commencement of an excess electricity purchasing scheme in November 2009 and the transition to a feed-in tariff scheme in July 2012. Moreover, government policy expects further installations of such power generation in the future. The Climate Change Adaptation Plan (Cabinet decision, October 2021) lists “introduction and use of renewable energy, such as self-sufficient PV power generation as a fundamental role of the people.” (Ministry of the Environment (MOE) 2021). The Sixth Strategic Energy Plan (Cabinet decision, October 2021) explicitly states “the aim of installing PV power generation facilities on 60% of newly built houses in 2030.” (Agency for Natural Resources and Energy (ANRE) n.d.).

According to the following previous research, factors affecting the installation of residential PV power generation can be broadly divided into the characteristics of residents, houses, and the surrounding environment.

The characteristics of residents have been analyzed in aggregation units based on census data. Kosugi et al. (2019) documented that factors affecting installation in census block units in Kyoto, Kyoto Prefecture were lower population density, greater household residents, and shorter residence periods (Kosugi et al. 2019). Schaffer and Brun (2015) argued that the installation of residential PV power generation in Germany is positively related to the home ownership rate and per-capita gross regional product (Schaffer and Brun 2015).

The characteristics of houses focus on the building’s height, area, volume, and age; the building method; and changes to the building. Based on residential PV installation permit data from Baltimore, Maryland, USA, Irwin (2021) established that the houses wherein it was installed were relatively larger, newer, and not attached houses (residences that have at least one wall shared with the neighboring residence) (Irwin 2021). Kawaguchi et al. (2020) investigated Nagoya, Aichi and found that compared to buildings wherein PV was not installed, those with PV installed had greater area, height, volume, and solar radiation (Kawaguchi et al. 2020). According to Bollinger and Gillingham (2012), the performance of residential repairs is one factor affecting the installation of residential PV power generation in California, USA (Bryan Bollinger and Kenneth Gillingham 2012).

The third factor comprises characteristics of the surrounding environment. Hachem-Vermette and Singh (2019) created patterns for the arrangement of neighboring houses and buildings as effects from the surrounding buildings and simulated amounts of solar radiation (Caroline Hachem-Vermette and Kuljeet Singh 2019). Narumi and Kim (2017) computed the amount of electricity generated in Yokohama, Kanagawa, accounting for building use, area class, and use districts (Daisuke Narumi and Kim Younghyo 2017). Furthermore, numerous studies have focused on distance, with Müller and Rode (2013) revealing that in Wiesbaden, Germany, installation tends to increase as the installed residential PV capacity in the neighborhood increases (Sven Müller and Johannes Rode 2013). Graziano and Gillingham

(2015) documented that in Connecticut, USA, residential PV installations in the previous 6 months caused an increase in those within 0.5 miles (Marcello Graziano and Kenneth Gillingham 2015). Researchers have noted that distance includes not only physical distance but also peer effects. According to Palm (2017), peer effects refer to “the social influence of peers, such as colleagues, neighbours or friends.” Moreover, he concluded that in Sweden, peer effects accompanying direct contact between people were more important than those from simply observing PV panels (Palm 2017). Curtius et al. (2018) revealed a tendency for the number of residential PV installations in a neighborhood and recognition of social expectations for PV installation to increase homeowners’ desire for installation (Curtius et al. 2018).

However, these three characteristics were interrelated, and which factor truly had an effect was unclear. Owing to data limitations, controlling all of the characteristics of residents, houses, and surrounding environment was difficult. Therefore, we deliberately focused on housing estates¹ as a space wherein the three aforementioned characteristics were highly homogeneous. Specifically, we assumed that residents would have lived there from the time of development and would be of similar ages and income classes. The houses were built around the same time and have similar building shapes pursuant to building agreements. The surrounding environment was assessed by average distance between nearest houses (see Table 8.1, interval between adjacent buildings (m)), which was similar. However, whether residential PV was installed differs between houses even within a housing estate.

Revealing the factors affecting installation in housing estates is a finding that is useful when evaluating support for residential PV installation in housing estates and residential areas in Japan, which we believe is this study’s significant contribution to the literature.

This study aimed to gather information regarding the types of houses and surrounding environments wherein residential PV power generation was installed in housing estates. Moreover, it aimed to verify the robustness of the factors affecting installation in housing estates by conducting analysis adding houses in neighboring areas outside the housing estates.

As presented below, we established hypotheses regarding the factors affecting residential PVs installation. Concerning housing characteristics, PV power generation was more likely to be installed if the building area is larger, the building height is higher, and the building shape changes, such as through being renovated, rebuilt, or newly built. By contrast, if a building agreement contains particulars about roofs, these must be considered and PVs must not be installed. Regarding the characteristics of the surrounding environment, installation makes less progress if the interval between adjacent buildings is closer, owing to the effects of light pollution from light reflecting off the PVs.

¹ A housing estate is defined as “a residential area on the National List of New Towns or judged to be a ‘housing estate’ by a local government,” with reference to the MLIT “National List of Housing Estates (FY2018).” (Ministry of Land, Infrastructure, Transport, and Tourism (MLIT) n.d.).

Table 8.1 Outline of housing estates and areas for comparison in Kakegawa City

		Area mean (see Sect. 8.3.1 for an explanation of variables)												
Area	Housing estates	Date residence commenced (year)	Project method at development entity	Area (ha)	No. of houses	No. of houses with residential PVs	Residential PV installation rate (%)	Area of houses (m ²)	Height houses (m)	Interval between adjacent buildings (m)	Building agreement dummy	Renovation dummy	Rebuilding dummy	New build dummy
Katsuragaoka estate	1980	General public (prefecture)	30	604	32	5.3%	87.7	8.2	11.8	0.005	0.015	0.070	0.008	
Asahigaoka estate	1985	Development permit (private)	16	379	12	3.2%	83.2	8.1	11.0	1.000	0.013	0.055	0.021	
Akidihamichi	1992	Development permit (private)	10	344	8	2.3%	100.4	8.4	11.2	0.305	0.015	0.026	0.029	
Mizutari	—	—	97	358	38	10.6%	110.1	8.0	14.2	0.000	0.014	0.106	0.131	
Otarō	—	—	11	129	11	8.5%	96.1	8.5	11.9	0.000	0.016	0.062	0.140	
Kamiyashiki	—	—	11	157	17	10.8%	97.5	8.2	13.2	0.000	0.019	0.051	0.299	

Sources: Housing estates: created with reference to MLIT, "National List of Housing Estates (FY2018)"

Areas for comparison: scope and areas identified based on Statistics Bureau, Ministry of Internal Affairs and Communications, "2015 Census: Border Data by Neighborhood, Etc."

No. of houses: used polygons that had apartment building names or private house names in the Zmap-TOWN II Digital Residential Map

Interval between adjacent buildings: used straight-line distance from the center of the building polygon to that of the nearest building polygon in 2020 in Kakegawa City for each house

8.2 Research Methods

8.2.1 Research Subjects

This study's subjects were PVs installed on the roofs of houses in Kakegawa City, Shizuoka.

We selected Kakegawa City, Shizuoka, for the following reasons: a 3D urban model (Project PLATEAU) provided by the City Bureau of the Ministry of Land, Infrastructure, Transport and Tourism (MLIT) has been developed, making it easier to gain information on building heights. Additionally, it seems that residential PV installations will continue into the future because—as a target under the Third Kakegawa City Climate Change Countermeasure Action Plan (Area Policy Volume)—the city aims to grow from 3994 “installations of general residential PV power generation (cumulative total)” as of FY2017 to 6000 in FY2023 and 8000 in FY2030 (Kakegawa City [n.d.-a](#)).

Kakegawa City has implemented “New Energy Device, Etc. Installation Support Project”, which offers assistance for up to half the expenses (to a maximum of 30,000 yen) incurred for installing devices in PV power generation facilities installed on new houses (connected to the system within 1 year of completion of construction or from purchase of a ready-built house) and up to half (to a maximum of 60,000 yen) those incurred for installing devices installed on existing houses (connected to the system 1 year or more from completion of construction or from purchase of a ready-built house) (Kakegawa City [n.d.-b](#)).

According to Kakegawa City’s Environmental Policy Division, the aforementioned project has been used for 2216 installations from April 2013 to February 2022 for an installed capacity totaling 12,668.36 kW. The number of houses using the project each fiscal year—divided into new builds and existing buildings—is illustrated in Fig. 8.1. Its usage in new builds has been greater since FY2018, when eligibility for assistance was classified into new builds and existing buildings. The cost of installing PVs on existing buildings is greater than for new builds because Kakegawa City authorities recognized that it would be more expensive than for new builds.².

² According to the “Opinion on Procurement Prices for FY2022 Onward, Etc.” by the Procurement Price Calculation Committee, ANRE (2022), the mean system cost for residential PV power generation installed in 2021 was 302,000 yen/kW and 280,000 yen/kW for existing and new buildings, respectively (Procurement Price Calculation Committee [n.d.](#)).

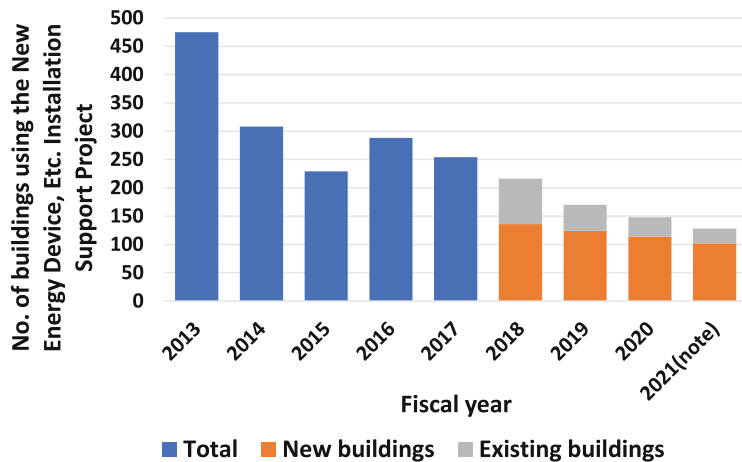


Fig. 8.1 Number of buildings using the Kakegawa City New Energy Device, Etc. Installation Support Project, by new builds and existing buildings. Source: Provided by Environmental Policy Division, Kakegawa City. Note: The figures for FY2021 end in February 2022

8.2.2 Data

8.2.2.1 Building Polygons

We acquired building polygon data on Kakegawa City for 2008/2009 (“2008”) and 2020 from the Zmap-TOWN II Digital Residential Maps provided by Zenrin. Only those polygons that had apartment building names or private house names in the Zmap-TOWN II Digital Residential Map were extracted. Consequently, public facilities and business premises were not included in the analysis.

8.2.2.2 Building Height

We acquired building heights from the 3D urban model (Project PLATEAU) provided by MLIT (“Plateau data”). However, because the Plateau data did not match (Sect. 8.2.2.1), we excluded buildings that lacked a height value from the Plateau data and spatially linked data in Sect. 8.2.2.1 with a center of gravity closest to the that in the former on ArcGIS Pro to include building heights in Sect. 8.2.2.1.

8.2.2.3 Presence or Absence of Residential PV Installations

To confirm whether residential PV power generation had been installed, we used the Geospatial Information Authority of Japan’s National Up-to-Date Photographs (Seamless) as a background map in ArcGIS Pro. The aerial photographs in

Kakegawa City were based on simple aerial photography (photographed in June to August 2020).

8.2.3 *Process of the Study*

We analyzed three housing estates to identify the factors affecting residential PV installation in housing estates based on houses and the surrounding environment. To verify the robustness of the factors affecting installation, we examined three neighboring areas outside the housing estates. To confirm the state of residential PV installations, we conducted an on-site survey (January 2022), an interview survey with the Environmental Policy Division of Kakegawa City (March 2022), and an interview survey with the mayor of Akihamichi (April 2022).

8.3 Presence or Absence of Residential PV Installations (Analysis 1)

8.3.1 *Analysis Method*

Kakegawa City has six housing estates within a 3.5-kilometer radius from the center of Kakegawa Station.³

To establish the factors affecting installation of residential PV power generation, we focused on Katsuragaoka, Asahigaoka, and Akihamichi. These housing estates have established building agreements that stipulate particulars relating to roofs pertaining to some or all of the houses in the estate.

An outline of the housing estates and neighboring areas for comparison in 8.4 was presented in Table 8.1, and their positional relationship was illustrated in Fig. 8.2.

In the Third Kakegawa City Climate Change Countermeasure Action Plan (Area Policy Volume), the residential PV installation rate among all households in FY2017 was 9.0% (Kakegawa City n.d.-c), but Akihamichi had a lower rate—only 2.3%. In neighboring areas, the residential PV installation rate was higher than in the housing estates, at a similar level to that for the entire city. The neighboring areas have farmland surrounding houses. Compared to the housing estates, houses in the neighboring areas had a mean area and height of a similar scale but a larger

³ The housing estates in Kakegawa City were selected based on MLIT, “National List of Housing Estates (FY2018).” Katsuragaoka, Asahigaoka, and Akihamichi estates were identified as the target houses based on polygons in the Statistics Bureau, Ministry of Internal Affairs and Communications, “2015 Census: Border Data by Neighborhood, Etc.” because the estate borders corresponded to the neighborhoods.

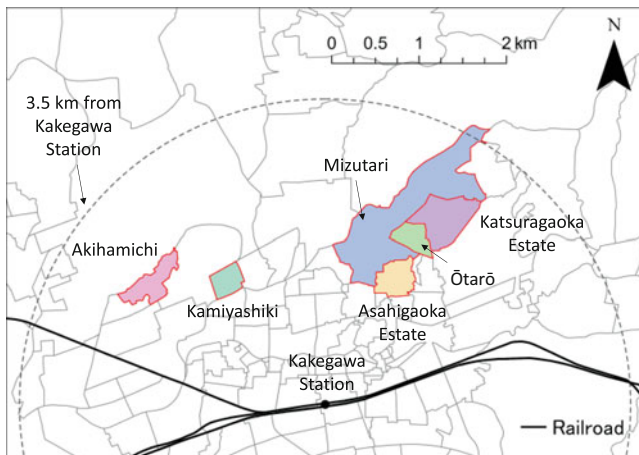


Fig. 8.2 Positional relationship in Kakegawa City. Source: created based on Statistics Bureau, Ministry of Internal Affairs and Communications, “2015 Census: Border Data by Neighborhood, Etc.”, National Land Information, “2020 Railway Data”

mean interval between adjacent buildings. Regarding changes to building shape, renovations were about the same level in the housing estates and neighboring areas. While rebuilds occurred predominantly in Mizutari, few occurred in Akihamichi. New builds were observed more in the neighborhoods for comparison than in the housing estates.

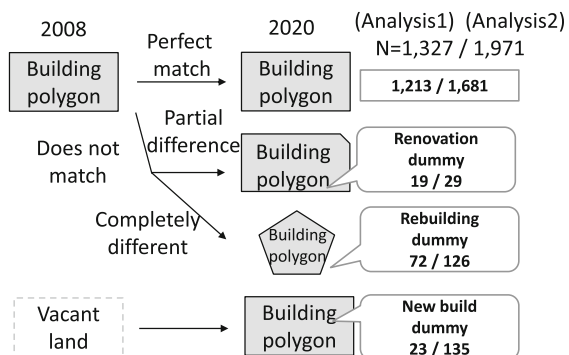
We conducted a logistic regression analysis of all 1327 houses in the housing estates⁴ using R4.1.2.

The outcome variable was whether residential PV power generation was installed on each house (a dummy variable that was 1 if installed and 0 if not). We adopted the following explanatory variables.

- (a) Building area (m^2): We computed the area in ArcGIS Pro from the building polygons in 2020.
- (b) Building height (m): We used the building heights acquired from the Plateau data.
- (c) Interval between adjacent buildings (m): We measured the straight-line distance from the center of the building polygon to that of the nearest building polygon in 2020 in Kakegawa City in ArcGIS Pro.
- (d) Renovation, rebuilding, new build dummies: To clarify the timing when residential PVs were installed on each house, we set three dummy variables (see Fig. 8.3). The renovation dummy represents building polygons that do not accurately match between 2008 and 2020 but, on visual inspection, were

⁴ When we confirmed the intra-class correlation coefficient, it was low at 0.005, and therefore, we did not select a multilevel model.

Fig. 8.3 Flowchart for determining renovation, rebuild, or new build



determined to exhibit partial differences. The rebuilding dummy represents building polygons that do not accurately match between 2008 and 2020 but, on visual inspection, were determined to have greatly different shapes. The new build dummy represents building polygons that did not exist in 2008 but do exist in 2020, and these were assigned to building polygons that did not intersect with 2008 building polygons in ArcGIS Pro.

- (e) Building agreement dummy: The provisions on roof coloring and materials thought to affect residential PV installation were presented in Table 8.2. Building agreements covered the entirety of the Asahigaoka estate but only some houses in the Katsuragaoka and Akihamichi estates. Houses included in the areas covered were assigned the building agreement dummy (1 if in an area was covered by a building agreement, 0 if not).

Notably, we took the natural logarithm of (a) to (c) calculated the mean of each housing estate where the houses were located, and centered them within the cluster (cwc). Considering the aforementioned relationships between (a) to (c) and (d) and (e) we forced the use of interaction terms.

8.3.2 Analysis results

The analysis results were reported in Table 8.3. The variance inflation factor (VIF) was at most 1.92, and the effects of multicollinearity seemed small.

As main effects, $\ln(\text{building height (m)})_{\text{cwc}}$, rebuilding dummy, and new build dummy were significant. Lower building heights compared to the mean in each estate tended toward residential PV installation if the houses were rebuilt or newly built. Among the interaction terms, $\ln(\text{building area (m}^2\text{)})_{\text{cwc}} \times \text{New build dummy}$ was significant. Compared to the mean in each estate, new houses with larger building areas had residential PVs installed more frequently.

Table 8.2 Outline of building agreements with provisions concerning roofs

Area	Building agreement	Provisions concerning roofs	No. of houses affected
Katsuragaoka estate	Kakegawa Oregon village building agreement	Article 11.5. The colors of the roofs and external walls of the buildings will be predominantly white, black, green, or brown, and have sober coloring in harmony with the surroundings.	3 (Katsuragaoka 3-chōme only)
Asahigaoka estate	Green Square Kakegawa building agreement	Article 10 (4). The colors of the roofs of the buildings will be predominantly gray, and mixtures of dark gray and green, blue, or brown may be applied. Furthermore, television antennas and similar items must not be installed on roofs.	379
Akihamichi	Akihamichi building agreement	Article 13.2. In zone B, the roofs of the buildings must be roofed with Japanese tiles, copper roofing, or other similar materials, except for the roofs of eaves, garages, sheds, and similar items.	105
	Akihamichi no. 2 west building agreement	Article 13.2. The colors of the roofs and external walls of the buildings will be predominantly white, black, green, or brown, and have sober coloring in harmony with the surroundings.	

Source: Created with reference to Kakegawa City authorities' "On Building Agreements," <https://www.city.kakegawa.shizuoka.jp/gyosei/docs/8135.html> (accessed April 2, 2022). The number of affected houses was confirmed visually in ArcGIS Pro

Table 8.3 Logistic regression analysis of whether residential PV power generation is installed

	Analysis 1: Housing estates only ($N = 1327$)				Analysis 2: Housing estates and neighboring areas ($N = 1971$)			
	B	S.E.	P-value		B	S.E.	P-value	
Constant term	-3.528	0.210	0.000	***	-3.345	0.155	0.000	***
ln(building area (m^2)) _{cwc}	0.228	0.931	0.806		0.834	0.488	0.088	
ln(building height (m)) _{cwc}	-2.460	0.901	0.006	**	-1.811	0.685	0.008	**
ln(interval between adjacent buildings (m)) _{cwc}	0.226	0.772	0.770		-0.145	0.531	0.785	
Building agreement D	-0.619	0.389	0.112		-0.680	0.327	0.038	*
Renovation D	1.462	0.964	0.129		1.120	0.980	0.253	
Rebuilding D	2.236	0.374	0.000	***	1.909	0.286	0.000	***
New build D	2.584	1.071	0.016	*	1.835	0.365	0.000	***
ln(building area (m^2)) _{cwc} × building agreement D	-3.237	1.682	0.054		-1.296	1.169	0.267	
ln(building height (m)) _{cwc} × building agreement D	0.329	2.320	0.887		-0.404	1.847	0.827	
ln(interval between adjacent buildings (m)) _{cwc} × building agreement D	1.794	1.326	0.176		1.762	1.205	0.144	
ln(building area (m^2)) _{cwc} × renovation D	1.025	4.836	0.832		-1.933	2.143	0.367	
ln(building height (m)) _{cwc} × renovation D	13.371	8.707	0.125		10.600	6.140	0.084	
ln(interval between adjacent buildings (m)) _{cwc} × renovation D	-0.928	2.935	0.752		-3.803	2.351	0.106	
ln(building area (m^2)) _{cwc} × rebuild D	-0.678	1.635	0.678		-1.610	0.987	0.103	
ln(building height (m)) _{cwc} × rebuild D	2.136	2.031	0.293		1.666	1.636	0.308	
ln(interval between adjacent buildings (m)) _{cwc} × rebuild D	-0.439	1.289	0.733		0.299	0.980	0.760	
ln(building area (m^2)) _{cwc} × new build D	9.639	4.523	0.033	*	-2.530	0.978	0.010	**
ln(building height (m)) _{cwc} × new build D	2.034	6.128	0.740		3.180	1.709	0.063	
ln(interval between adjacent buildings (m)) _{cwc} × new build D	-7.370	4.794	0.124		0.469	0.945	0.620	
Nagelkerke R^2	0.15				0.19			
AIC	420.15				796.06			

D Dummy variable ***, **, and * indicate <0.001, <0.01, and <0.05, respectively. Significant variables with a positive and negative coefficient are highlighted in bold and italics, respectively

8.4 Comparison of Housing Estates and Neighboring Areas (Analysis 2)

8.4.1 Analysis Method

Subsequently, we verified the robustness of the factors affecting installation by analyzing the neighboring areas outside the housing estates in addition to the estates themselves. We conducted a logistic regression analysis of 1971 houses, adding three neighborhoods analyzed in 8.3 (Ōtarō, Mizutari, Kamiyashiki)—near to the Katsuragaoka, Asahigaoka, and Akihamichi estates—that comprise housing.⁵

As in 8.3, the outcome variable was whether residential PV power generation was installed on each house. For the explanatory variable, we used the explanatory variables (a) to (e) used in 8.3 and forced use of interaction terms in consideration of the relationships between (a) to (c) and (d) and (e) using R4.1.2 for the analysis.

8.4.2 Analysis Results

The analysis results were reported in Table 8.3. The VIF was at most 5.29—a somewhat greater result—but the effects of multicollinearity seemed slight owing to it being from interaction effects.

The significant main effects were $\ln(\text{building height (m)})_{\text{cwc}}$; and building-agreement, rebuilding, and new build dummies. Having expanded the areas for analysis, the building-agreement dummy was significant. The results indicated that houses covered by a building agreement must show consideration regarding their roofs and tended not to have residential PV power generation installed.

Regarding the interaction terms, $\ln(\text{building area (m}^2\text{)})_{\text{cwc}} \times \text{new build dummy}$ was significant. Compared to the mean in each area, new houses with smaller building areas had residential PVs installed more often. This trend differed from the results of Analysis 1.

Between Analyses 1 and 2, the latter has a larger value for the pseudo-coefficient of determination Nagelkerke R^2 , which suggested a good fit. To confirm the divergence between predictions and actual results in Akihamichi, which exhibited the lowest rate among the three housing estates, the installation probability in houses computed from the state of residential PV installation and building changes and the results for Analysis 2 in Table 8.3 were illustrated in Fig. 8.4.

Analysis 2 revealed that the probability of installation was higher in houses that had been rebuilt. However, in Akihamichi, none of the nine such houses had installed residential PVs. In Akihamichi, several new houses have a small area,

⁵ When we confirmed the intra-class correlation coefficient, it was low at 0.02, and therefore, we did not select a multilevel model.

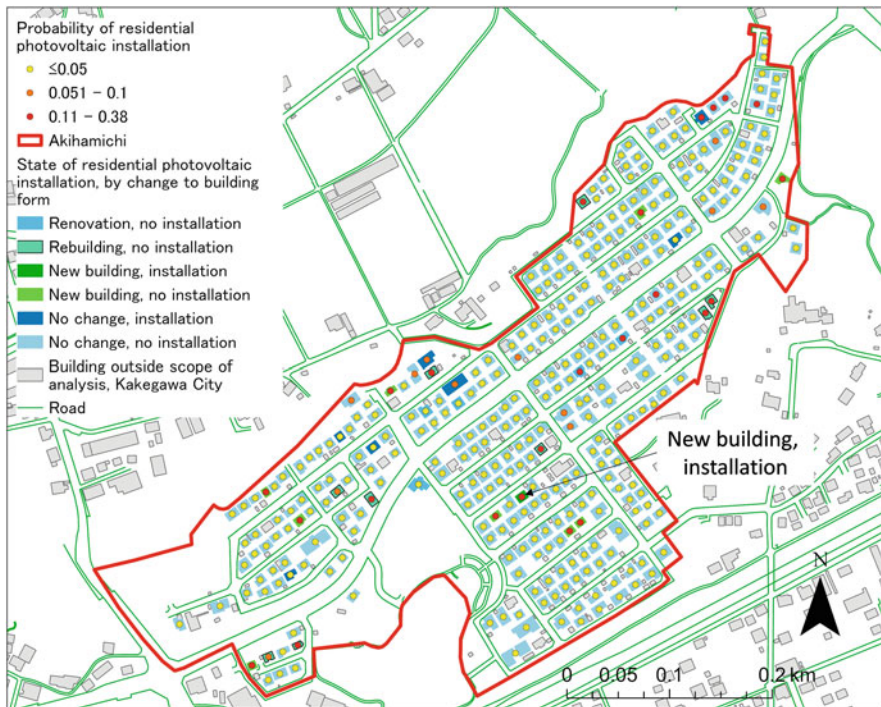


Fig. 8.4 Analysis 2: Probability of residential PV installation in Akihamichi. Sources: Buildings and roads: Zenrin Zmap-TOWN II Digital Residential Map (2020), Akihamichi: Created from Statistics Bureau, Ministry of Internal Affairs and Communications, “2015 Census: Border Data by Neighborhood, Etc.”

which was suggested as the cause of the low installation probability computed in Analysis 2, despite these houses being new builds. In fact, of the 10 new houses, only one had installed a residential PV.

8.5 Discussion

8.5.1 House Characteristics

8.5.1.1 Relationship with Building Area and Height

In Analysis 1, contrary to our hypothesis, houses with lower building heights than the mean in each estate had residential PVs installed more often. If there were no tall buildings nearby, installations appeared to spread if houses can obtain sufficient sunlight, even if they were not tall. This trend was also observed in Analysis 2.

In the housing estates, residential PVs were installed in new houses with larger areas compared to the mean in each estate.

Including the neighboring areas as well, it was installed in new houses with areas smaller than the mean in each estate. The mean area of new houses that have residential PV power generation installed was 99.9 and 70.8 m² in the housing estates and neighboring areas, respectively. Aerial photographs of the neighboring areas confirmed numerous installations in small-scale detached houses that were newly built on former farmland.

Residential PVs being installed in new houses seem common to Analyses 1 and 2, but the interaction between new houses and house area was affected by characteristics of the area. In housing estates, comparatively large new houses were developed owing to the fixed nature of the lots for each house; however, in the neighboring areas, smaller-scale new houses were developed on former farmland, and residential PVs were installed when each was newly built.

8.5.1.2 Relationship with Changes in Building Form

In both Analyses 1 and 2, rebuilds and new builds exhibited significant results. Larger-scale changes in building form occur than in renovations; hence, seemingly, a greater scope exists for installing PV panels. The rebuilds and new builds were subsidized by new houses under the New Energy Device, etc. Installation Support Project, and the subsidy amount for them was less than that for existing houses. There was a tendency to install residential PVs on the occasion of a change in building form, such as a rebuild or new build, and support for these may expand in the future with the aim of PV installation in more houses on these occasions.

8.5.1.3 Relationship with Building Agreements

Analysis 1 did not reveal any trends unique to houses covered by a building agreement. Analysis 2, which expanded the scope of analysis, established a clear trend against residential PV installation in houses covered by a building agreement. Although building agreements designate colors and materials, they do not directly prohibit the PV installation.

According to the mayor of Akihamichi, areas covered by the Akihamichi Building Agreement were sold in lots in 1992, and areas covered by the Akihamichi No. 2 West Building Agreement on the western side were sold in lots approximately 10 years later. Solar water heaters were popular when the Akihamichi houses were sold, but the building agreements prohibited the installation of these and antennas to preserve the landscape. With PV power generation, the panels can be installed closely attached to the roof; therefore, installation is not prohibited, and it does not seem that the landscape would exhibit any issue. However, according to the mayor of Akihamichi, the estate sales occurred before PV power generation became popular, and as the residents—in their 30 and 40 s when they purchased the houses—have grown older, they may have missed the timing to install such power generation.

8.5.2 Characteristics of the Surrounding Environment (Relationship with the Interval Between Adjacent Buildings)

In Analyses 1 and 2, the interval between adjacent buildings was not a significant result. This may be attributable to area, height, and changes in building form being more important factors affecting installation than the distance between houses.

8.6 Conclusion

Focusing on houses and the surrounding environment, this study determined the factors affecting the installation of residential PV power generation with a focus on houses and the surrounding environment. We adopted housing estates with similar characteristics among residents, houses, and the surrounding environment in Kakegawa City, Shizuoka as a case study.

Common to the housing estates and the neighboring areas, residential PVs were installed more in buildings with heights lower than the mean in each area and as more changes in building form, such as rebuilding and new building, occurred.

In the housing estates, residential PVs were installed more in new houses with larger building areas than the mean in each estate in particular. Irwin (2021) and Kawaguchi et al. (2020) revealed a trend favoring residential PV installation on larger, taller buildings, but the result here differed. In addition to the house repairs noted by Bollinger and Gillingham (2012), rebuilds and new builds were also opportunities to install residential PV power generation. Although the results pertaining to the area of new houses differed outside the housing estates, we hope to conduct a more detailed analysis by expanding the scope in the future.

Regarding the characteristics of the surrounding environment, the interval between adjacent buildings was not a significant result, even when including interactions with dummy variables. This leads to the conclusion that the factors affecting residential PV installation in housing estates were predominantly owing to characteristics of the houses, not those of the surrounding environment.

We may not have been able to accurately gather information regarding residential PV power generation overall because it was determined by visual inspection—a limitation of our study. Currently, the only public data on residential PV power generation (less than 10 kW) are aggregate values by local government area⁶; therefore, owing to information on installation locations being published in the future, we may expect the factors affecting the installation to be revealed in greater

⁶ The only business plan approval information for PV power generation projects that is publicly available on ANRE's Website for Publishing Project Plan Approval Information relates to projects for 20 kW or above. The website publishes approved and installed volumes by local government area.

detail. Moreover, owing to data limitations, we could not gather information on resident attributes (e.g., age, household type) or the age of the houses, but we intend to address this as a research question in the future.

Acknowledgments In conducting this research, we interviewed and were provided with information by the Environmental Policy Division of Kakegawa City. The mayor of Akihamichi cooperated for an interview. This study is part of the outcomes of the joint research with CSIS, the University of Tokyo (No. 917) and using the following data (Zenrin, Zmap-TOWN II 2008/09 (Shape version) Shizuoka Prefecture data set and Zmap-TOWN II 2020 (Shape version) Shizuoka Prefecture data set. We sincerely thank the abovementioned individuals and entities.

References

- Agency for Natural Resources and Energy (ANRE) (n.d.) “Dai-6-ji enerugī kihon keikaku”[Sixth Strategic Energy Plan], p. 59, Japanese. <https://www.meti.go.jp/press/2021/10/20211022005/20211022005-1.pdf> (issued 22 Oct 2021; Accessed 2 April 2022)
- Bryan Bollinger and Kenneth Gillingham (2012) Peer effects in the diffusion of solar photovoltaic panels. *Mark Sci* 31(6):900–912
- Caroline Hachem-Vermette and Kuljeet Singh (2019) Mixed-use neighborhoods layout patterns: impact on solar access and resilience. *Sustain Cities Soc* 51:101,771
- Curtius HC, Hille SL, Berger C, Hahnel UJJ, Wüstenhagen R (2018) Shotgun or snowball approach? Accelerating the diffusion of rooftop solar photovoltaics through peer effects and social norms. *Energy Policy* 118:596–602
- Daisuke Narumi and Kim Younghyo (2017) Research on the measures to promote introduction of rooftop-type photovoltaic power generation system considering economic efficiency. *AIJ J Technol Design* 23(55):925–930
- Irwin NB (2021) Sunny days: spatial spillovers in photovoltaic system adoptions. *Energy Policy* 151:112192
- Kakegawa City (n.d.-a) Dai-3-ki Kakegawa-shi chikyū ondanka taisaku jikkō keikaku (kuiki shisaku hen) [Third Kakegawa City climate change countermeasure action plan (zone policy volume)], p. 56, Japanese. https://www.city.kakegawa.shizuoka.jp/fs/8/4/9/1/2/_kuikisesakuhens3rd.pdf (issued March 2019; Accessed 2 April 2022)
- Kakegawa City (n.d.-b) Shin enerugī kiki tō no setchi ni tai suru josei [Assistance for the installation of new energy devices, etc.] Japanese. <https://www.city.kakegawa.shizuoka.jp/gyosei/docs/101882.html>. Accessed 2 April 2022
- Kakegawa City (n.d.-c) Dai-3-ki Kakegawa-shi chikyū ondanka taisaku jikkō keikaku (kuiki shisaku hen) [Third Kakegawa City climate change countermeasure action plan (zone policy volume)], p. 22, Japanese. https://www.city.kakegawa.shizuoka.jp/fs/8/4/9/1/2/_kuikisesakuhens3rd.pdf (issued March 2019; Accessed 2 April 2022)
- Kawaguchi N, Hayashi K, Yamada T, Tomino Y (2020) The analysis of the installation indicator for the rooftop-type photovoltaic power generation system of residential districts. *Jpn Assoc Human Environ Symbiosis J Human Environ Symbiosis* 36(2):151–161
- Kosugi T, Shimoda Y, Tashiro T (2019) Neighborhood influences on the diffusion of residential photovoltaic systems in Kyoto City, Japan. *Environ Econ Policy Stud* 21:477–505
- Marcello Graziano and Kenneth Gillingham (2015) Spatial patterns of solar photovoltaic system adoption: the influence of neighbors and the built environment. *J Econ Geogr* 15(4):815–839
- Ministry of Land, Infrastructure, Transport, and Tourism (MLIT) (n.d.) Zenkoku no jütaku danchi risuto ni tsuite [On the national list of housing estates], Japanese. https://www.mlit.go.jp/jutakukentiku/house/jutakukentiku_house_mn5_000016.html. Accessed 2 April 2022

- Ministry of the Environment (MOE) (2021) “Chikyū ondanka keikaku” [Climate Change Adaptation Plan], p. 27, Japanese, <http://www.env.go.jp/earth/211022/mat01.pdf> (issued 22 Oct 2021; Accessed 2 April 2022)
- Palm A (2017) Peer effects in residential solar photovoltaics adoption—a mixed methods study of Swedish users. *Energy Res Soc Sci* 26:1–10
- Procurement Price Calculation Committee (n.d.) ANRE, Reiwa 4-nendo ikō no chōtatsu kakaku tō ni kan suru iken [Opinion on procurement prices for FY2022 onward, etc.], Japanese, p. 22. https://www.meti.go.jp/shingikai/santei/pdf/20220204_1.pdf (accessed August 10, 2022)
- Schaffer AJ, Brun S (2015) Beyond the sun—socioeconomic drivers of the adoption of small-scale photovoltaic installations in Germany. *Energy Res Soc Sci* 10:220–227
- Sven Müller and Johannes Rode (2013) The adoption of photovoltaic systems in Wiesbaden, Germany. *Econ Innov New Technol* 22(5):519–535

Part II

Urban Analysis

Chapter 9

Statistical Multi-dimensional Scaling with a Geographical Penalty



Development of Bayesian Multi-dimensional Scaling and Its application to Time–Space Mapping

Hayato Nishi and Yasushi Asami

Abstract Understanding the structure of cities and facilities in terms of similarity and proximity when considering wide-area or national land planning is crucial. For this purpose, this chapter proposed a novel method to visualize the similarities or various distances of regions, referred to as Bayesian geographical multi-dimensional scaling. Multi-dimensional scaling (MDS) is the fundamental method that is generally used for this purpose; however, its projections are often substantially different from the geographical locations to facilitate appropriate comparison or understanding. Thus, to overcome this weakness, we introduced a geographical penalty for MDS, and its weight was determined using a statistical criterion. This penalty was introduced because dissimilarities or distances should be small if the two regions are geographically close in many cases. Furthermore, this method was applied to visualize the accessibility of public transit in Japan. The obtained results can be easily compared with geographical locations and facilitate an understanding of the transitions that improve accessibility in each prefecture.

The contents of this chapter are based on the following paper originally published in a Japanese journal: Nishi, H. and Asami, Y. (2019) Statistical multi-dimensional scaling under the geographical constraints: The development of Bayesian multi-dimensional scaling and its application to timespace mapping. *Journal of City Planning Institute of Japan* 54(3):826–832 (in Japanese).

H. Nishi (✉)
Hitotsubashi University, Kunitachi, Tokyo, Japan
e-mail: h.nishi@r.hit-u.ac.jp

Y. Asami
Department of Urban Engineering, The University of Tokyo, Bunkyo-ku, Tokyo, Japan
e-mail: asami@csis.u-tokyo.ac.jp

Keywords Multi-dimensional scaling · Time–space map · Visualization method · Similarity · Bayesian statistics

9.1 Introduction

Understanding the structure of cities and facilities in terms of similarity and proximity when considering wide-area or national land planning is vital, where the relationships among facilities are important. Various indices can be used to define such relationships, such as simple linear distance, time distance, road distance, and similarity indices. The relationships described with these indices are relatively easy to understand when the number of cities and facilities is small. However, it is difficult to understand the overall structure directly from the defined indices when the number of cities and facilities increases.

Multi-dimensional scaling (MDS) is a useful method for visualizing the relationships among cities and facilities located in a geographical space (Shimizu 1992). When the relationship between points such as cities or regions is defined in terms of dissimilarity, MDS arranges these points (typically on a two-dimensional plane) such that the dissimilarity corresponds to the distance between points. This facilitates an understanding of the overall structure as a dissimilarity map.

A typical application is a time–space map. In a time–space map, the time distance between points can be determined on a scale of time units (Shimizu 1992). In particular, several methods of time–space map representation were proposed by Kotoh (2000) based on MDS.

Although MDS is a basic and useful method, its projection can be difficult to understand because the optimal layout solution is not uniquely determined. Moreover, the layout of cities deviates from their actual geographical locations (Kotoh 1997).

To resolve this problem, we focused on the fact that many relationships between cities and facilities are strongly related to actual geographical relationships. For example, time distance has a close relationship with the linear geographical distance between cities and facilities, even if they are not the same. Cities that are close to each other tend to have relatively similar industrial and demographic structures. The method by Tanaka (2018), which is similar to MDS, also provides similarities to the actual geographical location.

However, the comparison of a map constructed using MDS with an actual geographic map can be challenging because MDS ignores rotation, translation, and scaling. A simple solution to this problem involves the application of Procrustes transformation (Dryden and Mardia 1998; Kendall et al. 1999) to the MDS map and then comparing it with an actual map. However, in this two-step method, the expectation that the projected location of the city should be close to the actual geographic location is not reflected in the first-step MDS projection. Therefore, the point-to-point relationships do not reflect this expectation. However, if we introduce a geographical penalty to MDS, the weight that should be assigned to it is not apparent.

Based on the motivations described above, this chapter proposed a method to add a geographical penalty to the relationships among cities and facilities on a projected map by modifying MDS. This method aimed to create maps that can be easily compared to actual geographic maps. To systematically introduce a penalty, this chapter statistically interpreted the MDS. Despite certain existing statistical (probabilistic) MDSs, such as the approach based on maximum likelihood estimation by Zinnes and MacKay (1983), we employed a Bayesian approach to introduce geographical penalties as prior distributions of city locations. Bayesian MDS was introduced for dimension selection in Oh and Raftery (2001) and for variable selection in Lin and Fong (2019). However, to the best of our knowledge, no previous study has introduced this concept from a geographical perspective.

The Bayesian geographical MDS (BGMDS) proposed in this chapter offers the following advantages. First, the geographical penalty introduced into the MDS reflects intuitive expectations in the dissimilarity maps described above and renders its comparison with an actual geographical map easier. Second, the Bayesian approach facilitates an evaluation of the uncertainty of the layouts of cities or facilities in the dissimilarity maps. Third, it provides a statistical criterion for determining the weight of geographical penalties.

The remainder of this chapter is structured as follows. Section 9.2 discusses the standard MDS and its probabilistic interpretation. Section 9.3 proposes BGMDS, which introduces a geographical penalty as a prior distribution to the MDS. In Sect. 9.4, we briefly summarize the inference method employed in the proposed method. In Sect. 9.5, we generate travel time–space maps among prefectures by public transportation using BGMDS as an application of the proposed method to a real-world problem. Section 9.6 presents a comparison of the proposed method with a standard MDS. Finally, Sect. 9.7 provides a discussion and presents future work prospects.

The Python implementation of BGMDS is available at <https://github.com/hayato-n/BGMDS>.

9.2 Multi-dimensional Scaling

The MDS method creates a dissimilarity map by solving the following optimization problem:

Let $n \in \mathcal{S} = \{1, \dots, N\}$ denote the index of each observation (city or facility) and the vector $\mathbf{z}_n = (z_{n,i} : i \in \{1, 2\})^\top$ denote its location on the dissimilarity map. In this chapter, we assumed a projection onto a two-dimensional map $i \in \{1, 2\}$; however, it is easy to generalize for three or more dimensional maps. Let $d_{n,m}$ be the dissimilarity (or distance) defined between two points $n, m \in \mathcal{S}$ ¹ and $\delta_{n,m} =$

¹ Here, we assumed that the dissimilarity is symmetric.

$\delta(z_n, z_m)$ is the distance on the MDS map defined in the same manner. Note that $\delta(z_n, z_m)$ is the Euclidean distance function between two points. z_n, z_m ².

MDS solves the minimization problem

$$\min_{z_n, z_m \in S} \sum_{n < m} (d_{n,m} - \delta_{n,m})^2. \quad (9.1)$$

This formulation is consistent with the “divergence evaluation model focusing on difference” in Tanaka (2018). As this optimization result is independent of rotation, translation, and scaling, an appropriate retransformation is required for comparison with the actual map.

If we interpret this MDS model statistically, minimization is the maximum likelihood estimation of the statistical model. Specifically, we assume that the observed dissimilarity $d_{n,m}$ contains random errors. Thus, we assume a Gaussian distribution as follows:

$$\mathcal{N}(d_{n,m} | \delta_{n,m}, \tau^{-1}). \quad (9.2)$$

Note that $\mathcal{N}(\cdot | \mu, \sigma^2)$ indicates that the random variable \cdot follows a Gaussian distribution with mean μ and variance σ^2 . In this model, the potential (unobserved) distance $\delta_{n,m}$ is the mean parameter, and τ is the precision (inverse of variance) parameter.

The maximum likelihood estimation of this statistical model is equivalent to minimization in the MDS. This relationship is similar to that between the maximum likelihood estimation and least squares in linear regression models.

9.3 Bayesian Geographical Multi-dimensional Scaling

The BGMDS method proposed in this chapter introduces a prior distribution that imposes a geographic penalty on the latent position $z_{n,m}$. Specifically, we assumed that it follows a Gaussian distribution.

$$\mathcal{N}(z_{n,i} | x_{n,i}, \lambda^{-1}). \quad (9.3)$$

This implies that the BGMDS projection z_n is distributed around the corresponding observed geographic location x_n . Note that λ is the precision (inverse of the variance) parameter of a Gaussian distribution.

Let $p(\cdot)$ be the probability density function of \cdot . We define $\mathbf{X} = \{x_1, \dots, x_N\}$, $\mathbf{Z} = \{z_1, \dots, z_N\}$, and \mathbf{D} is the matrix whose (n, m) element is $d_{n,m}$. The

² The distance function on the dissimilarity map can also be generalized to a symmetric function; however, it should be differentiable for efficient inference.

statistical model $p(\mathbf{D} \mid \mathbf{Z})$ and its prior distribution $p(\mathbf{Z} \mid \mathbf{X})$ are defined by Eqs. (9.2) and (9.3). The potential locations \mathbf{Z} are the parameters (latent variables). Considering two hyperparameters, λ and τ , the posterior distribution of \mathbf{Z} is formally obtained from Bayes' theorem as follows (Suyama 2017):

$$p(\mathbf{Z} \mid \mathbf{X}, \mathbf{D}) = \frac{p(\mathbf{D} \mid \mathbf{Z}) p(\mathbf{Z} \mid \mathbf{X})}{p(\mathbf{D} \mid \mathbf{X})}. \quad (9.4)$$

The hyperparameters λ and τ control the strength of the geographic penalty. Specifically, the larger λ is relative to τ , the stronger the penalty for the latent location z_n . As the marginal likelihood $p(\mathbf{D} \mid \mathbf{X})$ is the probability of obtaining the observed data \mathbf{D} from the given model and prior distribution, it can be used to evaluate the model. Thus, λ and τ can be chosen to maximize the marginal likelihood $p(\mathbf{D} \mid \mathbf{X})$; λ, τ , which is a function of the hyperparameters³ (Bishop 2006).

9.4 Inference on BGMDS

In BGMDS, we cannot analytically evaluate the posterior distribution of \mathbf{Z} and the marginal likelihood. Therefore, an approximate method is required. Variational inference is an approach for approximating the posterior distribution of \mathbf{Z} using a parametric distribution $q(\mathbf{Z})$ (Bishop 2006; Suyama 2017). Oh and Raftery (2001) and Lin and Fong (2019) used Markov chain Monte Carlo sampling, which is an alternative approach for approximation. An advantage of variational inference is that it is scalable, even in the presence of many cities or facilities. In variational inference, the “closeness” of the true posterior $p(\mathbf{Z} \mid \mathbf{X}, \mathbf{D})$ and its approximation $q(\mathbf{Z})$ is measured with the Kullback–Leibler (KL) divergence $\text{KL}[q(\mathbf{Z}) \parallel p(\mathbf{Z} \mid \mathbf{X}, \mathbf{D})]$, which is a non-negative measure between distributions. The relationship between the marginal likelihood and the KL divergence is

$$\log p(\mathbf{D} \mid \mathbf{X}) = \mathcal{L}[q(\mathbf{Z})] + \text{KL}[q(\mathbf{Z}) \parallel p(\mathbf{Z} \mid \mathbf{X}, \mathbf{D})], \quad (9.5)$$

where $\mathcal{L}[q(\mathbf{Z})]$ is the lower bound of the log-marginal likelihood, referred to as evidence lower bound (ELBO).

In variational inference, the KL divergence is minimized to determine the $q(\mathbf{Z})$ that is “close” to $p(\mathbf{Z} \mid \mathbf{X}, \mathbf{D})$. Upon fixing the hyperparameters, this minimization problem is equivalent to the maximization of ELBO \mathcal{L} because the marginal likelihood is constant. Therefore, we can use ELBO to approximate the log-marginal

³This procedure can be interpreted as a maximum likelihood estimation wherein the marginal likelihood is the likelihood function to be maximized. Therefore, it is referred to as the “type II maximum likelihood” method.

likelihood. The specific functional form of ELBO⁴ is as follows:

$$\begin{aligned}\mathcal{L}[q(\mathbf{Z})] = & \langle \log q(\mathbf{Z}) \rangle_q \\ & - \left\langle \sum_{n < m} \log \mathcal{N}(d_{n,m} | \delta_{n,m}, \tau^{-1}) \right\rangle_q \\ & - \left\langle \sum_{n=1}^N \sum_{i=1}^2 \log \mathcal{N}(z_{n,i} | x_{n,i}, \lambda^{-1}) \right\rangle_q,\end{aligned}\quad (9.6)$$

where $\langle \cdot \rangle_q$ is the expectation with an approximate distribution $q(\mathbf{Z})$. Both q and \mathcal{N} are the probability density functions of the corresponding distributions.

The specific inference procedure is as follows: First, we restricted the approximate distribution $q(\mathbf{Z})$ to a Gaussian distribution.⁵ This restriction facilitates the use of Bayes by Backprop algorithm (Blundell et al. 2015) for the inference. This algorithm was proposed to estimate Bayesian neural networks. In this algorithm, the gradient of the ELBO is unbiasedly estimated with a reparameterization trick. Gradient descent methods are used to update the parameters. In this chapter, we used the Adam Optimizer (Kingma and Ba 2015), which is an adaptive gradient descent method.

The hyperparameter settings are important; however, the model is not sensitive to small changes in hyperparameters. In addition, Blundell et al. (2015) reported that simultaneous optimization with variational inference does not work. Therefore, we selected hyperparameters that maximized ELBO using a grid search.

9.5 Time–Space Map Among Prefectures in Japan

As an example of the application of BGMDS, we employed it to visualize travel time with public transportation between prefectures as time–space maps. Such a time–space map expresses accessibility among cities and facilitates an understanding of the relationship between cities and the national land structure.

⁴ However, it is difficult to compute expectations in ELBO. Therefore, the Bayes by Backprop algorithm approximates them using the Monte Carlo method, which provides an unbiased estimator.

⁵ In the Bayes by Backprop algorithm, the approximate distribution is constrained to the following form:

$$q(\mathbf{Z}) = \sum_{n=1}^N \sum_{i=1}^2 \mathcal{N}(z_{n,i} | \mu_{n,i}, \sigma_{n,i}^2),$$

where $\mu_{n,i}, \sigma_{n,i}^2$ are the parameters of the approximate distributions optimized in the variational inference.

Table 9.1 Major railroad station on each prefecture

Prefecture	Major Station	Prefecture	Major Station
Aomori	Aomori	Shiga	Maibara
Iwate	Morioka	Kyoto	Kyoto
Miyagi	Sendai	Osaka	Osaka
Akita	Akita	Hyogo	San-no-miya
Yamagata	Yamagata	Nara	Nara
Fukushima	Fukushima	Wakayama	Wakayama
Ibaraki	Mito	Tottori	Tottori
Tochigi	Utsunomiya	Shimane	Matsue
Gunma	Takasaki	Okayama	Okayama
Saitama	Omiya	Hiroshima	Hiroshima
Chiba	Funabashi	Yamaguchi	Shimonoseki
Tokyo	Tokyo	Tokushima	Tokushima
Kanagawa	Yokohama	Kagawa	Takamatsu
Nigata	Nigata	Ehime	Matsuyama
Toyama	Toyama	Kochi	Kochi
Ishikawa	Kanazawa	Fukuoka	Hakata
Fukui	Fukui	Saga	Saga
Yamanashi	Kofu	Nagasaki	Nagasaki
Nagano	Nagano	Kumamoto	Kumamoto
Gifu	Gifu	Oita	Oita
Shizuoka	Shizuoka	Miyazaki	Miyazaki
Aichi	Nagoya	Kagoshima	Kagochima–Chuo
Mie	Tsu		

Broad railroad networks cover Japan, and they are used by people to move from one city to another. Furthermore, major cities connected by Shinkansen (bullet train) should be placed closer to each other on the time–space map because of the shorter travel time. Moreover, if traveling by airplanes is allowed, cities near popular airports will be placed closer to each other.

In this chapter, an inter-prefectural time–space map was generated using the following procedure. First, we selected a major railroad station (Table 9.1) for each of the 45 prefectures, excluding Hokkaido and Okinawa, which are located far from Honshu Island (the main island of Japan).⁶ Next, the travel times among the selected stations were obtained separately in the following two scenarios: (1) people cannot

⁶ Hokkaido and Okinawa were excluded for the following reasons. First, travel to Okinawa is more time-consuming than travel to other prefectures, particularly when airplanes are not used owing to available transits being only ships and airplanes. Access routes to Hokkaido from Honshu are also broader than routes to Okinawa, although they are still limited. Thus, the time to Hokkaido is longer than that to the other prefectures.

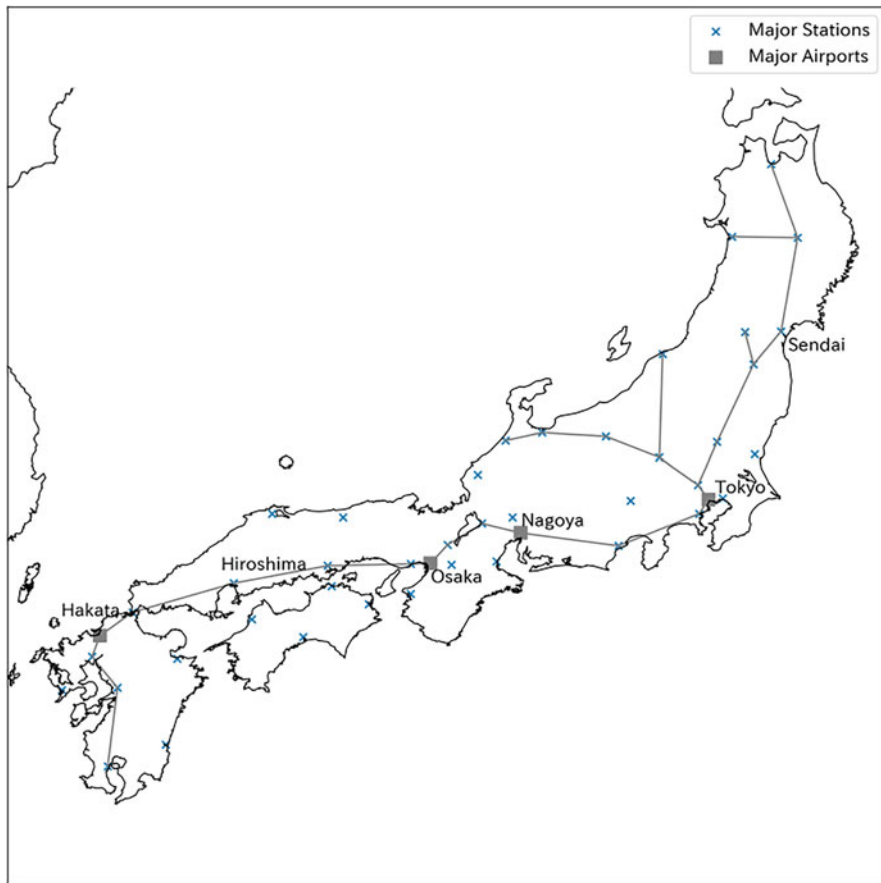


Fig. 9.1 Gray crosses and squares indicate the geographical locations of major stations. Prefectures connected with Shinkansen (bullet train) lines are tied with gray line segments. Gray squares indicate the presence of major airports nearby the stations

use airplanes and (2) people can use airplanes.⁷ Thus, we obtained two time distance matrices. Using these matrices and the geographic coordinates of the stations, we generated a time–space map using BGMDs for each matrix.

Figure 9.1 shows the geographical locations of the selected major stations. The prefectures are connected with Shinkansen lines and gray line segments. The Tokyo, Nagoya, Osaka, and Hakata stations are indicated with gray squares because there are major airports near these stations.

⁷ We obtained the travel times from <https://www.jorudan.co.jp> with the departure time set at 12:00 on 2019/4/1. It was assumed that the travel times were symmetrical. In addition, we adjusted the time units such that the average value was the same as that of the geographic Euclidean distance.

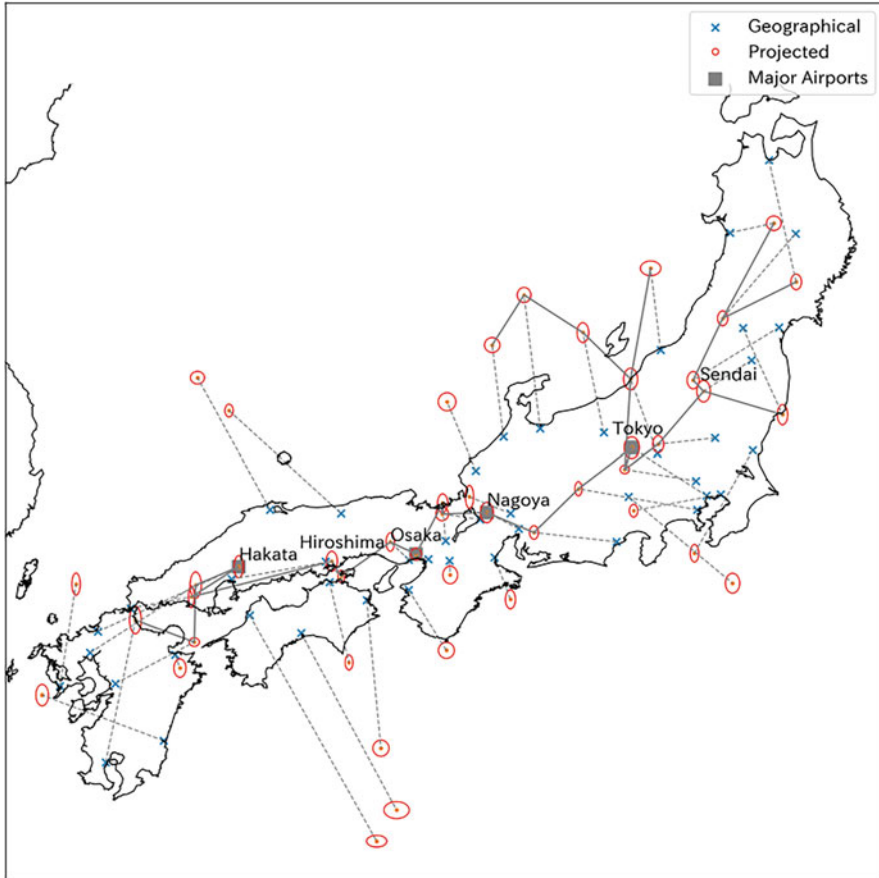


Fig. 9.2 Time–space map provided by BGMS. Airplanes are not available on this map. Red ellipses show the standard deviations of the approximated posterior distributions. The geographical locations (gray crosses) and the locations in the time-space map (red dots) are connected with gray dashed lines

Before presenting the results of the BGMS projection, we clarify the results of the hyperparameter selection. We selected the hyperparameters λ , τ to maximize the ELBO from the combinations of $\{0.1, 1, 10, 100\}$ using a grid search. Consequently, $(\lambda, \tau) = (1, 1)$ was selected with and without airplanes.

Figure 9.2 presents the BGMS results without airplanes. Red ellipses represent the standard deviations of the posterior distributions. The large ellipses indicate the existence of a large amount of locational uncertainty in the BGMS map. We connected the geographic location and the mean of the posterior distribution using gray dashed lines to clarify the relationship between the geographic and projected locations. The dashed lines indicate that the stations connected by the Shinkansen lines agglomerated toward the center of Japan. However, the prefectures on the Sea

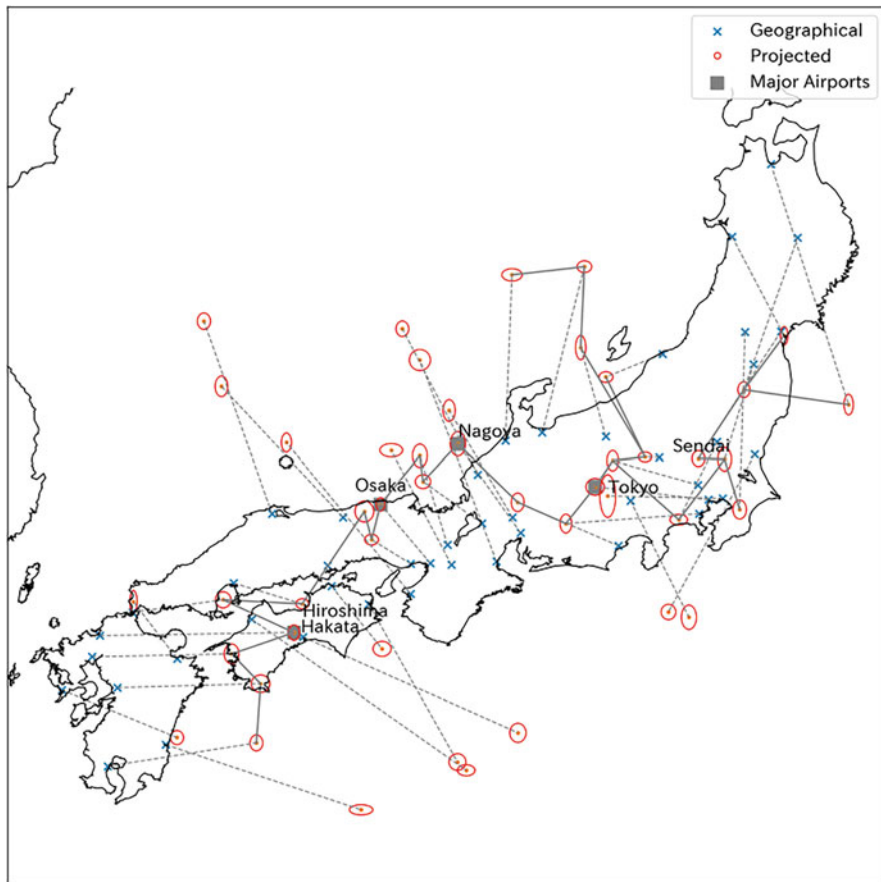


Fig. 9.3 Time–space map provided by BGMDS. Airplanes are available on this map. Red ellipses show the standard deviations of the approximated posterior distributions. The geographical locations (gray crosses) and the locations in the time–space map (red dots) are linked with gray dashed lines

of Japan side (west side of Japan) in the Shikoku and Chugoku regions, which are not connected to Shinkansen lines, are located far from the Shinkansen routes. This result indicates that Shinkansen lines improve accessibility between prefectures in Japan.

Figure 9.3 shows the BGMDS results when airplanes are available in the same format as that shown in Fig. 9.2. In this case, the effect of the Shinkansen is not apparent; however, the entire station layout was distorted such that Hakata Station and Tokyo Station become closer. In addition, Hakata Station dragged the stations in Kyushu (the western island) toward itself. This result indicates that airlines have improved their accessibility from Kyushu to Tokyo. However, prefectures on the

Sea of Japan side of Shikoku and Chugoku tended to move away from the other prefectures.

9.6 Comparison to MDS

To verify the effect of the geographical penalties introduced in the BGMDS, we compared them with the standard MDS. Because BGMDS and standard MDS optimize different evaluation criteria, an alternative criterion was required for a fair comparison. Therefore, in this section, we introduced a measurement criterion to compare time–space maps, which quantified the magnitude of the distortion of the time–space maps from the original geographical maps. We focused on the distortions because we should easily understand the locational relationships among cities if the magnitude of the distortion is small. We only compared the magnitude of the distortion using the time–space map under the scenario without airplanes because the use of airplanes justifies a large distortion of the time–space map.

The comparison procedure is as follows. First, we selected three cities from the time–space map and checked whether the relative positional relationships among the three cities were preserved. The triangles of the three cities were considered here. Without a loss of generality, we can choose an arbitrary city as its origin. Suppose that the left–right relationship of the other two cities from the origin is the same as that in the original map. In this case, the relative position relationships among these cities are preserved.⁸ This judgment was made for all city combinations, and we employed the rate of violation of the relative position relationship as a measurement criterion for the magnitude of the distortion. The smaller the violation ratio of the relative position relationship, the closer is the relative position relationship to the geographical map. Thus, the time–space map should easily be compared with the original geographical locations.

Figure 9.4 shows a time–space map generated by MDS. We applied the Procrustes transformation (Dryden and Mardia 1998; Kendall et al. 1999)⁹ for the result of MDS before mapping because it is not always appropriate for comparison with the original locations. For BGMDS, such a transformation was not required.

The violation rates of the relative position relationship were 56.0% for MDS and 24.0% for BGMDS. Thus, the relative position relationship was better preserved in the BGMDS time–space map than in MDS.¹⁰ A comparison among certain maps

⁸ From a computational perspective, we can examine the left–right relationship with the sign of the outer products of the vectors from the origin to other cities.

⁹ The Procrustes transformation is a combination of parallel transition, scaling, and rotation that minimizes the distance between two shapes of points.

¹⁰ The possible reasons for the high violation rate in the MDS are as follows. The prefectures are almost along a straight line because the overall shape of the Japanese islands is long and narrow. Focusing on three cities arranged almost in a straight line, a small locational difference in cities breaks their relative position relationship, for example, when the city in the center moves slightly.

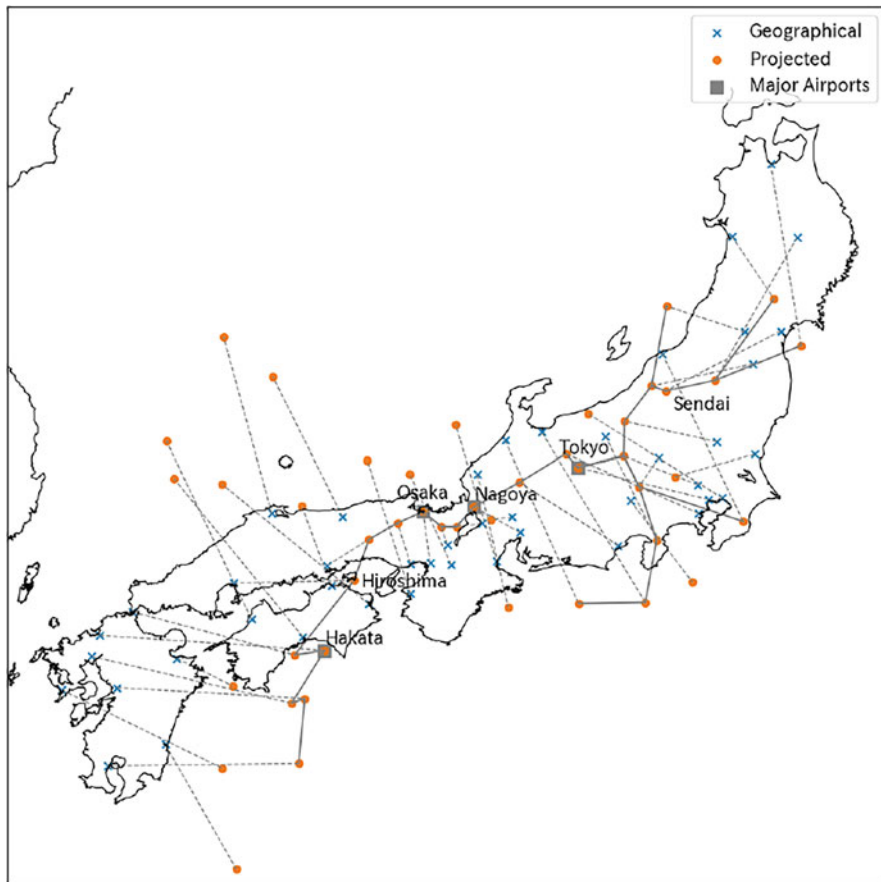


Fig. 9.4 Time–space map provided by MDS + Procrustes transformation. Airplanes are not available on this map

using BGMDS showed that the stronger the geographical penalties, the lower the violation rate. This suggests that geographical penalties are somewhat effective in maintaining relative positional relationships.

The locational characteristics of the time–space maps generated by the MDS are as follows: First, the prefectures in Hokuriku region are located to the south of Tokyo. This provides a large discrepancy with the actual geographical relationships. Prefectures in the Shikoku region are located on the Sea of Japan side. This also contributes to the high violation rate. In the BGMDS, the prefectures in Hokuriku

Hence, the violation rate increases if the MDS is applied to Japanese cities. In contrast, it would decrease if we applied MDS for countries such as the United States, where cities are not arranged in a straight line.

region are located to the north of Tokyo and prefectures in the Shikoku region are located on the Pacific Ocean side. Thus, the time–space map using BGMDS is relatively easier to read than that using MDS. However, the locations of prefectures in the Kyushu region were disrupted in both the MDS and BGMDS. This is a common problem in both the methods.

9.7 Discussion and Conclusion

To clarify the features of BGMDS from a different perspective, we interpreted BGMDS as an optimization problem and examined the effect of geographical penalties on the optimization process. As discussed in Sect. 9.4, when we employ variational methods, the approximation of the posterior distribution becomes a maximization problem of ELBO. This is equivalent to the minimization problem of the sign reversal of ELBO, which is the loss function. Because the posterior distributions are proportional to the product of the statistical model $p(\mathbf{D} | \mathbf{Z})$ and the prior distribution $p(\mathbf{Z} | \mathbf{X})$, the term related to the prior distribution can be isolated from ELBO. Therefore, we can interpret the variational approximation as a penalized optimization with this isolated term as the penalty term.

From this perspective, we obtained the following findings on the optimization process of BGMDS. Figure 9.5 shows how the loss function (the sign reversal of ELBO) changes during the optimization process of the BGMDS model for the scenario without airplanes (blue line). The isolated penalty term related to the prior distribution is indicated by the red line.

First, we focus only on the loss function (blue line). The loss values decreased almost constantly during the iterative optimization procedures (Fig. 9.5, left panel). Next, we focus on the penalty term (red line). It increased temporarily at the beginning and then gradually decreased after reaching a peak (Fig. 9.5, right panel). Thus,

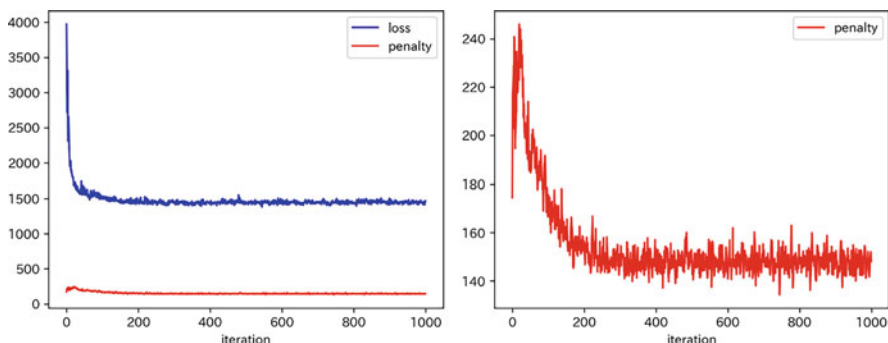


Fig. 9.5 Trajectory of loss values in the optimization procedure of BGMDS for the time–space map in Figure 9.2. The right panel omits the blue line in the left panel to exaggerate the trajectory of the penalty term (red line)

in summary, BGMDS allocated cities without much consideration of geographical penalties at the beginning of the optimization procedure. Subsequently, the locations of the cities were adjusted to be closer to their geographical positions.

Regarding the setting of the hyperparameters λ and τ , the following properties were observed in the time–space maps generated in this chapter. First, if the optimized values of ELBO are similar, we obtained similar city allocations regardless of the hyperparameter settings. However, differences in the size of the standard deviation ellipse were observed in certain cases. Therefore, we should be careful about the setting of the hyperparameters when discussing the uncertainty of the layout from the standard deviation ellipses.

The setting of the hyperparameters also affected the learning of the BGMDS. Specifically, the larger the values of the accuracy parameters λ and τ , the larger the ELBO gradient.¹¹ Hence, a low learning rate must be selected for the gradient method. Additionally, it is undesirable to set extremely large or small values for the hyperparameters because they make the learning unstable for the reasons mentioned above. Empirically, learning procedures tend to be more stable when the Adam optimizer is used¹² compared with the use of the simple stochastic gradient descent method. In our analyses, the stable values of the learning rate of the Adam optimizer were approximately the reciprocal of the smaller values of the two hyperparameters.

Despite its many advantages, BGMDS has several practical limitations. First, the dissimilarity between cities or facilities $d_{n,m}$ must be symmetric. This constraint condition is reasonable in most scenarios; however, it can limit its applicability to certain situations,¹³ such as the road distance, when there are many one-way roads. Second, the units of dissimilarity must be adjusted such that the scales d and δ are comparable because BGMDS provides penalties on the projected location z_n with the distance from the geographical location x_n . In the time–space maps presented in Sect. 9.5, the time units were scaled such that the average of time matched the average of the Euclidean distances among geographical locations to visualize the accessibility on the original geographical map. However, there is no optimal scaling method that is applicable to many objectives. An example of a situation wherein our scaling method is unsuitable is as follows. The metaphor “Japan gets smaller” is often used when, for instance, a new transit improves accessibility. The scaling method employed in this chapter does not match this intuitive metaphor. In addition, this method does not allow a direct comparison of, for example, Figs. 9.2 and 9.3 because the distance units of these maps are different. Therefore, when creating two

¹¹ When the value of the accuracy parameter is large, a small change in the parameter causes a large fluctuation in the loss function. Consequently, the larger the accuracy parameter, the larger the gradient.

¹² The Adam optimizer is an optimization method often used to train deep neural networks, which aims for efficient learning by providing different learning rates and momentums for each parameter.

¹³ Another example of a situation that requires asymmetric distances is the travel time of airplanes with long east–west travels. In this case, travel times are asymmetric because of the effects of westerlies and trade winds.

or more time–space maps for comparison, the scaling must be selected such that the distance units are the same.

Despite these limitations, the practical advantages of BGMDS are significant. In particular, the following two facts have notable advantages. First, the coordinates on the dissimilarity map are directly controlled to be close to the geographical coordinates, and second, the strength of the geographical penalties can be determined based on a statistical criterion.

Finally, we discuss the possible future developments in this field. First, certain approaches are required to scale the problem of scaling dissimilarity units, as discussed.¹⁴ In addition, the geographical penalty in BGMDS does not guarantee that relative position relationships, such as top, bottom, left, and right, are preserved (Shimizu 1992). As discussed in Sect. 9.6, BGMDS tends to preserve these relative position relations more often than MDS; however, it is worth explicitly introducing the relative position relations as new penalties or constraints.

Acknowledgments We appreciate the Journal of the City Planning Institute of Japan, where our original Japanese article was published. They have allowed us to publish the English version.

References

- Bishop CM (2006) Pattern Recognition and Machine Learning. Springer, New York
- Blundell C, Cornebise J, Kavukcuoglu K, Wierstra D (2015) Weight uncertainty in neural network. In: Proceedings of the 32nd International Conference on Machine Learning, vol 37
- Dryden I, Mardia K (1998) Statistical shape analysis. Wiley series in probability and statistics. Wiley, Chichester
- Kendall D, Barden D, Carne T, Le H (1999) Shape and shape theory. Wiley series in probability and statistics. Wiley, Chichester
- Kingma DP, Ba J (2015) Adam: a method for stochastic optimization. In: Proceedings of the 3rd International Conference on Learning Representations. arXiv:1412.6980
- Kotoh H (1997) Regional structure and visualized time-distance network. Theory Appl GIS (in Japanese) 5(2):1–10. https://doi.org/10.5638/thagis.5.2_1
- Kotoh H (2000) Several time maps and their features. In: The Fall National Conference of Operations Research Society of Japan, abstracts (in Japanese)
- Lin L, Fong D (2019) Bayesian multidimensional scaling procedure with variable selection. Comput Stat Data Anal 129:1–13
- Oh MS, Raftery AE (2001) Bayesian multidimensional scaling and choice of dimension. J Am Stat Assoc 96(455):1031–1044
- Shimizu E (1992) Time-space mapping and its application in regional analysis. Infrastruct Plann Rev (in Japanese) 10:15–29. <https://doi.org/10.2208/journalip.10.15>
- Suyama A (2017) Introduction to machine learning by Bayesian inference (in Japanese). Kodansha, Tokyo

¹⁴ For example, if we wish to reflect the feeling that “Japan gets smaller” due to new transit in a time–space map, a possible scaling approach is the adjustment of the time units by the ratio of travel times before and after the introduction of the new transit. However, the validity of this method depends on the purpose of the time–space map, and it cannot be employed for all purposes.

- Tanaka K (2018) Visualization method of spatial flow data based on similarity of destination choice patterns. *J City Plann Inst Jpn* (in Japanese) 53(3):1464–1471. <https://doi.org/10.11361/journalcpij.53.1464>
- Zinnes JL, MacKay DB (1983) Probabilistic multidimensional scaling: complete and incomplete data. *Psychometrika* 48(1):27–48

Chapter 10

Factors that Influence Estimation of Building Location in City Blocks in Tokyo Commercial Zones



Masahiro Taima, Yasushi Asami, Kimihiro Hino, and Wataru Morioka

Abstract In the central commercial zones of Tokyo, the importance of city-block restructuring has been strongly emphasized. The predictability of the building development in city blocks is crucial for their planning. This study classifies city blocks by the difference in influential factors of the building location and examines if the city blocks have steady tendencies of building locations. Furthermore, the probability of building coverage for each point in a block is visualized to grasp the spatial image. For our analysis, we used 205 city blocks as reference blocks. Results show influential factors of building location, such as the presence of a wide road and its adjacent direction, the north-south length of city blocks, and the same use of buildings. Further, the study visualizes the probability that each point covered by buildings in a given block and judged for classes has a steady tendency of building location.

Keywords City-block restructuring · Building location · Urgent urban renewal area

The contents of this paper are based on the following paper originally published in a Japanese journal: Masahiro Taima, Yasushi Asami, Kimihiro Hino, Wataru Morioka. (2016). Factors that influence estimation of building location in city blocks in Tokyo commercial zones. *Theory and Application of GIS*, 2016, Vol. 24, No.2, pp.85–96. (in Japanese).

M. Taima (✉)
Kyoto University, Kyoto, Japan
e-mail: taima.masahiro.85p@st.kyoto-u.ac.jp

Y. Asami · K. Hino
Department of Urban Engineering, The University of Tokyo, Tokyo, Japan
e-mail: asami@csis.u-tokyo.ac.jp; hino@ua.t.u-tokyo.ac.jp

W. Morioka
University of Illinois at Urbana-Champaign, Champaign, IL, USA
e-mail: watarum2@illinois.edu

10.1 Introduction

10.1.1 Background

Japan is currently entering an era of maturing cities, and the central issue in urban development is the restructuring of existing urban areas through the formation of new ones. There has been recently a strong demand in city centers for the restructuring of the existing urban areas.

The Ministry of Land, Infrastructure, Transport and Tourism formulated the “Guidelines for developing large city blocks” in 2011 and “Work reference materials for utilizing large city blocks to promote urban development” in 2014. These guidelines showed the effectiveness of large city blocks and promoted the efforts of local governments and private urban development businesses (Urban Development and Improvement Division, Ministry of Land, Infrastructure, Transport and Tourism 2011) to restructure them. Restructuring of city blocks and re-organizing them to the desired size enable development by utilizing their regional potentials, such as underutilized land in city centers, motivation for developers, and globally attractive features, such as in business, commerce, and lifestyle.

Based on the above social circumstances, city-block restructuring, particularly in central Tokyo, is thought to be actively implemented in the future. However, empirically predicting how buildings will be located in city blocks following future city-block restructuring is not easy.

10.1.2 Summary of Previous Research

Determining how buildings will be located in city blocks following future city-block restructuring requires a model for estimating building locations in a city block. Existing research that analyzes the relationship between city blocks and building locations includes studies. For example, Saito (2002) has conducted experiments on building locations and showed that rules that maintained road efficiency had formed city blocks. Saito (2004, 2011) has also analyzed how city blocks and road networks differ depending on the adjacency of buildings and measured the state of the surrounding space and used it as an explanatory variable to build a model for estimating the probability that a building is located in an urban area. Vialard (2011) has measured the goodness-of-fit of the buildings already arranged in one city block for another city block. However, no studies estimate building locations from city-block shapes; therefore, in the future, when city blocks are restructured, how buildings will be located within that city block cannot be determined. Asami and Ohtaki (2000) estimate the location of detached houses from the shape of a site; however, this study has a small sample size and a small number of estimated sites. Estimating the location of buildings in a city block requires the use of a larger number of sample sites.

There is research on the utilization of spaces, such as city blocks. Makio et al. (2006) examined changes in the location of buildings owing to condominium conversion at the city-block level for existing residential urban areas. Saito and Kato (2013) targeted central urban areas of provincial cities to clarify changes in land use and current circumstances in terms of city-block units. Nam et al. (2007, 2008) analyzed methods for securing parking spaces in apartment complexes located in existing urban areas as a problem of the balance between securing parking lots and securing green spaces. Nagatomi et al. (2007) determined the current state of land use along major arterial roads for each city block. Nakao and Ito (2012) determined the aspect of urban areas from the density of buildings and building-coverage ratio in a city block. Kawaguchi et al. (2014) quantitatively clarified at the city scale how the size and fluctuations of non-building land were related to the size and fluctuations of green spaces. Matsumiya et al. (2014) measured the distribution of gap rates among buildings in urban areas. However, though these studies have determined spaces to date, they do not estimate future spaces, which requires further analysis.

Various factors determine the location of buildings (henceforth, “influential factors”). Research on the determination of the impact of influential factors on the location of buildings is extensive. Aoki et al. (2010) determined the causal relationship between the regulation of sky-exposure rate and building shape. Kirita et al. (2007) determined the relationship between the location of buildings, such as setbacks, regulation of sky-exposure rate, slopes with front roads, and cut corners. Kawakami and Ohnishi (2013) created a model of usable space for buildings corresponding to building form regulations. Katsuragi and Watanabe (2000) discussed the factors forming building groups lacking continuity from changes in building form regulations. Nakanishi et al. (1996) examined how to introduce wall-line specifications as a method of “placement control” without reducing the feasible volume. Usui and Asami (2011) focused on the densities of buildings and roads to derive the setback distance of buildings. These studies focus on the influence of city-planning regulations on the layout of buildings. However, it is unclear how these urban planning regulations impact which city block characteristics are more or less likely to exhibit building-location trends. Determining building-location trends during future city-block restructuring enables its use in city-block restructuring plans.

10.1.3 Purpose

This study aimed to discuss factors that influence building locations by clarifying the characteristics of city blocks, which are more or less likely to exhibit building-location trends. For city blocks that exhibit these trends, we seek to visualize the probability of building-covered points being within those city blocks and estimate the location of buildings.

In Sect. 10.2, we design a model for estimating the location of buildings in city blocks with an arbitrary shape. In Sect. 10.3, we classify city blocks and use the

model for estimation accuracy (magnitude of error) to assess city blocks that are more or less likely to exhibit building-location trends. In Sect. 10.4, we visualize the probability of points being covered by buildings within those city blocks and estimate the location of buildings for city blocks that are likely to exhibit building-location trends. In Sect. 10.5, we discuss the results. Additionally, we discuss factors that influence the building location based on the judgment of city blocks that are likely to exhibit building-location trends within them, as discussed in Sect. 10.3, and the results of estimation of building location outlined in Sect. 10.4. Finally, in Sect. 10.6, we conclude the findings and offer the perspective of this study.

10.2 Research Method

10.2.1 Data Analysis

This study analyzed GIS data provided by Tokyo City (March 2013 edition of Tokyo Metropolitan Planning Geographic Information System).

A city block is an urgent urban renewal area, and a strong demand for city-block restructuring was the target of the study. Different floor-area ratios resulted in big changes in the building location, and detailed analysis becomes difficult. Therefore, targets were limited to city blocks where the floor-area ratio was designated to 600%, which was the largest number for city blocks. We excluded city blocks designated with district plans, districts with special floor-area ratio application, and districts with heights.

10.2.2 Construction of Model for Estimating City-Block Buildings

We adopted the method for estimating the location of detached homes from the site shape (Asami and Ohtaki 2000) in order to build a model for the estimation of the city-block building location.

When two city blocks had similar shapes and environments, the location of the buildings in those city blocks was considered to be similar. This assumption enabled the estimation of building locations from the city-block shape and other environments. We built a model for estimating the location of buildings in a city block based on this assumption.

Building locations in a city block were estimated by superimposing city blocks with the same centroids. The building location was expressed as a probability in the city-block area. For a city block that was referenced by the magnitude of similarity in shape with the city block whose building location we wanted to estimate (henceforth, “reference city block”), we changed the magnitude of the

weighting (henceforth, “weight”) of the building locations in the reference city block. The probability of the building position estimated from a city block with high similarity is evaluated higher.

The degree of similarity s is defined as following an index representing the degree of similarity between city blocks. A city block is a compact set on a two-dimensional plane. A point on the plane is set as \mathbf{x} . A point in the city block X is expressed as $\mathbf{x} (\in X)$. The centroid position vector of city block X is expressed as $\mathbf{g}(X)$, and the area of city block X is expressed as $A(X)$. We calculated the degree of similarity s between two city blocks— X and Y —taking the product set when the centroids of the two city blocks were matched and by dividing it with the union set. Therefore, the set obtained by translating the centroid of city block X so that it overlaps the origin was set as $G(X)$. Namely, this is defined in Eq. (10.1):

$$G(X) = \{\mathbf{z} : \mathbf{z} = \mathbf{x} - \mathbf{g}(X), \mathbf{x} \in X\} \quad (10.1)$$

The provisional degree of similarity s^* of city blocks— X and Y —is defined as shown in Eq. (10.2) below based on the concept of Lee and Sallee (1970):

$$s^*(X, Y) = \frac{A(G(X) \cap G(Y))}{A(G(X) \cup G(Y))} \quad (10.2)$$

In reality, the directions of the roads adjacent to the city block are different, and the buildings in a city block are greatly affected by the direction of roads. Therefore, we considered that city blocks with the changed direction in the range of $\pm\pi/4$ (45°) were almost identical. Therefore, allowing for such directional fluctuations, we defined the final degree of similarity s between city blocks. When a city block is obtained by rotating the city block X by θ with the centroid at its center as $R(X, \theta)$, the degree of similarity s is defined as in Eq. (10.3):

$$s(X, Y) = \max_{-\pi/4 \leq \theta \leq \pi/4} \frac{A(G(X) \cap R(G(Y), \theta))}{4A(G(X) \cup R(G(Y), \theta))} \quad (10.3)$$

The set of reference city blocks used for estimating the probability of a position of a building in an actual city block is set as reference city block group I . If the city block’s shape is similar, the location of the buildings that exist in it is also thought to be similar. Therefore, for a city block X whose building location we wanted to estimate, preferentially using information on the location of buildings in a city block was desirable with a high degree of similarity among those in the reference-city block group I . The degree of similarity value defined above directly could be used as a weight. However, it means that the degree of similarity would never become zero, and no matter how dissimilar the city blocks are, the weight would be positive and would be used in the estimation model of the building location. A better model can be created after city blocks whose shapes are clearly different are excluded. Since city blocks with major differences in shape are excluded, the building location weight needs to be set to 0 for city blocks with clearly different shapes. Therefore,

we define the relationship between the degree of similarity s and weight function $f(s)$ as shown in Eq. (10.4):

$$f(s) = \begin{cases} \frac{s-t}{1-t} & s > t \\ 0 & s \leq t \end{cases} \quad (10.4)$$

where t is a parameter between 0 and 1 ($t \in [0, 1]$). When the degree of similarity s is less than or equal to t , the weight becomes 0. The degree of similarity s and weight function $f(s)$ of city block X and city block Y are $s(X, Y), f(s(X, Y))$, respectively.

Next, we described how to estimate the location of buildings. Estimating the exact shape of a building is difficult; so, we estimated the probability that each point in a city block is covered by buildings. The city block whose building location we wanted to estimate is set as X , and the set of building locations on the set $i(\in I)$ of reference city blocks when the centroid of reference city block $G(i)$ is moved to the origin is set as B_i . When the point \mathbf{z} in $G(X)$ is $\mathbf{z} \in B_i$, it indicates that a building existed at the point \mathbf{z} . It is judged that the more B_i covers point \mathbf{z} , the more likely the buildings cover the point $\mathbf{x} (\in X)$. We define the probability of the estimation of a building's existence as $p(\mathbf{x}, X, I)$, which is the probability that a point $\mathbf{x} (\in X)$ is covered by a building, and which is weighted by the weight from the degree of similarity of the city block shape defined earlier. First, we defined an indicator function that expressed whether a building B_i of a reference city block existed at an arbitrary point \mathbf{x} on the plane by Eq. (10.5):

$$\chi(\mathbf{x}, B_i) = \begin{cases} 1 & \mathbf{x} \in B_i \\ 0 & \mathbf{x} \notin B_i \end{cases} \quad (10.5)$$

Then, the probability of the estimation of a building's existence— $p(\mathbf{x}, X, I)$ at the point $\mathbf{x} (\in X)$ on the city block X —is defined as shown in Eq. (10.6):

$$p(\mathbf{x}, X, I) = \frac{\sum_{i \in I} f(s(X, i)) \chi(\mathbf{z}, B_i)}{\sum_{i \in I} f(s(X, i))}, \mathbf{x} (\in X) \quad (10.6)$$

The parameter t of the weight function $f(s)$ was set to maximize the estimation accuracy of the building. This was done by extracting an arbitrary city block i from the reference city-block group I and estimating the location of buildings with other reference city blocks (the set of remaining reference city blocks after taking i from I is set as I_{-i}), and conducting this operation for each reference city block $i(\in I)$, and finding the value that maximizes the estimation accuracy index ρ defined below. We define the estimation accuracy index ρ as in Eq. (10.7):

$$\rho = \sum_{i \in I} \int_{\mathbf{x} \in B_i} [p(\mathbf{x}, i, I_{-i}) \chi(\mathbf{x}, B_i) - p(\mathbf{x}, i, I_{-i}) (1 - \chi(\mathbf{x}, B_i))] d\mathbf{x} \quad (10.7)$$

We obtained the estimation accuracy index by subtracting the integral value of the estimation probability of a building's existence at the point where the building was not actually present from the integral value of the probability of the building's existence at the point where the building was actually present. When this sum reached a maximum, the accuracy of a building location's estimation also reached a maximum, and the t at this time was used in the city-block building location estimation model.

10.3 Classification of City Blocks

Next, we classified city blocks to examine whether the error in building-location estimation as per model for estimating city blocks became small. A smaller error after classification than before classification indicated that this classification extracted a city block with a similar building location. Namely, in this classification, a city block was considered where trends were more likely to appear in the city-block building location. Meanwhile, a larger error after classification indicated that the city block of that classification had a large variation in the building location. Namely, in this classification, a city block was considered where trends were less likely to appear in the city-block building location. The above method was used to judge city blocks where trends in city-block building locations were more or less likely to appear.

10.3.1 *Method for Calculating Estimation Accuracy (Error Rate) in Model for Estimating City-Block Building Location*

First, we calculated the error in estimating the building location in the model for estimating the city-block building location. Research that examined the error of the plane position exists. For example, Teraki (2000a, b, c, d, e) used an error model created under the assumption that the planar position of spatial information was normally distributed around the true position. Chrisman (1987) calculated errors by superimposing spatial information. This study considered it appropriate to calculate the error in estimating the location of the buildings by superimposing the estimated position and true position.

In the present study, the error is calculated as follows. The estimation of the probable existence of the building of a point \mathbf{x} ($\in i$) in reference city block i ($\in I$) is expressed as $p(\mathbf{x}, i, I_{-i})$. Meanwhile, the function that takes 1 when $\mathbf{x} \in B_i$ and 0 when $\mathbf{x} \notin B_i$ is expressed as $\chi(\mathbf{x}, B_i)$. The error rate of the estimation of the building location as per the model for estimating city-block building location at i is calculated by taking the integral of the absolute value of the difference between $p(\mathbf{x}, i, I_{-i})$ and

$\chi(\mathbf{x}, B_i)$ over the domain of i and dividing by the area $A(i)$ of i . Then this error rate is calculated for each reference city block, and the sum is divided by the total number of reference city-block groups N_I to obtain the error rate of I . If the error rate is set as E , it is defined as shown in Eq. (10.8):

$$E = \frac{\sum_{i \in I} \frac{\int_{\mathbf{x} \in i} |p(\mathbf{x}, i, I_{-i}) - \chi(\mathbf{x}, B_i)| d\mathbf{x}}{A(i)}}{N_I} \quad (10.8)$$

In the present study, E is set as an index of the estimation accuracy of the city-block building location estimation model. Next, city blocks were classified, with city blocks whose error rate E increased or decreased being analyzed, and we clarified city blocks that were more or less likely to exhibit building-location trends.

10.3.2 City-block Classification

Focusing on factors that were thought to impact the location of buildings in city blocks, we classified city blocks.

First, the width of the road in front of the site is thought to be a factor that can affect building locations. Regulations regarding buildings considerably vary depending on the width of the front road. The Building Standards Act sets a width of 12 m as a boundary. In cases where the width of the front road is less than 12 m, the smallest specified floor-area ratio and road width-based floor-area ratio were used as the floor-area ratio of the site. In cases where the width of the front road is 12 m or more, measures, such as the relaxation of setback regulations applied in Category 1 Medium-to-high-rise Exclusive Residential Districts, Category 2 Medium-to-high-rise Exclusive Residential Districts, Category 1 Residential Districts, Category 2 Residential Districts, or Quasi-residential Districts, were stipulated. Additionally, the Tokyo Metropolitan Comprehensive Design Permission Guidelines set an application requirement in the city center residential comprehensive design system—a comprehensive design system applied to city centers. The requirement is that the width of the front road must be 12 m or more for sites where the floor-area ratio exceeds 600% after the ratio is increased. This shows that the 12-m width of the front road is used as a standard in many circumstances, and the 12-m width of the front road is likely to be a factor that largely impacts the building location.

A width of 12 m is relatively wide for a road. In a few cases in the city center of Tokyo, which is the target area, all roads connected to a city block are wide with a width of 12 m or more. Shape regulations include those that affect the north-south direction of the site, such as regulations on setbacks on adjacent land on the north side, regulations on shade, etc., and the direction is also an important consideration. Also, front roads may impact the building location depending on which direction a wide road connects to the city block.

The shape of a city block can also impact the location of buildings. Kawakami and Ohnishi (2013) show that the vertical shape of the site and the size of the frontage largely impact building-shape regulations and that the magnitude of regulations on shade and on setbacks on the north side differed depending on the north-south width of the city block. When we consider these findings, we can see that the location of buildings is impacted by whether the shape of the city block is long in the east-west direction or in the north-south direction.

Though previous studies have not analyzed the relationship between the land value of a city block with the building location, from the perspective of maximum effective use the land value may impact the building location. The judgment of maximum effective use in real estate appraisal considers the application and shape of the building (Yoshino 2006). The maximum effective use and shape of the building are expected to differ depending on the land value. Therefore, we classify city blocks by their land value.

The building application is thought to be a factor that impacts the building location. The building-design policy differs depending on its application (Naito et al. 2010). Therefore, the building location may differ depending on the building application. City blocks consisting of single-use buildings are expected to exhibit building-location trends more easily. Tokyo commercial zones—the target area of the present study—had city blocks whose building application included only offices, so we decided to consider these city blocks. We also considered limiting the analysis only to other applications (e.g., commercial facilities, housing complexes), but there were few city blocks that consisted of single-use buildings. So we could not conduct such analyses.

We classified city blocks based on the above-mentioned factors—width of the front road, shape of the city block shape, land value, and building application. City blocks whose surrounding roads were classified as less than 12 m or at least 12 m were set as classifications I and II, respectively. We considered the direction in which the front road with a width of at least 12 m is connected to a city block. City blocks connected to a front road with a width of at least 12 m on all four directions were set as classifications III, IV, V, and VI, respectively. City blocks that were long in the east-west and north-south direction were set as classifications VII and VIII, respectively. The average land price per unit area of all city blocks (205 in total) was taken. City blocks with values greater or lower than that average value were set as classifications IX and X, respectively. City blocks where all buildings were used as offices were set as classification XI. For each classification, we applied the model for estimating the city-block building location as explained in Sect. 10.2.2, and we calculated the model-estimation accuracy (error rate E) using the method described in Sect. 10.3.1.

10.3.3 Results

The results of the analysis are summarized in Table 10.1.

Table 10.1 Error rate E of estimations for each classification E

Classifications		N_1	t	E
Not classified	All blocks	205	0.79	0.330
Classification I ^a	City blocks whose surrounding roads less than 12 m	127	0.79	0.322
Classification II	City blocks whose surrounding roads at least 12 m	78	0.74	0.350
Classification III ^a	City blocks connected to a front road with a width of at least 12 m on north	30	0.72	0.319
Classification IV ^a	City blocks connected to a front road with a width of at least 12 m on south	21	0.72	0.300
Classification V	City blocks connected to a front road with a width of at least 12 m on east	14	0.64	0.363
Classification VI	City blocks connected to a front road with a width of at least 12 m on west	13	0.68	0.400
Classification VII	City blocks that were long in the east-west direction	101	0.76	0.337
Classification VIII ^a	City blocks that were long in the north-south direction	104	0.79	0.323
Classification IX	City blocks with values greater than that average value	67	0.71	0.356
Classification X	City blocks with values lower than that average value	138	0.74	0.335
Classification XI ^a	City blocks where all buildings were used as offices	34	0.63	0.319

^aClassification with reduced error rate compared to error rate without classification

City blocks that might exhibit building-location trends were judged as follows. The error rate E in model for estimating city blocks' building location when they were not classified was 0.330. We then classified city blocks, and a lower error rate E of a given classification than 0.330 indicated that this classification extracted city blocks whose building location was similar. This could be thought of as city blocks that were more or less likely to exhibit building-location trends. Meanwhile, a higher error rate E of a given classification than 0.330 indicated that the city block in this classification had a large variation in the building location. It can be said that these city blocks were less likely to exhibit the building-location trends. However, the error rate E increased as the total number of reference city block groups N_f became smaller. So, a definitive conclusion could be made that building-location trends were less likely to appear with these classifications based on our sample size, though its potential could be suggested here. We used this method to judge city blocks whose building-location trends were more or less likely to appear.

The results showed that in classifications I, III, IV, VIII, and XI, the error rate E decreased compared to those that were not classified. Therefore, the building-location trends of these city blocks were more likely to appear. Meanwhile, in classifications II, V, VI, VII, IX, and X, the error rate E increased compared to those that were not classified. So it can be said that building-location trends were less likely to appear in city blocks. We used the above analysis to clarify city blocks whose building-location trends were more or less likely to appear.

10.4 Estimation of City-block Building Locations

In the previous section, we identified city blocks that might exhibit building-location trends. However, how buildings are located in the city block could not be visually understood only through this judgment. When a city block whose building-location trends were more likely to appear was formed by city-block restructuring in the future, knowledge of this building location in advance could provide suggestions for city-block restructuring plans. Therefore, in this section, we used a model for estimating the city-block building location to visualize the building-covered points (estimating the probability of a building's existence) among the city blocks judged to be likely to exhibit building-location trends (classifications I, III, IV, VIII, XI), and we estimated the building location.

The probability of the estimation of a building's existence in the city block was visualized as shown in Figs. 10.1, 10.2, 10.3. A virtual city block was set, and one point per square meter was placed on it. Then, the probability of a building's existence in each point was estimated. This was then converted to raster data, and the probability of the estimation of a building's existence in each point in the city block was visualized. The brightness represents the probability of estimating a building's existence estimation in that part, with brighter areas having a probability closer to 1, and darker areas having a probability closer to 0. The orientation of the figure is north at the top.

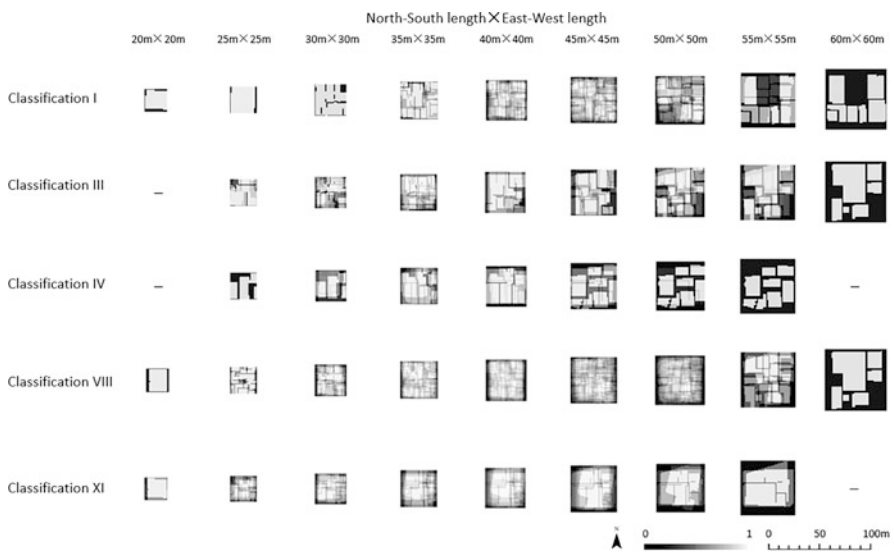


Fig. 10.1 Building existence probability in square city block

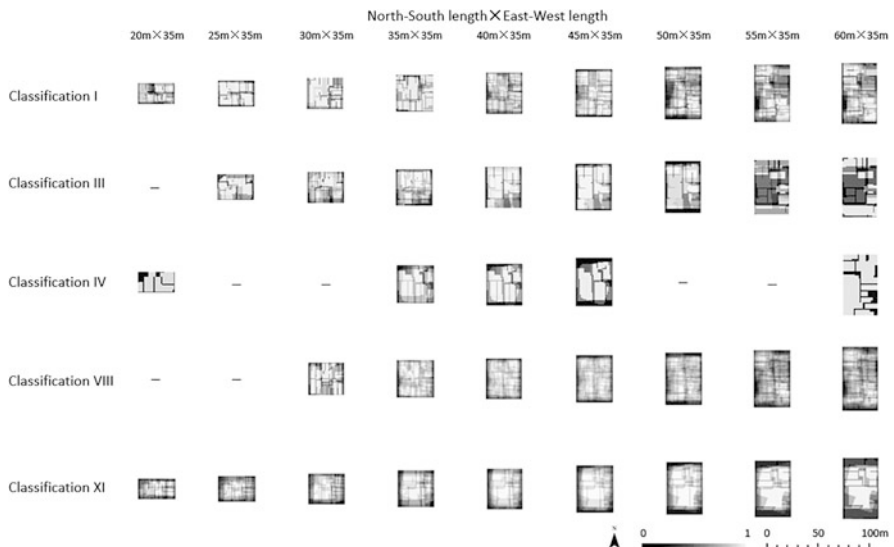


Fig. 10.2 Building existence probability in city block where side extending in east-west direction was unified to 35 m

The shape of the virtual city block was set as a rectangle, and multiple 35 m square city block shapes were set as standards. This shape was set as a standard because the average area and perimeter of all city blocks were 1285.54 m² and 147.41 m, respectively. If a city block was set as a rectangle, a city shape with an

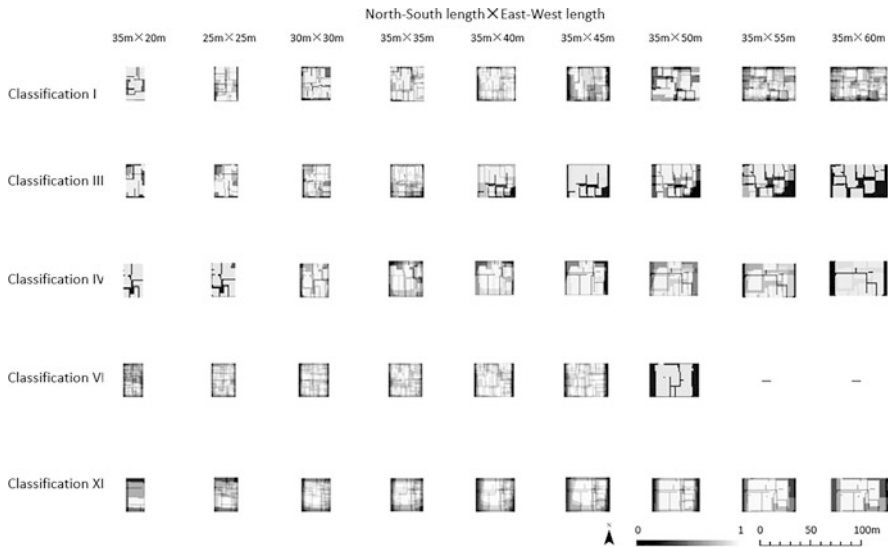


Fig. 10.3 Building existence probability in city block where side extending in north-south direction was unified to 35 m

average shape would be calculated as a city block of roughly 35 m square. A 35 m-square city block was set as a standard for the virtual city block, and the length of one side of the city block was changed at intervals of 5 m between 20 m and 60 m, which is the length in which all city blocks can be roughly accommodated. We then conducted a sensitivity analysis.

Probabilities of estimating a building's existence were visualized when the following city blocks were set: a square virtual city block with a side length of 20–60 m in Fig. 10.1. A virtual city block with a side extending in the east-west direction unified at 35 m with the side extending in the north-south direction to 20–60 m as shown in Fig. 10.2. A virtual city block with a side extending in the north-south direction unified at 35 m with the side extending in the east-west direction to 20–60 m as shown in Fig. 10.3. A virtual city block that does not have a reference city block with similarity greater than, or equal to, t cannot have its building location estimated according to the model for estimating the building location of a city block. So the corresponding virtual city block in the figure is marked with a “—” symbol.

10.5 Discussion

In this section, we discuss the above results.

Among classifications I and II, only classification I resulted in an error rate E , which was lower than that for unclassified cases. So, the presence or absence of a

city block connected to a front road with a width of 12 m impacted the location of buildings in that city block. This was an influential factor which occurred because buildings in the city block of classification I were evenly located throughout the block and its location was not biased in the center of the block owing to regulations on setbacks from narrow roads. It can also be seen in Figs. 10.1, 10.2, 10.3. Classification I showed the trend of buildings being more evenly located in a city block compared to other classifications.

Among classifications III, IV, V, and VI, classifications III and IV had an error rate E that was lower than that of unclassified cases. Namely, if the direction where the city block connected the wide road was north or south, it was an influential factor in building location. The north-south direction should be particularly considered for securing sunlight, and it is thought that this affects the location of buildings. Looking at classifications III and IV in Figs. 10.1, 10.2, 10.3, we can see that building locations in classifications III and IV are the north and south sides.

Among classifications VII and VIII, only classification VIII had an error rate E that was lower than the error rate of unclassified cases. The north-south direction is important for securing sunlight, and the buildings in city blocks whose shape is short in the north-south direction needed to be arranged by shifting them to the east and west to secure sunlight, whereas city blocks whose shape is long in the north-south direction can secure sufficient space in the north-south direction, and their buildings do not need to be arranged by shifting them to the east and west. Namely, it is predicted that city block with long shapes in the north-south direction has little building-location variation in the east-west direction, and this becomes an influential factor in the building location. Looking at Fig. 10.2, we can see that city blocks that are longer in the north-south direction (Fig. 10.2: 50 m × 35 m, 55 m × 35 m, 60 m × 35 m) have more buildings concentrated in the north and south sides of the city block.

Both classifications IX and X had an error rate E that was higher than the error rate of unclassified cases. As described in Sect. 10.3.3, a smaller total number of reference city block groups N_I decreases the accuracy of the estimation of the block's building location. Therefore, a higher error rate E in these classifications than that in the non-classified buildings is thought to be simply the absence of building-location trends, rather than the building location variation becoming bigger owing to the classification. If a trend emerges in the building location based on a given land-value boundary, the error rate E of either classification IX or X is expected to be lower than that for unclassified cases. However, since all the target city blocks were city centers, the overall land value was high, and no building-location trends were thought to have appeared. Namely, the land value did not impact the location of the city-block building in the targeted Tokyo commercial zones.

Classification XI had an error rate E lower than that for unclassified cases. Offices are required to have a high rentable ratio and an efficient workplace environment. These characteristics are reflected in the design (Naito et al. 2010). Therefore, city blocks consisting only of offices are thought to have similar building locations. The result of classification XI suggests that, even for non-office applications,

constructing a city block with the same building application would be an influential factor for building location. Figures 10.1, 10.2, 10.3 show that classification XI has buildings located in the center of the city block compared to other classifications.

In Sect. 10.4, we used the model for estimating the building location of city blocks judged to be likely to exhibit building-location trends (classifications I, III, IV, VIII, XI). In Sect. 10.3, results showed that the location of buildings could be determined in city blocks of various shapes. In the future, city-block restructuring is expected to be actively implemented in Tokyo commercial zones. However, when a city block formed by city-block restructuring in the future is similar to a virtual city block as shown in Figs. 10.1, 10.2, 10.3 in terms of shape and classification, the location of buildings in the city block after city-block restructuring can be similar to the location of buildings in the corresponding virtual city block. This may not only provide suggestions for city-block restructuring plans, but also be applied to various aspects, such as its utilization in residents' consensus building and rough estimation of future townscapes and wind direction.

10.6 Conclusion

The present study provides an outlook that a future study should analyze in detail—building-location trends and building locations with different floor-area ratios and expand the building-shape estimation from two dimensions on the first-floor level, as was done in this study, to the third dimension.

Acknowledgments The data received in the analysis for this study was provided by the Tokyo Metropolitan Bureau of Urban Development. We would like to express our gratitude here. This paper is translated from the original paper published in Theory and Application of GIS, 2016, Vol. 24, No.2, pp. 85–96.

References

- Aoki M, Ohsawa Y, Kirita H, Kobayashi T (2010) Building shape caused by architectural volume maximization under sky exposure criterion regulation. *J Archit Plan (Trans AIJ)* 75(648):403–410
- Asami Y, Ohtaki T (2000) Prediction of the shape of detached houses on residential lots. *Environ Plan B Plan Design* 27:283–295
- Chrisman HC (1987) The accuracy of map overlays: a reassessment. *Landsc Urban Plan* 14:427–439
- Katsuragi K, Watanabe S (2000) An analysis of the process in mixed townscape with strange form buildings under the changes of building controls. *J City Plan Inst Jpn* 35:763–768
- Kawaguchi N, Murayama A, Shimizu H, Takatori C (2014) The state of scale of open space/green covered space in city blocks and their temporal change, and the characteristic feature of their distribution on Nagoya blocks. *J City Plan Inst Jpn* 49(3):207–212
- Kawakami M, Ohnishi H (2013) Study on assessment of regulation on building form using modeling of building space, form and its simulation. *J Archit Plan (Trans AIJ)* 78(687):1041–1048

- Kirita H, Ohsawa Y, Hasuka F, Nakagawa M (2007) Effect of sky exposure rate regulation on building layout. *J Archit Plan (Trans AIJ)* 78(617):71–78
- Lee DR, Sallee GT (1970) A method of measuring shape. *Geogr Rev* 60(4):555–563
- Makio H, Sugiyama S, Tokuono T, Nakaniwa Y (2006) The increases of apartments and the changes in land uses of street-facing open spaces in extent residential areas. *J Archit Plan (Trans AIJ)* 604:1–7
- Matsumiya K, Washizaki M, Oikawa K, Gota M (2014) Quantitative analysis of gap between buildings. *J Archit Plan (Trans AIJ)* 79(697):693–699
- Nagatomi T, Sato S, Kobayashi Y, Himeno Y (2007) Elucidation of the land use condition on the Main road side by building distribution conditions for block units: main roadside of Oita City, Oita prefecture. *J City Plan Inst Jpn* 42(3):517–522
- Naito K, Hashimoto M, Hiroy M, Fujita D (2010) Architectural planning utilized in design. *Gakugei Publishing*, Kyoto
- Nakanishi M, Nakai N, Saito C (1996) A study of building line control and building arrangement. *J City Plan Inst Jpn* 31:523–528
- Nakao N, Ito Y (2012) Study on aspects of city urban space based on building density on blocks. *J Archit Plan (Trans AIJ)* 77(677):1689–1697
- Nam T, Usami M, Sugiyama S, Tokuono T (2007) The parking lot installation methods in the apartment housings located in built-up areas. *Journal of Architecture and Planning (Transactions of AIJ)* 614:17–24
- Nam T, Sugiyama S, Tokuono T (2008) The characteristic of apartment houses located in built-up areas from the parking location and building dispositions. *J Archit Plan (Trans AIJ)* 73(623):23–30
- Saito C (2002) Urban block pattern and efficiency of road network: a study on simulation method of block generation by building arrangement. *J City Plan Inst Jpn* 37:85–90
- Saito C (2004) Effect of lattice on urban block pattern and city shape: a study on influence of neighborhood relations of buildings on urban space. *J City Plan Inst Jpn* 39:847–852
- Saito C (2011) Prediction of buildings emergent position from accessibility, independence and distribution of shortest path between buildings: logistic regression model of buildings arrangement in typical urban block. *J City Plan Inst Jpn* 46(3):397–402
- Saito M, Kato M (2013) An approach to the change and the actual condition of land use in the block unit: case study on Taira central city area in Iwaki City. *J City Plan Inst Jpn* 48(3):315–320
- Teraki A (2000a) Error model of horizontal position on spatial information: estimation of horizontal precision of spatial information: part 1. *Theory Appl GIS* 8(1):83–90
- Teraki A (2000b) Error model of horizontal position on spatial information: estimation of horizontal precision of spatial information: part 2. *Theory Appl GIS* 8(1):91–97
- Teraki A (2000c) Error model of horizontal position on spatial information: estimation of horizontal precision of spatial information: part 3. *Theory Appl GIS* 8(1):99–105
- Teraki A (2000d) Error model of horizontal position on spatial information: estimation of horizontal precision of spatial information: part 4. *Theory Appl GIS* 8(2):33–41
- Teraki A (2000e) Evaluation of accuracy of horizontal position on spatial information. *Theory Appl GIS* 8(2):43–49
- Urban Development and Improvement Division, Ministry of Land, Infrastructure, Transport and Tourism (2011) Formulation of “guidelines for developing large city blocks”. *Land Readjustment* 54(3):12–13
- Usui H, Asami Y (2011) Setback distance and density of buildings and roads. *J City Plan Inst Jpn* 46(3):829–834
- Vialard A (2011) Measures of the fit between street network, urban blocks and building footprints Savannah and Atlanta. In Proceedings of the 8th international symposium on space syntax, 8101, pp. 1–17
- Yoshino S (2006) Regional analysis and individual analysis. “5th ed: Special areas and appraisals” (Land Appraisal Theory Study Group). Seibunsha, Osaka, pp 199–202

Chapter 11

A Diagnostic Approach to the Multicollinearity Problem for Better Model Selection in the Hedonic Pricing Method



Yuki Hiruta and Yasushi Asami

Abstract The hedonic pricing method is an effective technique for estimating land and building prices. Nonetheless, numerous analysts have expressed concerns regarding the potential for multicollinearity to inflate the variance of the estimated coefficients. Hedonic pricing often involves spatially situated objects, and so strong correlations between two or more variables frequently arise. There are several diagnostics for evaluating multicollinearity, although most—sourced from explanatory variables—only measure the severity of this condition. To assess the risk of multicollinearity in a comprehensive manner, it is imperative to develop diagnostics that consider both the probability of occurrence and the severity of multicollinearity. This paper presents a numerical method for evaluating the influence of multicollinearity from these two perspectives.

Keywords Hedonic regression · Multicollinearity · Variance inflation factor · Numerical analysis · Generalized linear model

The contents of this paper are based on the following paper originally published in a Japanese journal: Yuki, H. and Asami, Y. (2018) A diagnostics of multicollinearity problem for better model selection in hedonic approach. *Urban housing sciences* 102: 113–122 (in Japanese).

Y. Hiruta (✉)

Research Center for Net Zero Carbon Society, Institutes of Innovation for Future Society, Nagoya University, Nagoya, Japan
e-mail: hiruta.yuki.m3@f.mail.nagoya-u.ac.jp

Y. Asami

Department of Urban Engineering, The University of Tokyo, Tokyo, Japan
e-mail: asami@csis.u-tokyo.ac.jp

11.1 Introduction

The hedonic method is frequently used to estimate prices for assets such as land and buildings and to evaluate the economic value associated with environmental factors. Within the hedonic approach, the prices of commodities like real estate are perceived as aggregates of various attributes, encompassing aspects such as convenience and performance. These prices are subsequently modeled through regression analyses, as outlined by Rosen (1974) and Witte et al. (1979). Challenges arise when multiple variables within a regression model exhibit some degree of correlation, inducing multicollinearity effects. In urban contexts, where structures are spatially oriented, it is especially challenging to maintain full independence among the explanatory variables, often because of the spatial locations and underlying, non-explicit common factors (Heikkila 1988; Deaton and Hoehn 2004). The existence of multicollinearity can inflate the variance of the regression coefficients,¹ thereby compromising the model's reliability (e.g., Alin 2010; Kutner et al. 2005, p. 283). Multicollinearity is technically defined in terms of the lack of linear relationships and orthogonality (e.g., Chatterjee and Hadi 2006). Although perfect collinearity is rare in real-world datasets, the more pervasive concern is the near-linear dependence between explanatory variables, leading to a form of imperfect multicollinearity (Asteriou and Hall 2007).

In empirical studies that employ the hedonic approach, the primary objective is often to evaluate the economic value of environmental factors. Inaccurate estimations of the regression coefficients can significantly skew the conclusions. However, excessive cautiousness in variable selection as a result of concerns about multicollinearity can lead to the omission of valuable information. Thus, an accurate diagnosis of the effects of multicollinearity is essential.

Numerous methods for detecting the effects of multicollinearity in advance have been proposed. These include the correlation matrix of explanatory variables, R ; the determinant of the correlation matrix, $\det(R)$; the variance inflation factor (VIF); the maximum VIF among all explanatory variables, VIF_{\max} ; the mean value of VIF_k , \overline{VIF} ; and the eigenvalues and eigenvectors of R (Alin 2010). Typically, when constructing hedonic models, these indicators are used to provide a preliminary estimate of the severity of collinearity. If the effects of collinearity are of concern, variable selection or variable consolidation can be applied through principal component analysis or factor analysis (e.g., Yoshida 1987; Chatterjee and Hadi 2006). Among the detection methods for multicollinearity, VIF_k is widely used

¹ The variance inflation of regression coefficients as a result of multicollinearity is explained by a mathematical formula. Regarding Eq. (11.1), the variance of the estimated partial regression coefficient \hat{a}_k is given by $V(\hat{a}_k) = \sigma^2(\mathbf{X}'\mathbf{X})^{-1}$. Specifically, when $p = 2$, the variance of the estimated partial regression coefficient \hat{a}_1 , $V(\hat{a}_1)$ can be written as $V(\hat{a}_1) = \sigma^2/n(1 - r_{12}^2)$. Here, r_{12} is the correlation coefficient between variables x_1 and x_2 . From this, it can be understood that a larger correlation coefficient r_{12} between the two variables corresponds to a larger variance $V(\hat{a}_1)$ of the partial regression coefficient \hat{a}_1 .

as a formal measure (Kutner et al. 2005); when a single metric for a regression model is required, the mean of VIF_k , denoted as \overline{VIF} , is often employed.

When considering the multiple regression Eq. (11.1), the dependent variable is represented by the vector $y = (y_1, \dots, y_i, \dots, y_n)$, which consists of n observations. The explanatory variables are denoted by the matrix $X = [x_1, \dots, x_k, \dots, x_p]$, which comprises n observations and p types of variables. The regression coefficients are represented by the vector $a_k = (a_1, \dots, a_k, \dots, a_p)'$. VIF_k is expressed by Eq. (11.2). In this context, R_k^2 is the coefficient of determination when a particular explanatory variable x_k is linearly regressed using explanatory variables other than x_k in Eq. (11.1). VIF_k can be considered as an indicator that represents the extent to which the variance of a particular regression coefficient estimate expands in comparison with the case of no collinearity.²

$$\mathbf{y} = \mathbf{X}\mathbf{a} + \boldsymbol{\mu} \quad \boldsymbol{\mu} \sim N(\mathbf{0}, \sigma^2 \mathbf{I}) \quad (11.1)$$

$$VIF_k = \frac{1}{1 - R_k^2} \quad k = 1, 2, \dots, p \quad (11.2)$$

\overline{VIF} is defined by Eq. (11.3). This indicator illustrates the extent to which the regression coefficients estimated in the model deviate from the true values (hereafter referred to as the “deviation of the regression coefficients”) compared with a model that has no collinearity, $\sum_{k=1}^p VIF_k = p$. This is represented using only explanatory variables and reflects the deviation of the regression coefficients regardless of their variance.³

$$\overline{VIF} = \frac{\sum_{k=1}^p VIF_k}{p} \quad (11.3)$$

However, the deviation of the regression coefficients, as indicated by \overline{VIF} , is merely an expected value. Even for regression models with the same \overline{VIF} , there

² In the standardized regression model $\mathbf{y}^* = \mathbf{X}^* \mathbf{a}^* + \boldsymbol{\mu}^*$, with $\boldsymbol{\mu}^* \sim N(\mathbf{0}, \sigma^2 \mathbf{I})$ and using standardized variables from Eq. (11.1), the term $\mathbf{X}^t \mathbf{X}$ in the variance $V(\hat{a}_k) = \sigma^2 (\mathbf{X}^t \mathbf{X})^{-1}$ becomes the correlation matrix \mathbf{r}_{xx} . Thus, $V(\hat{a}_k)$ is equivalent to $V(\hat{a}_k^*) = (\sigma^*)^2 (\mathbf{r}_{xx})^{-1}$, with its k -th diagonal element being VIF_k . If the determination coefficient R_k^2 is 0, $VIF_k = 1$; otherwise, as R_k^2 increases, VIF_k grows.

³ The product of the sum of VIF_k and the variance of the error term $(\sigma^*)^2$ become the expected value of the sum of the squared differences between the estimated regression coefficient \hat{a}_k^* and its true value t_k^* , given the standardized regression model $\mathbf{y}^* = \mathbf{X}^* \mathbf{a}^* + \boldsymbol{\mu}^*$, where $\boldsymbol{\mu}^* \sim N(\mathbf{0}, \sigma^2 \mathbf{I})$, which is derived by standardizing all the variables in Eq. (11.1) (see below). When $R_k^2 \equiv 0$, $VIF_k \equiv 1$, and $\sum_{k=1}^p VIF_k$ equals p . Therefore, the mean value of VIF_k , $\overline{VIF} = \sum_{k=1}^p VIF_k / p$, can be said to be the expected value that indicates the extent to which the estimated regression coefficient deviates from the true regression coefficient when considering the case where all explanatory variables are not linearly related to other explanatory variables (Kutner et al. 2005).

can be instances where no deviation occurs, or the deviation can be several times larger than the expected value depending on the sample applied. Moreover, there is no objective criterion that indicates the level metrics such as VIF_k or \bar{VIF} can reach before multicollinearity becomes a concern. This often leads to ambiguous judgments of the form “If VIF_k exceeds 10, the variance might be too large, and its reliability could be compromised” (Minotani 2015). As a result, analysts might consider strategies to address multicollinearity without fully understanding its direct impact on the estimated regression coefficients and values of the dependent variable. When constructing regression models, it is not only important to know the expected deviation of the regression coefficients represented by \bar{VIF} , but also to understand the following:

1. The potential severity of the deviation.
2. The probability of such a deviation occurring (probability of deviation).

It therefore becomes essential to consider not only the expected values, but also the distribution of the deviations of the regression coefficients. This is because, even if \bar{VIF} (expected value) and the variance are consistent, different distributions of the deviations can change the likelihood of exceeding a certain level of deviation.

The goal of this research is to provide insights for analysts constructing hedonic models in their professional or research endeavors, enabling a better understanding of the implications of multicollinearity. Specifically, this study offers methods and numerical benchmarks for determining the maximum possible deviation of the regression coefficients when a specific \bar{VIF} is derived, as well as the likelihood of such deviations occurring. Although previous studies have examined the extent of the deviation of the regression coefficients for different explanatory variables through simulations (Yoo et al. 2014), there are no studies with similar objectives and methods to the present research.

11.2 Methods

In this study, we use the generalized linear model (GLM) to simulate the relationship between (1) the deviation of the regression coefficient from its theoretical value, denoted as \bar{VIF} , and (2) the actual deviation of the estimated regression coefficient from its true value. The GLM framework enables the expected value to be estimated and the error structure (residuals) of the dependent variable to be modeled as a probability distribution, allowing for the determination of its parameters. This approach is advantageous for understanding the relationship between the theoretical deviation value \bar{VIF} and the actual deviation, as it illustrates the variation in the actual deviation for each theoretical value. In contrast, existing methods only evaluate the expected value, without considering the variation.

To elucidate these relationships using the GLM without any dependency on the configuration, we construct regression models across a spectrum of scenarios: from those where explanatory variables have minimal correlation to those with

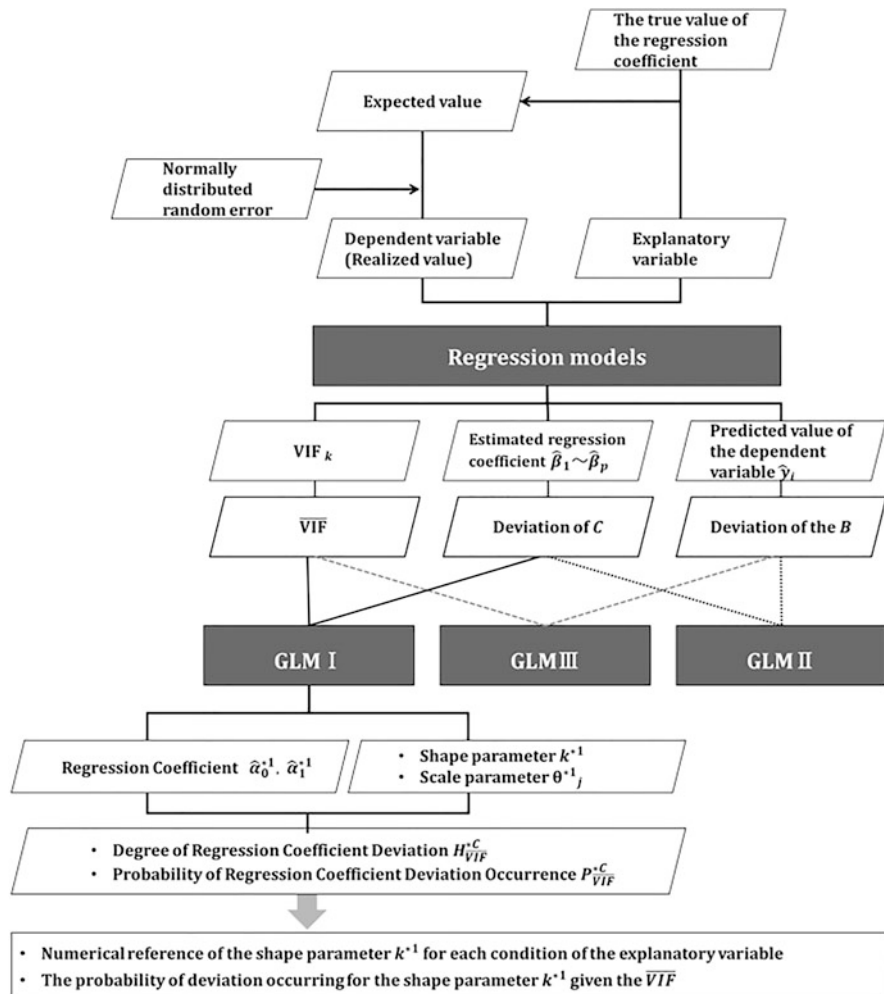


Fig. 11.1 Overview of proposed method

strong correlation. We employ a method that produces diverse variable sets through numerical simulations using random numbers.

An overview of the methodology is depicted in Fig. 11.1. Initially, we create several datasets of explanatory variables with a variety of inter-variable correlations. Using each dataset and pre-defined true regression coefficients, we calculate the true dependent variable (expected value). Subsequently, by incorporating random error terms in the expected value, we derive the actual values for the dependent variable in the regression model. Using the obtained dependent variables (actual values) and the primary explanatory variables, we fashion multiple regression models. Through these models, the deviation between the estimated regression coefficients and their

true values is quantified. Furthermore, $\overline{\text{VIF}}$ is directly derived from each explanatory variable dataset. We form a GLM with the metric representing the genuine deviation as the dependent variable and $\overline{\text{VIF}}$ as the explanatory variable.

The proposed method is applied to seven distinct regression model types to illustrate the different impacts of multicollinearity. In addition, the robustness of the constructed GLM and the extracted probability distribution parameters is verified. Finally, considering the influence of multicollinearity on the estimated values of the dependent variable in relation to $\overline{\text{VIF}}$ and the deviation of the regression coefficients, we suggest a diagnostic approach for assessing the effects of multicollinearity.

11.2.1 Construction of Regression Models

11.2.1.1 Generation of Explanatory Variables

The focus of this study is the influence of multicollinearity resulting from the correlation relationships among individual variables in regression models with 2–4 explanatory variables. For regression models with three or more variables, we consider both the presence and absence of independent variables. In this section, we describe the types of datasets and the method for generating variables that exhibit diverse correlations.

1. Types of Datasets

Figure 11.2 presents seven conditions that differ in their number of explanatory variables. The double-lined arrows in the conceptual diagram indicate that the variables were generated using the method described below, ensuring that the 5000 sets of explanatory variables encompass a broad spectrum of correlation relationships, ranging from sets with a correlation coefficient of -1 to those with a correlation coefficient of $+1$. The bold arrows denote correlation relationships that are automatically determined by the correlations of variables not linked by these bold arrows. The dotted arrows symbolize independent relationships between explanatory variables. Variables connected solely by dotted arrows are derived from random numbers that follow a normal distribution with a mean of 0 and a variance of 1. All the generated explanatory variables have been standardized to have a mean of 0 and a variance of 1.

2. Method for Generating Variables Demonstrating Diverse Correlations

The double-lined arrows in Fig. 11.2 imply that the 5000 sets of explanatory variables uniformly include sets exhibiting a variety of correlation relationships, from those with a correlation coefficient of -1 to those with a correlation coefficient of $+1$. These sets of explanatory variables were generated using the method

Explanation	Number of explanatory variables	Concept Diagram
a. Two variables showing various correlation coefficients	$p = 2$	$x_1 \longleftrightarrow x_2$
b. Three variables showing various correlation coefficients	$p = 3$	$x_1 \longleftrightarrow x_2$ $x_1 \rightarrow x_3$ $x_2 \rightarrow x_3$
c. Two variables showing various correlation coefficients and one variable with little to no correlation with the others	$p = 3$	$x_1 \longleftrightarrow x_2$ $x_1 \rightarrow x_3$ $x_2 \rightarrow x_3$
d. Four variables showing various correlation coefficients	$p = 4$	$x_1 \longleftrightarrow x_2$ $x_1 \rightarrow x_3$ $x_1 \rightarrow x_4$ $x_2 \rightarrow x_3$ $x_2 \rightarrow x_4$ $x_3 \rightarrow x_4$
e. Three variables showing various correlation coefficients and one variable with little to no correlation with the others	$p = 4$	$x_1 \longleftrightarrow x_2$ $x_1 \rightarrow x_3$ $x_1 \rightarrow x_4$ $x_2 \rightarrow x_3$ $x_2 \rightarrow x_4$ $x_3 \rightarrow x_4$ $x_3 \rightarrow x_1$
f. Two variables showing various correlation coefficients and two variables with little to no correlation with the others	$p = 4$	$x_1 \longleftrightarrow x_2$ $x_1 \rightarrow x_3$ $x_1 \rightarrow x_4$ $x_2 \rightarrow x_3$ $x_2 \rightarrow x_4$ $x_3 \rightarrow x_4$ $x_3 \rightarrow x_1$ $x_4 \rightarrow x_1$
g. Two sets of two variables each showing various correlation coefficients	$p = 4$	$x_1 \longleftrightarrow x_2$ $x_1 \rightarrow x_3$ $x_1 \rightarrow x_4$ $x_2 \rightarrow x_3$ $x_2 \rightarrow x_4$ $x_3 \rightarrow x_4$ $x_3 \rightarrow x_1$ $x_4 \rightarrow x_1$

The figure contains three scatter plots side-by-side, each with a horizontal axis ranging from -1 to +1.

- The first plot shows a horizontal band of points between two vertical dashed lines labeled -1 and +1. Above the plot are two horizontal double-headed arrows. The text "Various correlation coefficients" is centered below the plot.
- The second plot shows a narrow vertical band of points centered at 0, with a very sharp peak. Above the plot are two horizontal double-headed arrows. The text "Determined by correlation coefficients between other variables" is centered below the plot.
- The third plot shows a single point located exactly at the center (0) on the horizontal axis. Above the plot are two horizontal dotted arrows. The text "Little correlation" is centered below the plot.

Fig. 11.2 Patterns of explanatory variable generation (seven conditions)

outlined below, leveraging Eq. (11.4), where the variable x_2 predominantly exhibits a correlation coefficient of ρ with x_1 :

$$x_2 = \rho x_1 + \sqrt{1 - \rho^2} a \quad (11.4)$$

Initially, a distinct ρ is determined for each set of explanatory variables. The value of ρ is randomly selected from a uniform distribution ranging from -1 to 1. Subsequently, the explanatory variable x_1 and the variable a are formed by

randomly drawing 2000 values from a normal distribution with mean 0 and variance 1. The dependent variable x_2 is computed by applying the determined correlation coefficient ρ along with the independent variables x_1 and a to Eq. (11.4). Repeated iterations of this procedure produce sets of variables (x_1, x_2) with correlation coefficients that span from -1 to $+1$.⁴

11.2.1.2 Generation of the Dependent Variable (Realized Value)

We elucidate the effects of multicollinearity by analyzing the differences between the estimated regression coefficients and the dependent variable in regression models where the true regression coefficients are known. To do this, we set the explanatory variables x_{ik} (where $i = 1, 2, \dots, n; k = 1, 2, \dots, p$) and the true regression coefficients ($\beta_0 = 0, \beta_k = 1$) during the variable-generation stage. Using Eq. (11.5), we first calculate the expected value (true value) λ_i . Then, by adding a random error ε_i that is normally distributed with mean 0 and variance σ^2 , we generate the dependent variable (realized value) y_i using Eq. (11.6). Note that y_i is not standardized so that the actual degree of discrepancy can be captured.

Expected value:

$$\lambda_i = E[y_i] = \beta_0 + \beta_1 x_{i1} + \beta_2 x_{i2} + \cdots + \beta_p x_{ip} \quad (11.5)$$

Realized value:

$$y_i = \lambda_i + \varepsilon_i \quad \varepsilon_i \sim N(0, \sigma^2) \quad (11.6)$$

11.2.1.3 Construction of Regression Models

Using datasets consisting of explanatory and dependent variables, we perform regression according to Eq. (11.7). This regression formula provides the estimated regression coefficients $(\hat{\beta}_0, \dots, \hat{\beta}_p)$. The estimated value of the dependent variable \hat{y}_i is given in Eq. (11.8). (The estimated value of the dependent variable is simply referred to as the “estimated value”).

Regression formula:

$$y_i = \beta_0 + \beta_1 x_{i1} + \beta_2 x_{i2} + \cdots + \beta_p x_{ip} + \varepsilon_i \quad (11.7)$$

⁴ Using this method to generate a set of variables introduces some bias. Therefore, we produced a variable set 1.5 times larger than the required sample size. By stratifying and randomly selecting based on the correlation coefficients calculated from the generated variable sets (x_1, x_2) at intervals of 0.005, we ensured that the correlation coefficients of the generated pairs of explanatory variables were as uniform as possible, ranging from -1 to 1 .

Estimated value:

$$\hat{y}_i = \hat{\beta}_0 + \hat{\beta}_1 x_{i1} + \hat{\beta}_2 x_{i2} + \cdots + \hat{\beta}_p x_{ip} \quad (11.8)$$

11.2.2 Indicators Representing the Impact of Multicollinearity

11.2.2.1 Calculation of Indicators

To understand the effects of multicollinearity, we calculate the following indicators: \overline{VIF} using Eq. (11.10); the deviation C of the regression coefficients using Eq. (11.11); and the deviation B of the estimated values using Eq. (11.12). \overline{VIF} reflects the expected deviation of the regression coefficients, representing how many times greater the deviation is in comparison with a model that has no collinearity. This metric is derived from the explanatory variables. Conversely, C signifies the discrepancy between the estimated regression coefficients $(\hat{\beta}_1, \dots, \hat{\beta}_p)$ obtained from the regression model and the actual regression coefficients $(\beta_1, \dots, \beta_q)$. Both \overline{VIF} and C are crucial in comprehending the deviation in the regression coefficients because they provide insights into the relationship between the theoretical and actual deviations.

The deviation B of estimated values highlights the difference between the predicted value of the dependent variable \hat{y}_i and its true or expected value, denoted as λ_i . This indicator is especially helpful in gauging the extent to which the deviation of the regression coefficients, induced by multicollinearity, influences the estimated values of the dependent variable.

$$VIF_k = \frac{1}{1 - R_k^2} \quad k = 1, 2, \dots, p \quad (11.9)$$

$$\text{Mean of } VIF_k : \overline{VIF} = \frac{\sum_{k=1}^p VIF_k}{p} \quad (11.10)$$

$$\text{Deviation of regression coefficients : } C = \frac{\sum_{k=1}^p (\hat{\beta}_k - \beta_k)^2}{p} \quad (11.11)$$

$$\text{Deviation of estimated values : } B = \sum_{i=1}^n (\hat{y}_i - \lambda_i)^2 \quad (11.12)$$

11.2.2.2 Basic Statistics of the Indicator Values

For each of the seven conditions illustrated in Fig. 11.2, we construct 5000 independent regression models with a sample size of 2000. From each regression model, we derive \overline{VIF} , C, and B, yielding 5000 values for each indicator. Using these indicator values as variables, we formulate three GLMs with a sample size of 5000:

GLM-I: Explains the deviation C of regression coefficients using \overline{VIF} .

GLM-II: Explains the deviation B of estimated values using \overline{VIF} .

GLM-III: Explains the deviation B of estimated values using the deviation C of regression coefficients.

Each of these GLMs is constructed 500 times using different samples. Table 11.1 presents statistics for all 2,500,000 indicator values employed in the analysis (5000×500) for conditions a–g.

11.3 Results

11.3.1 Impact on Estimated Regression Coefficients

In this section, we address the following questions:

- To what extent can the deviation C of regression coefficients arise (severity)?
- What is the likelihood of observing a deviation in the regression coefficients that would not occur in the absence of multicollinearity (probability of deviation)?

These aspects are investigated for each \overline{VIF} , illustrating the risks associated with the deviation of regression coefficients. By constructing GLM-I with the deviation C of regression coefficients as the dependent variable and \overline{VIF} as the independent variable, we can determine the regression coefficient that describes the relationship between \overline{VIF} and C and identify the parameters of the probability distribution representing the error structure of C (specifically, k^{*1} and $\theta^{*1}\overline{VIF}$). This study leverages these insights.

11.3.1.1 Relationship Between \overline{VIF} and Deviation C of Regression Coefficients: GLM-I

For each conditions a–g outlined in Fig. 11.2, we construct GLM-I 500 times with a sample size of $l = 5000$ to determine the relationship between \overline{VIF} and the actual deviation C of the regression coefficients. After considering the link functions and the error structure of C, we adopt the formula with the smallest value of Akaike's information criterion (AIC). In Eq. (11.13), the subscript $j = 1, 2, \dots, l$ indicates

Table 11.1 Descriptive statistics for indicator values

	a.	b.	c.	d.	e.	f.	g.
VIF							
Min.	1.0	1.0	1.0	1.0	1.0	1.0	1.0
Qu.1st	1.1	1.3	1.0	1.5	1.2	1.0	1.2
Median	1.3	1.8	1.2	2.2	1.6	1.2	1.6
Qu.3rd	2.3	3.3	1.9	4.0	2.8	1.6	2.8
Max.	366,270.1	977,262.1	244,320.9	545,388.1	733,226.5	183,256.6	734,766.7
Mean	7.1	10.1	5.1	10.9	7.8	4.1	7.8
sd.	456.1	930.7	304.2	634.9	698.3	228.3	699.0
Deviation C of regression coefficients							
Min.	0.000	0.000	0.000	0.000	0.000	0.000	0.000
Qu.1st	0.000	0.000	0.000	0.000	0.000	0.000	0.000
Median	0.001	0.001	0.001	0.001	0.001	0.001	0.001
Qu.3rd	0.001	0.002	0.001	0.002	0.001	0.001	0.001
Max.	133.202	708.652	306.634	317.798	778.280	151.332	765.021
Mean	0.003	0.005	0.003	0.005	0.004	0.002	0.004
sd.	0.193	0.536	0.234	0.325	0.572	0.146	0.564
Deviation B of estimated values							
Min.	0.000	0.001	0.002	0.006	0.002	0.014	0.004
Qu.1st	1.213	1.923	1.923	2.676	2.677	2.675	2.677
Median	2.366	3.357	3.358	4.351	4.354	4.351	4.355
Qu.3rd	4.111	5.388	5.386	6.625	6.628	6.626	6.625
Max.	30.777	33.182	37.556	38.944	35.740	40.588	34.634
Mean	3.002	4.001	4.001	5.000	5.001	5.000	5.001
sd.	2.452	2.828	2.830	3.161	3.160	3.164	3.161

the data number, C_j is the dependent variable, and \overline{VIF}_j is the independent variable. E represents the expected value, α_0^{*1} , α_1^{*1} denote the regression coefficients, η^{*1} is the linear predictor, and f is a logarithmic link function that connects the linear predictor η^{*1} with the expected value $E(C_j)$. Concerning the error structure of C_j , it is assumed that C_j follows a gamma distribution with shape parameter k^{*1} and scale parameter θ^{*1}_j .

$$\text{GLM} - \text{I} : f [E(C_j)] = \eta^{*1} = \alpha_1^{*1} \log(\overline{VIF}_j) + \alpha_0^{*1}$$

where C_j follows a gamma distribution:

$$C_j \sim \gamma \left(C_j | k^{*1}, \theta^{*1}_j \right) \quad (11.13)$$

Table 11.2 presents the estimated regression coefficients $(\hat{\alpha}_0^{*1}, \hat{\alpha}_1^{*1})$ and the shape parameter k^{*1} for the gamma distribution. Figure 11.3 (left and center panels) shows the estimated values and confidence intervals for conditions a, b, and d using the mean values of the regression coefficients $(\hat{\alpha}_0^{*1}, \hat{\alpha}_1^{*1})$ and the shape parameter k^{*1} derived from 500 regression models. The dots in the diagrams indicate the distribution of all observation values used in constructing the regression models. Figure 11.3 (right panel) shows the probability distribution (gamma distribution) of C for the \overline{VIF} values marked by gray vertical lines in Fig. 11.3 (left and center panels), i.e., at points $\overline{VIF} \in (2^0, 2^{0.5}, \dots, 2^{10})$ and for $\overline{VIF} = 10$.

All models indicate that the regression coefficients $(\hat{\alpha}_0^{*1}, \hat{\alpha}_1^{*1})$ are significant at the 1% level. The values of $\hat{\alpha}_0^{*1}$, $\hat{\alpha}_1^{*1}$, and α_{11} are broadly consistent across the seven conditions, with $\hat{\alpha}_0 \approx -7.60$ and $\alpha_1 \approx 1.00$ (as listed in Table 11.2). From Fig. 11.3 (left and center panels), it is evident that the relationship between the expected value of C and \overline{VIF} for conditions a, b, and d is largely consistent and linear. In contrast, the shape parameter k^{*1} presented in Table 11.2 varies among the seven conditions, and the probability distribution (gamma distribution) of C shown in Fig. 11.3 (right panel) differs in conditions a, b, and d. The probability distribution (gamma distribution) is determined by the shape parameter k^{*1} and the scale parameter $\theta^{*1}_j = E(C_j)/k^{*1}$. Therefore, if the expected values $E(C_j)$ estimated for each \overline{VIF} are identical, the shape parameter k^{*1} determines the form of the distribution.

This implies that even if \overline{VIF} remains consistent, the expected value of C is stable across explanatory variable conditions a–g. Despite this consistency, the probability distribution of C varies by condition. Even when the expected values align, differences in the probability distributions can lead to variations in the likelihood of observing deviations exceeding a particular threshold.

Table 11.2 GLM-I estimated regression coefficients $(\hat{\alpha}_0^{*1}, \hat{\alpha}_1^{*1})$ and shape parameter k^{*1}

GLM-I		Estimated regression coefficients $\hat{\alpha}_0^{*2}, \hat{\alpha}_1^{*2}$ are all 1% significant				Shape parameter k^{*1}					
		Min.	Qu.1st	Mean	Qu.3rd	Max.	Min.	Qu.1st	Mean	Qu.3rd	Max.
2 variables	a.	$\hat{\alpha}_0^{*1}$	-7.662	-7.613	-7.600	-7.587	-7.549	a.	0.794	0.834	0.844
		$\hat{\alpha}_1^{*1}$	0.927	0.985	1.001	1.017	1.072			0.853	0.886
3 variables	b.	$\hat{\alpha}_0^{*1}$	-7.661	-7.613	-7.600	-7.587	-7.549	b.	1.030	1.069	1.081
		$\hat{\alpha}_1^{*1}$	0.934	0.987	0.999	1.011	1.056			1.093	1.166
c.		$\hat{\alpha}_0^{*1}$	-7.645	-7.612	-7.600	-7.588	-7.551	c.	1.143	1.181	1.195
		$\hat{\alpha}_1^{*1}$	0.907	0.984	1.000	1.016	1.065			1.208	1.208
d.		$\hat{\alpha}_0^{*1}$	-7.661	-7.613	-7.600	-7.587	-7.541	d.	1.208	1.250	1.264
		$\hat{\alpha}_1^{*1}$	0.953	0.986	0.998	1.010	1.046			1.277	1.332
e.		$\hat{\alpha}_0^{*1}$	-7.646	-7.611	-7.599	-7.587	-7.548	e.	1.279	1.329	1.346
		$\hat{\alpha}_1^{*1}$	0.945	0.985	0.999	1.014	1.057			1.364	1.423
f.		$\hat{\alpha}_0^{*1}$	-7.642	-7.610	-7.600	-7.590	-7.547	f.	1.459	1.512	1.532
		$\hat{\alpha}_1^{*1}$	0.923	0.982	0.999	1.015	1.083			1.553	1.631
g.		$\hat{\alpha}_0^{*1}$	-7.650	-7.611	-7.599	-7.588	-7.540	g.	1.294	1.341	1.358
		$\hat{\alpha}_1^{*1}$	0.940	0.985	0.999	1.014	1.056			1.374	1.460

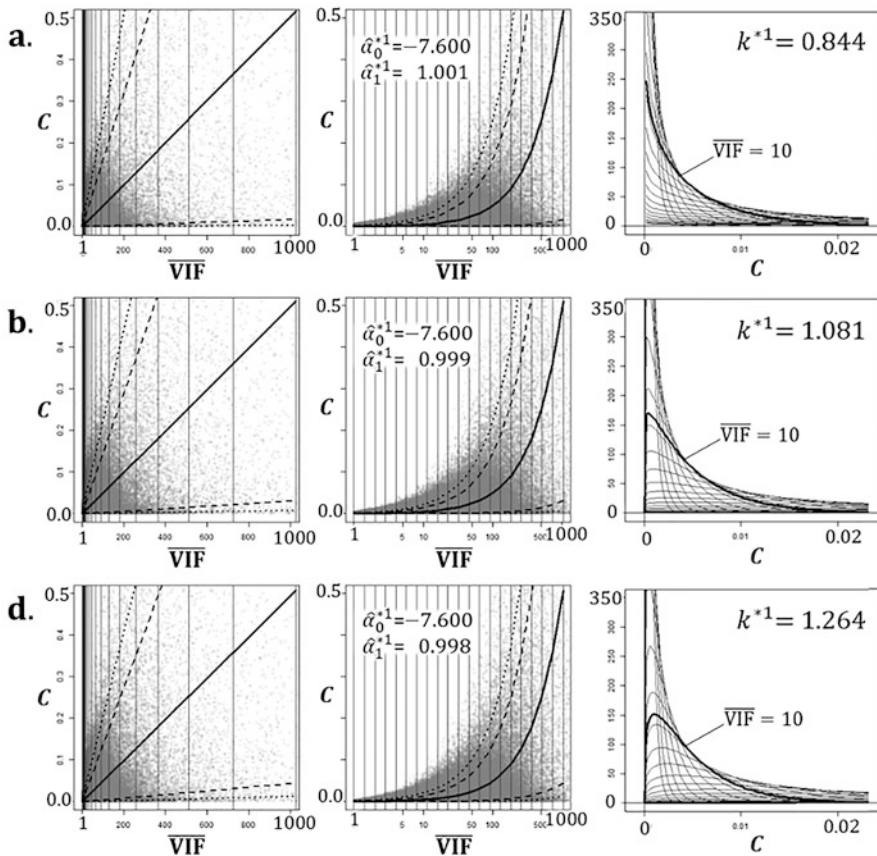


Fig. 11.3 GLM-I for conditions a, b, and d. Left: Relationship between $\overline{\text{VIF}}$ and C . Center: Relationship between $\overline{\text{VIF}}$ and C (with a logarithmic scale on the x -axis). Right: Probability distribution for each $\overline{\text{VIF}}$. *For the left and center panels, the solid line represents the mean (estimated value), the dashed line represents the 95% confidence interval, and the dotted line indicates the 99% confidence interval. For clarity, the x -axis ($\overline{\text{VIF}}$) only extends to 1000 and the y -axis (C) only extends to 0.5. For the right panel, for clarity, the x -axis (C) is limited to 0.02 and the y -axis (density) only extends to 350

11.3.1.2 Concepts of Severity and Probability of Deviation

We wish to determine the extent to which the deviation C of the regression coefficients can occur (severity) and the likelihood of such a deviation compared with the absence of collinearity (probability of deviation occurrence). However, the maximum deviation that occurs in a regression model showing a certain $\overline{\text{VIF}}$ cannot be specified solely from its probability distribution. In this study, we consider a large deviation that occurs with a 1/1000 probability (the 99.9th percentile) in the gamma distribution as the “maximum deviation.” We denote this by $(Z_{.999}^C)_{\overline{\text{VIF}}}$.

When a particular explanatory variable x_k is regressed linearly using other explanatory variables (i.e., excluding x_k) and the determination coefficient is $R_k^2 = 0$, there is no collinearity between x_k and the other explanatory variables and $VIF_k = 1$. Because VIF_k takes values in the range $1 \leq VIF_k < \infty$, if $\overline{VIF} = \sum_{k=1}^p VIF_k/p = 1$, we can infer that the regression model is not affected by multicollinearity. For $\overline{VIF} = 1$, we consider a large deviation that occurs with a 1/1000 probability (the 99.9th percentile of the probability distribution) as the maximum deviation in the absence of collinearity, and denote this by $(Z_{.999}^C)_1$. We define the ratio $(Z_{.999}^C)_{\overline{VIF}}/(Z_{.999}^C)_1$ as an indicator of the extent to which the deviation C of the regression coefficients can occur, and denote this as the degree of regression coefficient deviation, $H_{\overline{VIF}}^{*C}$. Moreover, in the gamma distribution of C for a regression model with a certain \overline{VIF} , we use the probability $Q((Z_{.999}^C)_1, k^{*1}, \theta^{*1}_{\overline{VIF}})$ of a larger deviation than $(Z_{.999}^C)_1$ occurring as an indicator of the likelihood of such a significant deviation in the absence of collinearity. We denote this as the probability of regression coefficient deviation occurrence, $P_{\overline{VIF}}^{*C}$. The concepts of $H_{\overline{VIF}}^{*C}$ and $P_{\overline{VIF}}^{*C}$ are illustrated in Fig. 11.4.

11.3.1.3 Degree of Regression Coefficient Deviation and Probability of Regression Coefficient Deviation Occurrence

The left side of Table 11.3 displays the mean values of the degree of regression coefficient deviation $H_{\overline{VIF}}^{*C}$ for 500 models with $\overline{VIF} = (2^0, 2^1, \dots, 2^{10})$ and $\overline{VIF} = (5, 10, 100)$ under conditions a–g. Figure 11.5 (upper panel) illustrates the relationship between \overline{VIF} and $H_{\overline{VIF}}^{*C}$ for conditions a, b, and d. For conditions a–g, \overline{VIF} and $H_{\overline{VIF}}^{*C}$ align almost perfectly. From these results, it is clear that the expected value of C (represented by \overline{VIF} , but also the maximum deviation when using $\overline{VIF} = 1$, i.e., without the influence of collinearity) can be directly determined by \overline{VIF} .

The right side of Table 11.3 presents the mean values of the probability of regression coefficient deviation occurrence $P_{\overline{VIF}}^{*C}$ for 500 models with $\overline{VIF} = (2^0, 2^1, \dots, 2^{10})$ and (5, 10, 100) under conditions a–g. Figure 11.5 (lower panel) depicts the relationship between \overline{VIF} and $P_{\overline{VIF}}^{*C}$ for conditions a, b, and d. Whereas $H_{\overline{VIF}}^{*C}$ aligns with \overline{VIF} and does not vary across conditions a–g, $P_{\overline{VIF}}^{*C}$ tends to be higher when there are more explanatory variables. This indicates that even if the expected value of the C is the same, the probability of such a deviation occurring depends on the number of explanatory variables and other factors associated with conditions a–g.

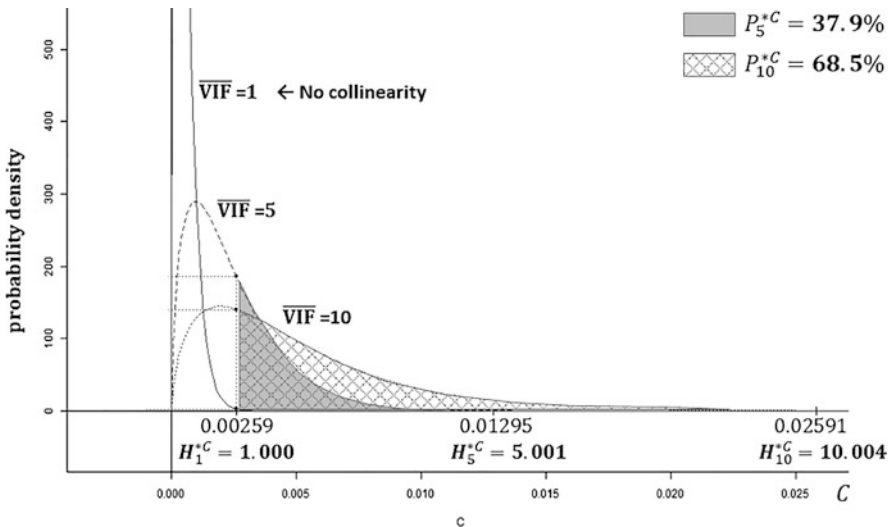


Fig. 11.4 Concepts of the degree of regression coefficient deviation and probability of regression coefficient deviation occurrence. In this figure, the 99.9th percentile of the probability distribution with $\overline{\text{VIF}} = 1$, denoted as $(Z_{999}^{*C})_1$, is 0.00259. We consider this as the “maximum deviation” that occurs when there is no collinearity. Moreover, the 99.9th percentile of the probability distribution with $\overline{\text{VIF}} = 10$, denoted as $((Z_{999}^{*C})_{10})$, is 0.02591, and this represents the “maximum deviation” when $\overline{\text{VIF}}$ is 10. The value $(Z_{999}^{*C})_{10} = 0.02591$ is roughly ten times $(Z_{999}^{*C})_1 = 0.00259$. Therefore, the degree of regression coefficient deviation for the model with $\overline{\text{VIF}} = 10$ ($H_{\overline{\text{VIF}}}^{*C}$) is 10. In the probability distribution with $\overline{\text{VIF}} = 10$, the likelihood of a deviation greater than the maximum deviation of a model without collinearity ($(Z_{999}^{*C})_1 = 0.00259$) is represented by the area of the shaded region and is given by $Q((Z_{999}^{*C})_1, k^{*1}, \{\theta \wedge \{*\}\} - \{10\}) = 0.685$, which means that the probability of regression coefficient deviation occurrence for the model with $\overline{\text{VIF}} = 10$, denoted as P_{10}^{*C} , is 68.5%

11.3.1.4 Robustness of GLM-I

Tables 11.2 and 11.3 and Figs. 11.3 and 11.5 summarize the consistency across the 500 models in terms of the GLM-I parameters $H_{\overline{\text{VIF}}}^{*C}$ and $P_{\overline{\text{VIF}}}^{*C}$, indicating that the constructed GLM-I is not heavily dependent on the sample. We further demonstrate the robustness of the model by constructing GLM-I with a constraint that limits $\overline{\text{VIF}}$ to a fixed value of l or below. Table 11.4 presents the results from constructing GLM-I in a similar manner, but using samples that restrict $\overline{\text{VIF}}$ to values of $l = 10, 50, 100, 500, 1000, 5000$, and $10,000$. The estimated regression coefficients $(\hat{\alpha}_0^{*1}, \hat{\alpha}_1^{*1})$ and the shape parameter k^{*1} remain largely consistent, suggesting that GLM-I is a stable model that does not depend on the range of $\overline{\text{VIF}}$.

Table 11.3 Left: Mean value of \mathbf{H}_{VIF}^{*C} ; Right: Mean value of \mathbf{P}_{VIF}^{*C}

VIF	Degree of regression coefficient deviation H_{VIF}^{*C}						Probability of regression coefficient deviation P_{VIF}^{*C}					
	Mean of 500 simulations						Mean of 500 simulations					
a.	b.	c.	d.	e.	f.	g.	a.	b.	c.	d.	e.	f.
$2^0 =$	1	1.0	1.0	1.0	1.0	1.0	1.0	0.1	0.1	0.1	0.1	0.1
$2^1 =$	2	2.0	2.0	2.0	2.0	2.0	2.0	2.8	3.3	3.6	3.8	4.0
$2^2 =$	4	4.0	4.0	4.0	4.0	4.0	4.0	15.4	19.0	20.8	21.8	23.1
$2^3 =$	8	8.0	8.0	8.0	8.0	8.0	8.0	37.1	44.7	48.1	50.0	52.4
$2^4 =$	16	16.1	16.0	15.9	16.0	16.0	16.0	58.7	67.8	71.5	73.5	75.9
$2^5 =$	32	32.2	32.0	31.9	32.0	32.0	32.0	74.9	83.0	85.9	87.4	89.1
$2^6 =$	64	64.6	64.0	64.2	63.7	64.1	64.0	85.4	91.5	93.4	94.4	95.4
$2^7 =$	128	129.5	128.1	127.4	128.3	128.1	128.2	91.6	95.8	97.0	97.6	98.1
$2^8 =$	256	259.7	256.5	257.6	254.9	256.9	256.6	95.3	98.0	98.7	99.0	99.2
$2^9 =$	512	521.0	513.5	516.2	509.8	514.6	514.2	97.4	99.0	99.4	99.6	99.7
$2^{10} =$	1024	1045.3	1028.2	1034.7	1019.8	1030.8	1030.6	1030.0	98.5	99.5	99.7	99.9
5	5.0	5.0	5.0	5.0	5.0	5.0	5.0	21.8	26.8	29.2	30.5	32.3
10	10.0	10.0	10.0	10.0	10.0	10.0	10.0	44.5	52.8	56.5	58.6	61.1
100	101.1	100.1	100.4	99.6	100.2	100.1	100.2	89.8	94.6	96.1	96.7	97.4

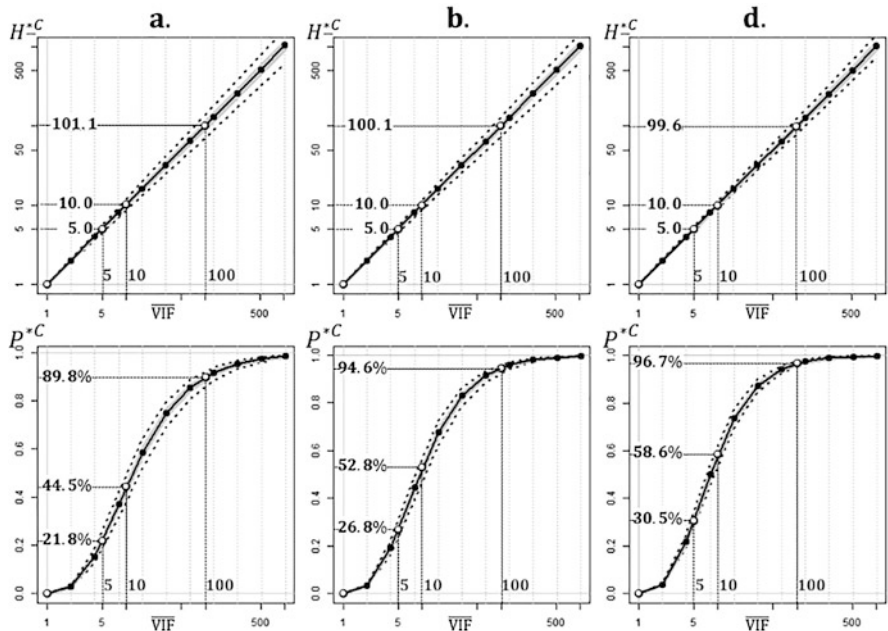


Fig. 11.5 GLM-I for conditions a, b, and d. Upper: Degree of deviation $H_{\overline{VIF}}^{*C}$; Lower: Probability of deviation occurrence $P_{\overline{VIF}}^{*C}$. Solid lines with black dots represent the mean of 500 simulations. The gray area indicates the range from the first quartile to the third quartile, and the dotted lines show the maximum and minimum values

11.3.1.5 Comparison and Test for Differences

Figure 11.6 compares $P_{\overline{VIF}}^{*C}$ and $H_{\overline{VIF}}^{*C}$ across models under the seven different conditions for the example cases of $\overline{VIF} = 5$ and 10 . These models differ based on the number of explanatory variables and whether independent variables are present or absent. The kernel density⁵ is based on the results of 500 simulations.

For every combination of these seven conditions (21 combinations in total), Welch's t -test⁶ is applied to examine the difference in means. For H_5^{*C} and H_{10}^{*C} , the null hypothesis that “the means of the two groups are equal” is only rejected at the 1% level (p -value ≥ 0.01) in conditions a and d. For the other conditions, this

⁵ The bandwidth of a Gaussian kernel density estimator is selected based on a rule-of-thumb (Silverman 1986). The default value is 0.9 times the minimum of the standard deviation and the interquartile range divided by 1.34 times the sample size to the power of -0.2 .

⁶ Before using Welch's t -test, we tested for normality with the Kolmogorov–Smirnov test and checked for homoscedasticity with the F -test. All data met the 5% significance level for normality. While the variance results varied by group, both the Welch's and Student's t -tests were consistent, so we reported Welch's t -test results.

Table 11.4 Regression coefficient estimates ($\hat{\alpha}_0^{*1}, \hat{\alpha}_1^{*1}$) and shape parameter k^{*1} from GLM-I trained using samples limited to \overline{VIF} less than or equal to a constant value I

GLM-I		Estimated regression coefficients $\hat{\alpha}_0^{*2}, \hat{\alpha}_1^{*2}$ are all 1% significant					Shape parameter k^{*1}				
		≤10	≤50	≤500	≤1000	≤5000	≤10	≤50	≤100	≤500	≤1000
2 variables	a.	$\hat{\alpha}_0^{*1}$ -7.604	-7.598	-7.597	-7.596	-7.597	-7.600	a.	0.874	0.856	0.850
	$\hat{\alpha}_1^{*1}$	1.016	0.998	0.996	0.994	0.995	1.002				0.850
3 variables	b.	$\hat{\alpha}_0^{*1}$ -7.605	-7.611	-7.615	-7.620	-7.618	-7.616	b.	1.118	1.089	1.080
	$\hat{\alpha}_1^{*1}$	1.025	1.036	1.042	1.050	1.047	1.044				1.072
c.	$\hat{\alpha}_0^{*1}$ -7.591	-7.586	-7.589	-7.592	-7.592	-7.591	c.	1.227	1.205	1.203	1.197
	$\hat{\alpha}_1^{*1}$	0.981	0.964	0.971	0.980	0.980	0.978				1.197
d.	$\hat{\alpha}_0^{*1}$ -7.589	-7.615	-7.608	-7.605	-7.608	-7.605	d.	1.371	1.302	1.289	1.281
	$\hat{\alpha}_1^{*1}$	0.977	1.017	1.008	1.004	1.007	1.005				1.281
e.	$\hat{\alpha}_0^{*1}$ -7.577	-7.571	-7.565	-7.567	-7.567	-7.565	e.	1.423	1.368	1.355	1.350
	$\hat{\alpha}_1^{*1}$	1.004	0.994	0.981	0.985	0.985	0.983				1.350
f.	$\hat{\alpha}_0^{*1}$ -7.608	-7.613	-7.611	-7.607	-7.607	-7.607	f.	1.567	1.523	1.519	1.506
	$\hat{\alpha}_1^{*1}$	1.021	1.040	1.032	1.021	1.021	1.021				1.506
g.	$\hat{\alpha}_0^{*1}$ -7.571	-7.569	-7.563	-7.566	-7.566	-7.565	g.	1.431	1.378	1.363	1.357
	$\hat{\alpha}_1^{*1}$	0.985	0.983	0.972	0.978	0.978	0.976				1.357

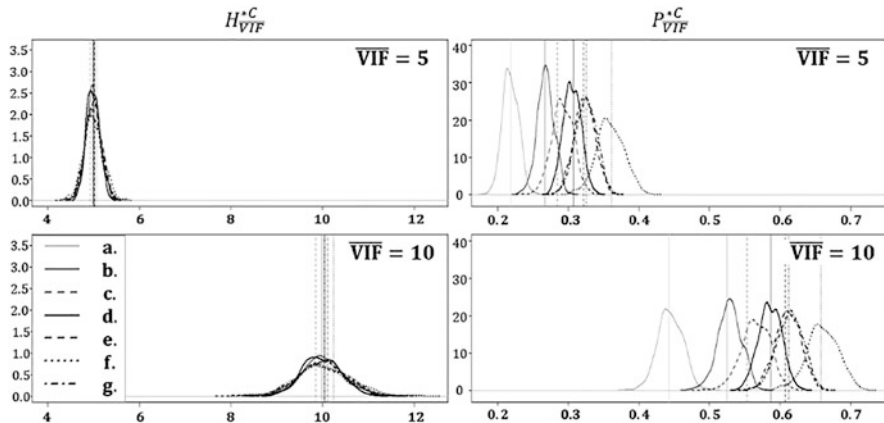


Fig. 11.6 Left: Degree of deviation in regression coefficients $H_{\overline{VIF}}^{*C}$ (no significant difference observed); Right: Probability of deviation in regression coefficients $P_{\overline{VIF}}^{*C}$ (significant difference at the 5% level)

hypothesis is not rejected at the 5% significance level (p -value ≥ 0.05), indicating that there is no substantial difference between the two groups. For P_5^{*C} and P_{10}^{*C} , however, all combinations have p -values of less than 0.05, supporting the conclusion that a difference exists between the groups. This suggests that while regression models with the same \overline{VIF} display little variance in the degree of deviation, the probability of such deviations occurring varies, indicating differing risks of deviations in the regression coefficients.

11.3.2 Impact on the Estimated Values of the Dependent Variable

When multicollinearity influences the estimated regression coefficients, it is postulated that the estimated values of the dependent variable (often referred to as “estimates”) will also be affected. In this section, using an approach akin to that applied in Sect. 11.3.1.1, we explore the relationship between \overline{VIF} and the deviation B of the estimates, as well as the relationship between the deviation C of regression coefficients and the deviation B of estimates.

11.3.2.1 Relationship Between \overline{VIF} and Deviation B of Estimates: GLM-II

For conditions a–g listed in Fig. 11.2, GLM-II is constructed 500 times with $l = 5000$ to determine the relationship between \overline{VIF} and the deviation B of estimates. This model is created considering the link function and the error structure of B.

Ultimately, the equation with the smallest AIC is adopted. In Eq. (11.14), the subscript $j = 1, 2, \dots, l$ represents the data index, B_j is the dependent variable, and \overline{VIF}_j is the explanatory variable. E represents the expected value, α_0^{*2} , α_1^{*2} are the coefficients, η^{*2} is the linear predictor, and g is a logarithmic link function connecting the linear predictor η^{*2} to the expected value $E(B_j)$. Regarding the error structure, it is assumed that B_j obeys a gamma distribution characterized by the shape parameter k^{*2} and the scale parameter θ_j^{*2} .

$$\text{GLM - II : } f [E (B_j)] = \eta^{*2} = \alpha_1^{*2} \log (\overline{VIF}_j) + \alpha_0^{*2}$$

where B_j follows a gamma distribution:

$$B_j \sim \gamma \left(B_j | k^{*2}, \theta_j^{*2} \right) \quad (11.14)$$

For each condition of GLM-II, the estimated regression coefficients $(\hat{\alpha}_0^{*2}, \hat{\alpha}_1^{*2})$ and the shape parameter k^{*2} are presented in Table 11.5. Figure 11.7 (left and center panels) shows the estimated values and confidence intervals for conditions a, b, and d. This representation is derived using the mean values of the regression coefficients $\hat{\alpha}_0^{*2}$ and $\hat{\alpha}_1^{*2}$, and the shape parameter k^{*2} from 500 regression models. The right side of Fig. 11.7 shows the probability distribution (gamma distribution) of the deviation B of estimated values for $\overline{VIF} \in (2^0, 2^{0.5}, \dots, 2^{10})$, and specifically for $\overline{VIF} = 10$, as indicated by the gray vertical lines in the left and center of Fig. 11.7.

The regression coefficient $\hat{\alpha}_1^{*2}$ for GLM-II is not significant in any scenario and is close to zero. Additionally, as illustrated by Fig. 11.7, both the estimated values and confidence intervals of GLM-II are uniform. The probability distribution of B does not change for the various \overline{VIF} values. This implies that \overline{VIF} , which represents the expected deviation of the regression coefficient, cannot explain the deviation in the estimated values. However, the intercept $\hat{\alpha}_0^{*2}$ is significant at the 1% level for all conditions. This suggests that, although differences in the expected deviation of regression coefficients do not influence the deviation in the estimated values, any variation in factors such as the number of explanatory variables could impact the estimates.

11.3.2.2 Relationship Between Deviation C of Regression Coefficients and Deviation B of Estimates: GLM-III

We now examine the relationship between the deviation of the regression coefficient C and the deviation of the estimated value B using the same method as with GLM-II. For each of conditions a–g presented in Fig. 11.2, we construct GLM-III 500 times with a sample size of $l = 5000$. This demonstrates the relationship between

Table 11.5 GLM-II estimated regression coefficients $(\hat{\alpha}_0^{*2}, \hat{\alpha}_1^{*2})$ and shape parameter k^{*2}

		Estimated regression coefficients $\hat{\alpha}_0^{*2}$ are all 1% significant, $\hat{\alpha}_1^{*2}$ are not significant					Shape parameter k^{*1}			
		Min.	Qu.1.st	Mean	Qu.3rd	Max.	Min.	Qu.1.st	Mean	Qu.3rd
2 variables		a.	$\hat{\alpha}_0^{*2}$ -0.049	1.065 -0.010	1.090 0.000	1.099 0.009	1.110 0.009	1.141 0.037		
3 variables	b.	$\hat{\alpha}_0^{*2}$ -0.031	1.337 -0.008	1.378 0.000	1.386 0.007	1.396 0.049	1.429 0.049		a.	1.420 1.519
	c.	$\hat{\alpha}_0^{*2}$ -0.052	1.351 -0.009	1.378 0.000	1.387 0.009	1.395 0.039	1.432 0.039		b.	1.480 1.577
4 variables		d.	$\hat{\alpha}_0^{*2}$ -0.029	1.567 -0.007	1.601 0.000	1.609 0.007	1.619 0.030	1.657 0.030		
e.		$\hat{\alpha}_0^{*2}$ -0.027	1.572 -0.008	1.601 0.000	1.610 0.006	1.619 0.032	1.645 0.032		c.	1.888 1.977
	f.	$\hat{\alpha}_0^{*2}$ -0.045	1.575 -0.010	1.602 -0.001	1.610 0.009	1.618 0.035	1.648 0.035		d.	1.893 1.977
g.		$\hat{\alpha}_0^{*2}$ -0.027	1.565 -0.007	1.601 0.000	1.610 0.007	1.618 0.038	1.649 0.038		e.	2.350 2.468
								f.	2.359 2.470	2.501 2.530
								g.	2.375 2.478	2.506 2.537

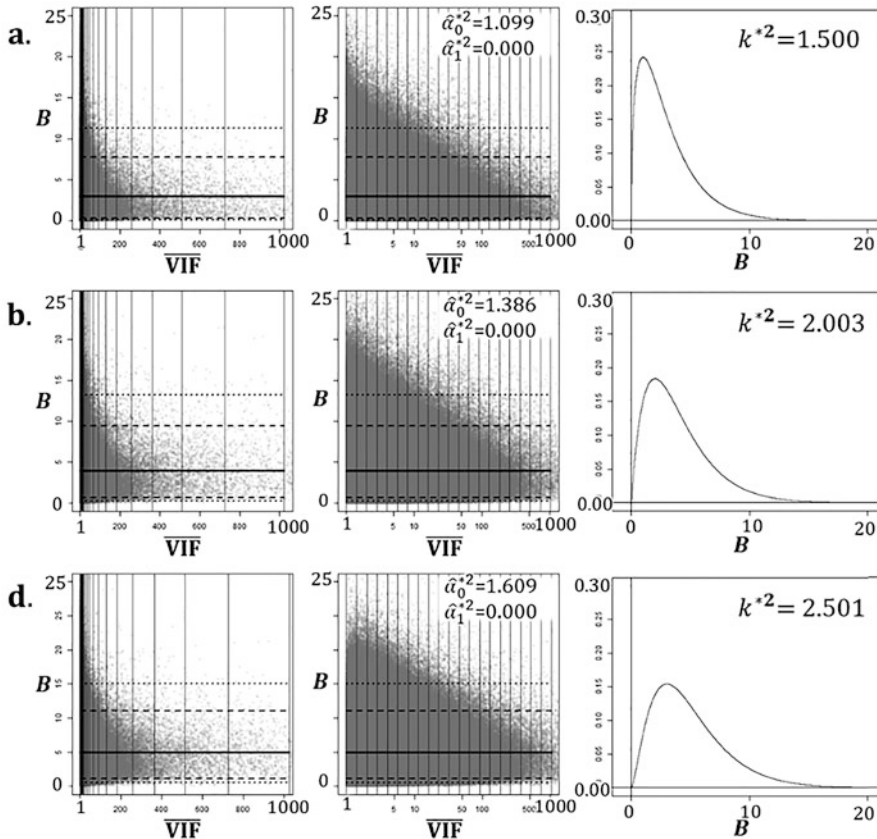


Fig. 11.7 GLM-II for conditions a, b, and d. Left: Relationship between $\overline{\text{VIF}}$ and B . Center: Relationship between $\overline{\text{VIF}}$ and B (with a logarithmic scale on the x-axis). Right: Probability distribution for each $\overline{\text{VIF}}^2$. For the left and center panels, the solid line represents the mean (estimated value), the dashed line represents the 95% confidence interval, and the dotted line indicates the 99% confidence interval. For clarity, the x-axis ($\overline{\text{VIF}}$) only extends to 1000 and the y-axis (B) only extends to 25. For the right diagram, for clarity, the x-axis (B) is limited to 20 and the y-axis (density) only extends to 0.30

the deviation of the regression coefficient C and the deviation in the estimated value B. The model accounts for the link function and error structure of B. Ultimately, the equation with the smallest AIC is adopted. In Eq. (11.15), the subscript $j = 1, 2, \dots, l$ represents the data number, B_j is the dependent variable, C_j is the explanatory variable, E denotes the expected value, and α_0^{*3} and α_1^{*3} represent coefficients. η^{*3} is a linear predictor. The logarithmic link function h connects the linear predictor η^{*3} to the expected value $E(B_j)$. We assume that the error structure of B_j obeys a gamma distribution with shape parameter k^{*3} and scale parameter θ^{*3}_j .

$$\text{GLM - III : } h[E(B_j)] = \eta^{*3} = \alpha_1^{*3} \log(C_j) + \alpha_0^{*3}$$

where B_j follows a gamma distribution:

$$B_j \sim \gamma \left(B_j \mid k^{*3}, \theta^{*3} \right) \quad (11.15)$$

The estimated regression coefficients of GLM-III for each condition, namely $\hat{\alpha}_0^{*3}$ and $\hat{\alpha}_1^{*3}$ along with the shape parameter k^{*3} , are listed in Table 11.6. Figure 11.8 (left and center panels) is similar to Fig. 11.7, showing the estimated values and confidence intervals for conditions a, b, and d based on the mean values of $\hat{\alpha}_0^{*3}$, $\hat{\alpha}_1^{*3}$, and k^{*3} derived from 500 regression models. Figure 11.8 (right panel) depicts the probability distribution (gamma distribution) of B for points $C \in ((Z_{.999}^{*C})_{20}, (Z_{.999}^{*C})_{20.5}, \dots, (Z_{.999}^{*C})_{210})$, and $C = (Z_{.999}^{*C})_{10}$, marked by gray vertical lines in the left and center panels of Fig. 11.8.

From the estimated regression coefficient $\hat{\alpha}_1^{*3}$ for GLM-III (see Table 11.6), we observe that a larger value of C is correlated with an increased expected value for the deviation in the estimated value $(Z_{.999}^{*B})_C$. However, this trend is not as pronounced as for GLM-I. For example, with $\overline{VIF} = 5$ (i.e., the expected deviation of the regression coefficient C is five times that in a scenario without collinearity), the maximum deviation, $(Z_{.999}^{*C})_1$, becomes five times that of a collinearity-free scenario. However, even if C reaches five times its value for a collinearity-free scenario, the resulting maximum deviation of the estimated value $(Z_{.999}^{*B})_C$ is only about 1.6 times larger, and the difference is not significant.⁷

Although the expected deviation of the regression coefficient C , represented by \overline{VIF} , does not directly explain the deviation in the estimated value B , models with larger values of C tend to exhibit a larger deviation in B . However, the growth in B is more subtle than the increase in C .

11.4 A Method for Diagnosing the Risk of Multicollinearity

Typically, analysts estimate the degree (severity) of deviation in regression coefficients based on metrics such as \overline{VIF} derived from explanatory variables and diagnose the regression model accordingly. In this paper, we have proposed a more accurate model diagnosis method by referring to the shape parameter k^{*1} derived from GLM-I in addition to \overline{VIF} .

Table 11.7 presents the shape parameter k^{*1} for each variable condition, as revealed by the numerical experiments. Additionally, Table 11.8 and Fig. 11.9

⁷ $(Z_{.999}^{*B})_C$ represents the 99.9th percentile (or “maximum deviation”) from the probability distribution (gamma distribution) of the deviation B of the estimated values when a deviation C in a certain regression coefficient is indicated. $(Z_{.999}^{*B})_1$ denotes the 99.9th percentile (or “maximum deviation”) from the probability distribution (gamma distribution) of the deviation B of the estimated values at the maximum deviation of the regression coefficient, $(Z_{.999}^{*C})_1$, in the model with $\overline{VIF} = 1$ (a model without collinearity).

Table 11.6 GLM-III estimated regression coefficients $(\hat{\alpha}_0^{*3}, \hat{\alpha}_1^{*3})$ and shape parameter k^{*3}

GLM-III		Estimated regression coefficients $\hat{\alpha}_0^{*3}, \hat{\alpha}_1^{*3}$ are all 1% significant				Shape parameter k^{*1}					
		Min.	Qu.1st	Mean	Qu.3rd	Max.	Min.	Qu.1st	Mean	Qu.3rd	Max.
2 variables	a.	$\hat{\alpha}_0^{*3}$	-7.662	-7.613	-7.600	-7.587	-7.549	a.	0.794	0.834	0.844
	$\hat{\alpha}_1^{*3}$	0.927	0.985	1.001	1.017	1.072					
	b.	$\hat{\alpha}_0^{*3}$	-7.661	-7.613	-7.600	-7.587	-7.549	b.	1.030	1.069	1.081
3 variables	$\hat{\alpha}_1^{*3}$	0.934	0.987	0.999	1.011	1.056					
	c.	$\hat{\alpha}_0^{*3}$	-7.645	-7.612	-7.600	-7.588	-7.551	c.	1.143	1.181	1.195
	$\hat{\alpha}_1^{*3}$	0.907	0.984	1.000	1.016	1.065					
4 variables	d.	$\hat{\alpha}_0^{*3}$	-7.661	-7.613	-7.600	-7.587	-7.541	d.	1.208	1.250	1.264
	$\hat{\alpha}_1^{*3}$	0.953	0.986	0.998	1.010	1.046					
	e.	$\hat{\alpha}_0^{*3}$	-7.646	-7.611	-7.599	-7.587	-7.548	e.	1.279	1.329	1.346
f.	$\hat{\alpha}_1^{*3}$	0.945	0.985	0.999	1.014	1.057					
	$\hat{\alpha}_0^{*3}$	-7.642	-7.610	-7.600	-7.590	-7.547	f.	1.459	1.512	1.532	1.553
	$\hat{\alpha}_1^{*3}$	0.923	0.982	0.999	1.015	1.083					
g.	$\hat{\alpha}_0^{*3}$	-7.650	-7.611	-7.599	-7.588	-7.540	g.	1.294	1.341	1.358	1.374
	$\hat{\alpha}_1^{*3}$	0.940	0.985	0.999	1.014	1.056					

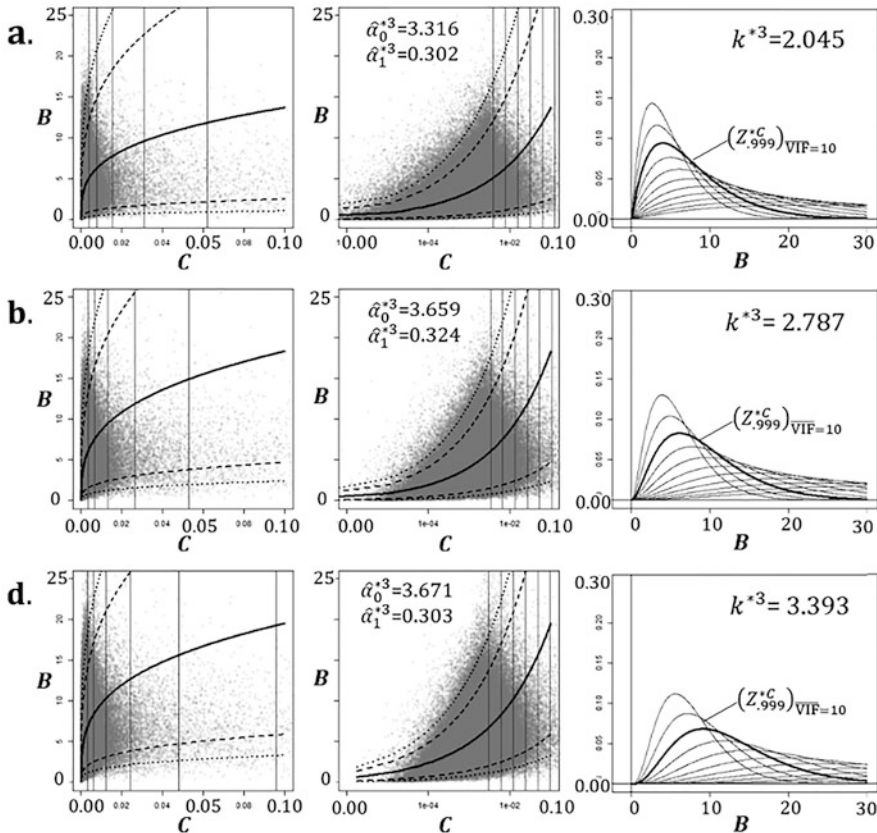


Fig. 11.8 GLM-III for conditions a, b, and d. Left: Relationship between C and B . Center: Relationship between C and B (with a logarithmic scale on the x -axis). Right: Probability distribution for each C . For the left and center panels, the solid line represents the mean (estimated value), the dashed line represents the 95% confidence interval, and the dotted line indicates the 99% confidence interval. For clarity, the x -axis (C) only extends to **0.10** and the y -axis (B) only extends to **25**. For the right diagram, for clarity, the x -axis (B) is limited to 20 and the y -axis (density) only extends to 0.30

illustrate the probability of a deviation in the regression coefficients in relation to both $\overline{\text{VIF}}$ and the shape parameter k^* . By consulting information similar to that contained in Table 11.8 and Fig. 11.9, the probability P^*C of experiencing significant deviations can be determined. Such deviations, in the absence of multicollinearity, are exceptionally rare, occurring only with a 1/1000 probability. This comprehension is based on the $\overline{\text{VIF}}$ derived from the explanatory variables and the shape parameter k^* dictated by the conditions of these variables. Furthermore, as GLM-II and GLM-III have shown, variations in the probability of a deviation in the regression coefficients influence the degree of impact on the estimated values of

Table 11.7 Conditions of variables and shape parameter k^{*1}

Conditions of the explanatory variables	Shape parameter k^{*1}
a. 2 variables	0.844
b. 3 variables	1.081
c. 3 variables, one is independent	1.195
d. 4 variables	1.264
e. 4 variables, one is independent	1.346
f. 4 variables, two are independent	1.532
g. 4 variables, two correlated pairs	1.358

Table 11.8 Probability of deviation P^{*C} for \overline{VIF} and shape parameter k^{*1} (in %)

\overline{VIF}	Shape parameter k^{*1}	1	2	4	8	16	32	64	128	256	512	1024
0.8	0.1	2.7	14.7	35.5	56.7	73.0	83.8	90.5	94.5	96.8	98.2	
0.9	0.1	2.9	16.2	38.9	61.0	77.1	87.1	92.9	96.2	97.9	98.9	
1	0.1	3.2	17.8	42.2	64.9	80.6	89.8	94.7	97.3	98.7	99.3	
1.1	0.1	3.4	19.3	45.3	68.5	83.6	91.9	96.1	98.2	99.1	99.6	
1.2	0.1	3.6	20.9	48.3	71.7	86.1	93.6	97.1	98.7	99.4	99.8	
1.3	0.1	3.9	22.4	51.2	74.7	88.3	94.9	97.9	99.1	99.6	99.9	
1.4	0.1	4.1	23.9	53.9	77.3	90.1	96.0	98.4	99.4	99.8	99.9	
1.5	0.1	4.3	25.4	56.6	79.7	91.7	96.8	98.8	99.6	99.9	99.9	
1.6	0.1	4.6	26.9	59.1	81.9	93.0	97.5	99.1	99.7	99.9	100.0	
1.7	0.1	4.8	28.4	61.4	83.8	94.1	98.0	99.4	99.8	99.9	100.0	
1.8	0.1	5.1	29.9	63.7	85.6	95.1	98.5	99.5	99.9	100.0	100.0	
1.9	0.1	5.3	31.4	65.9	87.1	95.9	98.8	99.7	99.9	100.0	100.0	
2	0.1	5.6	32.9	67.9	88.6	96.6	99.1	99.8	99.9	100.0	100.0	

the dependent variables. Employing the proposed method facilitates the comparison of the following aspects:

- The severity of impacts directly inferred from \overline{VIF}
- The probability of a deviation in the regression coefficients
- The magnitude of the impact on the dependent variable across various potential regression models

11.5 Discussion

In empirical studies that use the hedonic model to quantify the economic value of environmental factors, the accurate estimation of regression coefficients is paramount. When constructing such a hedonic model, analysts aim to gauge several potential risks, specifically the maximum extent of the influence of multicollinearity, termed the “severity,” and the probability of its occurrence, referred to as the “probability of deviation.” This study has provided insights for both practitioners and researchers when building hedonic models, placing particular emphasis on

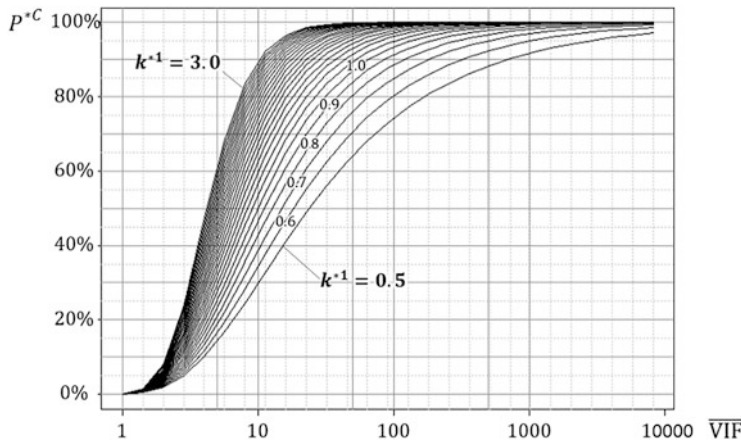


Fig. 11.9 Probability of deviation $P_{\overline{\text{VIF}}}^{*C}$ for $\overline{\text{VIF}}$ and shape parameter k^{*1}

understanding the effects of multicollinearity. To be more precise, we have used GLMs to elucidate the relationships among the mean of VIF_k (denoted as $\overline{\text{VIF}}$), the deviation C in the regression coefficients of the constructed regression model, and the deviation B of the estimated values for dependent variables within the same model.

When using the deviation observed in the absence of collinearity as a baseline, we have confirmed that the actual deviation C of the regression coefficients aligns with the value of $\overline{\text{VIF}}$. For instance, if $\overline{\text{VIF}} = 5$, there is a risk that C might be approximately five times the deviation observed in scenarios without collinearity. This remains consistent irrespective of the number of explanatory variables in the regression model; it holds as long as $\overline{\text{VIF}}$ is the same. Conversely, the probability that C in a specific model surpasses the maximum deviation (which represents the 99.9th percentile) observed without collinearity depends on the number of explanatory variables, even if $\overline{\text{VIF}}$ remains the same. For example, when $\overline{\text{VIF}} = 5$ in a model, the likelihoods with two, three, and four explanatory variables are approximately 21.8%, 26.8%, and 30.5%, respectively.

Although $\overline{\text{VIF}}$ cannot explain the deviation B in the estimated values of the dependent variable, we have observed that as the probability of a deviation in the regression coefficient increases, B also tends to increase. Thus, when comparing the extent of impact on estimated values across multiple models, it is vital to understand the probability of a deviation in the regression coefficients rather than merely relying on $\overline{\text{VIF}}$. Such findings can be attributed to the nature of the ordinary least-squares method, indicating that when a regression coefficient deviates significantly from its true value, other coefficients adjust to minimize the residuals.

Most existing metrics for diagnosing the effects of multicollinearity are based on explanatory variables. However, understanding the risk of multicollinearity solely from these metrics is challenging. Alin (2010) stated that, to genuinely comprehend

the real impact, it is essential to consider the variation in the actual deviations. Thus, both analytical and numerical approaches are required.

In this study, through numerical experiments, we have empirically demonstrated that the shape parameter k^{*1} from the GLM provides valuable information for model selection. More specifically, we showed that the variability in the deviations of regression coefficients can be expressed as differences in the probability distribution for each \overline{VIF} and is manifested in the gamma distribution. Additionally, the differences in the probability distribution for each \overline{VIF} are governed by the shape parameter k^{*1} of the gamma distribution. We have proposed a method for understanding the likelihood of observing deviations which, in the absence of multicollinearity, are almost negligible (occurring with only a 1/1000 probability), by referring to both the \overline{VIF} derived from explanatory variables and the shape parameter k^{*1} . Furthermore, we have provided numerical guidelines for the shape parameter k^{*1} across seven different conditions, each distinguished by different numbers of explanatory variables and variations in other parameters.

There are countless combinations of the number of explanatory variables and potential correlations among them. The numerical benchmarks (shape parameter k^{*1}) offered in this study for the seven conditions might not suffice. Moreover, this study has not accounted for the impacts of linear relationships among multiple variables. The methodology used for generating variables might also influence the estimated value of the shape parameter k^1 . Therefore, refining and presenting a more precise shape parameter k^{*1} will be addressed in future research. An additional future challenge is to formulate the relationship between the number of explanatory variables used in the regression model and the shape parameter k^1 , with the aim of providing a more widely applicable diagnostic method.

In recent years, available computational resources have expanded rapidly, enhancing our ability to understand the full scope of the impacts of multicollinearity. With these advanced resources, it will be possible to clearly present the probability of deviations and the effects on the estimated values of dependent variables, based on the explanatory variables. This will enable technicians and researchers building hedonic models to choose those that are better aligned with their objectives, supported by clearer reasoning.

References

- Alin A (2010) Multicollinearity. Wiley Interdiscip Rev Comput Stat 2(3):370–374. <https://doi.org/10.1002/wics.84>
- Asteriou D, Hall SG (2007) Applied econometrics: a modern approach using EViews and Microfit (Rev. ed). Palgrave Macmillan. <http://ci.nii.ac.jp/ncid/BA81825890.bib>
- Chatterjee S, Hadi AS (2006) Regression analysis by example, 4th edn. Wiley-Interscience. <http://ci.nii.ac.jp/ncid/BA78320728>
- Deaton BJ, Hoehn JP (2004) Hedonic analysis of hazardous waste sites in the presence of other urban disamenities. Environ Sci Pol 7(6):499–508. <https://doi.org/10.1016/j.envsci.2004.08.003>

- Heikkila E (1988) Multicollinearity in regression models with multiple distance measures. *J Reg Sci* 28(3):345–362. <https://doi.org/10.1111/j.1467-9787.1988.tb01087.x>
- Kutner M, Nachtsheim C, Neter J, Li W (2005) Applied linear statistical models. McGraw-Hill Irwin. <https://books.google.co.jp/books?id=OHqBQgAACAAJ>
- Minotani C (2015) Series statistics library, linear regression analysis (in Japanese). Asakura Publishing Co., Ltd
- Rosen S (1974) Hedonic prices and implicit markets: product differentiation in pure competition. *J Polit Econ* 82(1):34–55. <https://doi.org/10.1086/260169>
- Silverman BW (1986) Density estimation for statistics and data analysis. Chapman and Hall
- Witte AD, Sumka HJ, Erikson H (1979) An estimate of a structural hedonic price model of the housing market: an application of Rosen's theory of implicit markets. *Econometrica* 47(5):1151–1173. <https://doi.org/10.2307/1911956>
- Yoo W, Mayberry R, Bae S, Singh K, He Q, Lillard JW (2014) A study of effects of multicollinearity in the multivariable analysis. *Int J Appl Sci Technol* 4(5):9–19. <http://www.ncbi.nlm.nih.gov/pmc/articles/PMC4318006/>
- Yoshida M (1987) Multicollinearity and ridge regression in regression analysis. 13:227–242. <https://doi.org/10.18910/9749>

Chapter 12

Theoretical Relationships Between Building Setback, Plot Frontage, and Plot Depth in Terms of Road and Building Densities



Hiroyuki Usui and Yasushi Asami

Abstract A theoretical investigation into the relationships between building setback, plot frontage, and plot depth in terms of building density (number of buildings per unit area) and road-network density (total length of road networks per unit area) is sparsely documented. Hence, in this study, we constructed a mathematical model to analyze the above relationship and maximize the average plot frontage. We found that (1) the average plot frontage is inversely proportional to the gross building density and is a convex upward quadratic function of the road-network density; (2) the average plot depth and setback allowance do not depend on the building density and are a monotonically decreasing function of the road-network density; and (3) the ratio of average plot depth to frontage is proportional to the gross building density and is a monotonically decreasing function of the road-network density. Based on the above findings, we developed a criterion for determining whether the average plot frontage is longer than the average plot depth. Further, the model was validated via an empirical analysis of the Tokyo metropolitan region. The results revealed that the modes of the average plot frontage, average plot depth, and ratio of plot depth to frontage were 11 m, 16 m, and 1.4, respectively. The mode of setback allowance was 5 m. The ratio of building setback to the setback allowance was in the range 0.4–0.6, which indicated that typically approximately half of the allowance is assigned to building setback. The findings of this study will provide urban planners and practitioners with a firm theoretical foundation for understanding the relationship between building setbacks, plot shape, building density, and road-network density in the district scale.

The contents of this paper are based on the following paper originally published in a Japanese journal: Usui, H. and Asami, Y. (2011) Setback distance and density of buildings and roads. *Journal of City Planning Institute of Japan* 46(3): 829–834 (in Japanese).

H. Usui (✉) · Y. Asami

Department of Urban Engineering, The University of Tokyo, Tokyo, Japan
e-mail: usui@ua.t.u-tokyo.ac.jp; asami@csis.u-tokyo.ac.jp

Keywords Building density · Road-network density · Plot frontage · Plot depth · Ratio of plot depth to frontage · Building setback

12.1 Introduction

Urban spaces primarily consist of buildings and roads (Hillier and Hanson 1989; Kropf 2018; Oliveira 2016). The boundaries between building and road spaces in Western and Japanese cities are discernibly different from each other (Ashihara 1986). Western cities have distinct boundaries between building and road spaces because the buildings along streets have well-defined outlines. However, in Japanese cities, this demarcation tends to be ambiguous because the outlines of the buildings along streets often lack precise definition (Ashihara 1986). The ambiguity in the demarcation between building and road spaces characterizes the physical urban form of Japanese cities (Maki 1980).

The ambiguity between building and road spaces in current Japanese cities can be attributed to the Japanese building-form regulations. In Japan, a building form is governed by land-use zoning regulations, namely the maximum building coverage ratio (BCR) and floor area ratio (FAR) for a given plot. BCR is defined as the maximum ratio of the building area to the plot area, and FAR is defined as the maximum ratio of the total floor area of a building to the area of the plot. The maximum BCR and FAR are legally established in the Japanese building codes and the City Planning Act. Such building-form regulations are called *indirect building-form regulations* because they do not directly determine the building form. Furthermore, building façades are often not aligned with their adjacent front roads, which blurs the boundary between the building and road spaces.

However, building forms in Western cities (for example, cities in France and Germany) are directly controlled by *direct building-form regulations* that mandate guidelines regarding building façade locations and heights according to the proportion of building height, front road width, and building setbacks (Marshall 2011). Although building façades must be aligned with a legally established building line (road perimeter), an adherence to a maximum BCR and FAR is not legally required and is followed only if necessary (Wada 2007). Direct building-form regulations ensure that buildings maintain a uniform height and their facades align with the building lines. However, the close relationship between building façades and roads, as commonly observed in traditional Western cities, has gradually disappeared in modern Western cities since the publication of Buchan's report *Traffic in Towns* (Marshall 2005).

In this study, the ambiguity in the demarcation between building and road spaces in a 2D plane is quantified as the building setback, which is defined as the distance between the façade of a building and the edge of its front road. A comparison between the building-form regulations in Japanese and traditional Western cities indicates that the ambiguous demarcations between building and road spaces in current Japanese cities can be regarded as facilitating an allowance for the building

setback. In the literature, this ambiguity has been compared with international urban planning policies and physical urban forms (e.g., building location patterns and road-network patterns) (Kropf 2018; Marshall 2005, 2009; Oliveira 2016) (see a detailed literature review from Japanese journals in the next section). However, the relationship between the setback allowance, average plot area, and plot shape (plot frontage and plot depth) in a district (a collection of urban blocks encircled by roads and large-scale non-built areas) had not been mathematically formulated until the Japanese version of this paper was published in a journal in 2011 (Usui and Asami 2011). Furthermore, qualitatively, the higher the road-network density, the lower the average plot depth and building setback; however, a quantitative and theoretical investigation involving the derivation of a mathematical formulation describing the above relationship had not been undertaken before 2011.

The objective of this study is to investigate the theoretical and empirical relationship between the building setbacks, average plot depth, plot frontage, and plot size within a district in terms of the building density (the number of buildings per unit area) and road-network density (the total length of road-networks represented as road centerlines per unit area) in the district.

The remainder of this chapter is organized as follows. Previous literature is briefly reviewed in the second section. In the third section, the average plot frontage, plot size, and plot depth are mathematically formulated as functions of building density and road-network density. Subsequently, the average allowance for building setback in a plot is mathematically formulated. In the fourth section, we discuss the application of these formulations to approximately 3000 districts in the Tokyo metropolitan region, statistical distributions of the average plot frontage and depth, and ratio of the average plot depth to plot frontage. Next, the relationship between the average setback allowance and road-network density is theoretically investigated. In addition, the ratio of building setbacks to the allowance is empirically analyzed. The final section concludes this chapter.

12.2 Literature Review

In urban planning, the first step to understand the physical form and environment of urban spaces is to compute building density, road-network density, district BCR (the ratio of the total area of building footprints in a district to the area of the district), and district FAR (the ratio of the total floor area of buildings in a district to the area of the district), for which several appropriate criteria have been proposed (Asami 2001; Koshizuka 1988; Koshizuka and Kotoh 1989). Several methods have been proposed to categorize urban forms into different types at the district scale (e.g., *Space Matrix* (Berghauer-Pont and Haupt 2010) and *Morpho* (Oliveira and Medeiros 2016)). The relationship between urban form and density (BCR, road-network density, and FAR) has been theoretically analyzed (e.g., Berghauer-Pont and Haupt 2007, 2010).

In the literature, the ambiguity between building and road spaces has been studied with respect to the physical urban form (the open space around buildings

and adjacency of buildings to roads). A previous study investigated the theoretical relationship between the open space area around a building—called the effective vacant area—and building density in a district using a simple mathematical model. The results revealed that the effective vacant area decreased as the average building footprint area increased (Koshizuka 1988; Koshizuka and Kotoh 1989).

In addition, Koshizuka (1985) modelled road networks as a set of random lines uniformly distributed on a 2D plane. He found that the average distance from a location to the nearest road network was inversely proportional to the road-network density. As per theoretical analyses, building density and road-network density must be proportional to each other because all buildings are adjacent to their front roads (Koshizuka 1992). Saito (2004) developed an urban form simulation model on the assumption that the lattice density and building location rule are fixed and investigated the changes in the patterns of urban blocks and road networks with respect to the changes in lattice patterns (e.g., grids, triangles, and hexagons).

Asami and Ohtaki (2000) developed a method for predicting the shape of detached houses from the shape of residential plots by introducing an associative memory model. Empirical analyses conducted in a city in the Kanagawa prefecture revealed that the building setback increased with plot depth. On the basis of the above result, several methods have been developed to assess the adjacency of buildings and roads. The methods involve generating buffer domains from the centerlines of road networks, where the optimal buffer distance can be estimated from the inverse square root of building density (Usui and Asami 2010a, b).

12.3 Mathematical Formulation of the Average Plot Frontage, Depth, and Allowance for Building Setback in a District

12.3.1 Semi-Gross Building Density

Consider a district k of area S and perimeter L . Let the number of buildings in the district be n . The gross building density is defined as $\rho_G \equiv n/S$, and the semi-gross building density is defined as

$$\rho_N \equiv n / (S - S_R), \quad (12.1)$$

where S_R is the area of the roads in the district.¹ In this study, all road networks, including those forming the boundary of the district (denoted by ∂L_k), are represented as road centerlines. Assuming that the maximum degree of road intersections

¹ A district area, S , includes non-residential plots such as urban parks and car parking space. However, the plots containing n number of buildings do not include such non-residential plots. Hence, ρ_G and ρ_N are smaller when non-residential plots are not considered than when they are.

(hereafter called intersections) is four, S_R can be formulated as follows:

$$S_R(\Lambda, \bar{w}, v_3, v_4) \equiv \bar{w}\Lambda - \left(\frac{\bar{w}}{2}L + \bar{w}^2 \right) - \left(v_3 \frac{\bar{w}^2}{2} + v_4 \bar{w}^2 \right), \quad (12.2)$$

where Λ denotes the total length of the road networks, v_3 and v_4 denote the number of intersections of degree three and four, respectively, and \bar{w} denotes the average road width. In Eq. (12.2), the second term on the right-hand side is the area of the road network that forms the boundary of the district but is not included in the district. The third term represents the area of the intersections, which is subtracted to avoid counting it twice.

Intersections of degrees three and four are classified into (1) those inside the district and (2) those on the road network forming the boundary of the district. In the former case, the number of intersections of degree three and four are denoted by $v_{3\text{in}}$ and v_4 , respectively. Assuming that all roads extending beyond the district are omitted, all intersections of degree four in the latter case can be regarded as those of degree three. The number of intersections of degree three in the latter case is denoted as $v_{3\text{peri}}$.

Using this notation, Eq. (12.2) can be rewritten as follows:

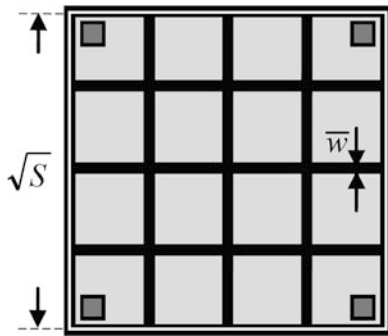
$$\begin{aligned} S_R(\Lambda, \bar{w}, v) &\equiv \bar{w}\Lambda - \left(\frac{\bar{w}}{2}L + \bar{w}^2 + \frac{\kappa_3 + 2\kappa_4}{2}v\bar{w}^2 \right) \\ &= \bar{w}\Lambda - \left\{ \frac{\bar{w}}{2}L + (1 + cv)\bar{w}^2 \right\}, \end{aligned} \quad (12.3)$$

where $v_3 = v_{3\text{in}} + v_{3\text{peri}}$ and $v \equiv v_3 + v_4$. Additionally, $\kappa_3 \equiv v_3/v$ and $\kappa_4 \equiv v_4/v$ denote the ratio of the number of intersections of degree three and four, respectively, to the sum of the number of both intersections, and $c \equiv (\kappa_3 + 2\kappa_4)/2$; $c \in [0.5, 1]$. If $v = v_3$, then $c = 0.5$. If $v = v_4$, then $c = 1$. Using Eq. (12.3), Eq. (12.1) can be rewritten as follows:

$$\begin{aligned} \rho_N &= \frac{n}{S - \bar{w}\Lambda + \left\{ \frac{\bar{w}}{2}L + (1 + cv)\bar{w}^2 \right\}} \\ &= \frac{n}{S} \cdot \frac{1}{1 - \bar{w} \left\{ \frac{\Lambda}{S} - \frac{1}{2} \cdot \frac{L}{S} - \frac{(1+cv)}{S} \bar{w} \right\}} \\ &= \rho_G \frac{1}{1 - \bar{w} \left\{ \frac{\Lambda}{S} - \frac{1}{2} \cdot \frac{L}{S} - \frac{(1+cv)}{S} \bar{w} \right\}}. \end{aligned} \quad (12.4)$$

The adjacency of a building plot to its front road is not explicitly considered in Eq. (12.4). To address this issue, it is assumed that a building plot has no more than one building, which is termed *the rule of one plot for one building*. This rule has advantages and disadvantages. The rule does not hold true, for example, when the use of two buildings on a lot is inseparably related to one another. Nevertheless, the assumption of the rule can help overcome data limitations regarding plot shapes. Under this assumption, the number of building plots is equal to n .

Fig. 12.1 A district modeled as a square of edge length \sqrt{S} . It is composed of a square grid of $m \times m$ urban blocks, where m denotes the number of urban blocks along one edge of the square. The white lines show the centerlines of the road networks forming the edges of the square



12.3.2 Average Plot Frontage as the Function of Building Density and Road-network Density

Assuming the rule of one plot per building and that all plots are adjacent to their front roads, the relationship between building density and road-network density was theoretically investigated using the average plot frontage in the district. As illustrated in Fig. 12.1, the district is modeled as a square of edge length \sqrt{S} , and it is composed of a square grid of $m \times m$ urban blocks, where m denotes the number of urban blocks along one edge of the square. The white lines show the centerlines of the road networks that form the edges of the square.

The total perimeter of the urban blocks can be formulated using m , \sqrt{S} , and \bar{w} as follows:²

$$B \equiv 4 \frac{\sqrt{S} - m\bar{w}}{m} m^2 = 4m (\sqrt{S} - m\bar{w}). \quad (12.5)$$

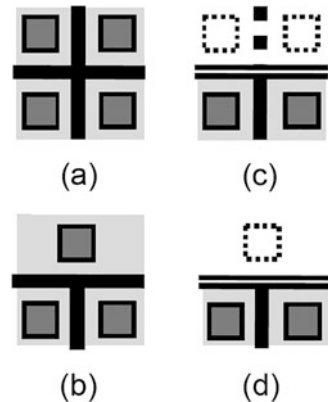
Because the relationship between A and m is formulated as $A = 2(m + 1)\sqrt{S}$, Eq. (12.5) can be rewritten as a function of A as follows:

$$B = 2\sqrt{S} \left(\frac{A}{\sqrt{S}} - 2 \right) - \left(\frac{A}{\sqrt{S}} - 2 \right)^2 \bar{w}. \quad (12.6)$$

To compute the average plot frontage, the number of plots facing a street in the district, n_F , is expressed in terms of n , v , and c . Inside the district, the numbers of corner plots and plot edges facing an intersection of degree four are four and eight, respectively. Hence, the numbers of corner plots and plot edges facing the total number of intersections of degree four are $4v_4$ and $2 \times 4v_4 = 8v_4$, respectively (see Fig. 12.2a). By contrast, one plot and two corner plots face an intersection of degree three inside the district; therefore, the number of plot edges facing an

² B is equivalent to the total plot frontage in the district.

Fig. 12.2 Number of corner plots and the plot frontages:
 (a) corner plots facing an intersection of degree four inside a district, (b) corner plots facing an intersection of degree three inside a district, (c) corner plots facing an intersection of degree four on the perimeter of a district, (d) corner plots facing an intersection of degree three on the perimeter of a district



intersection of degree three is five. Hence, the numbers of plots and plot edges facing the total number of intersections of degree three inside the district are $3v_{3_{in}}$ and $1 \times v_{3_{in}} + 2 \times 2v_{3_{in}} = 5v_{3_{in}}$, respectively (see Fig. 12.2b). The number of corner plots facing an intersection of degree three on the boundary of the district is two, and the corresponding number of plot edges is four. Hence, the numbers of corner plots and plot edges facing the total number of intersections of degree three on the boundary of the district are $2v_{3_{peri}}$ and $4v_{3_{peri}}$, respectively (see Fig. 12.2c,d). Therefore, n_F can be formulated as follows:

$$\begin{aligned}
 n_F &= 8v_4 + 5v_{3_{in}} + 4v_{3_{peri}} + \{(n+4) - (4v_4 + 3v_{3_{in}} + 2v_{3_{peri}})\} \\
 &= (n+4) + 4v_4 + 2v_3 \\
 &= (n+4) + (2\kappa_4 + \kappa_3)v \\
 &= n + 4(1 + cv),
 \end{aligned} \tag{12.7}$$

where $(n+4) - (4v_4 + 3v_{3_{in}} + 2v_{3_{peri}})$ is the number of plot edges not facing any intersections. Because the corner plots facing the vertices of the square have two edges each facing the vertices, four was added to the right-hand side of Eq. (12.7).

Using Eqs. (12.6) and (12.7), the average plot frontage in the square district is formulated as shown below.

$$\begin{aligned}
 \bar{F} &\equiv \frac{B}{n_F} = \frac{S}{n} \cdot \frac{n}{n_F} \left\{ 2 \left(\frac{\Lambda}{S} - \frac{2}{\sqrt{S}} \right) - \left(\frac{\Lambda}{S} - \frac{2}{\sqrt{S}} \right)^2 \bar{w} \right\} \\
 &\approx \frac{1}{\rho_G} \cdot \frac{n}{n_F} \lambda (2 - \bar{w}\lambda), \text{ if } \frac{2}{\sqrt{S}} \ll \frac{\Lambda}{S},
 \end{aligned} \tag{12.8}$$

where $\lambda \equiv \Lambda/S$ denotes road-network density and n_F/n can be regarded as a constant; from empirical analyses in the Tokyo metropolitan region, $n_F/n \simeq 1.2$. Hence, \bar{F} can be regarded as a function of three variables: road-network density, gross building density, and average road width. The average plot frontage is inversely proportional to the gross building density and is a convex upward quadratic function of the road-network density. Therefore, there exists a λ^* that maximizes \bar{F} .

$$\bar{F}_{\max} = \frac{n}{n_F} \cdot \frac{S}{n\bar{w}} = \frac{n}{n_F} \cdot \frac{1}{\bar{w}\rho_G}. \quad (12.9)$$

$$\lambda^* = \frac{1}{\bar{w}} + \frac{2}{\sqrt{S}} \approx \frac{1}{\bar{w}}. \quad (12.10)$$

If $\lambda < \lambda^*$, then increasing λ increases the average plot frontage. Otherwise, increasing λ decreases the average plot frontage. In addition, Eqs. (12.9) and (12.10) show that (1) \bar{F}_{\max} is inversely proportional to ρ_G , \bar{w} , and n_F/n , and (2) λ^* is inversely proportional to \bar{w} .

\bar{F} in Eq. (12.8) can be regarded as a three-variable function that characterizes the number of buildings and roads in a district. If the infimum of \bar{F} , denoted by \bar{F}_{\inf} , is a policy variable and the number of roads in a district (λ and \bar{w}) is fixed, the supremum of ρ_G can be computed using λ , \bar{w} , and $n_F/n (\simeq 1.2)$ as follows:

$$\rho_G \leq \frac{1}{\bar{F}_{\inf}} \cdot \frac{n}{n_F} \lambda (2 - \bar{w}\lambda) = \sup \rho_G. \quad (12.11)$$

As $\sup \rho_G$ is regarded as a convex upward quadratic function of λ , there exists a λ^{**} that maximizes $\sup \rho_G$ as follows:

$$\max \sup \rho_G = \frac{n}{n_F} \cdot \frac{1}{\bar{w}\bar{F}_{\inf}}, \quad (12.12)$$

$$\lambda^{**} = \lambda^*. \quad (12.13)$$

If $\lambda < \lambda^{**}$, then increasing λ increases $\sup \rho_G$. Otherwise, increasing λ decreases $\sup \rho_G$. Eqs. (12.12) and (12.13) imply that an optimal road-network density exists that maximizes the gross building density, satisfying $\bar{F} \geq \bar{F}_{\inf}$.

12.3.3 Average Plot Depth and Average Plot Depth to Frontage Ratio

The average plot size is given by the inverse of the semi-gross building density, ρ_N .

$$\begin{aligned}\bar{s} &\equiv \frac{1}{\rho_N} = \frac{S}{n} \left[1 - \bar{w} \left\{ \frac{\Lambda}{S} - \frac{1}{2} \cdot \frac{L}{S} - \frac{(1+cv)}{S} \bar{w} \right\} \right] \\ &= \frac{1}{\rho_G} \left[1 - \bar{w} \left\{ \lambda - \frac{1}{2} \cdot \frac{L}{S} - \frac{(1+cv)}{S} \bar{w} \right\} \right].\end{aligned}\quad (12.14)$$

Assuming that the plot frontage and depth are independently distributed, the average plot depth can be approximated to \bar{s}/\bar{F} as follows:

$$\begin{aligned}\bar{D} &\approx \frac{\bar{s}}{\bar{F}} = \frac{\frac{S}{n} \left[1 - \bar{w} \left\{ \frac{\Lambda}{S} - \frac{1}{2} \cdot \frac{L}{S} - \frac{(1+cv)}{S} \bar{w} \right\} \right]}{\frac{S}{n} \cdot \frac{n}{n_F} \left\{ 2 \left(\frac{\Lambda}{S} - \frac{2}{\sqrt{S}} \right) - \left(\frac{\Lambda}{S} - \frac{2}{\sqrt{S}} \right)^2 \bar{w} \right\}} \\ &= \frac{n_F}{n} \cdot \frac{1 - \bar{w} \left\{ \lambda - \frac{1}{2} \cdot \frac{L}{S} - \frac{(1+cv)}{S} \bar{w} \right\}}{\left\{ 2 \left(\lambda - \frac{2}{\sqrt{S}} \right) - \left(\lambda - \frac{2}{\sqrt{S}} \right)^2 \bar{w} \right\}} \\ &\approx \frac{n_F}{n} \cdot \frac{1 - \bar{w} \left\{ \lambda - \frac{1}{2} \cdot \frac{L}{S} - \frac{(1+cv)}{S} \bar{w} \right\}}{\lambda (2 - \bar{w} \lambda)}, \text{ if } \frac{2}{\sqrt{S}} \ll \frac{\Lambda}{S}.\end{aligned}\quad (12.15)$$

The validity of this assumption has been confirmed empirically in previous studies (Usui 2019; Usui and Asami 2013). Assuming the rule of one plot for one building and that all plots are adjacent to their front roads, Eq. (12.15) implies that the average plot depth depends not on building density but on λ , intersection density (v/S), \bar{w} , and $n_F/n (\simeq 1.2)$.

The ratio of average plot depth to frontage is defined as follows:

$$\begin{aligned}\gamma &\equiv \frac{\bar{D}}{\bar{F}} = \rho_G \left(\frac{n_F}{n} \right)^2 \frac{1 - \bar{w} \left\{ \frac{\Lambda}{S} - \frac{1}{2} \cdot \frac{L}{S} - \frac{(1+cv)}{S} \bar{w} \right\}}{\left(\frac{\Lambda}{S} - \frac{2}{\sqrt{S}} \right)^2 \left\{ 2 - \left(\frac{\Lambda}{S} - \frac{2}{\sqrt{S}} \right) \bar{w} \right\}^2} \\ &\approx \rho_G \left(\frac{n_F}{n} \right)^2 \frac{1 - \bar{w} \left\{ \lambda - \frac{1}{2} \cdot \frac{L}{S} - \frac{(1+cv)}{S} \bar{w} \right\}}{\lambda^2 (2 - \bar{w} \lambda)^2} = \rho_G C(\lambda), \text{ if } \frac{2}{\sqrt{S}} \ll \frac{\Lambda}{S}.\end{aligned}\quad (12.16)$$

Because $C(\lambda) \equiv \left(\frac{n_F}{n}\right)^2 \frac{1-\bar{w}\left\{\lambda - \frac{1}{2} \cdot \frac{L}{S} - \frac{(1+c\gamma)\bar{w}}{S}\right\}}{\lambda^2(2-\bar{w}\lambda)^2}$ is a monotonically decreasing function of λ , (1) increasing ρ_G increases γ , and (2) increasing λ decreases γ . In addition, the dimensional analysis of Eq. (12.16) implies that, because γ is a dimensionless quantity, $C(\lambda)$ must have two dimensions in length; if the other variables are fixed, $C(\lambda)$ can be regarded as the gross average plot size determined by the road-network density. Moreover, if $\gamma < 1$ (i.e., $1/\rho_G < C(\lambda)$), then $\bar{F} > \bar{D}$. Otherwise, $\bar{F} < \bar{D}$. Therefore, $C(\lambda)$ can be used to determine which of \bar{F} and \bar{D} is smaller.

12.3.4 Average Allowance for Building Setback

The average allowance for building setback in a plot is mathematically formulated assuming that (1) the building footprint and its plot are rectangular in shape and similar to each other and (2) the BCR in each plot is the district BCR, denoted by $\mu \equiv S_B/(S - S_R)$, where S_B is the total area of the building footprints. As illustrated in Fig. 12.3, the building frontage and depth that satisfy Eqs. (12.17) and (12.18) can be defined as the typical building frontage, \bar{F}_B , and typical building depth, \bar{D}_B , respectively.

$$\mu \bar{F} \bar{D} = \bar{F}_B \bar{D}_B. \quad (12.17)$$

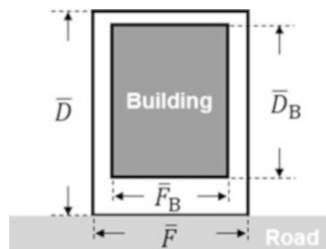
$$\frac{\bar{D}_B}{\bar{F}_B} = \frac{\bar{D}}{\bar{F}} = \gamma. \quad (12.18)$$

On solving the above two equations, we obtain $\bar{D}_B = \sqrt{\mu} \bar{D}$. The average allowance for building setback in a plot is defined as

$$\bar{D}_{\text{Free}} \equiv \bar{D} - \bar{D}_B = (1 - \sqrt{\mu}) \bar{D}. \quad (12.19)$$

Equations (12.15) and (12.19) indicate that \bar{D}_{Free} depends not on the gross building density but on the road-network density when the other variables such as μ , v/S , \bar{w} ,

Fig. 12.3 Allowance for building setback in a plot, \bar{D}_{Free} . The building frontage and depth that satisfy Eqs. (12.17) and (12.18) are defined as the typical building frontage, \bar{F}_B , and typical building depth, \bar{D}_B , respectively



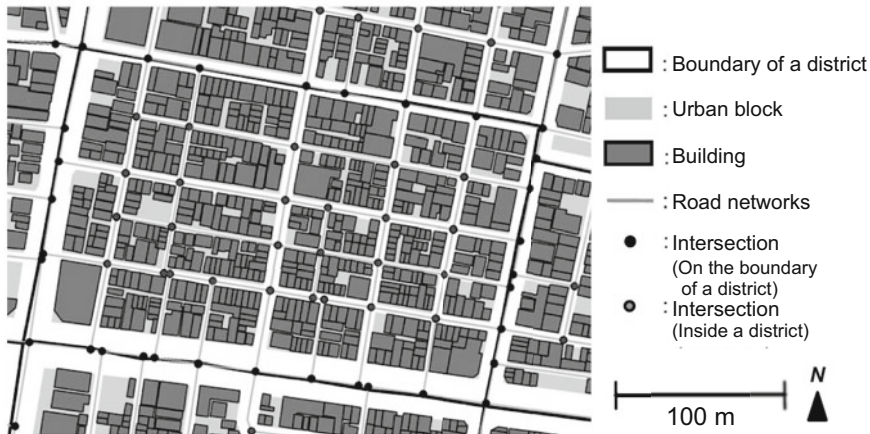


Fig. 12.4 A district in the Tokyo metropolitan region (Torigoe 1 chome). Road networks are modeled as a graph $G = (V, E)$, where $V = \{v_j\}$ denotes a set of nodes representing intersections and $E = \{e_i\}$ denotes a set of edges representing the road segments connecting adjacent intersections

and $n_F/n (\simeq 1.2)$ are regarded as constant. Evidently, $\overline{D}_{\text{Free}}$ is inversely proportional to the square root of μ .

12.4 Empirical Case Analyses in the Tokyo Metropolitan Region

12.4.1 Computing the Empirical Area of the Road Networks

We selected 3115 districts in the Tokyo metropolitan region for the empirical case analysis. Figure 12.4 shows a district in the Tokyo metropolitan region (Torigoe 1 chome: “chome” means the name of district). For each district, n , Λ , v_3 , v_4 , \overline{w} , S_R , and S_B were computed using GIS software (ArcGIS).³,⁴ Hereafter, the software is referred to as GIS. Certain innovative approaches were necessary to compute Λ and $v = v_3 + v_4$ using GIS.

As shown in Fig. 12.4, road networks are modeled as a graph denoted by $G = (V, E)$, where $V = \{v_j\}$ denotes a set of nodes representing the intersections and $E = \{e_i\}$ denotes a set of edges representing the road segments connecting

³ The spatial data used are *Residential Maps* as of 2005 by Zenrin, Co., LTD. for building footprints and *Mapple 10,000 Digital Data* as of 2007 released by Shobunsha Publications, Inc. for road networks.

⁴ Assuming that the maximum degree of intersection is four.

adjacent intersections. A set of polygons representing the urban blocks in the district ($UB = \{UB_k\}$, where UB_k denotes the set of urban blocks in district k) was generated by subtracting the polygons representing roads from the polygon representing the district. In general, ∂L_k and the road networks forming ∂L_k correspond to each other; however, a slight difference between them triggers a significant difference in Λ and v .

To address this issue, the following five-step data processing method must be followed. First, buffer domains are generated from $E = \{e_i\}$. Each buffer domain is denoted by $N(e_i)$, and the buffer distance is computed as the sum of [width of e_i]/2 and $0.35/\sqrt{\rho_G}$ (Usui and Asami 2010a). Second, e_i is considered a part of ∂L_k if $N(e_i)$ includes some parts of ∂L_k , denoted by $N(e_i) \cap \partial L_k \neq \emptyset$. The set of edges satisfying $N(e_i) \cap \partial L_k \neq \emptyset$ is denoted by $E' \equiv \{e_i | N(e_i) \cap \partial L_k \neq \emptyset\}$. Third, a set of edges satisfying the condition $N(e_i) \cap \partial L_k = \emptyset$ is denoted by $E'' \equiv \{e_i | N(e_i) \cap \partial L_k = \emptyset\} = E - E'$ and decomposed as $E'' = \bigcup_k E'_k$, where E'_k denotes the subset of edges satisfying $N(e_i) \cap \partial L_k = \emptyset$ in district k . Fourth, the number of nodes $v_j \in V$ on E'_k is computed and represented as v . Finally, the total length of edges representing the road segments satisfying the condition $N(e_i) \cap UB_k \neq \emptyset$, including the road networks forming ∂L_k , is computed as Λ . The average road width \bar{w} , in a district is then computed as shown below:

$$\bar{w} \equiv \sum_h w_h \Lambda_h / \Lambda, \quad (12.20)$$

where w_h and Λ_h denote the width and total length of the edges of the road whose class of road width is h , respectively.

The scatter plot shown in Fig. 12.5 (left) illustrates the relationship between $S_R(\Lambda, \bar{w}, v)$ (given by Eq. (12.3)) and S_R computed using GIS. S_R was estimated by measuring the areas common to the polygon representing the district and those representing the roads. As can be observed from the figure, S_R tends to be lower than $S_R(\Lambda, \bar{w}, v)$. Fig. 12.5 (right) shows the relative frequency distribution of $S_R/S_R(\Lambda, \bar{w}, v) \equiv r$. The average and standard deviation of r are 0.86 and 0.17, respectively. We found that (1) the relative frequency distribution of r is unimodal, and (2) its mean and mode are almost equal.

S_R was lower than $S_R(\Lambda, \bar{w}, v)$ because we treated the width of the roads forming the boundary of the district ∂L_k inappropriately. As can be observed from Fig. 12.4, (1), approximately half of the area of roads forming ∂L_k is not included in district k , and (2) the width of the roads forming ∂L_k tends to be wider than those inside district k . The former was considered for computing $S_R(\Lambda, \bar{w}, v)$ by incorporating the second term on the right-hand side of Eq. (12.3). Because the width of the roads forming ∂L_k tends to be wider than those inside the district, $S_R \simeq 0.86 S_R(\Lambda, \bar{w}, v)$ on average. This property should be considered when estimating S_R from $S_R(\Lambda, \bar{w}, v)$. Hence, it was not $S_R(\Lambda, \bar{w}, v)$ but S_R that we adopted to compute \bar{F} , \bar{D} , and γ in empirical analyses.

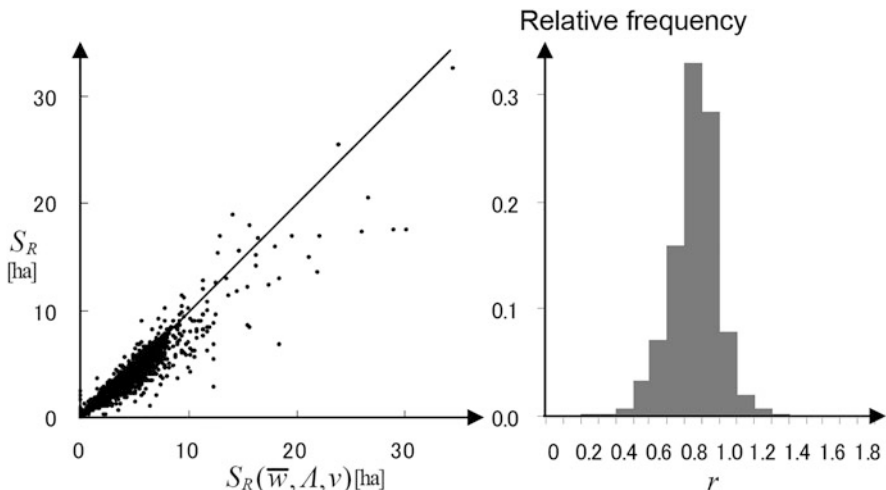


Fig. 12.5 Relationship between $S_R(A, \bar{w}, v)$ and S_R (left) and the relative frequency distribution of $S_R/S_R(A, \bar{w}, v) = r$ (right)

12.4.2 Frequency Distribution of the Average Plot Frontage, Depth, and the Average Plot Depth to Frontage Ratio and Their Geographical Distribution in Tokyo

Figure 12.6 (top) shows the frequency distribution of the average plot frontage, \bar{F} , and average plot depth, \bar{D} , in the districts of the Tokyo metropolitan region. Evidently, (1) the two distributions are unimodal, and (2) the modes of \bar{F} and \bar{D} are 11 m and 16 m, respectively. Figure 12.6 (bottom) shows the frequency distribution of the ratio of average plot depth to frontage, γ , in the districts of the Tokyo metropolitan region. As can be observed, this distribution is also unimodal and the mode of γ is 1.4. This implies that, on average, plot depth tends to be higher than plot frontage in the Tokyo metropolitan region.⁵

The geographical distribution of γ over the districts in the Tokyo metropolitan region is shown in Fig. 12.7. As can be observed, the plot frontage tends to be higher than the plot depth in the districts surrounding the center of the Tokyo metropolitan region (defined as the Tokyo central station). By contrast, the plot depth tends to be higher than the plot frontage in districts that are 5–10 km away from the Tokyo central station.

⁵ Considering plots not adjacent to their front roads, \bar{F} computed using Eq. (12.8) is smaller than the observed value. \bar{D} computed using Equation (12.15) is higher than the observed value because $\bar{D} = \bar{s}/\bar{F}$, and γ computed using Equation (12.16) is higher than the observed value because $\gamma = \bar{s}/\bar{F}^2$.

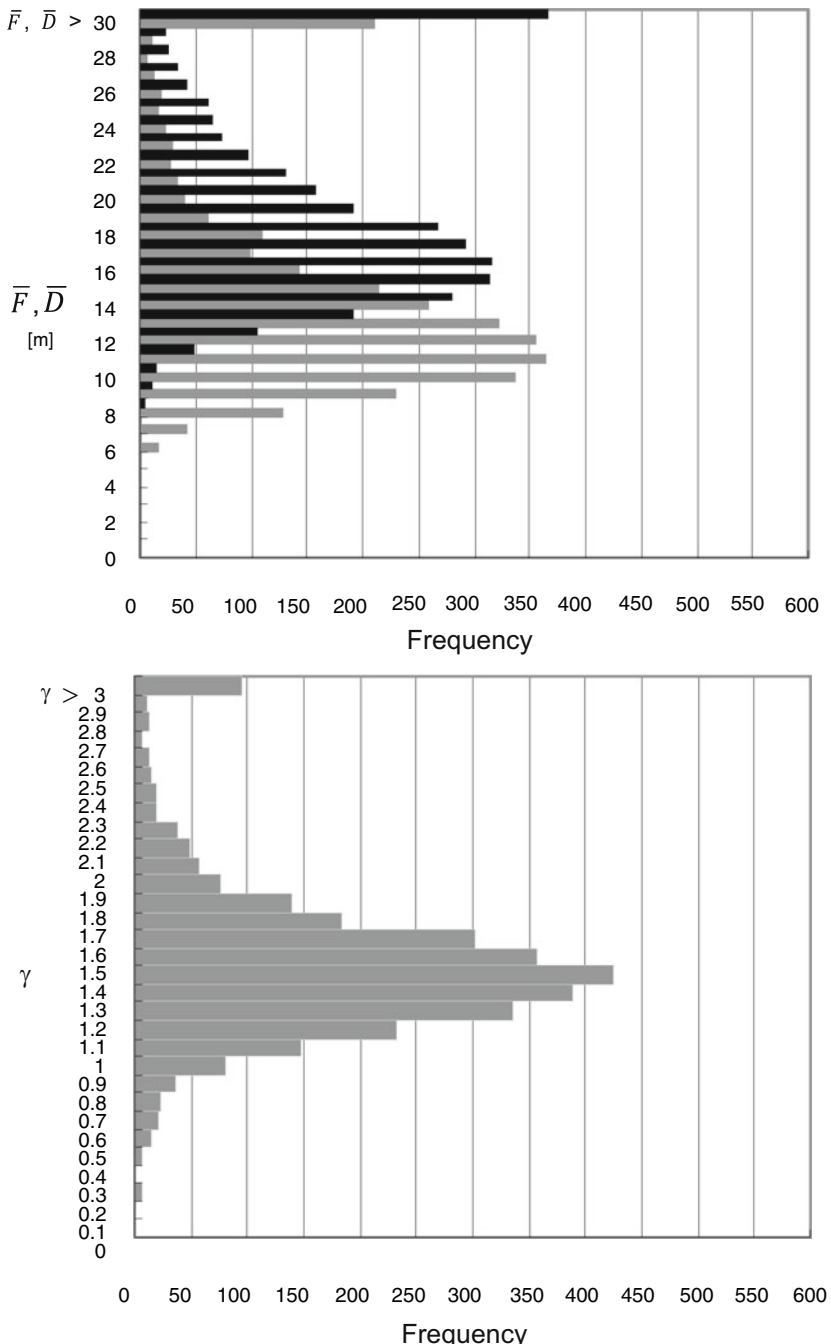


Fig. 12.6 Frequency distribution of the average plot frontage, \bar{F} , (gray) and average plot depth, \bar{D} , (black) (top) and the frequency distribution of the ratio of average plot depth to frontage, γ , in the district of the Tokyo metropolitan region (bottom)

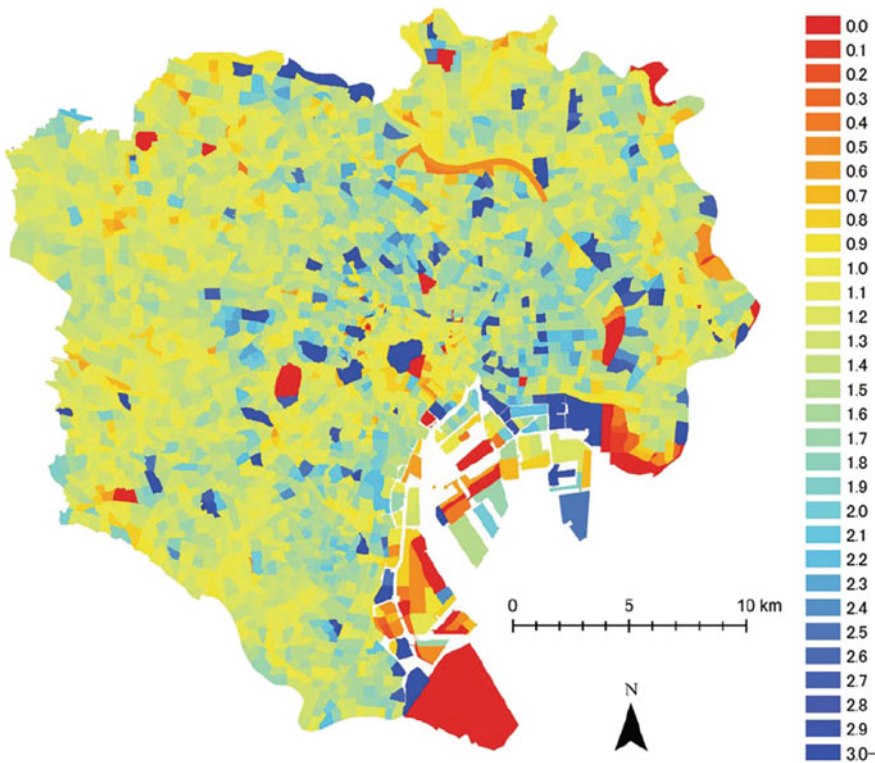


Fig. 12.7 Geographical distribution of γ of each district in the Tokyo metropolitan region

The above empirical findings can be theoretically validated by focusing on the relationship between gross building density and road-network density. Figure 12.8 shows the relationship between road-network density λ and $C(\lambda)$, as defined in Eq. (12.16). The black dots represent the value of $C(\lambda)$ when the values of the other variables in $C(\lambda)$ are the average values over the Tokyo metropolitan region, i.e., $v/S = 45 \text{ ha}^{-1}$, $c = 0.56$, $\bar{w} = 8.7 \text{ m}$, $n_F/n = 1.38$, and $L/S = 124 \text{ m ha}^{-1}$. The gray dots represent the values of $C(\lambda)$ when the values of the other variables are those in each district. Compared to the districts of the Tokyo metropolitan region shown in Fig. 12.4, where $c = 0.70$, the average number of intersections of degree three is higher than those of degree four. The gray dots in Fig. 12.8 are distributed along the black dots.

As mentioned previously, $C(\lambda)$ can be used to determine which of \bar{F} and \bar{D} is smaller in each district. In this respect, Fig. 12.8 shows whether the gross building density is higher compared to the road-network density in terms of the comparative relationship between \bar{F} and \bar{D} in each district. The road-network density in the districts with $\gamma > 1$ is less than the building density. By contrast, the road-network density in the districts with $\gamma < 1$ is higher than the building density.

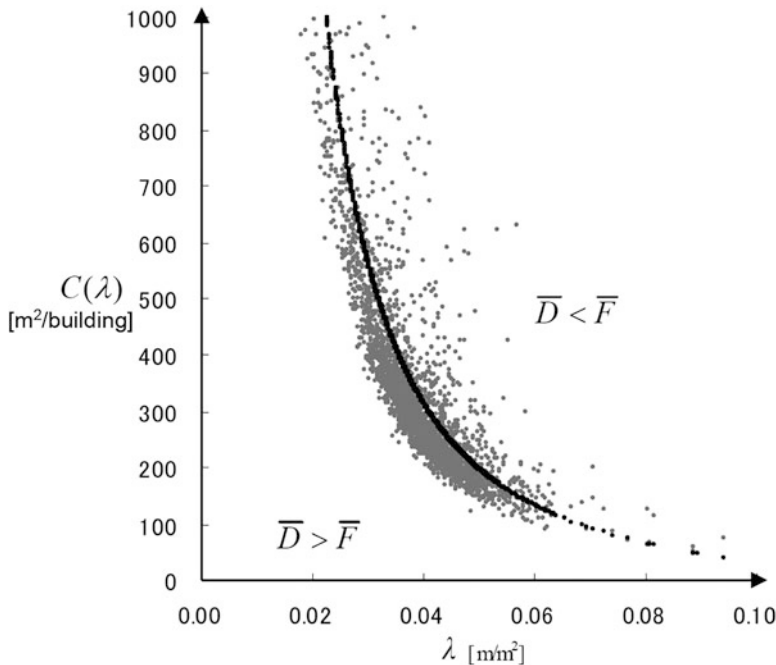


Fig. 12.8 Relationship between the road-network density λ and $C(\lambda)$, as defined in Eq. (12.16). Black dots are the values of $C(\lambda)$ when the values of the other variables in $C(\lambda)$ are their average in the Tokyo metropolitan region, i.e. $v/S = 45 \text{ ha}^{-1}$, $c = 0.56$, $\bar{w} = 8.7 \text{ m}$, $n_F/n = 1.38$, and $L/S = 124 \text{ m ha}^{-1}$. Gray dots are the values of $C(\lambda)$ when the values of the other variables are those in each district

12.4.3 Relationship Between Building Setback and Average Plot Depth in a District

Figure 12.9 shows the relationship between road-network density and \bar{D}_{Free} wherein the values of the variables that constitute \bar{D}_{Free} are the average values in the Tokyo metropolitan region: $v/S = 45 \text{ ha}^{-1}$, $c = 0.56$, $\bar{w} = 8.7 \text{ m}$, $n_F/n = 1.38$, and $L/S = 124 \text{ m ha}^{-1}$. As can be observed (1) \bar{D}_{Free} is a monotonically decreasing function of λ , and (2) as λ increases, the ratio $|\bar{d}\bar{D}_{\text{Free}}/\bar{d}\lambda|$ decreases. This implies that (1) the construction of a road network in districts with low road-network density can effectively decrease \bar{D}_{Free} compared to that in the districts with high road-network density, and (2) relaxing the maximum BCR in each plot can effectively decrease \bar{D}_{Free} in the districts with high road-network density.

Fig. 12.10 shows the frequency distribution of \bar{D}_{Free} in the districts of the Tokyo metropolitan region. It is a unimodal distribution with a mode of 5 m. Interestingly, \bar{D}_{Free} in 33 districts is zero, which implies that the building façades in the districts are aligned with their front roads. The geographical distribution of \bar{D}_{Free} in each district of the Tokyo metropolitan region is shown in Fig. 12.11. As can be observed,

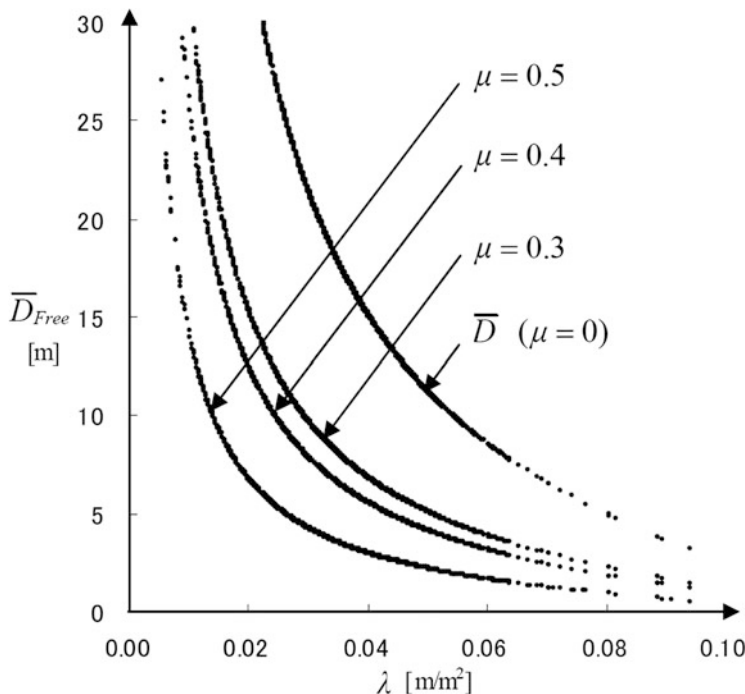


Fig. 12.9 Relationship between the road-network density λ and \bar{D}_{Free} wherein the values of the other variables in \bar{D}_{Free} are the average values in the Tokyo metropolitan region; i.e., $v/S = 45 \text{ ha}^{-1}$, $c = 0.56$, $\bar{w} = 8.7 \text{ m}$, $n_F/n = 1.38$, and $L/S = 124 \text{ m ha}^{-1}$. If $\mu = 0$, $\bar{D}_{\text{Free}} = \bar{D}$

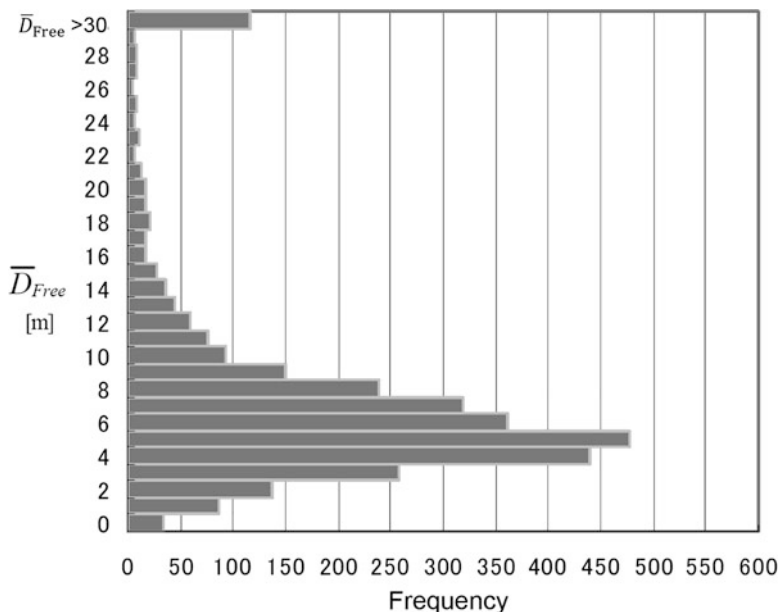


Fig. 12.10 Frequency distribution of \bar{D}_{Free} in the districts of the Tokyo metropolitan region

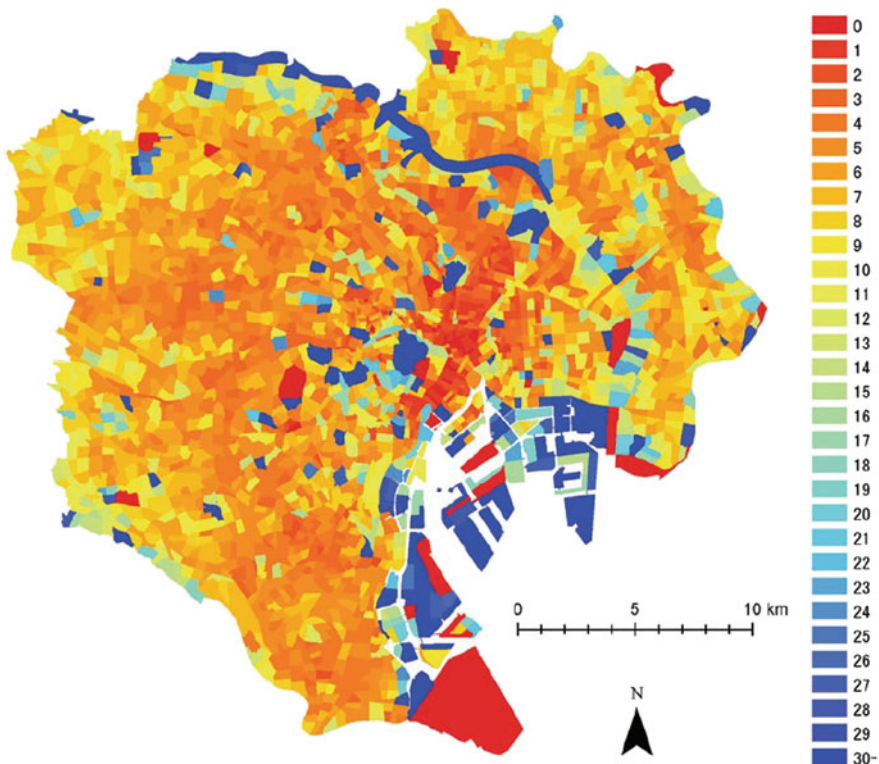


Fig. 12.11 Geographical distribution of \bar{D}_{Free} over the Tokyo metropolitan region

(1) districts with $\bar{D}_{\text{Free}} = 0$ are geographically clustered around the Tokyo central station and where land readjustment projects were carried out after the Great Kanto earthquake in 1923. By contrast, the districts with $\bar{D}_{\text{Free}} \simeq 5$ m are distributed within 5 km from the Tokyo central station.

Finally, the ratio of building setback to \bar{D}_{Free} is empirically analyzed for five districts in the Tokyo metropolitan region. On average, \bar{D}_{Free} in a district can be regarded as the upper limit of the average building setback, denoted by \bar{D}_{SB} .⁶ In a real urban space, \bar{D}_{SB} ranges from zero to \bar{D}_{Free} according to building-form regulations, namely the BCR and FAR. Table 12.1 shows the ratios $\bar{D}_{\text{SB}}/\bar{D}$ and $\bar{D}_{\text{SB}}/\bar{D}_{\text{Free}}$ in the five districts where the edge length of the square plot computed by $1/\sqrt{\rho_G}$ are 10, 12.5, 15, 17.5, and 20 m. For each district, D_{SB} is computed by measuring the building setbacks using the method developed by Usui and Asami (2010a, b). As shown in the fig. (1) $\bar{D}_{\text{SB}}/\bar{D}$ ranges from 0.1 to 0.2, and

⁶ \bar{D}_{Free} includes the minimum setback distance from the edge of an adjacent building plot as stipulated by the article 236 of Japan Civil Code.

Table 12.1 Computation results of $\overline{D}_{\text{SB}}/\overline{D}$ and $\overline{D}_{\text{SB}}/\overline{D}_{\text{Free}}$

District name	ρ_G	λ	\overline{D}_{SB}	$\overline{D}_{\text{Free}}$	\overline{D}	γ	$\overline{D}_{\text{SB}}/\overline{D}$	$\overline{D}_{\text{SB}}/\overline{D}_{\text{Free}}$
Kyojima 3	98.4	482	1.3	2.8	12.1	1.86	0.11	0.46
Sendagi 2	63.4	503	1.7	3.0	13.1	1.33	0.13	0.57
Yushima 3	44.4	461	1.3	2.8	14.1	1.27	0.09	0.46
Kami-shakujii-Minami	32.3	360	3.2	8.3	18.5	1.32	0.17	0.39
Minami-Shinozakicho 2	25.0	411	3.3	7.5	17.6	1.02	0.19	0.44

Note: ρ_G is in ha^{-1} , λ is in m ha^8 , and \overline{D}_{SB} , $\overline{D}_{\text{Free}}$, and \overline{D} are in m

(2) $\overline{D}_{\text{SB}}/\overline{D}_{\text{Free}}$ ranges from 0.4 to 0.6. Therefore, $\overline{D}_{\text{SB}}/\overline{D}$ and $\overline{D}_{\text{SB}}/\overline{D}_{\text{Free}}$ tend to remain stable against the changes in \overline{D} and γ . In addition, irrespective of the values of \overline{D} and γ , the fact that \overline{D}_{SB} is approximately half of $\overline{D}_{\text{Free}}$ is useful in estimating \overline{D}_{SB} from road-network density using Eq. (12.19).

12.5 Conclusion

The objective of this study is to understand the relationship between the allowance for a building setback in its plot, average plot size, and plot shape (plot frontage and plot depth) in a district by theoretically and empirically investigating the relationship in terms of building density and road-network density in a district. We showed that computing the building density and road-network density enables us to compute the average plot size, plot frontage, and plot depth and understand the relationship between the building density, road-network density, and plot shape dimensions. The theoretical and empirical findings of this study will provide urban planners and practitioners with a firm theoretical foundation for understanding the relationship between building setbacks (via allowance for the building setback in its plot), plot shape, building density, and road-network density at the district scale. The study contributes significantly toward understanding the relationship between the part (plot) and whole (district) of physical form of urban space.

Acknowledgment This research was the result of joint research with CSIS, University of Tokyo (No. 785), and used the residential maps provided by Zenrin Co., Ltd.

References

- Asami Y (ed) (2001) Residential environment: methods and theory for the evaluation. University of Tokyo Press
- Asami Y, Ohtaki T (2000) Prediction of the shape of detached houses on residential lots. Environ Plan B Plan Design 27(2):283–295
- Ashihara Y (1986) The hidden order Tokyo through the twentieth century. Chuko Bunko

- Berghäuser-Pont MY, Haupt P (2007) The relation between urban form and density. *Urban Morphol* 11:62–64
- Berghäuser-Pont MY, Haupt P (2010) Spacematrix: space, density and urban form. NAi Publishers
- Hillier B, Hanson J (1989) The social logic of space. Cambridge University Press
- Koshizuka T (1985) On the relation between the density of urban facilities and the distance to the nearest facility from a point in a given area. *J City Plan Inst Japan* 20:85–90. (in Japanese)
- Koshizuka T (1988) A theoretical study on building density as an indicator of urban environments. *J City Plan Inst Japan* 23:19–25. (in Japanese)
- Koshizuka T (1992) Spatial distribution model. In: Architectural Institute of Japan (ed) Analytic models for architecture and urban planning. Inoueshoin, pp 35–50
- Koshizuka T, Kotoh H (1989) Estimations of effective vacant areas by building densities. *J City Plan Inst Japan* 24:337–342. (in Japanese)
- Kropf K (2018) The handbook of urban morphology. John Wiley & Sons
- Maki F (1980) City with a hidden past. Kajima Institute Publishing
- Marshall S (2005) Street & Patterns. Spon Press
- Marshall S (2009) Cities, design and evolution. Routledge, Abingdon
- Marshall S (2011) Urban coding and planning. Routledge
- Oliveira V (2016) Urban morphology: an introduction to the study of the physical form of cities. Springer
- Oliveira V, Medeiros V (2016) *Morpho*: combining morphological measures. *Environ Plan Plan Design* 43(5):805–825
- Saito C (2004) Effect of lattice on urban block pattern and city shape: a study on influence of neighborhood relationships of buildings on urban space. *J City Plan Inst Japan* 39(3):847–852. (in Japanese)
- Usui H (2019) Statistical distribution of building lot depth: theoretical and empirical investigation of downtown districts in Tokyo. *Environ Plan B Urban Analys City Sci* 46(8):1499–1516
- Usui H, Asami Y (2010a) Method for determining buffer distance for judging adjacency of lots to roads. *J Archit Plan* 75(651):1175–1180. (in Japanese)
- Usui H, Asami Y (2010b) Comparison of accuracy of methods of judging adjacency of buildings to roads. *Theory Appl GIS* 18(2):53–62. (in Japanese)
- Usui H, Asami Y (2011) Setback distance and density of buildings and roads. *J City Plan Inst Japan* 46(3):829–834. (in Japanese)
- Usui H, Asami Y (2013) Estimation of mean lot depth and its accuracy. *J City Plan Inst Jpn* 48(3):357–362. (in Japanese)
- Wada H (2007) France no keikan wo yomu: Hozon to kisei no gendai toshikeikaku (understanding landscape in France: modern urban planning for preservation and restrictions of landscape). Kajima Institute Publishing. (in Japanese)

Chapter 13

A Method of Visual Analytics and Data Visualization in Design Context: Case Study of Spatiotemporal Data Visualization of Urban Retail Agglomeration Growth



Akiyoshi Inasaka

Abstract Urban commercial facilities significantly influence neighborhood residents, with changes like store closures disrupting their routines. Especially for the elderly, proximity to these facilities is crucial. Although introducing well-known brands can rejuvenate areas, they might also lead to overcrowding, potentially diminishing the quality of life for locals. It is imperative in urban planning to understand these dynamics and their implications. This chapter delves into the formation of commercial clusters in urban zones and introduces techniques for analyzing and visualizing these trends. Utilizing data from Shibuya Ward, Tokyo, the study demonstrates the efficacy of these methods. The analysis focuses on the expansion direction of commercial clusters using spatiotemporal point data. By tracking when each store opened, the research identifies how new establishments influence the growth trajectory of existing commercial conglomerates. Using a circular statistical method, the study visualizes the expansion of commercial clusters.

Keywords Visualization · Spatiotemporal data · Circular statistics · Retail agglomeration

This contents of this paper are based on the following papers originally published in a Japanese journal: Inasaka, A. and Sadahiro, Y. (2010): A Method of Analysis and Visualization of Expanding Direction of Retail Distribution, *Transactions of AIJ, Journal of Architecture Planning and Environmental Engineering*, Vol.75, No. 650, pp.889–896 (in Japanese). Inasaka, A. (2013): Visualization of Expanding Direction Pattern of Retail Distribution using High Resolution Spatiotemporal Data, *The 36thSymposium on Computer Technology of Information, Systems and Application of Architectural Institute of Japan*, pp.265–268 (in Japanese).

A. Inasaka (✉)

Department of Design, Faculty of Creative Engineering, Chiba Institute of Technology,
Narashino, Chiba, Japan
e-mail: akiyoshi.inasaka@p.chibakoudai.jp

13.1 Introduction

13.1.1 *Urban Events as Manifestations of Urban Activities*

In urban space, many spatial phenomena manifest people's diverse urban activities. These events have various effects on urban activities, affecting other urban activities. Some of these events affect people's daily lives directly or indirectly. In particular, in urban commercial areas, people's daily lives are intermingled with urban activities that are easily influenced by social conditions, such as commercial activities, and the effects of each of these activities are significant. There are two major types of events in urban commercial areas: visible events that can be seen with the naked eye and invisible events that cannot be seen with the naked eye. The first type of invisible phenomenon is typical of each region's unique atmosphere and image. Although invisible to the eye, they are important indicators for people to choose a good place to live or to verify the affinity between the image of a store and that of the local area. They should be understood when people make important decisions about urban activities.

On the other hand, visible events include, for example, various construction activities such as new building construction and remodeling and the accompanying store closings and vacancies. It is necessary to understand exactly how these activities are manifested and positioned in urban planning to create a harmonious streetscape and a convenient commercial area for residents. Thus, urban events are important in all urban activities, including residents' lives and urban planning, and must be accurately understood.

Many of the urban events mentioned above can be grasped and understood to some extent by reading various spatial data provided by government and public agencies, such as numerical maps, census data, various statistical data, data from basic urban planning surveys, and residential maps and telephone directories provided by private companies. In recent years, with the development of information technology and ubiquitous technology, it has become possible to obtain more detailed spatial data on events in a given location than was previously possible, and data that captures time-series changes at the same location has also been developed. However, displaying a large amount of detailed data does not always accurately capture the essential events. For example, a large amount of data may be graphically close together, densely packed, or overlapping, and the essential event that is being captured may be buried. It is necessary to select, aggregate, or transform the information necessary to capture the essence of the event and perform operations to remove excess information (Monmonier and Watanabe 1995 "How to Lie with a Map"). This study defines visualization as displaying information extracted from such operations.

13.1.2 Visualization Methods Using Large Amounts of Spatial Data

Exploratory Spatial Data Analysis (ESA), which utilizes Geographic Information Systems (GIS), has attracted attention in recent years as a method for clarifying phenomena from a large amount of detailed spatial data. Among them, visualization methods are very versatile for two reasons: visualization of information allows for quick and easy verification of more information, and graphical representation allows non-specialists to deepen their understanding of the data intuitively. The graphical representation allows non-specialists to understand the data intuitively (Haining 2003).

Numerous studies have been conducted in various fields on spatial data visualization methods. Here, we will discuss the different types of spatial data and their visualization methods. Specifically, spatial data is divided into low-dimensional spatial data with relatively few attributes and variables ranging from one to three dimensions and high-dimensional spatial data with various variables and attributes of four or more dimensions. The visualization method is organized along two axes: non-spatial visualization, such as graphs and tables of aggregate data, and visualization, in which spatial relationships can be seen on maps. (Table 13.1).

13.1.2.1 Low-dimensional Spatial Data, Non-spatial Visualization

It refers to the visualization of the results of aggregation or statistical processing of data provided in tables, such as census data or various statistical survey data at a certain point in time, by extracting specific attributes or items of the data and visualizing the trends among the data utilizing a numerical line for one-dimensional data, or a two-dimensional or three-dimensional scatter diagram for two-dimensional or three-dimensional data. For one-dimensional data, it is possible to visually capture the trend among the data through a number line. This also applies to histograms, which display data aggregated by section. Methods that belong to this category are used to grasp relationships that do not depend so much on the position of the data as on the attributes of the spatial data or the values of the variables. Since this type of method is generalized and there are abundant research examples, we will not go into detail in this study.

Table 13.1 Organization of existing visualization methods

	Non-spatial	Spatial
Low dimension	Scatterplot, histogram, and	Map, cell, 2D + 3DCG, area cartography Area cartogram
High dimension	Line plot, parallel Coordinate plot)	3DCG, VR, 2D + 3D animation Space syntax

13.1.2.2 High-dimensional Spatial Data, Non-spatial Visualization

This type of data and visualization refers to the visualization of the results of aggregation or statistical processing of comparing various attributes and items and their time-series changes in the census and statistical survey data, as described above. Many of the methods in this category capture the relationships among multiple attributes and variables of data as time-series transitions and changes. For example, in chemistry and physics, data capturing time-series changes of a certain substance, and in statistics, visualization of time-series changes of a certain variable value. In recent years, with the development of information technology, various types of data have become more detailed and voluminous, and the non-spatial visualization methods for low-dimensional spatial data described above are no longer sufficient to handle them. A method for efficiently understanding such multi-attribute and multi-variable data in a unified manner is needed, and many studies have been conducted.

There will be a tool to unify three types of plots: parallel coordinate plots by Gahegan (2005) that capture the variation among variables, scatter plots that look at correlations among multiple attribute variables, and plots that capture distribution trends such as variance, skewness, and kurtosis for each variable's data. (kurtosis) of each variable. As an example of its application, an attempt has been made to display the obtained results on a map (e.g., Theus 2005).

13.1.2.3 Low-dimensional Spatial Data and Spatial Visualization

It targets visualization based on the spatial positional relationship of each data, which the above-mentioned non-spatial visualization methods cannot capture. In addition to the census and statistical data described above, this method is used to visualize spatial data that captures spatial and geographical conditions and characteristics, such as topographic elevation data, road maps, and building maps. Many of these methods are based on maps. This type of research is conducted using GIS in cartography and geovisualization.

A GIS visualizes spatial entities (spatial entity) defined by points, lines, and surfaces, which are composed of five properties: position, shape, attribute, function, and time, with two relations: topology and order (Yan 2003, pp. 26). This section will discuss the visualization of spatial data represented by point, line, and surface events, respectively.

13.1.2.4 Point Event(s)

A representative example of point visualization is John Snow's cholera map, commonly used in epidemiology to display the location of disease outbreaks and the like. This is the first example of spatial analysis in epidemiology and has contributed greatly to the development of spatial analysis in epidemiological

research. In addition to the visualization of the point of occurrence of an event, there are also methods to represent the point of occurrence of an event and the magnitude of the event in terms of points and their magnitudes. For example, research has been conducted on a visualization method called the circle area cartogram, which represents the population distribution in each area by the location and size of circles (Dykes 1998, Inoue and Shimizu 2005, Dykes 2005, etc.). In recent years, the sophistication and generalization of Global Positioning System (GPS) technology have made it possible to record events at various points, and many studies have been conducted on this most primitive spatial visualization method.

13.1.2.5 Linear Event(line)

Next, visualization of linear events is generally used to represent linear elements in space, such as streets and roads, and to visualize the trajectory of an object's movement. Various navigation tools are a typical example of line data visualization that indicates the optimal route from a starting point to a destination based on the input of time required, distance, and other objectives.

Some methods do not preserve actual locations in real space but visualize their topological relationships. For example, many methods use multidimensional scaling (MDS) and graph theory to visualize the relationships among various locations and data by connecting them with lines (Rodger 2005; Robert 2005, etc.).

The axial map, a part of the space syntax originated by Hillier and Hanson (1984), visualizes the spatial connectivity and accessibility of urban space by dividing the street space into line segments. This is an effective visualization method (Kigawa and Furuyama 2004; Kigawa and Furuyama 2005; Kigawa and Furuyama 2006, etc.).

13.1.2.6 Surface

There are two main types of surface data: those expressed in terms of administrative boundaries such as prefecture, municipality, town, street, etc. Many census and statistical survey data are obtained in this way. In many cases, census and statistical survey data are obtained using this method, and each parcel is assigned a value. For example, a choropleth map is commonly used to visualize population data obtained from a census, in which differences in hue, saturation, and lightness of colors represent values. However, there is not necessarily a relationship between the importance of the value to be displayed and the size of the area of each compartment surrounded by administrative boundaries, etc. For example, when a small value is assigned to a large compartment, the overall distribution of the value appears to be small, which greatly affects the appearance of the information. To eliminate such differences as much as possible, there are many studies on the cartogram method, which expresses each value by the size of the area of each parcel while preserving

the spatial positional relationship and the topological shape of each parcel (Inoue and Shimizu 2005, etc.).

In addition, many studies have been conducted using methods that capture events continuously by smoothing point densities and other data using kernel functions. This operation aggregates what cannot be captured by displaying point data alone as a surface. This method is particularly effective for spatiotemporal data and other analyses in which the volume of data is necessarily large (e.g., Sadahiro 2007).

13.1.2.7 High-dimensional Spatial Data and Spatial Visualization

Information has become more abundant in recent years due to advanced information technology, and spatial data is no exception. Therefore, it has become necessary to handle various attributes and variables and their time-series changes simultaneously. Numerous visualization methods have been developed for this purpose. For example, animation methods have been recognized for their importance in visualization research and cartography (Dorling 1992; DiBiase et al. 1992 etc.). As a concrete example, animation is becoming popular as a method to grasp the aspect of change and transition by displaying the numerical change of each position at multiple points in time in a time-series frame-by-frame manner, even if it is not a dynamic object (Inoue et al. 2009, etc.).

With the recent development of remote sensing, GPS, and laser measurement technology in airplanes, wide-area and high-resolution data have become available. This has made it possible to visualize high-resolution 3D urban models (e.g., Yoshikawa 2007a, b). In addition, visualization methods that apply 3D computer graphics and virtual reality technology have become versatile and effective tools for consensus building in urban planning and landscape evaluation (e.g., Amin 2007; Yoshikawa 2007a, b etc.). The methods for capturing physical space have been rapidly improving with the progress of information and computer technology.

On the other hand, research is also being conducted on what is visible but difficult to capture due to the layering and complexity of events. In the aforementioned research related to space syntax, visual simulation methods that consider environmental indicators such as pedestrian distribution, light, wind, and atmospheric flow have been proposed and developed into tools (Takamatsu 2007, Batty 2003 etc.). The method has been used in architectural and urban design (Takamatsu 2007).

As described above, research on visualization has been conducted in various fields, and many of the visualization methods have been developed independently by practitioners and researchers, depending on the events they wish to capture and the attributes and variables they wish to display. The widespread use of GIS has made it easy to analyze data and display the results using a certain set of tools, enabling the capture of a wide range of events. Various general-purpose tools have also been developed by groups such as the GeoVISTA Center at Pennsylvania State University and the Center for Advanced Spatial Analysis (CASA) at University College London. However, both the quality and quantity of spatial data are limited. However, both the quality and quantity of spatial data are increasing daily, and there

is still room for further development of visualization methods due to the diversity and complexity of the data, as well as the complexity of spatial events caused by changes in social conditions.

In light of the above, this study proposes a method for analyzing and visualizing representative spatial data for various events in urban commercial areas, which are the most active in urban space. We focus on visualizing invisible events, latent patterns of events that conventional methods cannot grasp, and the visualization of complex and irregularly changing events.

13.2 Analytical Method and Visualization of the Direction of Commercial Concentration Expansion

13.2.1 *Introduction*

Commercial facilities are an essential part of urban life, and changes in these facilities always have some impact on neighborhood residents. For example, changes such as unexpected store closures in neighborhood shopping areas can disrupt the traditional shopping environment of residents. For the elderly, the commercial facilities they use daily should be located within a short distance from their residences, and this burden may be even greater. While the opening of popular brand-name stores is expected to attract many users and revitalize the surrounding area, there is also concern that the large influx of visitors may cause congestion and other problems that could adversely affect the living environment of residents in the surrounding area. Changes such as the opening and closing of commercial facilities are always occurring in commercial clusters. While such changes can be good for revitalizing the area, they can also significantly impact residents, such as the deterioration of the surrounding residential environment and the decline of the surrounding area due to unjustified development, etc. Therefore, in urban planning and development, it is important to grasp the changes and trends to control them appropriately and accurately. It is necessary to accurately grasp the changes and trends to control them appropriately in urban planning and development.

In light of the above, this chapter focuses on the formation process of commercial clusters in urban areas. It proposes a method for describing, analyzing, and visualizing the trends of changes in these clusters. Section 13.2 proposes a method for describing and analyzing the direction in which commercial clusters expand based on the time when each store in a commercial cluster opens. Section 13.4 describes, analyzes, visualizes, and discusses the results using data from Shibuya Ward, Tokyo, as an empirical analysis to verify the effectiveness of the proposed method. Finally, Section 13.4 summarizes the chapter and discusses future issues.

This chapter was added based on the content of “Analysis Method and Visualization of the Direction of Commercial Agglomeration Expansion” (Inasaka and Sadahiro 2010), which was accepted as a research paper in the Transactions of the Architectural Institute of Japan, Planning Division.

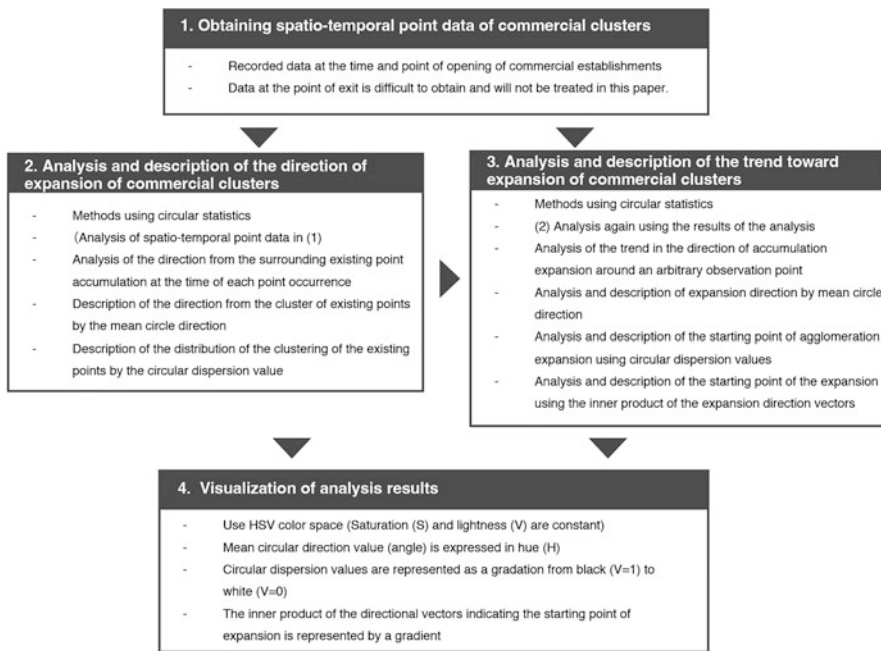


Fig. 13.1 The flow of this section

13.2.2 Analytical Method for Describing the Direction of Expansion of Commercial Clusters

13.2.2.1 Analysis and Description of the Direction of Commercial Agglomeration Expansion Using Spatiotemporal Point Data

Assume that we have spatiotemporal data on existing commercial establishments in a certain region. The location of each commercial facility is represented as a point, and the time when each store opened is recorded. Note that we do not include closed commercial establishments in our analysis since it is often difficult to obtain such information. However, in the “Survey of Establishments and Businesses,”¹ the number of closed and newly opened establishments is almost the same for commercial establishments related to retail, restaurants, and services. New establishments may open in the same location after closing. Therefore, it should be noted that it is necessary to consider the re-filling of commercial clusters, such as new store openings after store closures. In this chapter, we define this data as commercial clusters (Fig. 13.1).

¹ (Note 1) See Statistical Survey of Business Establishments and Enterprises 2004 (Tokyo Metropolitan Government, Table 20, Shibuya Ward). (<http://www.stat.go.jp/data/jigyou/2004/>)

Next, we propose a method for describing the direction in which commercial clusters expand during their formation process. For the above commercial clusters, we analyze in which direction the individual stores have expanded while joining the existing commercial clusters when they opened new stores. We use the circular statistical method² while tracing the past formation process.

From this data, we first determine the current commercial agglomeration. We define a commercial cluster as a set consisting of all stores.

Let us assume that the commercial facilities that comprise the existing commercial clusters are s_1, s_2, \dots, s_n . These facilities are located in the order of s_1 , and the aggregate $S = \{s_1, s_2, \dots, s_n\}$ constitute the current commercial agglomeration.

Next, a circular data is created that describes a certain direction of existing stores in the vicinity, centered on each store to be analyzed. The state of the commercial clusters at each of the intermediate points in time p can be determined by the following equation. s_p the set of existing commercial stores at the point in time when $S_{p-1} = \{s_1, s_2, \dots, s_{p-1}\}$. The set of points s_p and the set S_{p-1} and the unit vector formed by the points constituting the set $L_p = \{l_1, l_2, \dots, l_{p-1}\}$ and the angle formed concerning the east on the map is $\Theta_p = \{\theta_1, \theta_2, \dots, \theta_{p-1}\}$ and the angle formed concerning the east on the map is defined as Here, we assume that s_p on the unit circle centered at Θ_p is defined as the circle data. In this paper, unless otherwise noted, the angles are measured in radian with the east direction set to 0 (rad). This data uses the following equation Θ_p for the mean circular direction $\bar{\theta}$ (Fisher 1993; Brunsdon and Corcoran 2006; Corcoran et al. 2007).

$$C = \sum_i^{p-1} \cos \theta_i, S = \sum_i^{p-1} \sin \theta_i, R^2 = C^2 + S^2 \quad (R \geq 0) \quad (13.1)$$

The mean circular direction $\bar{\theta}$ is a composite vector of a set of unit vectors $L_p = \{l_1, l_2, \dots, l_{p-1}\}$, and its angle is given by using the value obtained in Eq. (13.1) according to the following:

$$\bar{\theta} = \begin{cases} \tan^{-1} \left(\frac{S}{C} \right) & S > 0, C > 0 \\ \tan^{-1} \left(\frac{S}{C} \right) + \pi & C < 0 \\ \tan^{-1} \left(\frac{S}{C} \right) + 2\pi & S < 0, C > 0 \end{cases} \quad (13.2)$$

R is the composite length of its composite vector, which lies in the range $[0, p - 1]$. \bar{R} represents average composite length as follow

$$\bar{R} = R / (p - 1) \quad (13.3)$$

² (Note 2) Sometimes referred to as directional statistics This method has recently been attracting attention in computational statistics, such as Shimizu (2008)

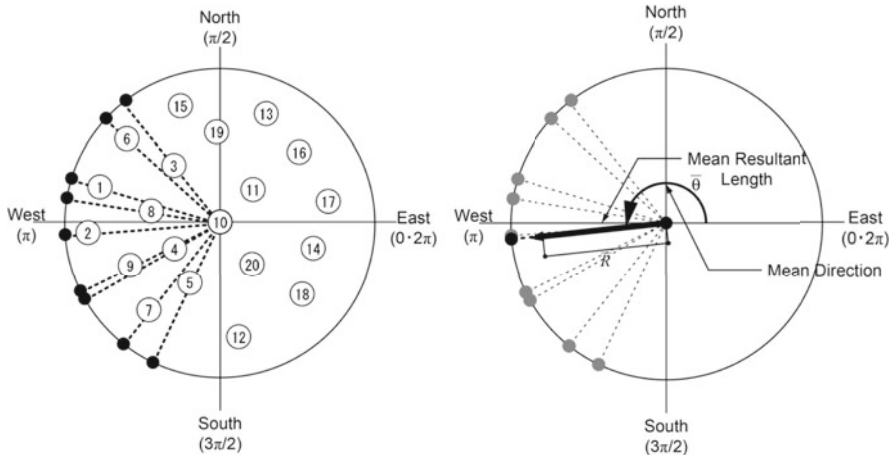
and are positioned in the range $[0, 1]$. \bar{R} the maximum and minimum values of $\bar{R} = 1$, indicating that all point data are matched. However, for the average composite length $\bar{R} = 0$ is the case for the average composite length $n(n \geq 3)$. It should be noted, however, that in the case of the average composite length, in addition to the case where the points are evenly distributed in many directions to divide the circumference equally, there is another case where the points are distributed in a straight line up through the center of the unit circle to bisect the circumference.

$$V = 1 - \bar{R} \quad (13.4)$$

V is defined as the circular variance (Note 5). As with the variance of linear data, the smaller the value of the circular variance, the more concentrated the data distribution. The circular variance $V = 1$ property is similar to the above property of the mean composite length $\bar{R} = 0$. Similarly to the above property of the mean composite length, the property of $n(n \geq 3)$ In addition to the case where the point sequences are evenly distributed in many directions to divide the circumference into two equal parts, there is also the case where the point sequences are distributed in the direction above the straight line passing through the center of the unit circle to divide the circumference into two equal parts. However, the cases in which the point sequences are uniformly distributed in multiple directions and the case in which they are distributed in a straight line correspond to the cases in which the accumulation expands in multiple directions around a certain base facility and the case in which it expands in a straight line along a main road, respectively, in urban space, and their meanings are quite different. In the above two cases, it cannot be interpreted that the distribution is uniformly distributed so that the dispersion value is 0 in the linear case. With the above properties in mind, $V < 1$ is considered in this method.

We propose a method for describing the direction of expansion of commercial agglomeration using the above circular statistics method. In this paper, this method is called the “expanded direction description method.” The calculation procedure is as follows.

First, the spatiotemporal data of the existing commercial facilities $i(0 < i < t)$ at the point in time $[0, t]$ of the existing commercial facility. p_i The first step is to consider a point that occurred at time $[0, t]$. The point p_i as the base point, and the points that occurred before the point $i(0 < i < t)$. The points that occurred before the point in time $\{p_0, p_1, p_2, \dots, p_{i-1}\}$ and plot the intersection of the points on the unit circle on the circumference of the circle. The angles formed by the unit vectors connecting the points plotted on the unit circle and the base point p_i . The angle formed by the unit vector connecting the points plotted on the unit circle and the base point is used in Eqs. (13.1) and (13.2) to obtain the average circle direction $\bar{\theta}$. The obtained mean circle direction is calculated using Eqs. (13.1) and (13.2). The



Flow up to the description of the direction using the circular statistical method

- (1) The numbers in the circle indicate the order in which the points occur.
- (2) In the left figure, the 10th generated point is the base point and connects it with a point that occurred in the past. Plot on the unit circle.
- (3) A line connecting a point plotted on the unit circle and the base point. The angle formed by the average circle direction using the circular statistics method. The following equation is obtained.
- (4) Invert the obtained result by $-\pi$ and calculate the existing accumulation or the direction of expansion is the direction of expansion of the
- (5) Also, the average of each unit vector in (3) is the average composite vector.

Fig. 13.2 Concept of circular statistics relationship between mean circular direction and circular variance

obtained average circle direction $\bar{\theta}$ by the following equation π . The obtained mean circle direction is inverted by (Note 5). Circular variance is a translation of circular variance.

$$d = \begin{cases} \bar{\theta} + \pi & (0 < \bar{\theta} \leq \pi) \\ \bar{\theta} - \pi & (\pi < \bar{\theta} \leq 2\pi) \end{cases}, \quad (0 < d \leq 2\pi) \quad (13.5)$$

Next, the length of the composite vector of each unit vector and the number of points i generated up to that point are substituted into Eq. (13.3) to obtain the average composite length, which is then substituted into Eq. (13.4) to obtain the circle variance V (Fig. 13.2).

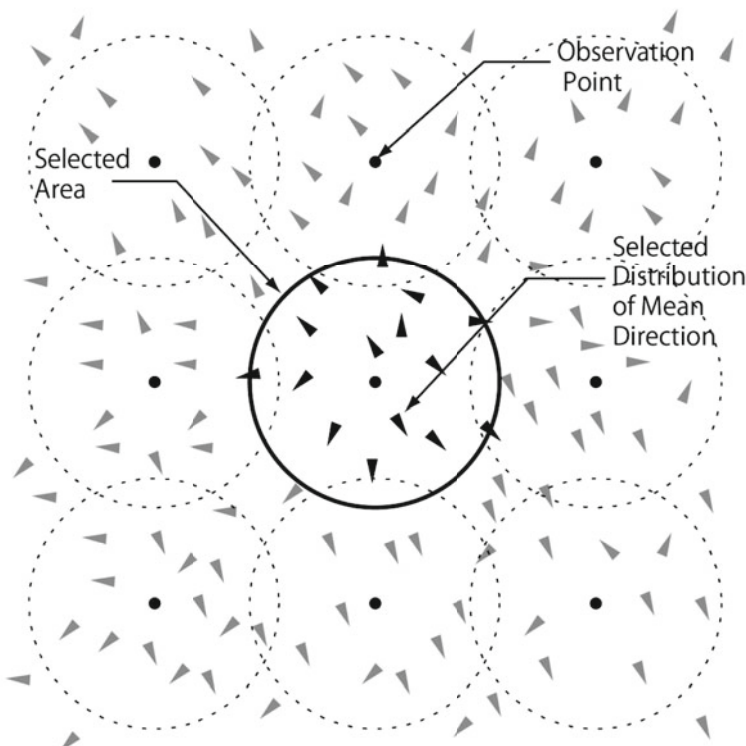
13.2.2.2 Analysis and Description of Trends in the Direction of Expansion of Commercial Clusters

Using the results of the expansion direction of each spatiotemporal point obtained through the above expansion direction description method, we analyze the trend

of the expansion direction of accumulation at an arbitrary observation point. This paper calls this method the “expansion direction trend description method.” The calculation procedure is as follows.

First, assume that there is a spatiotemporal point distribution that includes the magnification direction of each point calculated from the spatiotemporal data of existing commercial facilities at the obtained time using the magnification direction description method proposed earlier. Then, we generate uniform observation points at arbitrary distance intervals on the spatiotemporal point distribution. Generate a unit circle with an arbitrary radius centered on an observation point, and extract the spatiotemporal points encompassed by the circle. The unit circle defines the direction of expansion of each point.

Plot the result on a plot of the mean circle direction. The average circle direction is obtained using Eqs. (13.1) and (13.2). Substitute the length of the composite vector formed by the center of the unit circle and the expansion direction of each point plotted on the circumference of the unit circle and the number of space-time points included in Eq. (13.3) to obtain the average composite length, which is then



The observation points are generated at arbitrary intervals and encompassed within a buffer range of arbitrary radius.
The average direction of each above point is tabulated using circular statistical techniques.

Fig. 13.3 Description of expansion direction trend from an arbitrary observation point

substituted into Eq. (13.4) to obtain the circle variance value (Fig. 13.3). In this case, the observation points generated at arbitrary distance intervals will appear as differences in the resolution of the visualization when the analysis results are displayed, depending on the differences in the intervals. The radius of the circle used to select the spatiotemporal point data around the observation point is the scale that this analysis can read.

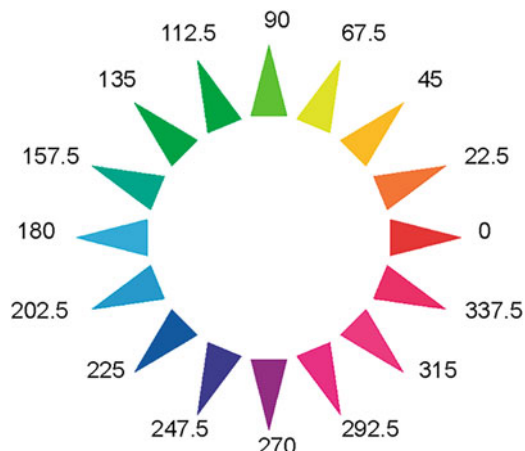
The average circle direction obtained here indicates the trend of the expansion direction of the accumulation concerning each observation point. If the circle dispersion is close to 0, the directionality is strongly in the direction of the obtained mean circle. If it is close to 1, the expansion is almost uniform in all directions.

13.2.2.3 Visualization of Analysis Results Using HSV Color Space

The values calculated by the above-mentioned expansion direction description method and the expansion direction trend description method are visualized as follows. The direction of expansion description method calculates the direction of expansion for each spatiotemporal point and the direction of expansion and circular dispersion values obtained. The direction of magnification was calculated for each point by describing the trend of magnification direction, and the mean circle direction and circle variance were obtained. Then, the magnification direction, mean circle direction, and circle dispersion are visualized on a map.

The direction of the mean circle is visualized using ArcGIS 9.3, with the east direction set to 0 (rad) and the angles indicated by the arrows. The HSV color space is defined by hue (H: hue), saturation (S: saturation), and value (V: value) and is suitable for representing the angles of the analysis results. The circular dispersion is visualized by a white-to-black gradient from a dispersion value of 0 to 1 (Fig. 13.4).

Fig. 13.4 Visualization of mean circle direction using HSV color space. Classify and assign observed angles within ± 11.25 degrees



13.2.2.4 A Method for Visualizing the Starting Point of Commercial Agglomeration Expansion Using Vector Analysis

Using directional data describing the angle of expansion of each store in a commercial cluster, we propose a method of searching for the starting point of the expansion of the commercial cluster by applying the method of vector analysis. The computational procedure is as follows.

From the previous method, for a set of commercial stores SH for each store in the commercial agglomeration to which they belong, a set of vectors $\vec{P}_n = \{\vec{p}_1, \vec{p}_2, \dots, \vec{p}_n\}$ and for a store \vec{p} for a store in the set, as defined by the vector (x, y) for a store in the set. The data are assumed to be arranged in ascending order by the time of the source.

Vector of stores opened at a given point in time i and the vector of commercial stores that have already opened at a given point in time \vec{p}_i and the set of vectors of commercial stores that have already opened in the surrounding area is defined by $\vec{P}_{i-1} = \{\vec{p}_1, \vec{p}_2, \dots, \vec{p}_{i-1}\}$ where the vectors \vec{p}_i and the vector $\vec{p}_o \in \vec{P}_{i-1}$ the inner product of these two vectors can be calculated using Eq. (13.5) below, and $\cos\theta$ is obtained by Eq. (13.6).

$$\vec{p}_o = (x_o, y_o), \quad \vec{p}_i = (x_i, y_i) \text{ than the} \\ \vec{p}_o \bullet \vec{p}_i = x_o x_i + y_o y_i = |p_o| |p_i| \cos\theta \quad (13.5)$$

$$\cos\theta = \frac{\vec{p}_o \bullet \vec{p}_i}{|p_o| |p_i|} = \frac{x_o x_i + y_o y_i}{\sqrt{x_o^2 + y_o^2} \sqrt{x_i^2 + y_i^2}} \quad (13.6)$$

From the above calculations, it can be seen that the vectors \vec{p}_i and the set \vec{P}_{i-1} for all vectors in the set $\cos\theta$ values are obtained for all vectors of using the results, the shape of the distribution of vectors indicating the direction of origin of the expansion of commercial concentration at the location of the store p_i . The following Eq. (13.7) gives the shape of the distribution of vectors that indicate the direction of origin of the expansion of commercial clusters at the location of a store.

$$C_i = \frac{\sum_{k=1}^{i-1} \cos\theta_k}{i - 1} \quad (13.7)$$

C_i takes values in the range $[-1, 1]$. Around 1, there is a concentration of the vector distribution, and around -1, there is a divergence of the vector distribution. Furthermore, a random situation is observed near 0. In other words, when the value of C_i around 1 indicates that the area is near the starting point of the expansion of commercial accumulation, while the area around -1 indicates that the area is at the boundary of the expansion.

Using the above method, the values of each store belonging to a commercial cluster are visualized on a map by painting them with a gradient. C_i the above

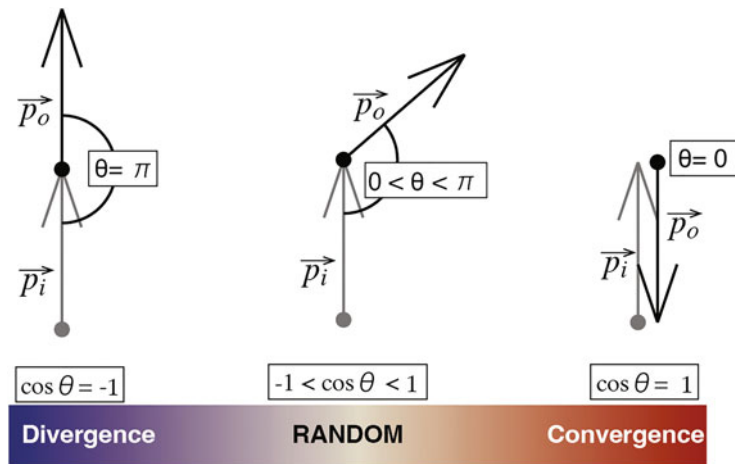


Fig. 13.5 $\cos \theta$ obtained from the inner product of vectors θ values and directional patterns obtained from the inner product of vectors

method is used to visualize the value of each store belonging to a commercial cluster by painting it in a gradation on a map and to examine the starting points of the expansion of commercial clusters, the boundaries of commercial clusters, and the scale and distribution of commercial clusters (Fig. 13.5).

13.3 Formation Process Analysis of Commercial Agglomeration in Shibuya

13.3.1 About Shibuya Ward

Shibuya Ward (Fig. 13.6) is located in the western part of Tokyo, bordered by Shinjuku and Nakano Wards to the north, Suginami, and Setagaya Wards to the west, Meguro and Shinagawa Wards to the south, and Minato Wards to the east. The area is long and narrow from north to south, with large green areas such as Yoyogi Park and Meiji Shrine in the center. The area is also home to some of Tokyo's most prominent commercial districts, including the areas around Shibuya, Ebisu, and Harajuku stations, as well as a variety of neighborhood shopping areas along the Keio Line, surrounding residential areas, and upscale residential areas such as Shoto. In addition, it is positioned as one of Tokyo's sub-centers, with many major railroad lines and main arterial roads intersecting the city. Therefore, it is considered a suitable site for the empirical analysis in this chapter.



Fig. 13.6 Schematic of Shibuya and Shinjuku Ward

13.3.2 About the Data Set

In this chapter, we use the address-matched “NTT Town Pages Data” for Shibuya Ward, Tokyo, from 1989 to 2007 as an example of applying the above method. This data is suitable for understanding time-series changes because it is published regularly on a yearly or, in recent years, bi-monthly basis. In this study, we use the data published in September of each fiscal year from 1989 to 1994 and published every other month in January, March, May, July, September, and November from 1995 to 2007. A total of 178,859 stores are included in the analysis. The stores covered here appear in the retail, restaurant, and service industries in the NTT Town Pages Data.

The data used in this study is based on the date when each store was first listed on the website, either annually or bi-monthly, and the store is assumed to have

opened at that time. However, the data do not show the detailed time of each store opening for each fiscal year or each bi-monthly period. In other words, the order in which stores were opened during each fiscal year or bi-monthly period is unclear. Therefore, in this paper, we assume that multiple store openings at each point in time occurred at the same time.

Since the relationship between stores close to each other is stronger than between stores as far away as possible, the analysis is based on the relationship between stores included within an arbitrary radius of a circle centered on each store to be analyzed.

13.3.3 Analysis of the Direction of Agglomeration Expansion as Seen in the Spatiotemporal Point Data and Discussion of Examples of the Application of Visualization

The method proposed in this chapter makes it difficult to determine its radius during the analysis uniquely. However, since the results depend on the radius distance, this paper analyzes data within a circle of radius 1000 m, 750 m, 500 m, 250 m, 100 m, 50 m, and 30 m, with each store as the base point. The results are as follows. We first discuss the analysis results for the circles with radii of 1000 m, 500 m, and 250 m, where the results are more pronounced.

In this chapter, considering the ease of viewing the analysis results, the angles indicating the direction were divided into 16 azimuths from 0 to 360 degrees, and the observed mean circle angles were classified and visualized for each 22.5-degree width range centered on each angle. The circular dispersion values were expressed as a 10-step gradation.

First, in the analysis of the 1000 m radius buffer (Fig. 13.7), we can observe arrows extending outward from the major railroad stations in Shibuya Ward, namely Shibuya, Ebisu, Yoyogi, and Shinjuku stations. From this, it can be inferred that the stations serve as the base points for the expansion of commercial clusters. Next, focusing on the locations estimated to be the base points of each expansion, we can see that the distribution is not uniform, with large and small distributions in each angular zone. For example, when we focus on the expansion based on the area around Shibuya Station, we observe that the distribution of arrows in the northeast direction is significantly smaller than those in other directions. This indicates that the directionality of expansion in that direction is strong. This is consistent with the location of Meiji-dori Avenue, which suggests that commercial clusters are expanding from Shibuya Station to Harajuku. Similarly, the distribution of arrows along the Keio Line and Koshu Kaido that extend westward from Shinjuku Station is also strongly oriented, suggesting that commercial clusters are expanding westward from the base point of Shinjuku Station.

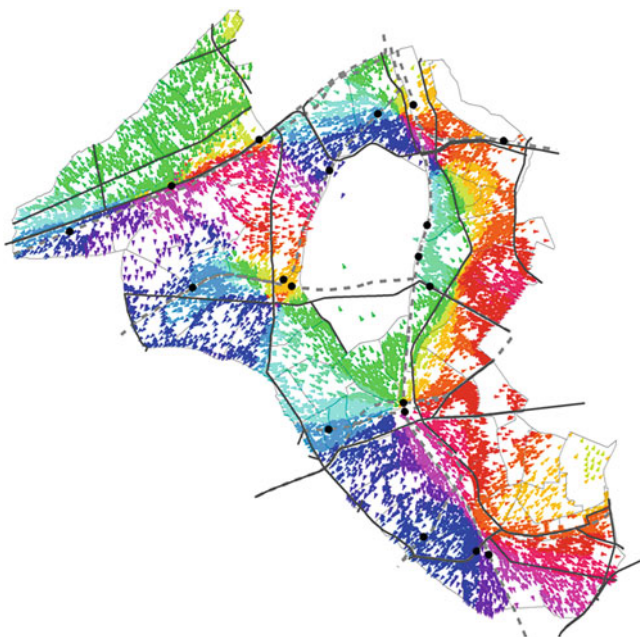


Fig. 13.7 Distribution of expanding direction at 1000 m buffer

In addition, in the circular dispersion distribution chart (Fig. 13.8), we can see results consistent with the above discussion of locations that serve as the base points for expansion. It can be seen that the locations with high circular dispersion are distributed around the major stations of Shibuya, Ebisu, Yoyogi, and Shinjuku. This indicates that relatively old stores are uniformly distributed near the commercial clusters, which is the base point for expanding the commercial clusters, as discussed in the expansion direction distribution map. Similarly, along the main roads, Meijidori and Koshu kaido, the locations with high circle dispersion are distributed in a long and thin line, and the commercial clusters are extended outward in parallel with these streets.

In the 500-m buffer (Fig. 13.9), as in the 1000-m buffer, in addition to the extensions centered on major stations, the distribution of arrows in the direction of extensions based on relatively small stations, such as Hatsudai, Hatagaya, and Sasazuka stations on the Keio Line and Yoyogi Uehara station on the Odakyu Line, which was not observed when the buffer radius was large, can be observed. The distribution of arrows in the direction of the road can be observed. We can also observe locations where opposite arrows collide along roads. This is caused by the collision of expansion based on each station and can be assumed to be the boundary line between each expanding commercial cluster.

As in the 1000 m buffer analysis, the circular dispersion distribution (Fig. 13.10) is also higher at the locations that can be inferred as the base points of the

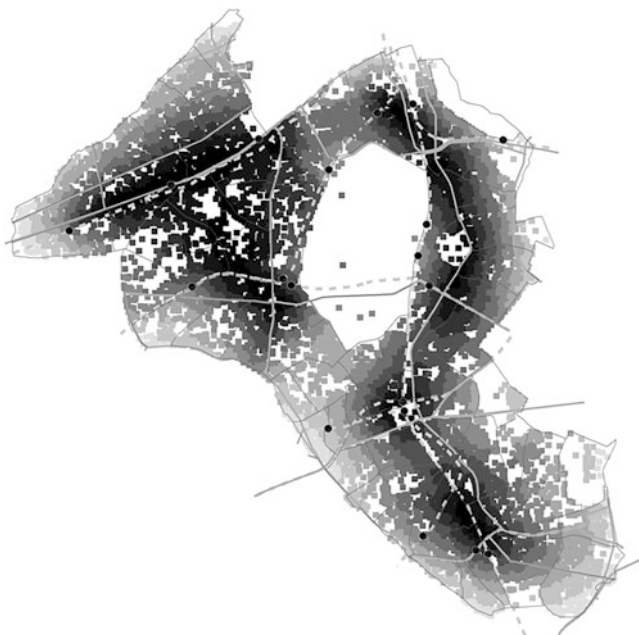


Fig. 13.8 Circular dispersion distribution at 1000 m buffer

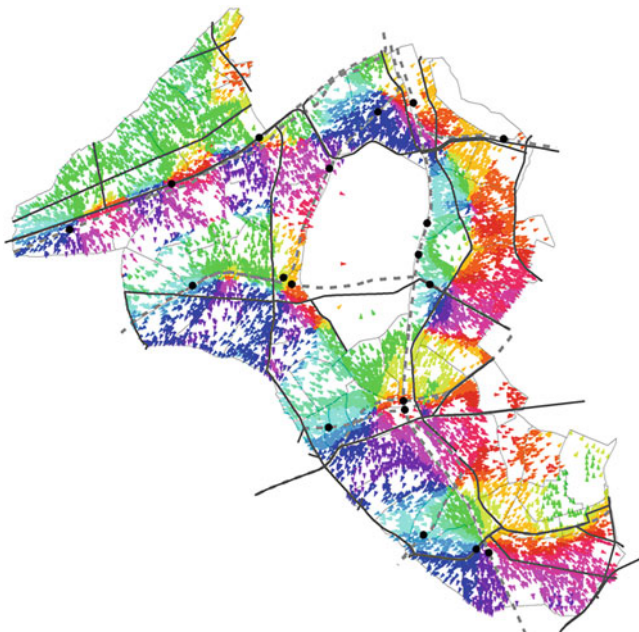


Fig. 13.9 Distribution of expanding direction at 500 m buffer



Fig. 13.10 Circular dispersion distribution at 500 m buffer

expansion by visualization of the mean circular direction. In addition, the circular dispersion is high at the locations where arrows pointing in opposite directions collide, which can be inferred as the locations where the expansion collides with the commercial accumulation. In addition, although not shown in the expansion direction distribution map, the Hiroo area on the east side of Ebisu station has a high dispersion value. Although there is no station or other base point, it is considered the base point of the expansion of the area in light of the other trends shown in the circular dispersion.

In the 250-m buffer (Fig. 13.11), we observed more detailed changes than in the analysis using a larger buffer radius. The arrow distribution in the direction of expansion is not observed in the above analysis. Still, it is based on the relatively small station area that does not face an arterial road, such as the Daikanyama station. The arrow distribution along arterial roads also shows a more localized change in the arrow distribution along roads, showing a strong expansion directionality in the analysis results for the large buffer radius. In light of the previous discussion, it can be inferred that the central facility within the smaller regional unit is located at the base of this change. As an example of this being particularly evident, we observed the distribution of arrows extending northward from Hatagaya and Sasazuka stations along the Keio Line. We captured relatively small changes, such as in neighborhood shopping areas.

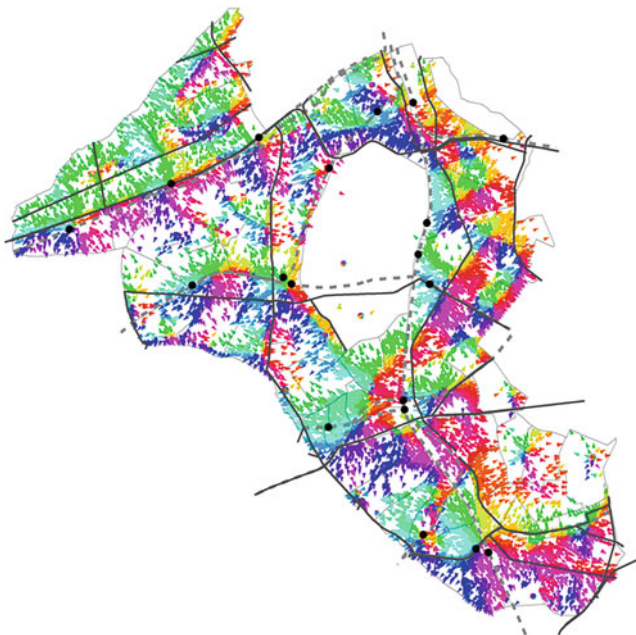


Fig. 13.11 Distribution of expanding direction at 250 m buffer

Similarly, the circular dispersion distribution map (Fig. 13.12) captures minute changes in commercial clusters, which were not observed when analyzing large buffer radii. As mentioned earlier, relatively high circular dispersion is observed for large and small railroad stations and arterial roads. At the same time, high values are also observed for locations where arrows pointing in opposite directions collide. In other words, the locations with high circular dispersion are related to the cases where they are the base points of the expansion of commercial clusters, and the boundary areas where the expansion of commercial clusters collides with each other and where a straight road passes between the clusters and stores are located on the line of the road. It corresponds to the case where the base point is on a straight line with the point sequence bisecting the circumference, which is a property of circular dispersion in this method.

It can be observed that the smaller the buffer radius, the more detailed the analysis results. By decreasing the buffer radius, more detailed changes that were not apparent when the analysis target was selected with a large radius can be captured, such as changes in small stations and areas with characteristics as a region but no facilities that can serve as a base point. On the other hand, if the buffer radius is too small, such as 50 m or 30 m, the arrows will be arranged irregularly, and no trend can be read. This is considered to be a limitation of this method.



Fig. 13.12 Circular dispersion distribution at 250 m buffer

13.3.4 Analysis of the Trend in the Direction of Agglomeration Expansion and Discussion of Examples of Application of Visualization

Based on the results of the previous analysis, we analyze the trend in the direction of expansion at arbitrary observation points. In this paper, the analysis was conducted using a grid of observation points at intervals of 100 m. The observation area centered on an observation point is affected by the circle's radius encompassing the observation target. The radii of the circles were 1000 m, 750 m, 500 m, 250 m, and 100 m, and the spatiotemporal point data were tabulated for each of these radii. The above analysis found that the 500 m buffer radius captured the relatively wide changes based on major stations and the relatively narrow changes based on arterial roads and small- and medium-scale stations, respectively. The results of this analysis were used to examine the trend in the direction of expansion within the radii of 500 m and 250 m, where the differences in the results from the previously defined observation points were pronounced. The same method was used for the visualization of the results.

As shown in Fig. 13.13, the distribution of arrows indicating the direction of expansion of the concentration is observed near Shibuya and Ebisu stations, which are the main stations in this area, and near the intersection of Meiji-Dori and

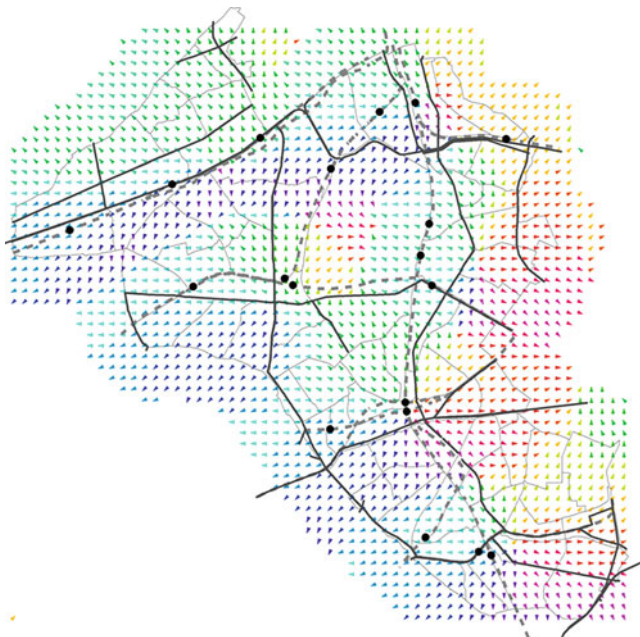


Fig. 13.13 500 m buffer result use of the distribution in the direction of expansion 500 m at buffer
Enlarged directional trend distribution

Omotesando, which are the main roads in this area. The same directional arrows can also be observed along Koshu Kaido in a uniform westerly direction, suggesting that the concentration tends to expand along the main road.

The results of this analysis (Fig. 13.14) show that the dispersion values are high near the major stations and trunk roads mentioned above, and these areas can be positioned as the base points for the expansion trend. In particular, the areas with high circular dispersion near trunk roads are long and narrow, indicating that roads are the standard for expansion.

(Expanding trend within a buffer radius of 250 m from the observation point) A more detailed change trend can be read when the observation buffer radius from the observation point in Fig. 13.15 is reduced. In addition to the trends based on major stations and intersections with main roads, small-scale expansion trends can be observed based on stations with residential areas around them, such as Hatsudai, Hatagaya, and Sasazuka stations on the Keio Line and Yoyogi Uehara station on the Odakyu Line. The areas with large values in the circular distribution map (Fig. 13.16) are concentrated near the aforementioned points, and by comparing them with the map showing the trend in the direction of expansion, it can be seen that they are the base points for the expansion of the agglomeration.

(Analysis results for other buffers and overall discussion) Similar to the discussion in the previous Sect. 13.3.3, it can be observed that the analysis results become

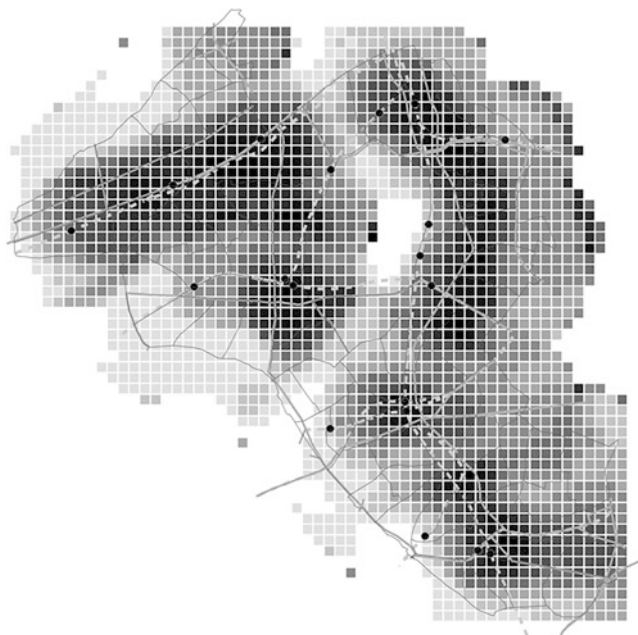


Fig. 13.14 500 m buffer results use of 500 m distribution in the direction of expansion 500 m buffer time Circular dispersion distribution

more detailed as the buffer radius becomes smaller, depending on the size of the buffer radius that determines the area to be analyzed. For the extended directional distribution map results with an irregular array of arrows, such as the results with a buffer radius of 50 m or 30 m, no significant trend can be read in both the extended directional trend distribution map and its circular dispersion distribution map. This is considered to be a limitation of this method.

13.3.5 Analysis and Discussion Using Commercial Agglomeration Expansion Origin Direction Data (Figs. 13.17 and 13.18)

Figures 13.4 and 13.7 show that vectors indicating the direction of origin are concentrated around major stations such as Shinjuku, Shibuya, and Takadanobaba Stations. The 500 m buffer in Fig. 13.7 shows that the vectors are concentrated around Hatsudai, Hatagaya, and Sasazuka stations along the Keio Line, around Kagurazaka, and near the intersection of Meiji-Dori and Omotesando, where many visitors come without depending on nearby shopping areas or major stations.

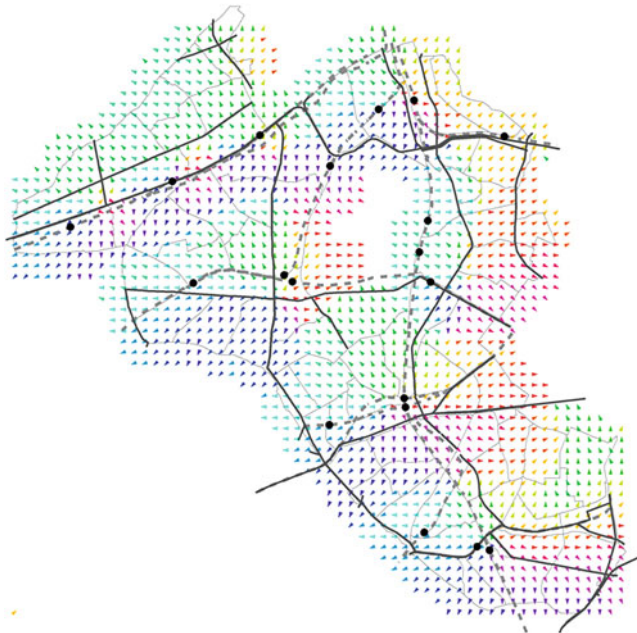


Fig. 13.15 500 m buffer result use of the distribution in the direction of expansion 250 m at buffer
Enlarged directional trend distribution

13.3.6 Visualization of 500 m Buffer Accumulation Expansion Starting Point (Figs. 13.19 and 13.20)

As explained above, the areas around the major stations are painted in red, indicating the starting points of the expansion of commercial clusters. In addition, some locations far from the main station are also indicated as the starting points, indicating that the neighborhood shopping areas and places frequented by many visitors also indicate the starting points of commercial cluster expansion.

Many of the points painted in blue are located between multiple origins, indicating locations where the expansion between each commercial agglomeration converges.

13.3.7 Visualization of 250 m Buffer Accumulation Expansion Starting Point (Figs. 13.21 and 13.22)

Next, when the buffer is set to 250 m to visualize the starting point of the expansion of commercial clusters, the results are almost the same as when the data is aggregated at 500 m. However, when we look at the area around major stations



Fig. 13.16 500 m buffer results use of 500 m distribution in the direction of expansion 250 m at buffer Circular dispersion distribution

such as Shibuya and Shinjuku stations, we can see differences by area divided by stations and railroad lines. In other words, by aggregating the data in 250-m buffers, we can more precisely read the differences in the expansion starting points of the regions.

13.3.8 Differences in Visualization Results Depending on Buffer Size

Regarding the effect of buffer size, a relatively large area, such as 500 m, is suitable for reading a more macroscopic situation, such as an expansion centered on a major station. On the other hand, when the buffer size is smaller than 250 m, it is possible to read differences in the area bounded by regional dividing elements such as major stations and railroad tracks, and it is considered to capture more microscopic aspects of the area.

Using detailed spatiotemporal data, we proposed a method to visualize the starting point and convergence point of the expansion of commercial clusters by applying a vector analysis method to the pattern of the expansion of commercial



Fig. 13.17 Commercial agglomeration expansion starting point directional diagram (750 m buffer)

clusters. We also conducted an empirical analysis using actual data. The starting points and convergence points of the expansion were visualized.

In the future, we would like to conduct Monte Carlo simulations and perform statistical tests on the probability distributions obtained from the simulations to investigate the usefulness of this method further.



Fig. 13.18 Commercial agglomeration expansion starting point directional diagram (500 m buffer)

13.4 Conclusion

13.4.1 Summary and Future Issues

We proposed a method for describing, analyzing, and visualizing changes accompanying the expansion of complex commercial clusters using a circular statistical method, which is difficult to grasp using conventional methods such as paper maps, analysis based on ordinary statistical data, and animation-like methods that

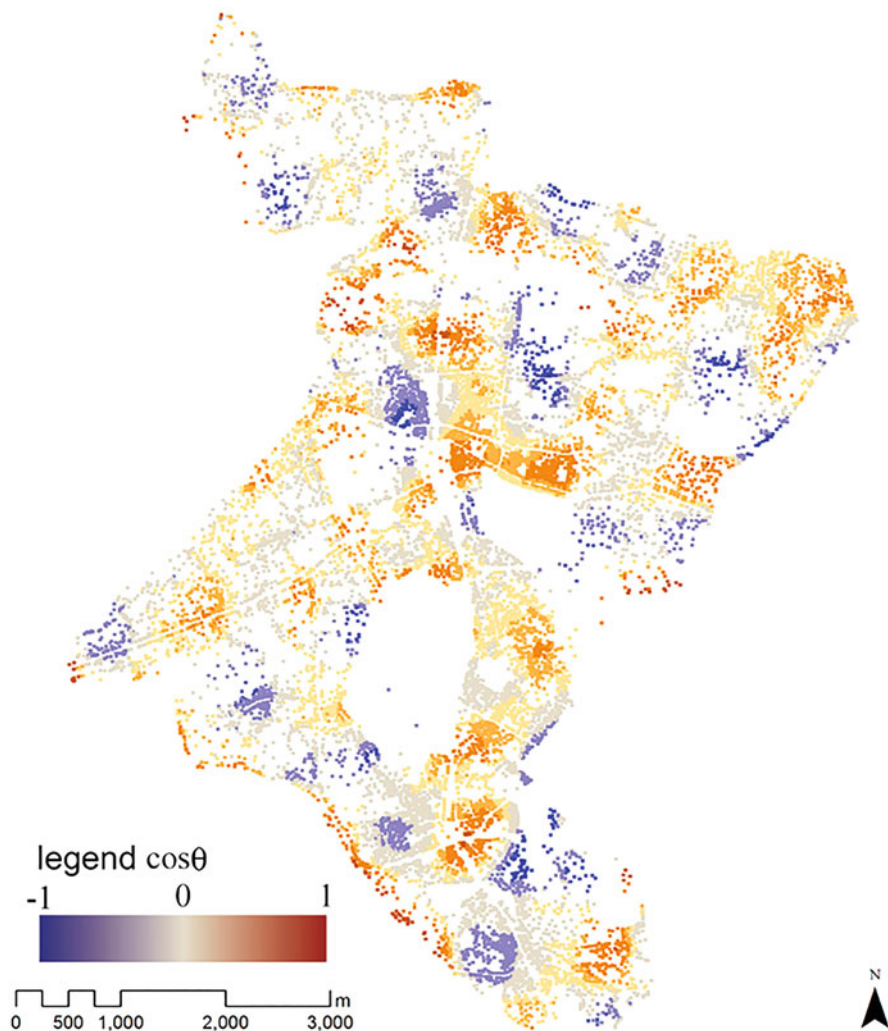


Fig. 13.19 $\cos\theta$ value distribution (at 500 m buffer) (750 m enlarged starting point directional map)

sequentially display time-series changes. The method is analyzed empirically using spatiotemporal point data of commercial stores in Shibuya Ward, Tokyo, and the results are discussed.

The results obtained are summarized below.

1. First, we analyzed the direction of expansion of commercial clusters by using the circular statistical method to analyze the direction of new store openings relative to existing clusters in each time cross-section and were able to visualize the results. The results show that the arrow points are concentrated and distributed

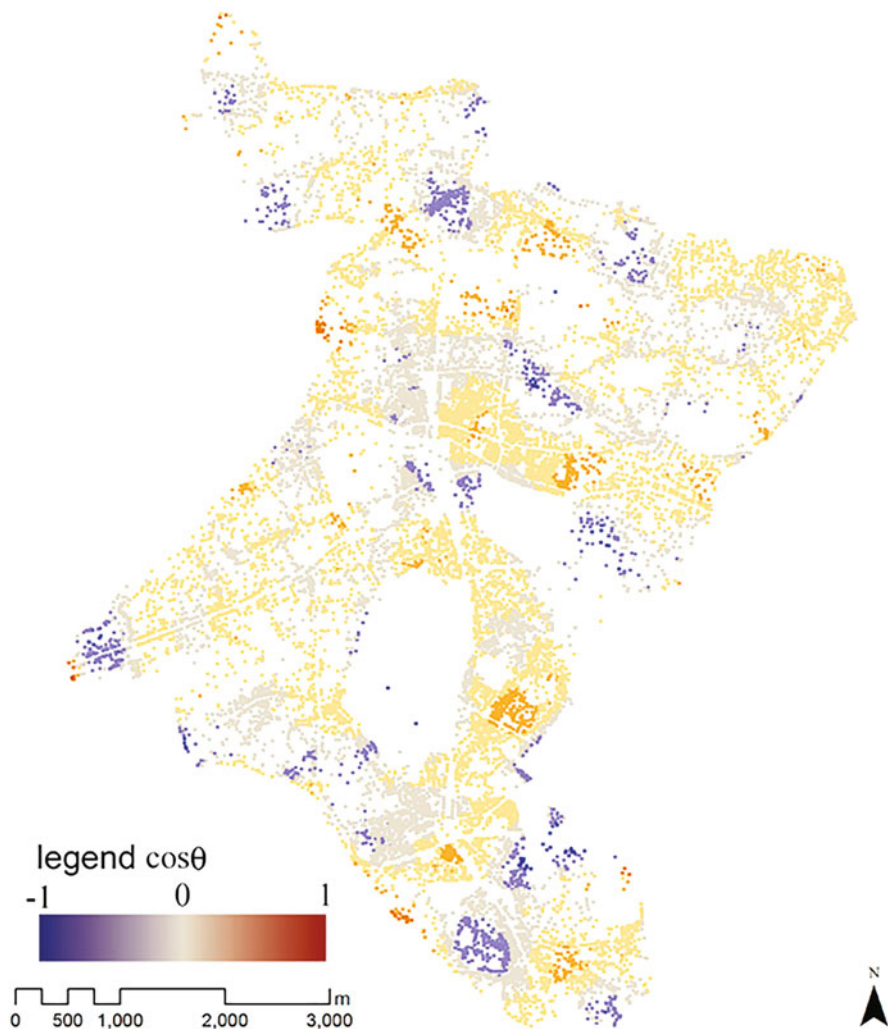


Fig. 13.20 $\cos\theta$ value distribution (at 500 m buffer) (500 m enlarged starting point directional map)

at the points that are the base points of the expansion of commercial clusters and that they are located near facilities and roads that are generally considered to be the base points of commercial cluster expansion, such as railroad stations and arterial roads, in comparison with the current situation in Shibuya Ward. While conventional mesh data analysis can provide a rough trend of expansion, the analysis using this method can be evaluated to a certain extent in that it can simultaneously identify the base points and directions of expansion.

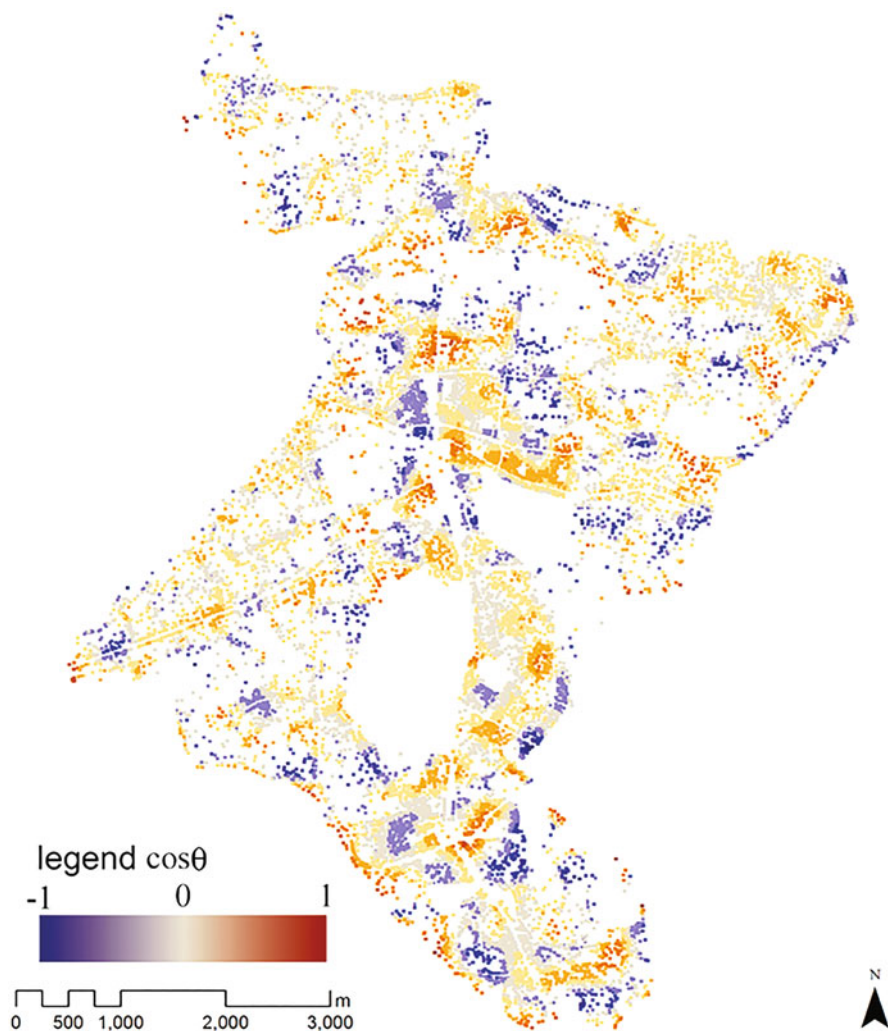


Fig. 13.21 $\cos\theta$ value distribution (at 250 m buffer) (750 m enlarged starting point directional map)

2. In the map of the distribution of circular dispersion, it was found that the circular dispersion value is decidedly high in the area that can be concluded as the base point in the above map showing the direction of expansion. In other words, high circular dispersion means that the points to be analyzed are uniformly distributed in all directions from the base point. In this case, the area is positioned where relatively old stores are concentrated. The conclusion is generally consistent that the area is the base point of commercial cluster expansion and is being extended outward from there. Although previous studies have captured changes

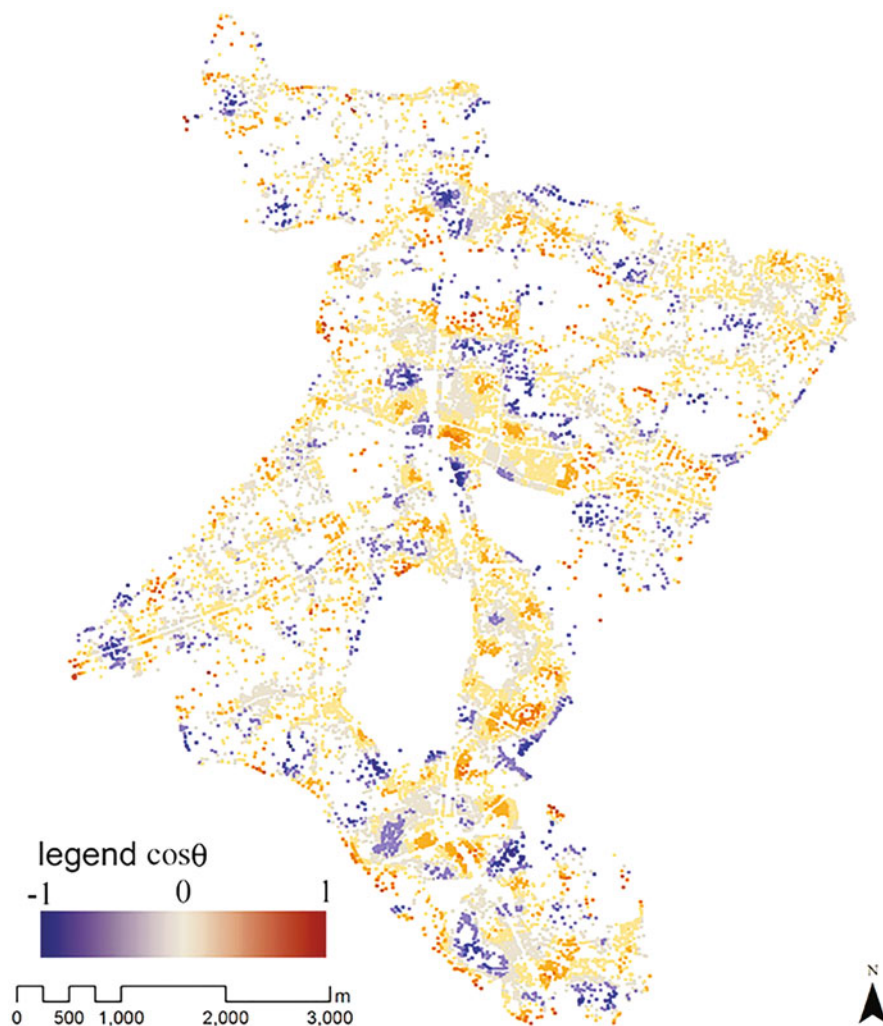


Fig. 13.22 θ value distribution (at 250 m buffer) (500 m enlarged starting point directional map)

in commercial clusters based on train stations, in reality, this method is not limited to such studies but also allows us to understand changes in areas without a clear base point, such as streets or train stations.

3. The conventional method made it difficult to analyze data at different scales, such as township units or mesh data. Still, with this method, it is possible to change the scale of analysis freely. For example, the smaller the buffer radius determining the analysis target area, the more detailed the results become. The smaller the radius, the more detailed the analysis results become. By reducing the buffer radius, we succeeded in capturing more detailed changes, such as changes

in small stations and areas with characteristics as a region but no facilities that can serve as a base point, which were not revealed when the analysis target was selected with a large radius.

4. The analysis from the equally spaced observation points enabled us to capture the expansion trend of the area around each observation point and to show each change more clearly. Similarly, the dispersion diagram showed that the high dispersion values are the points of almost uniform expansion in all directions at the observation points and are the base points of the expansion of commercial clusters.

The following three issues need to be addressed in the future.

1. To simplify the method, we use spatiotemporal data that only considers the location of stores and the time of their opening. In reality, many stores close, and their impact on the formation process is not small. To reproduce the formation process of commercial areas more faithfully, it is necessary to study an analysis method using data that considers store closures.
2. The visualization method of showing the circular dispersion distribution in addition to the expanded directional map and the expanded directional trend distribution sometimes results in a large amount of information, making it difficult to grasp each phenomenon in some cases. Several measures can be considered in the future. A method to automatically detect and highlight the singular points of the vector field from each of the extended directional maps and extended directional trend maps is considered. In addition, since the data display function of a general GIS was used in this study, there are limitations in how the results can be visualized.
3. Although we have only proposed a method to capture the trend of change in commercial clusters based on past changes, we would like to study a future forecasting method to estimate the direction in which commercial clusters are expected to expand in the future, using the results of the analysis based on the method proposed here as test data.

We want to discuss the above issues and others in the future.

13.4.2 Summary and Future Prospects

Urban commercial areas are not only areas with many commercial stores but also places where many people live and are subject to many changes in social and economic conditions, either directly or indirectly. Many of these changes can be seen in the image of the area, the process of formation, and the direction of expansion, which is the subject of this study. The detailed and large amount of spatial data that has become easily available in recent years can be used to capture such urban events, as shown by previous studies and the method proposed in this study.

In this study, we propose an analytical method for extracting correlations among events and the formation process of events and their changes from a large amount of detailed spatial data and a visualization method that enables intuitive interpretation of the data and demonstrates its effectiveness. The methods were empirically validated using actual data from various events in an urban commercial area. On the other hand, the methods are based on a simplified model of events and do not necessarily reproduce real-life events perfectly. Therefore, it should be noted that the method is still insufficient for practical use in urban planning and urban development.

In this study, events such as the exit of a commercial store were treated in a simplified manner to increase the generality of the method. For example, only the opening of a store was treated due to data limitations. In the future, when data that is difficult to obtain, such as at the point of store exit, become available, it will be necessary to consider a method that more closely matches real urban events, including such data.

Next, the analysis of the method proposed in this study uses point data to simplify the method. Many of the events we try to capture in this study are complex and irregular changes and their trends in commercial areas. They are at the basic stage of capturing the nature and aspects of the events themselves. Therefore, to simplify the methodology, we used a point data format to precisely define each attribute, location, and time of occurrence to some extent. However, in an actual urban space, the scale of buildings has not a small influence on each event, and analysis using data such as polygon data, which includes the general area and scale of buildings, as well as the names of tenants, is also conceivable.

In the future, it will be necessary to examine the scale and area of buildings in three dimensions to represent the reality of urban space better. First, we would like to study an analysis method that adds area and other morphological information as attributes to the point data used in this study. Then we would like to develop an analysis method using polygon data that considers shape and scale.

Third, in this study, we could go back to when the latest available data was obtained and capture the changes that occurred during that period and their trends. In urban planning and urban development, it is often discussed in advance what effects a certain plan will have after its implementation and the current situation. The results obtained using the methodology developed in this study capture the trends of each urban event. Therefore, it is thought that using them as test data to predict future changes and transitions will be useful. In the future, it is necessary to consider using the results and findings obtained in each case for methods to clarify the prediction of future changes. The analytical method for this analysis is an issue for the future. The urban commercial areas in this study will be affected by rapid changes in various social conditions, which will accelerate various changes in urban space, such as the exit and entry of commercial stores and the formation of their image. Rapid changes in urban space will burden the lives of residents and various urban activities, and it will continue to be necessary to accurately understand the resulting urban events. In recent years, the development of information technology and ubiquitous technology has made it possible to acquire large amounts of detailed data to ensure a

more comfortable life for people. The quality and quantity of spatial data capturing various events will become better and richer, and there will be no shortage of such data in the future. Various spatial analysis and visualization methods have been developed to accurately and efficiently extract various events from these data. As mentioned in Chap. 1, the main objective of this study is to develop an analytical method that can capture trends and structures of events from detailed, diverse, and abundant data resources and derive hypotheses from them, even for exploratory spatial data analysis. As a result, it can be evaluated that each analysis method and visualization method developed in this study can derive hypotheses in an exploratory manner from a discussion of the results of each empirical analysis. We hope this research will serve as a basis for developing analytical methods to capture more advanced spatial phenomena.

References

- Akiyoshi I, Yukio S (2010): “A Method of Analysis and Visualization of Expanding Direction of Retail Distribution”, *Journal of the Architectural Institute of Japan* 75(650) 889–895. (in Japanese)
- Amin H (2007) Urban visualization with virtual reality. *Urban Plan Urban Visual Simul* 270:39–42
- Batty M (2003) Agent-based pedestrian modelling. In: Longley P, Batty M (eds) *Advanced spatial analysis. The CASA book of GIS*. ESRI Press, Redland, CA, pp 81–106
- Brunsdon C, Corcoran J (2006) Using circular statistics to analyse time patterns in crime incidence. *Comput Environ Urban Syst* 30(3):300–319
- Corcoran J, Chhetri P, Stimson R (2007) Using circular statistics to explore the geography of the journey to work. *Reg Sci* 88(1):119–132
- DiBiase D, MacEachren AM, Krygien JB, Reeves C (1992) Animation and the role of map design in scientific visualization. *Cartogr Geogr Inform Syst* 19(4):201–214
- Dorling D (1992) Stretching space and splicing time: from cartographic animation to interactive visualization. *Cartogr Geogr Inform Syst* 19(4):β215–β227
- Dykes J (1998) Cartographic visualization: exploratory spatial data analysis with local indicators of spatial association using Tcl/Tk and cdv. *R Stat Soc Statistician* 47(Part 3):485–497
- Dykes, Jason (2005): “Facilitating interaction for geovisualization”, In: Dykes, J, MacEachren, AM., and Kraak, M-J, (eds.): *Exploring geovisualization*, Elsevier, Oxford, pp. 143–158
- Fisher NI (1993) Statistical analysis of circular data. Cambridge University Press, Cambridge
- Gahegan M (2005) Beyond tools: visual support for entire process of GIScience. In: Dykes J, MacEachren AM, Kraak M-J (eds) *Exploring geovisualization*. Elsevier Ltd, Oxford, UK, pp 83–99
- Haining R (2003) Spatial data analysis theory and practice. Cambridge University Press, Cambridge, UK
- Hillier B, Hanson J (1984) The social logic of space. Cambridge University Press, Cambridge, UK
- Inoue R, Shimizu E (2005) A new method for constructing circle area cartogram. *Theory Appl GIS* 13(1):43–50
- Inoue R, Shimizu E, Yoshida Y, Li Y (2009) Visualization of spatial distribution and temporal transition of land Price in Tokyo 23 wards based on Spatio-temporal kriging interpolation. *Theory Appl GIS* 17(1):13–24
- Kigawa T, Furuyama M (2004) The urban entropy coefficient: a measure describing urban conditions—a morphological analysis on evolutional process of Paris. *J City Plan Inst Japan* 39(3):823–828

- Kigawa T, Furuyama M (2005) Study on a vector in Kyoto's modernization by means of space syntax—a philosophy seen in an urban planning project for installation and broadening streets in Kyoto. *J City Plan Inst Japan* 40(3):139–144
- Kigawa T, Furuyama M (2006) Using space syntax to examine an evolutional process of a local town—a case study on the modernization of Otsu city in Shiga prefecture. *J City Plan Inst Japan* 41(3):229–234
- Monmonier M, Watanabe J (1995) *Chizu Ha Usotsukidearu*, Shobunsha, Tokyo. Monmonier, Mark (1991): how to lie with maps. University of Chicago Press, Chicago, IL. (Translation).
- Roberts, Jonathan, C (2005): "Exploratory Visualization with Multiple Linked Views", In: Dykes, Jason, MacEachren, Alan, M., and Kraak, Menno-Jan,(eds.): Exploring Geovisualization, Elsevier Ltd., Oxford, United Kingdom, pp.159–180
- Rodger, Peter (2005): "Graph Drawing Techniques for Geographic Visualization", In: Dykes, Jason, MacEachren, Alan, M., and Kraak, Menno-Jan,(eds.): Exploring Geovisualization, Elsevier Ltd., Oxford, United Kingdom, pp.143–158
- Sadahiro, Yukio (2007): "From Spatial Analysis to Spatio-Temporal Analysis: Issues and Future Prospects", *Urban Planning <Feature>: Beauty and Reality in Urban Analysis*, 264, pp. 31–35. (in Japanese)
- Shimizu K (2008) Recent developments in directional statistics: distributional aspects. *Japan Soc Comput Stat* 19(2):127–150
- Takamatsu S (2007) On visualization methods of form and function: developing techniques in the UK. *Urban Plan Urban Visual Simul* 270:13–16
- Theus M (2005) Statistical data exploration and geographical information visualization. In: Dykes J, MacEachren AM, Kraak M-J (eds) *Exploring geovisualization*. Elsevier, Oxford, p 127–142
- Yan W (2003) *GIS no Genri to Ouyou*. JUSE Press, Ltd, Tokyo. (in Japanese).
- Yoshikawa K (2007a) Application of 3D computer graphics to urban development: assuming its use in municipalities. *City Plan Urban Visual Simul* 270:43–46
- Yoshikawa M (2007b) Digital city and VR. *City Plan Urban Visual Simul* 270:47–50

Chapter 14

Theoretical Approach for Selection of Public Transport System Considering Urban Density and Travel Distance



Daisuke Hasegawa and Tsutomu Suzuki

Abstract The increasing popularity of ride-sharing services, car sharing, and other transportation options has led to a growing diversification of local public transportation services for short-distance travel. In this study, we aimed to understand how an appropriate public transportation system evolves based on density and travel impedance of passengers using an analytical model. Initially, we developed a model representing five typical transportation systems, each characterized by the presence of fixed routes and varying requirements for access and egress time. Subsequently, we analyzed the influence on expenses that satisfy the service level condition, focusing on the effect of demand density and travel distance. Furthermore, we investigated the current status of the introduction of local transportation in eastern Japan and compared the results with the calculation results of the model. Notably, we observed that increasing the number of buses and demand-responsive transit (DRT) operated by the local government led to enhanced effectiveness of car sharing, particularly in areas where DRT services were introduced.

Keywords Local public transportation · Trip length · Demand density · Operation efficiency · Demand-responsive transit

The contents of this paper are based on the following paper originally published in a Japanese journal: Daisuke, H., Tsutomu, S. (2017) Theoretical Approach for the Selection of Public Transport Systems Considering Ur-ban Density and Travel Distance. Journal of City Planning Institute of Japan, 52 (3), pp. 1284–1289 (in Japanese).

D. Hasegawa (✉)

The University of Tokyo, Tokyo, Japan
e-mail: hasega60@e.u-tokyo.ac.jp

T. Suzuki

University of Tsukuba, Ibaraki, Japan
e-mail: tsutomu@risk.tsukuba.ac.jp

14.1 Introduction

Motorization in Japan has made significant strides since the 1960s. The changing urban landscape has resulted in a growing reliance on suburban areas, as evident from the proliferation of roadside shops. Consequently, the number of urban public transportation users has seen a noticeable decline, significantly affecting urban buses with short operating distances. Consequently, an important issue concerning municipalities has been raised: the reduced public transportation threatens the daily lives of mobility-impaired people, such as the elderly, who cannot drive cars. In response to these challenges, there has been a nationwide effort to restructure local public transportation networks, with a primary focus on reorganizing bus route networks. This aims to create more accessible boarding points and ensure regular operation of vehicles to improve the overall public transportation experience.

In recent years, several municipalities have adopted demand-responsive transit (DRT) solutions, DRT systems offer the flexibility to adjust routes dynamically based on user demand taking into account modern modes of transportation like ride-sharing (e.g., Uber) and car-sharing services. These new local public transportation services are distinguished by operational factors including the accessibility of boarding locations and the presence of route/operation schedules. They play a crucial role in bridging transportation gaps (Kato and Takeuchi 1979; Niitani 1993) for individuals who lack access to existing means of transportation and those facing difficulties in utilizing existing means of transportation. However, one key challenge lies in the variable operating route lengths of these new transportation services, which vary based on user demand. Consequently, operational efficiency is heavily influenced by the demand density and the size of the target region. Therefore, the advantages and disadvantages of each means of transportation are determined based on user density and trip length; however, it is difficult to identify these specific conditions quantitatively.

Research has been conducted on the relationship between demand density and the means of transportation. For example, Niitani (1993) categorized public transportation based on running space and transportation capacity and proposed the appropriate coverage area for each mode of transportation based on demand density and trip length. Ishida et al. (1999) examined transportation costs from both supply and user perspectives and identified advantageous regions in the city. Nevertheless, these studies primarily focused on inter-city transport, concentrating on railroads and automobiles, without delving into low demand density and short-distance inter-city transport.

Considering research from the perspective of rationality in delivery, Ieda (1997) and Watanabe and Suzuki (2000) conducted studies focusing on the optimal hierarchical structure of transport transfer facilities (i.e., hubs) in the field of logistics. However, minimal research has addressed the difference in operation methods, such as direct and touring trips in the passenger sector, which exhibit limited hierarchy. Hasegawa and Suzuki (2011) focused on the effectiveness of DRT and quantitatively demonstrated the characteristics of its operational efficiency,

including its superiority in low-density cities, rapid decline in operational efficiency due to vehicle shortage, and improvement of operational efficiency through the use of both large and small vehicles. However, certain issues persist, such as the consideration of road density and shape and the continuous representation of the concentration and dispersion of travel demand.

To address these gaps, our study modeled five typical transportation services with varying operational factors, such as the accessibility of boarding locations and the presence of route/operation schedules. We analyzed the effects of demand density and user travel distance on the cost required for each transportation mode to achieve a certain service level. Additionally, we surveyed the current state of their introduction to local public transportation, identified the characteristics of demand density and travel distance, and compared these findings with the model results to theoretically derive the demand density and travel distance where each transportation service becomes advantageous, along with their advantageous regions.

14.2 Comparison of Suitability of Transportation Services Based on City Model

In this section, we provide an overview of the city model and five typical transportation services. The indicators for evaluating the superiority or inferiority of each service method were defined. We then quantitatively clarify the cost required to achieve a certain service level based on the demand density and user-mean travel distance.

14.2.1 City Model Settings

Three main assumptions were considered for our city model:

1. Users with a demand density ρ (people/km² h) are uniformly distributed on an infinite plane
2. Users head in various directions from their departure point
3. Travel demand to their destination is attenuated with distance according to an exponential distribution, as shown in Eq. (14.1):

$$q(x) = \lambda e^{-\frac{2}{d}x}. \quad (14.1)$$

Here, if the user mean travel distance d is obtained by averaging Eq. (14.1) over the range of x to infinity, then λ is a parameter related to diminishing distance and is set as $s \lambda = 2\rho/(d\pi)^2$.

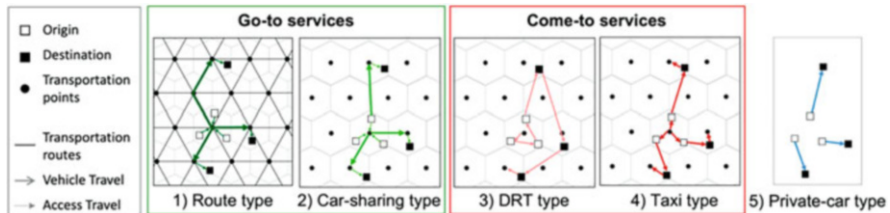


Fig. 14.1 Five types of transportation services

14.2.2 Modeling Transportation Services

We defined five transportation services and calculated the cost and service level achieved for each service (mean travel time). Figure 14.1 presents a conceptual diagram of each transportation service.

With respect to transportation points such as train stations, bus stops, and car-sharing parking lots, transportation services can be divided into two categories: go-to services, where users can access or egress the points, and come-to services, where a vehicle picks up the user from the transportation point to the user's departure point.

Five typical transportation services were assumed:

1. Route type: Users go to transportation points and ride vehicles that run at regular intervals on routes connecting the transportation points
2. Car-sharing type: Users access transportation points similarly to the route type but allows for free movement between transportation points
3. DRT type: Shared transportation is used from the user's departure point to the destination
4. Taxi type: These operate on non-fixed schedules and routes, and users are transported from their departure point to their destination on demand without carpooling
5. Private car type: Users go directly from the departure point to the destination by private car, bicycle, or foot

The route and car-sharing types are classified as go-to services, while the demand and taxi types are classified as come-to-services. It is assumed that in a given setting or situation, one of the five types is adopted.

14.2.3 Provision Cost and User's Mean Travel Time for Each Transportation Service

In this section, the cost of providing each transportation service and the user travel time achieved by each service are calculated. Each transportation service i has a uniform transportation point, with a travel distance d_{ai} for the access/egress part between the transportation point and departure point or destination, and a travel distance d_{ci} between the departure point and destination.

1) Route Type

A user accesses the nearest transportation point placed at density b_1 (points/km²) and the access time per unit distance (reciprocal of speed) t_{a1} (h/km) (Fig. 14.1). The user then boards a vehicle that arrives at a fixed operation interval f_1 (h) on a route that connects the transportation points and moves to the transportation point nearest to the destination at the vehicle travel time per unit distance t_{c1} (h/km). The user then conducts an egress movement from the transportation point to the destination for time t_{a1} . The user selects the shortest route to the transportation point nearest the destination and does not consider the time required for transfers or the acceleration and deceleration times required when the vehicle is stopping. For the user's mean access/egress time d_{a1} (km), the transportation points are assumed to be uniformly distributed in a hexagonal lattice, and because the mean distance to the center of a regular hexagonal region (access travel) is not significantly different from the distance from a disk-shaped region to the center of the circle, this distance is used as an approximation:

$$d_{a1} = \frac{2}{3\sqrt{\pi}} \frac{1}{\sqrt{b_1}}. \quad (14.2)$$

The vehicle travel distance d_{c1} (km) and route density l (km/km²) are obtained from the user's mean travel distance (from the origin point □ to the destination point ■) \hat{d} (km) and transportation point density b_1 as follows:

$$d_{a1} = \alpha \hat{d}, \quad (14.3)$$

$$l = \beta \sqrt{b_1}, \quad (14.4)$$

where α and β are constant terms in the network travel distance and density, respectively. Although the network distance naturally differs depending on its shape, it is considered proportional to the straight-line distance (Koshizuka and Kobayashi 1983). The α value approaches 1 as the network becomes denser. In this study, the transportation points, which are intersections of routes, are defined as uniformly arranged in a hexagonal lattice (i.e., the route network is connected in a triangular lattice); therefore, α is the area ratio of a sector with a central angle of 60° and an equilateral triangle, whereas β is the total distance of the triangular lattice network clarified by Watanabe (2006)

$$\alpha = \frac{2\pi}{3\sqrt{3}} \approx 1.209, \quad (14.5)$$

$$\beta = 3\sqrt{\frac{2\sqrt{3}}{3}} \approx 3.233. \quad (14.6)$$

The operation frequency f_1 is obtained by dividing the travel time of route density l by the vehicle density n_1 (vehicles/km²), with half of this value set as the mean waiting time.

$$f_1 = \frac{l t_{c1}}{n_1}. \quad (14.7)$$

The user mean travel time T_1 (h) is set as

$$T_1 = d_{c1} t_{c1} + d_{a1} t_{a1} + f_1/2, \quad (14.8)$$

and the route type provision cost C_1 (yen/h) is set as

$$C_1 = l CL_1 + b_1 CB_1 + n_1 CN_1, \quad (14.9)$$

where CL_1 (yen·km/h), CB_1 (yen·point/h), and CN_1 (yen·vehicle/h) are the cost parameters per hour for the route, transportation point, and vehicle, respectively. The route density l was obtained from the transportation point density using Eq. (14.4), where the total cost is determined using the transportation point and vehicle densities.

2) Car-sharing Type

A user accesses (→) a transportation point placed at density b_2 (points/km²) and unit time t_{a2} (h/km) in the same manner as in the route type, whereas distance d_{a2} (km) is set as follows, similar to Eq. (2):

$$d_{a2} = \frac{2}{3\sqrt{\pi}} \frac{1}{\sqrt{b_2}}. \quad (14.10)$$

It is assumed that the vehicle travels in a straight line (→) to the transportation point nearest to the destination at a unit vehicle travel time t_{c2} (h/km), and that travel distance d_{c2} (km) is set as the user's mean travel distance d (km). In addition, one-way drop-offs were assumed to be possible, and the time required for the vehicle to return to its original transportation point was not considered. Under the assumption that vehicles converge to a given point from multiple directions, the waiting time f_2 (h) until a user is assigned a vehicle is set as the total usage time, which is obtained by dividing the vehicle usage time per person by the demand density divided by the number of vehicles n_2 (vehicles).

$$f_2 = \frac{\rho \hat{d} t_{c2}}{n_2}. \quad (14.11)$$

The car-sharing users' mean travel time T_2 (h) and provision cost C_2 (yen/h) are expressed as follows:

$$T_2 = d_{c2}t_{c2} + d_{a2}t_{a2} + f_2/2, \quad (14.12)$$

$$C_2 = b_2CB_2 + n_2CN_2. \quad (14.13)$$

3) DRT Type

A user has a vehicle operating at regular intervals from a transportation point located at density b_3 (points/km²) come to them at the departure point at a unit vehicle travel time t_{c3} (h/km), after which the user travels to the destination (→). During this time, the vehicle passes through the departure points and destinations of other users who are riding together, and after completing the rounds of the departure points, the vehicle makes rounds of the destinations. The user requires additional boarding time because of the operation interval and detours to the departure points of other users.

The route length $2d_{c3}$ (km) that connects the user's departure point and destination after the vehicle picks up the user is obtained via the Beardwood–Halton–Hammersley (BHH) theorem (Beardwood et al. 1959). The value obtained by multiplying the region area (reciprocal of transportation point density b_3) of each transportation point by the demand density ρ is set as the number of passengers. For the region where the vehicle makes its rounds, if the departure point is set as a transportation point-specific region and the destination is set as a disk-shaped region where the user mean distance d is set as the radius, then the route distance converges to Eq. (14.14) (where $k = 0.765$):

$$2d_{c3} = \frac{k\sqrt{\rho}}{2} \left(\frac{1}{b_3} + \sqrt{\frac{\pi d^2}{b_3}} \right). \quad (14.14)$$

The mean ride distance d_{c3} (km) to the destination was set to half the value in Eq. (12). The operation interval f_3 (h) of the vehicle is set as the pickup time when a vehicle travels the route length $2d_{c3}$ at vehicle travel time t_{c3} divided by the product of the number of vehicles n_3 (vehicles/km²) and the transportation point density b_3 . Half of the resulting value is set as the mean waiting time of the user.

$$f_3 = \frac{2d_{c3}t_{c3}}{b_3n_3}. \quad (14.15)$$

Therefore, the DRT type user's mean travel time T_3 (h) and provision cost C_3 (yen/h) are as follows.

$$T_3 = d_{c3}t_{c3} + f_3/2, \quad (14.16)$$

$$C_3 = b_3CB_3 + n_3CN_3. \quad (14.17)$$

4) Taxi Type

A user has a vehicle coming to the departure point from a transportation point placed at density b_4 (points/km²), from which the user goes (\rightarrow) to the destination at time per distance t_{c4} (h/km). There is no carpooling when a user is directly transported from the departure point to the destination. If ride-sharing services are considered similar to taxis, then ride-sharing can be considered as a case wherein a high density of transportation points for a taxi-type service setup are present, except that instead of professional drivers providing the service, general drivers who are residents pickup and drop-off users. The distance d_{a4} (km) from the transportation point to the departure point and from the destination to the nearest transportation point was calculated based on the transportation point density b_4 using the following equation, which is similar to Eqs. (14.2) and (14.10) as follows:

$$d_{a4} = \frac{2}{3\sqrt{\pi}} \frac{1}{\sqrt{b_4}}. \quad (14.18)$$

The ride distance d_{c4} to the destination is assumed to be equivalent to the user's mean travel distance d . Vehicles are assigned to each user on a first-come-first-served basis; when all n_4 (vehicles/km²) vehicles are in use, the waiting time f_4 (h) is included. The pickup time when a vehicle travels a distance from the transportation point to the departure point and from the destination to the nearest transportation point at vehicle travel time t_{c4} per unit distance is divided by the product of the number of vehicles n_4 (vehicles/km²) and transportation point density b_4 , with half of the resulting value set as the user waiting time.

$$f_4 = \frac{2d_{c3}t_{c3}}{b_3n_3}. \quad (14.19)$$

Therefore, the taxi-type user's mean travel time T_4 (h) and provision cost C_4 (yen/h) are as follows:

$$T_4 = d_{c4}t_{c4} + f_4/2, \quad (14.20)$$

$$C_4 = b_4CB_4 + n_4CN_4. \quad (14.21)$$

5) Private Car Type

The user owns a vehicle and drives it directly to the destination at a unit vehicle time t_{c5} (h/km) (\rightarrow). Therefore, the private car type user's mean travel time T_5 (h) is as follows:

$$T_5 = \hat{d}t_{c5}. \quad (14.22)$$

The number of vehicles n_5 (vehicles/h) is defined as the product of demand density and travel time, assuming that each vehicle has a cost associated with the transportation point, which is the vehicle storage location. Therefore, the number of vehicles n_5 and the provision cost C_5 (yen/h) are as follows:

$$n_5 = \rho T_5, \quad (14.23)$$

$$C_5 = (CB_5 + CN_5) n_5. \quad (14.24)$$

14.3 Transportation Services that Minimize Costs

Table 14.1 lists the parameters used for the model analysis. For each transportation service type, T_i is given as a parameter from the equations obtained in Sect. 14.2, and the number of vehicles n_i is obtained by solving the equation for f_i . The user travel time T_i was set to 1/2 (h), and the cost to achieve a service level of 30 min on average was calculated. The parameter value per hour was set with reference to automobile transportation business management indicators(Automobile Business Association of Japan 2017). Figure 14.2 illustrates the cost per person c_i (yen/h/person) obtained by dividing the provision cost C_i by the demand density ρ when the transportation point density b_i is changed. Based on these results, the following insights were derived.

When the transportation point density b_i increases, the mean travel time decreases because the access distance d_{ai} and the number of users per transportation point decrease, and there exists an optimal transportation point density that minimizes c_i . However, the number of private vehicles n_5 and transportation density b_5 are uniquely determined by the demand density; thus, these values do not change.

Table 14.1 Parameter settings for each transportation service i

			(1) Route type	(2) Car-sharing type	(3) DRT type	(4) Taxi type	(5) Private car type
T_i	User travel time	(h)	1/2	1/2	1/2	1/2	1/2
t_{ai}	Reciprocal of access speed	(h/km)	1/3	1/3	–	–	–
t_{ci}	Reciprocal of vehicle speed	(h/km)	1/30	1/30	1/30	1/30	1/30
CL_i	Route cost	(Yen·km/h)	90	–	–	–	–
CB_i	Transportation point cost	(Yen·point/h)	50	100	100	100	200
CN_i	Vehicle cost	(Yen·vehicle/h)	5000	2500	2500	2500	2500

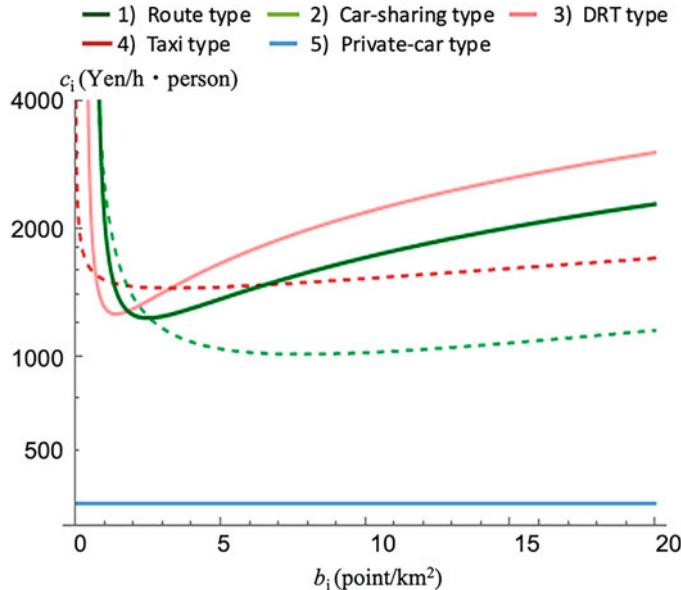


Fig. 14.2 Relationship between transportation point cost b_i and cost c_i per person ($\rho = 5, \hat{d} = 5$)

- The optimal transportation point density is higher for the go-to services category, which experiences a larger increase in mean travel time owing to an increase in access distance.

Here, we verify the change in c_i when the user's mean distance and demand density change when b_i where c_i is at a minimum and b_i^* is substituted. Figure 14.3 shows c_i as d changes. From the figure, the following can be observed.

- Route type exhibits increasing costs with travel distance, whereas other means of transportation exhibit diminishing costs. For short-travel distances, DRT is advantageous. As the distance increases, car-sharing becomes more advantageous. However, over time, the DRT type becomes advantageous again, because increases in d have little effect on the waiting time.

Figure 14.4 shows changes in c_i when the demand density ρ is changed, and Fig. 14.5 shows the changes in c_i when both d and ρ are changed. It can be inferred from these figures that:

- The route type is not affected by changes in demand density; thus, when demand is high, the cost per person decreases, and the route type becomes advantageous.
- For the other means of transportation, the cost per person decreases exponentially as demand increases. When demand is high, the most advantageous transportation service is car sharing, followed by private cars.

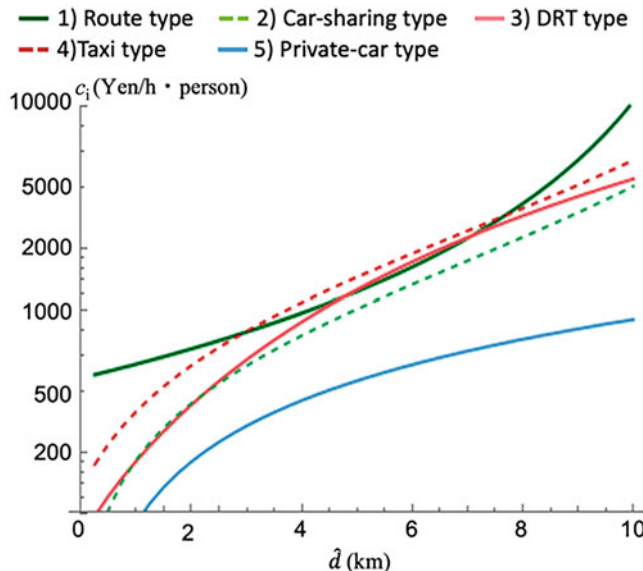


Fig. 14.3 Relationship between user's mean travel distance \hat{d} and cost c_i per person ($\rho = 5$)

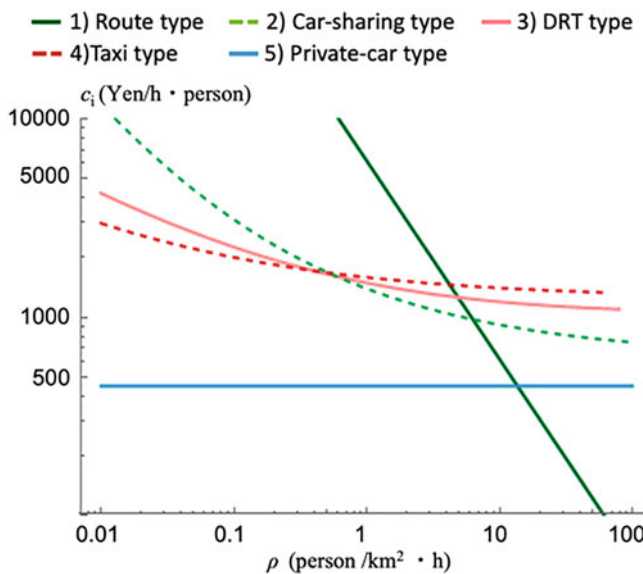


Fig. 14.4 Relationship between demand density ρ and cost c_i per person ($\hat{d} = 5$)

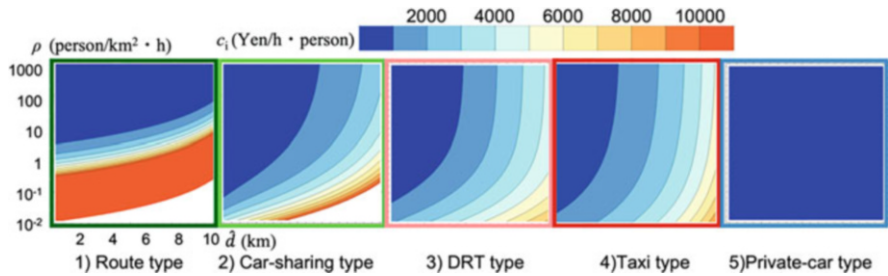


Fig. 14.5 Relationship between user's mean travel distance \hat{d} and demand density ρ and cost c_i per person

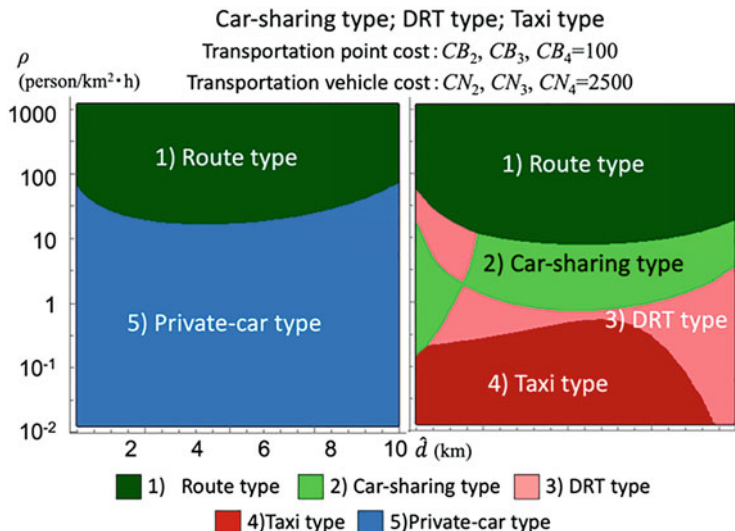


Fig. 14.6 Relationship between user's mean travel distance d and demand density ρ , and means of transportation where C_i is minimized (right: except private car type)

Figure 14.6 shows the means of transportation, where c_i is at a minimum as the ρ and d values are changed, divided between cases where the private car type is considered and where private cars can be used and cases where private cars cannot be used. This result shows that

- The private car type has a large advantageous region, demonstrating the overall superiority of private cars. However, when the demand is high, the route type becomes advantageous.
- When the private car type was not considered, as demand decreased, advantageous regions appeared for the car-sharing type for long distances and for the DRT type for short distances.

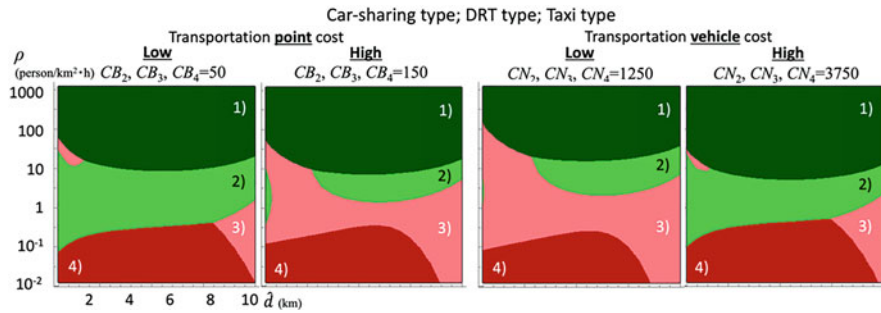


Fig. 14.7 Relationship between changes in car-sharing, demand, and taxi type transportation point and vehicle cost and advantageous regions

Figure 14.7 shows an analysis of the effects on advantageous regions when the car-sharing, demand, and taxi-type transportation point costs CB_2 , CB_3 , CB_4 , and vehicle costs CN_2 , CN_3 , and CN_4 are changed for unit cost sensitivity analysis. The following conclusions were drawn.

- As shown in Fig. 14.2, fluctuations in transportation-point costs have a significant effect on the car-sharing type, where the number of transportation points is large, whereas decreases in vehicle costs have a considerable effect on the DRT type.

These results show that when demand is low, the difference in costs between the car-sharing and DRT types is small and that the superiority of either type changes with slight changes in cost.

14.4 Comparison Between Actual Circumstances of Introduction of Transportation Services to Local Public Transportation and Results of Theoretical Model

In this section, we examine the circumstances surrounding the introduction of these services to local public transportation, primarily by municipalities in eastern Japan. After comparing the demand densities and travel distance values of the introduced means of transportation, we compared the advantageous regions for these transportation services according to the demand density and travel distance derived in the previous section.

14.4.1 Status of Introduction of Services to Local Public Transportation

Figure 14.8 presents the results of an Internet and literature survey of 734 municipalities across 14 prefectures in eastern Japan, focusing on community buses

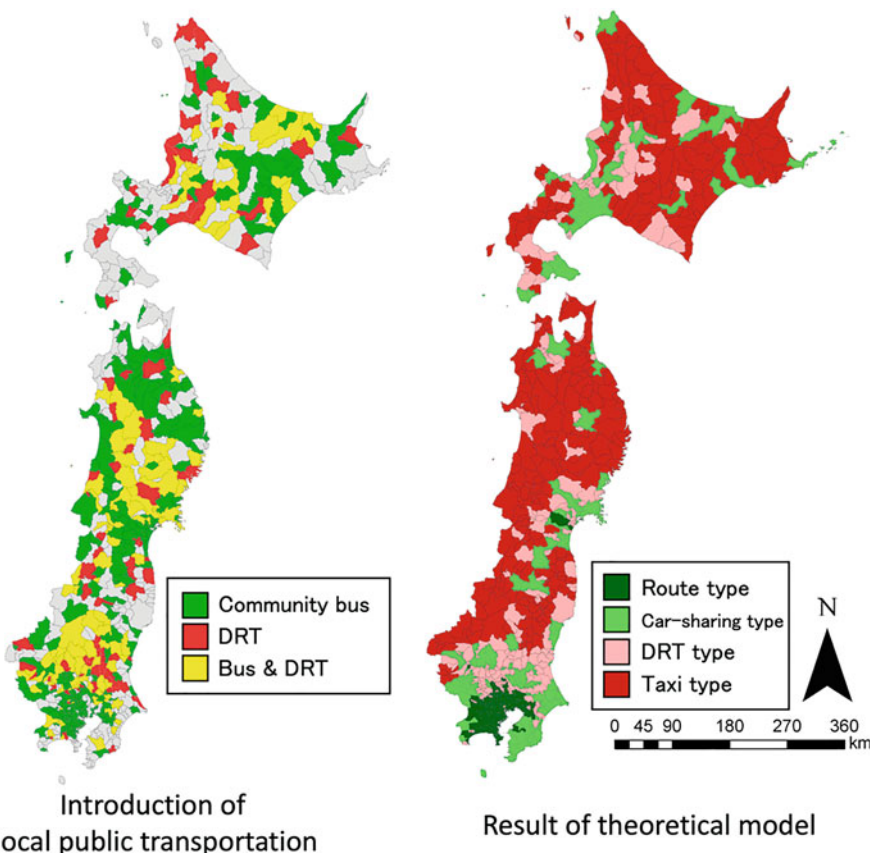


Fig. 14.8 Actual circumstances of local public transportation introduction and model-based classification results

and demand taxis operated mainly by municipalities. The survey identified 371 confirmed cases of introduction of community buses and 193 cases of demand taxis, with 115 cases utilizing both services. Comparing these results with a 2011 survey by Nihon Keizai Shinbunsha (2012), community buses and demand taxis increased by 199 and 117 cases, respectively, indicating the diversification of local public transportation in municipalities.

14.4.2 Comparison with Model Results

We investigated the correspondence between the advantageous regions of each transportation service and the introduction results for each municipality based on the relationship between d/ρ and provision cost. Demand density and travel distance

Table 14.2 Mean travel distance d and demand density ρ values for each local public transportation service

	Count	\hat{d} (km)	ρ (person/km ² .h)
Community bus	303	3.75	40.15
DRT	87	5.29	2.19
Bus and DRT	117	4.51	6.23
Not applicable	258	5.67	9.79

were calculated for each 1-km mesh, aggregated by municipality, and averaged. The demand density ρ_k per hour for a 1-km grid k is calculated using the following equation:

$$\rho_k = P_k (Day/7) (Hour/24), \quad (14.25)$$

where P_k is the total population (people) of mesh k in 2010, Day is the number of outings per week, and $Hour$ is the number of outings per day. Assuming that users visit the nearest hospital/supermarket for 1 h per day, we set $Day = 2$ and $Hour = 1$. The mean travel distance d_k of mesh k takes the straight-line distance from the representative point in each mesh to the nearest point among the 8657 hospital points (Wellness Corporation 2011) and 41,351 supermarket points (Shogyo Kai 2013) using GIS, and averages them. Table 14.2 shows the mean travel distance and demand density values by means of transportation, excluding the island areas. These data indicate that municipalities that have introduced community buses have a short mean travel distance and a high demand density of 40 people/h km², whereas those that have introduced demand taxis have long travel distances and low demand densities.

In the case illustrated in Fig. 14.6, which does not consider private car types, Fig. 14.9 shows the mean travel distance and demand density values for each municipality. Figure 14.8 (right) shows their geographical distribution. Although this analysis has limitations because of the assumption of uniform demand density by the model and the use of an estimated value for the travel distance, the boundary between the community bus and demand taxi is generally consistent with boundaries (1), (2), (3), and (4) shown in the figure.

Of the 774 municipalities included in the analysis, 154 were classified as route types corresponding to regions with high population densities and destinations within short distances, such as the Tokyo metropolitan area and Sendai City in Miyagi Prefecture. This result reflects the real world, where railroads and bus routes are already densely developed in these regions. In contrast, 148 municipalities were classified as car-sharing type, which included regions such as Chiba, Saitama, Kanagawa, and Miyagi, with demand densities similar to those of route-type settings: some areas of Hokkaido where the demand density is low, but the travel distance is long. However, unlike route-type municipalities, to date, no locations have achieved car-sharing-type local public transportation, with only a mixed presence of community buses and demand taxis. Finally, 188 municipalities were classified as the DRT type, including northern Kanto, the area around Sendai City in Miyagi Prefecture, and central Hokkaido. Among the cities classified as car-sharing

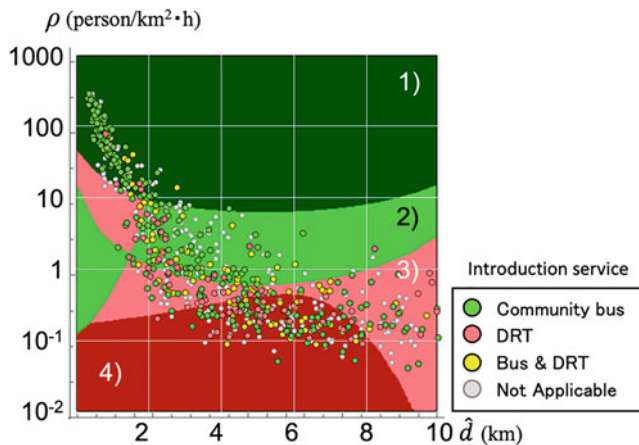


Fig. 14.9 Relationship between advantageous region by each transportation service and travel distance d and demand density ρ

and DRT types, 108 locations already had demand taxis in operation (of which 62 locations used community buses), which is consistent with the analysis results. Meanwhile, 287 municipalities were classified as taxi types, with many distributed in the Tohoku region. However, based on a comparison with Fig. 14.8 (left), many regions introduced community buses instead. Considering the per capita local bus route maintenance costs in Japan Bus Association (2016), Aomori Prefecture ranked third nationwide, whereas Akita Prefecture ranked seventh nationwide, indicating its high costs; thus, it is speculated that introducing a taxi-type service setup could reduce costs. In addition, the explanatory power of the analysis could be increased if cases where habitable land is limited (e.g., hilly and mountainous areas) and where actual demand density is high were considered in the study.

14.5 Summary and Future Issues

This study aims to provide a theoretical discussion on the benefits of increasingly diversifying local public transportation and its advantages over the current transportation situation. We derived the basic conditions for changes in costs for each means of transportation to achieve a certain service level based on the relationship between demand density and user travel distance. These results were then compared with the local transportation services introduced and implemented in specific regions. The following conclusions were drawn:

1. The route type is superior when the demand density is high, while the taxi type is superior when the demand density is low. The car-sharing type and DRT type

fall between these two types, with the DRT-type service setup becoming more advantageous as the travel distance increases.

2. The results of investigating the actual introduction of these transportation services to local public transportation revealed that regions where community buses were introduced tended to have high demand densities and short travel distances, while regions with DRT-type services were introduced showed the opposite tendencies.
3. A comparison of the advantageous regions for each transportation service and the values observed in different municipalities partially confirmed the consistency of the model with regions where route and DRT-type services were introduced.

For future studies, the following topics should be considered: correspondence of parameters to actual conditions, discussions that consider capacity, and addressing imbalanced demand distributions.

Acknowledgments This study was supported in part by JSPS KAKENHI (Grant Numbers JP 26560162 and 16 J02064), the Oobayashi Foundation, and the Division of Policy and Planning Science Commons at the University of Tsukuba.

References

- Automobile business Association of Japan (2017) Motor truck transportation business management indicators
- Beardwood J, Halton JH, Hammersley JM (1959) The shortest path through many points. *Proc Camb Philos Soc* 55:299–232
- Hasegawa D, Suzuki T (2011) Theoretical consideration of demand-based transportation establishment conditions focusing on urban scale and density. *J Urban Plan* 46(3):817–822
- Ieda H (1997) Formulation and solution of hierarchical transportation systems, such as hub-spokes/point-to-point and aggregated/direct transportation, on a homogeneous infinite plane. *J Civil Eng Plan* 14:773–782
- Ishida T, Taniguchi M, Suzuki T, Furuya H (1999) Analysis of the effectiveness of transportation policies focusing on the feasible range of transportation modes and favorable areas. *Transport Policy Res* 2(1):14–25
- Japan Bus Association (2016) Japanese bus business 2015
- Kato A, Takeuchi D (1979) New edition of urban transportation and urban planning. Gijutsu Shoin
- Koshizuka T, Kobayashi J (1983) Road distance and straight-line distance. *J Urban Plan* 18:43–48
- Nihon Keizai Shinbunsha (2012) Evaluation of sustainability of national cities
- Niiitani Y (1993) Urban transportation planning. Gihodo Publishing
- Shogyo Kai (2013) Japan supermarket directory
- Watanabe D (2006) Mathematical study on network form analysis and transportation system optimization from the perspective of proximity, Doctoral dissertation, graduate School of Tsukuba University, 2006
- Watanabe D, Suzuki T (2000) Study on hierarchical collection and distribution transportation systems considering economies of scale. *J Urban Plan* 35:1027–1032
- Wellness Corporation (2011) National hospital directory